

Institut universitaire romand de Santé au Travail

Assessment of particulate exposure and surface characteristics in association with urinary levels of 8-hydroxy-2'-deoxyguanosine, considered as marker of oxidative stress

Thèse de doctorat ès sciences de la vie (PhD)

**présentée à la Faculté de Biologie et de Médecine de
l'Université de Lausanne**

par

Ari SETYAN

Chimiste diplômé de l'Université de Genève, Suisse

Jury

Prof. Valentin Rousson, Président
Prof. Michel Guillemin, Directeur de thèse
Dr Michel J. Rossi, co-Directeur de thèse
Dr Thomas Kuhlbusch, Expert
Dr Jean-Jacques Sauvain, Expert
Dr Michael Riediker, Expert

Lausanne, 2009

Imprimatur

Vu le rapport présenté par le jury d'examen, composé de.

Président	Monsieur Prof.	Valentin Rousson
Directeur de thèse	Monsieur Prof.	Michel Guillemain
Co-directeur de thèse	Monsieur Dr	Michel J. Rossi
Experts	Monsieur Dr	Thomas Kuhlbusch
	Monsieur Dr	Jean-Jacques Sauvain
	Monsieur Dr	Michael Riediker

le Conseil de Faculté autorise l'impression de la thèse de

Monsieur Ari Setyan

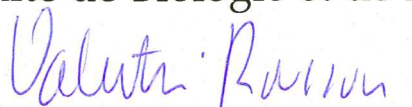
Chimiste diplômé de l'Université de Genève

intitulée

**Assessment of particulate exposure and surface characteristics
in association with urinary levels of 8-hydroxy-2'-deoxyguanosine
considered as markers of oxydative stress.**

Lausanne, le 4 mars 2009

pour Le Doyen
de la Faculté de Biologie et de Médecine



Prof. Valentin Rousson

Abstract

Epidemiological studies have demonstrated that exposure to fine particles is associated to adverse health effects, including cancer, respiratory and cardiovascular diseases. However, mechanisms by which particles induce health effects remain unclear. According to one of the most investigated hypotheses, particles cause adverse effects through the production of reactive oxygen species (ROS), which are very hazardous compounds able to attack directly biological structures, including the DNA strand or the lipid bilayer of the cells. If the defense mechanisms, constituted of antioxidants, are not able to counter ROS, then these compounds will cause in the body a range of oxidation reactions called “oxidative stress”.

The aim of the present research project was to better understand mechanisms by which exposure to fine particles induces oxidative stress. The first point of this project was to check whether exposure to high levels of fine particles is directly linked to oxidative stress, and whether this oxidative stress is accompanied by the activation of the defense mechanisms (antioxidants). The second point was to study the role played by the particle surface characteristics in the oxidative stress process.

For that purpose, a study was conducted in bus depots with the participation of 40 mechanics. First, occupational exposure to particles (PM₄) and to other pollutants (NO_x, O₃) was measured over a two-day period. Then, urine samples of mechanics were collected in order to measure levels of 8-hydroxy-2'-deoxyguanosine (8OHdG) and antioxidants. 8OHdG is a molecule formed by the oxidation of DNA and allowing to assess the oxidative stress status of the mechanics. Finally, particles were collected on filters, and functional groups located on the particle surface were analyzed in the laboratory using a Knudsen flow reactor. This technique allows not only to quantify functional groups on the particle surface, but also to measure the reaction kinetics.

Results obtained during the field campaign in bus depots showed that mechanics were exposed to rather low levels of PM₄ (20-85 µg/m³) and of pollutants (NO_x: 100-1000 ppb; O₃: <15 ppb). However, despite this low exposure, urinary levels of the oxidative stress biomarker (8OHdG) increased significantly for non-smoking workers over a two-day period of shift.

This oxidative stress was accompanied by an increase of antioxidants, indicating the activation of defense mechanisms. On the other hand, the analysis of functional groups on the particle surface showed important differences, depending on the workplace, the date and the activities of workers. The particle surface contained simultaneously antagonistic functional groups which did not undergo internal reactions (such as acids and bases), and was usually characterized by a high density of carbonyl functions and a low density of acidic sites. Reaction kinetics measured using the Knudsen flow reactor pointed out fast reactions of oxidizable groups and slow reactions of acidic sites. Several exposure parameters were significantly correlated with the increase of the oxidative stress status: the presence of acidic sites, carbonyl functions and oxidizable groups on the particle surface; reaction kinetics of functional groups on the particle surface; particulate iron and copper concentrations; and NO_x concentration.

Résumé

Des études épidémiologiques ont démontré qu'une exposition aux particules fines provoque des effets néfastes sur la santé, tels que cancer, maladies respiratoires et cardio-vasculaires. En revanche, de nombreuses zones d'ombre demeurent sur les mécanismes par lesquels ces particules agissent sur la santé. Selon l'une des hypothèses les plus étudiées actuellement, les particules agiraient par l'intermédiaire d'espèces oxygénées réactives, composés très dangereux capables d'attaquer directement des structures biologiques comme l'ADN ou les lipides membranaires. Si les mécanismes de défense, constitués d'antioxydants, ne sont pas capables de contrer les espèces oxygénées réactives, ces dernières provoquent dans l'organisme une série de réactions d'oxydation regroupées sous le terme « stress oxydatif ».

Le présent projet de recherche vise à mieux comprendre les mécanismes par lesquels une exposition aux particules fines aboutit à un stress oxydatif. Le premier but du projet est de vérifier si une exposition régulière à des niveaux élevés de particules fines est directement liée au stress oxydatif, et si ce stress oxydatif est accompagné par une activation des systèmes de défense (antioxydants). Le deuxième but est d'étudier plus précisément le rôle joué par les propriétés de la surface des particules dans le processus de stress oxydatif.

Pour répondre à ces questions, une étude a été menée dans des dépôts de bus avec la participation de 40 mécaniciens. Dans un premier temps, le niveau d'exposition des mécaniciens aux particules (PM_{10}) et à d'autres polluants (NO_x , O_3) a été mesuré sur une période de deux jours. Ensuite, des échantillons d'urines ont été collectés auprès des mécaniciens pour mesurer les concentrations en 8-hydroxy-2'-deoxyguanosine (8OHdG) et en antioxydants. La 8OHdG est une molécule provenant de l'oxydation de l'ADN et permettant d'évaluer le niveau de stress oxydatif des travailleurs. Finalement, des particules ont été échantillonnées sur filtres, et les groupes chimiques à la surface de ces particules ont ensuite été analysés en laboratoire avec un réacteur à écoulement de Knudsen. Cette technique permet non seulement de quantifier le nombre de groupes chimiques à la surface des particules, mais aussi d'étudier leur cinétique de réaction.

Les résultats obtenus lors de la campagne d'échantillonnage sur le terrain ont montré que les ouvriers des dépôts de bus étaient exposés à des concentrations relativement faibles de PM_{10} (20-85 $\mu g/m^3$) et de différents polluants (NO_x : 100-1000 ppb; O_3 : <15 ppb). Cependant, malgré ces faibles niveaux d'exposition, le biomarqueur de stress oxydatif (8OHdG) a augmenté de façon significative dans l'urine des mécaniciens non-fumeurs durant deux jours consécutifs de travail dans les dépôts de bus. Ce stress oxydatif était accompagné d'une augmentation des antioxydants, indiquant l'activation des systèmes de défense. Parallèlement, l'analyse des groupes chimiques à la surface des particules ambiantes dans les dépôts de bus a montré de très grandes différences en fonction du lieu, de la date et des activités des ouvriers. La surface des particules ambiantes contenait plusieurs fonctions antagonistes qui coexistaient sans subir de réactions internes (telles que des acides et des bases), et était généralement caractérisée par une densité élevée de fonctions carbonyles, et une faible densité de sites acides. La cinétique de réaction mesurée avec le réacteur de Knudsen a indiqué une vitesse de réaction rapide pour les groupes chimiques oxydables, ainsi qu'une vitesse de réaction lente pour les sites acides. Plusieurs paramètres d'exposition ont montré une corrélation significative avec l'augmentation du stress oxydatif : la présence d'acides, de carbonyles et de fonctions oxydables à la surface des particules; la cinétique de réaction des groupes chimiques à la surface des particules; les concentrations en fer et en cuivre particulières; et la concentration en NO_x .

Table of contents

Abstract.....	3
Résumé.....	5
Table of contents.....	7
List of figures.....	11
List of tables.....	15
Abbreviations.....	19
1. Introduction.....	21
1.1 The air.....	21
1.2 Particulate matter.....	21
1.3 Oxidative stress.....	26
1.4 Oxidative stress biomarkers.....	28
1.5 Aim of the research project.....	30
1.6 Institute for Work and Health.....	31
1.7 Swiss Federal Institute of Technology (Air and Soil Pollution Laboratory)..	32
1.8 Outline of the thesis.....	32
1.9 References.....	33
2. Design of the field campaign.....	41
2.1 Ethics Committee.....	41
2.2 Sampling sites.....	41
2.3 Population under study.....	47
2.4 Biological fluids sampling.....	50
2.5 Measurements and analysis.....	50
2.6 Reference.....	51
3. Exposure parameters.....	53
3.1 Introduction.....	53
3.2 Material and methods.....	56
3.2.1 Stationary sampling.....	56
3.2.2 Personal sampling.....	60
3.2.3 Statistical analyses.....	61
3.3 Results and discussion.....	61

3.3.1	<i>Stationary sampling</i>	61
3.3.2	<i>Personal sampling</i>	80
3.3.3	<i>Comparison between stationary and personal samplings</i>	83
3.3.4	<i>Summary</i>	84
3.4	Conclusion.....	84
3.5	References.....	85
4.	Particle surface characterization	89
4.1	Introduction.....	89
4.2	Material and methods.....	91
4.2.1	<i>Knudsen flow reactor</i>	91
4.2.2	<i>Probe gases</i>	95
4.2.3	<i>Samples</i>	98
4.2.4	<i>Particle mass</i>	104
4.2.5	<i>Particle size distribution</i>	104
4.2.6	<i>Kinetics of heterogeneous titration reactions</i>	106
4.2.7	<i>Statistical analyses</i>	107
4.3	Results and discussion.....	107
4.3.1	<i>Laboratory-generated aerosols</i>	109
4.3.2	<i>Carbonaceous particles</i>	112
4.3.3	<i>TiO₂ particles</i>	118
4.3.4	<i>Aerosols collected in the field</i>	121
4.3.5	<i>Kinetics of heterogeneous titration reactions</i>	128
4.4	Conclusion.....	131
4.5	References.....	132
5.	Markers of biological effects	141
5.1	Introduction.....	141
5.2	Material and methods.....	147
5.2.1	<i>Chemicals</i>	147
5.2.2	<i>Analytical method of urinary 8OHdG by HPLC-ECD</i>	148
5.2.3	<i>Analytical method of urinary 8OHdG by LC-MS/MS</i>	150
5.2.4	<i>Measurement of urinary creatinine</i>	151
5.2.5	<i>Measurement of urinary antioxidants</i>	153
5.2.6	<i>Statistical analyses</i>	153
5.3	Results and discussion.....	153

5.3.1	<i>Analytical method of urinary 8OHdG by HPLC.....</i>	153
5.3.2	<i>Analytical method of urinary 8OHdG by LC/MS-MS.....</i>	160
5.3.3	<i>Summary of the analytical methods.....</i>	165
5.3.4	<i>Levels of urinary 8OHdG for workers in bus depots.....</i>	166
5.3.5	<i>Levels of urinary antioxidants for workers in bus depots.....</i>	171
5.4	Conclusion.....	175
5.5	References.....	176
6.	Correlations between oxidative stress and exposure parameters.....	183
6.1	Introduction.....	183
6.2	Material and methods.....	184
6.3	Results and discussion.....	186
6.3.1	<i>Correlations between exposure parameters.....</i>	186
6.3.2	<i>Correlations between 8OHdG and personal data, lifestyle factors and exposure parameters.....</i>	188
6.3.3	<i>Normality test.....</i>	191
6.3.4	<i>Statistical models.....</i>	193
6.4	Conclusion.....	195
6.5	References.....	196
7.	Conclusion and perspectives.....	201
8.	Annexes.....	203
8.1	Questionnaire.....	203
8.2	Stationary sampling.....	205
8.3	Personal sampling.....	207
8.4	Uptake measurements on aerosols collected in the workplaces using the Knudsen flow reactor.....	208
8.5	Urinary concentrations of 8-hydroxy-2'-deoxyguanosine.....	209
8.6	Urinary concentrations of creatinine.....	210
8.7	Urinary concentrations of antioxidants.....	211
	Remerciements.....	213
	Curriculum Vitae.....	215
	List of publications.....	217

List of figures

1.1	Schematic drawing of the human respiratory tract, and modeled particle deposition probability in the respiratory tract.	24
1.2	Hierarchical oxidative stress model.	27
1.3	Repair of a damaged DNA base by non-specific endonucleases or specific glycolyses.	29
2.1	Drawing and pictures of the sampling site in bus depot 1.	43
2.2	Plan of the sampling sites in bus depot 2, and picture of the sampling site surveyed during daytime.	44
2.3	Plan of the sampling site surveyed in bus depot 3 during daytime.	45
2.4	Drawing and pictures of the metro construction site. Examples of activities in this sampling site: welding and grinding down of the rails.	46
2.5	Timeline of interventions during a sampling campaign.	50
3.1	Mean PM ₄ concentrations over an 8-hour period of shift.	62
3.2	Mean organic and elemental carbon concentrations over an 8-hour period of shift. Elemental carbon fraction to the total carbon (OC+EC).	63
3.3	Particulate iron, copper and manganese content.	64
3.4	Influence of the multiple charge correction on the particle size distribution.	66
3.5	Particle penetration into the SMPS (TSI Inc., model 3934). Influence of the diffusion loss correction on the particle size distribution.	67
3.6	Two examples of particle size distributions measured using a SMPS: without significant activity near the SMPS, and recorded immediately after the passage of a bus near the SMPS.	68
3.7	Example of particle number concentrations monitored using a SMPS during a whole period of shift.	69
3.8	Mean particle number, mass and surface area concentrations over an 8-hour period of shift, measured using the SMPS (also with LQ1-DC for the surface area). Correlation between particle surface areas measured using LQ1-DC and SMPS.	71
3.9	Mean aerodynamic diameter of particles, determined using the Andersen type cascade impactor.	73

3.10	Four examples of particulate mass size distribution determined using the Andersen type cascade impactor.	74
3.11	Mean NO _x concentrations over an 8-hour period of shift. NO ₂ contribution to NO _x	76
3.12	Mean ozone concentrations over an 8-hour period of shift.	77
3.13	Correlation between results obtained for PM ₄ using stationary pumps and the Andersen type cascade impactor.	78
3.14	Correlation between results obtained for PM ₄ using stationary pumps and those estimated with OC, EC and metal ions.	79
3.15	Correlation between results obtained for particle mass concentration using the SMPS and the Andersen type cascade impactor.	80
3.16	Box plots of mean PM ₄ concentrations over an 8-hour period of shift, measured on personal samples.	81
3.17	Box plots of mean organic and elemental carbon concentrations over an 8-hour period of shift, measured on personal samples.	82
4.1	Schematic drawing of the Knudsen flow reactor, and photograph of the reactor. ...	93
4.2	Typical raw data of a titration experiment using the Knudsen flow reactor, and example of a calibration curve obtained for the determination of K _{calibr}	94
4.3	Schematic drawing of the co-flow burner used to produce hexane soot.	101
4.4	Photographs of the samples collected using two high-volume samplers.	104
4.5	Particle size distributions of limonene SOA, Pb(NO ₃) ₂ , and Cd(NO ₃) ₂ measured using the SMPS.	109
4.6	Carbonaceous surface acidic oxide neutralization.	113
4.7	Carbonaceous surface basic oxide neutralization.	116
4.8	Uptake measurements of probe gases on silanized and non-silanized quartz fiber filters using the Knudsen flow reactor.	121
4.9	Uptake measurements of N(CH ₃) ₃ , NH ₂ OH, CF ₃ COOH, HCl, and O ₃ on aerosols collected in the workplaces using the Knudsen flow reactor.	123
5.1	Molecular structure and tautomeric forms of 8OHdG.	143
5.2	Molecular structure of 8OHdG under neutral, anionic and dianionic form. Relative abundance of these three forms depending on pH.	143
5.3	Typical chromatograms of standard solutions obtained by HPLC-ECD.	154
5.4	Six-point calibration curve measured in duplicates by HPLC-ECD.	155

5.5	Typical chromatograms of non-spiked and spiked urine samples. 1-step clean-up by SPE (Oasis WCX), followed by HPLC-ECD.	156
5.6	Recovery rate of 8OHdG in spiked urine samples. 1-step clean-up by SPE (Oasis WCX), followed by HPLC-ECD.	157
5.7	Typical chromatograms of non-spiked and spiked urine samples. 2-step clean-up by SPE (Discovery DSC-SAX, BondElut C ₁₈ /OH), followed by HPLC-ECD.	159
5.8	Recovery rate of 8OHdG in spiked urine samples. 2-step clean-up by SPE (Discovery DSC-SAX, BondElut C ₁₈ /OH), followed by HPLC-ECD.	160
5.9	Proposed fragmentation pathway of 8OHdG during negative ion electrospray tandem mass spectrometry with CID.	161
5.10	Typical chromatograms of standard solutions, obtained by LC-MS/MS.	161
5.11	Eight-point calibration curve measured in duplicates by LC-MS/MS.	162
5.12	Typical chromatograms of non-spiked and spiked urine samples, obtained by LC-MS/MS.	163
5.13	Examples of curves obtained for the recovery rate of 8OHdG in standard solutions and in spiked urine samples. 1-step clean-up procedure (BondElut C ₁₈ /OH), followed by LC-MS/MS.	164
5.14	Correlation between urinary levels of 8OHdG (raw data, without creatinine adjustment) and those of creatinine.	168
5.15	Box plots of urinary concentrations of 8OHdG.	169
5.16	Box plots of urinary concentrations of creatinine.	171
5.17	Example of voltammetric measurements of urine samples using the antioxidant redox sensor manufactured by EDEL Therapeutics S.A.	172
5.18	Correlation between urinary levels of antioxidants (raw data, without creatinine adjustment) and those of creatinine.	173
5.19	Box plots of urinary concentrations of antioxidants in their reduced state.	174
5.20	Correlation between urinary levels of 8OHdG and those of antioxidants.	175

List of tables

1.1	List of particle sizes and corresponding fractions.	23
2.1	List and description of the sampling sites surveyed during the field campaign.	42
2.2	Complete list of volunteers with sampling sites, dates and personal information. ...	48
2.3	Characteristics of the studied population.	49
3.1	Selected studies where occupational exposure to Diesel exhaust particles and other fine particulate matters was assessed.	53
3.2	Spearman's rank correlation matrix between stationary and personal samplings for PM ₄ , OC and EC.	83
3.3	Summary of results obtained for exposure parameters in the workplaces with stationary and personal samplings, and corresponding occupational exposure limits for Switzerland.	84
4.1	Parameters of the Knudsen flow reactor.	93
4.2	List of different chemical reactions during the titration experiments in the Knudsen flow reactor under the given experimental conditions.	96
4.3	Technical data of carbonaceous particles manufactured by Evonik Degussa GmbH.	100
4.4	Titration experiments on laboratory-generated aerosols, carbonaceous aerosols and TiO ₂ samples using the Knudsen flow reactor.	108
4.5	Uptake coefficient γ_0 of heterogeneous chemical reactions between probe gases and aerosol samples in the Knudsen flow reactor.	129
4.6	Uptake coefficient γ_0 of heterogeneous chemical reactions between probe gases and aerosols collected in the field.	130
4.7	List of Spearman's rank correlation coefficients between uptake coefficient γ_0 and number of probe gases taken up by the samples collected in the workplaces.	130
5.1	Non-exhaustive list of studies where 8OHdG was used as biomarker of oxidative stress.	142
5.2	Non-exhaustive list of analytical methods for 8OHdG.	144
5.3	Parameter settings for HPLC-ECD.	150
5.4	Parameter settings for LC-MS/MS.	151
5.5	Precision of the first analytical method by HPLC-ECD.	157

5.6	Precision of the second analytical method by HPLC-ECD.	160
5.7	Precision of the analytical method by LC-MS/MS.	165
5.8	Summary of the data related to the robustness of the three analytical methods of urinary 8OHdG.	166
5.9	Detailed results obtained for the reproducibility (inter-day variability) of the analytical method by LC-MS/MS.	167
5.10	Matrix of pairwise comparison probabilities obtained by analysis of variance for urinary levels of 8OHdG (non-smokers and former smokers).	170
5.11	Matrix of pairwise comparison probabilities obtained by analysis of variance for urinary levels of 8OHdG (smokers).	170
5.12	Matrix of pairwise comparison probabilities obtained by analysis of variance for urinary levels of creatinine (non-smokers and former smokers).	171
5.13	Matrix of pairwise comparison probabilities obtained by analysis of variance for urinary levels of creatinine (smokers).	171
5.14	Matrix of pairwise comparison probabilities obtained by analysis of variance for urinary levels of antioxidants (non-smokers and former smokers).	174
5.15	Matrix of pairwise comparison probabilities obtained by analysis of variance for urinary levels of antioxidants (smokers).	174
6.1	List of selected studies where urinary levels of 8OHdG were correlated with occupational or lifestyle factors.	184
6.2	Spearman's rank correlation coefficients between exposure parameters.	187
6.3	Spearman's rank correlation coefficients between 8OHdG and personal data.	188
6.4	Spearman's rank correlation coefficients between 8OHdG and exposure parameters.	189
6.5	Normality test using skewness and kurtosis values.	192
6.6	Normality test for log-transformed parameters using skewness and kurtosis values.	193
6.7	List of different statistical models describing the evolution of urinary levels of 8OHdG as a function of exposure parameters, obtained by multiple regression analysis.	194
8.2	Stationary sampling.	205
8.3	Personal sampling.	207
8.4	Uptake measurements on aerosols collected in the workplaces using the Knudsen flow reactor.	208

8.5	Urinary concentrations of 8-hydroxy-2'-deoxyguanosine.	209
8.6	Urinary concentrations of creatinine.	210
8.7	Urinary concentrations of antioxidants.	211

Abbreviations

8OHdG	8-hydroxy-2'-deoxyguanosine
ANOVA	analysis of variance
BD	bus depot
BET	Brunauer/Emmett/Teller
BMI	body mass index
CE	capillary electrophoresis
CFC	chlorofluorocarbon
CID	collision-induced dissociation
CPC	condensation particle counter
DC	diffusion charger
DEP	Diesel exhaust particle
DMA	differential mobility analyzer
DNA	deoxyribo-nucleic acid
DPF	Diesel particle filter
EC	elemental carbon
ECD	electro-chemical detector
EELS	electron energy loss spectroscopy
ELISA	enzyme-linked immuno-sorbent assay
FT-IR	Fourier transform infra-red
GC	gas chromatography
HPLC	high performance liquid chromatography
IARC	International Agency for Research on Cancer
ID	inner diameter
IR	infra-red
JaICA	Japan Institute for the Control of Aging
LC	liquid chromatography
LOD	limit of detection
MCS	metro construction site
MS	mass spectrometer
N/A	not available

N/D	not detected
NEXAFS	near-edge X-ray absorption fine structure
NIST	National Institute of Standards and Technology
NMR	nuclear magnetic resonance
OC	organic carbon
OEL	occupational exposure limit
PA	proton affinity
PAH	polycyclic aromatic hydrocarbon
PM_x	particulate matter with aerodynamic diameter smaller than x μm
RNOS	reactive nitrogen oxide species
ROS	reactive oxygen species
S/N	signal to noise ratio
SAX	strong anion exchange
SD	standard deviation
SE	standard error
SMPS	scanning mobility particle sizer
SOA	secondary organic aerosol
SOD	super-oxide dismutase
SPE	solid-phase extraction
SRM	standard reference material
TC	total carbon
TEM	transmission electron microscopy
UV	ultra-violet
VOC	volatile organic compound
WCX	weak cation exchange
XPS	X-ray photoelectron spectroscopy

Chapter 1 - Introduction

1.1 The air

The atmosphere is a layer of gases surrounding the Earth and retained by the Earth's gravity. It contains roughly 78.1% nitrogen (N_2), 20.9% oxygen (O_2), 0.93% argon (Ar), 0.038% carbon dioxide (CO_2), trace amounts of other gases, and a variable amount (average around 1%) of water vapor (U.S. National Aeronautics and Space Administration, 2007). This mixture of gases is commonly known as air.

There are many substances in the air which may impair the health of plants and animals (including humans). Chemical, physical or biological agents that cause harm or discomfort to humans and other living organisms, or damage the environment, constitute air pollution. Worldwide air pollution is responsible for large numbers of deaths and cases of respiratory and cardiovascular diseases. Although a number of physical activities (volcanoes, fire, etc.) may release different pollutants in the environment, human activities are the major cause of environmental air pollution (Kampa and Castanas, 2008).

Pollutants may be classified as either primary or secondary. Usually, primary pollutants are substances directly emitted from a process, such as the carbon monoxide (CO) gas from a motor vehicle exhaust, or sulfur dioxide (SO_2) released from factories. Major primary pollutants produced by human activities include sulfur oxides (SO_x), nitrogen oxides (NO_x), carbon monoxide, carbon dioxide, volatile organic compounds (VOCs), particulate matter (PM), toxic metals, chlorofluorocarbons (CFCs), ammonia (NH_3) and radioactive pollutants. Secondary pollutants are not emitted directly. Rather, they are formed in the air when primary pollutants react or interact. Secondary pollutants include particles formed from gaseous primary pollutants, and tropospheric ozone (O_3) formed from NO_x and VOCs. Note that some pollutants may be both primary and secondary.

1.2 Particulate matter

Particulate matter is a mixture of microscopic solids or liquid droplets suspended in a gas. In contrast, aerosol refers to particles and the surrounding gas together. Particle sources refer to the various locations, activities or factors which are responsible for the release of particles in

the atmosphere. These sources can be classified in two major categories: anthropogenic sources (owing to human activity) and natural sources. Anthropogenic sources mostly relate to combustion processes, such as smoke stacks of power plants, manufacturing facilities, municipal waste incinerators, motor vehicles, aircraft, ships, burn practices in agriculture and forestry management, burning wood, fireplaces, stoves, furnaces, incinerators, oil refining, and industrial activity in general. Particles may also occur naturally, originating from volcanoes, dust storms, forest and grassland fires, living vegetation, and sea spray. Some of these particles are emitted directly into the atmosphere (primary emissions), and some are emitted as gases and form particles in the atmosphere (secondary emissions, leading to gas-to-particle conversion). Averaged over the globe, aerosols released by human activities currently account for about 10% of the total amount of aerosols in our atmosphere (U.S. National Aeronautics and Space Administration).

Epidemiological studies have demonstrated that increased levels of particulate matter in the air are associated to adverse health effects, such as heart disease, altered lung function and cancer (Maynard and Kuempel, 2005). Activities of workers in many occupational situations are responsible for the release of important amounts of particles, leading to acute health hazards for exposed workers. Therefore, many epidemiological and toxicological studies related to particulate matter are undertaken at the workplace, in order to better understand health hazards due to particulate matter and to improve the safety of workers.

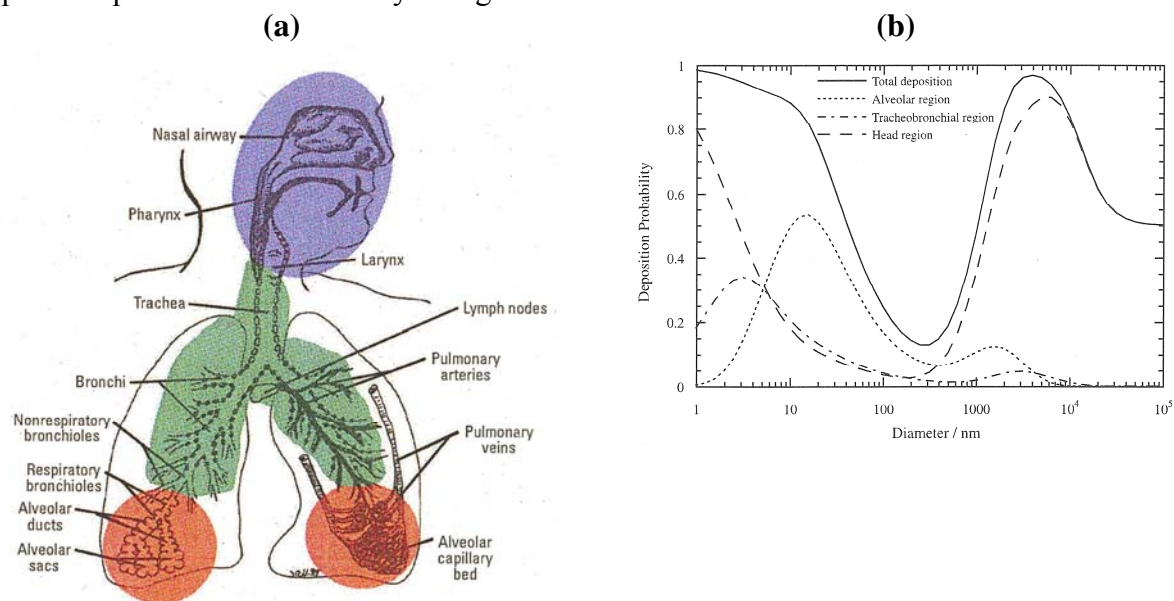
Health effects of particulate matter depend on many physical and chemical properties. One of the most important properties is the particle size, because it determines the region of the respiratory tract where particles deposit, and the way they interact with the biological system. As particles are often non-spherical, there are many definitions of particle size. The most widely used definition is the aerodynamic diameter, which is the diameter of a spherical particle, having a density of 1 g/cm^3 and the same terminal settling velocity in the gas as the particle of interest (European Standard EN 481, 1993). Particle diameters range from less than 10 nm to more than 100 μm . These dimensions represent the continuum from a few molecules up to the size where particles can no longer be carried by a gas. The notations PM_{10} and $\text{PM}_{2.5}$ are used to describe particles with an aerodynamic diameter smaller than 10 and 2.5 μm , respectively. Table 1.1 shows the different particle sizes and their names as they are described in the European Standard EN 481 (1993), which is also valid in Switzerland.

Table 1.1: List of particle sizes and corresponding fractions (European Standard EN 481, 1993).

Name	Fraction	Size
PM ₁₀₀	Inhalable fraction	≤ 100 µm
PM ₁₀	Thoracic fraction	≤ 10 µm
PM ₄	Respirable fraction	≤ 4 µm

There are three main routes by which workers can be exposed to particles: inhalation, ingestion and dermal penetration (Oberdörster *et al*, 2005). As with most particles in the workplace, inhalation is considered to be the main route by which particles will enter the bodies of workers. The respiratory tract is usually divided into three regions: the naso-pharyngeal region, which includes mouth, nose, larynx and pharynx; the tracheo-bronchial region; and the alveolar region (Figure 1.1(a)). Once inhaled, particles will deposit in all regions of the respiratory tract with high efficiency, dependent upon their particle size. Figure 1.1(b) shows the fractional deposition of inhaled particles in the naso-pharyngeal, tracheo-bronchial and alveolar regions of the human respiratory tract for nasal breathing at rest using the predictive mathematical model of the International Commission on Radiological Protection (1994). It is important to note that particles in the range 10-100 nm deposit mainly in the alveolar region, while deposition of particles larger than 1 µm takes place in the naso-pharyngeal region. Once deposited, nanoparticles, in contrast to larger particles, appear to translocate to different organs in the body after penetrating the cell epithelium and entering the blood or the lymphatic system.

Figure 1.1: (a) Schematic drawing of the human respiratory tract (taken from Oberdörster *et al*, 2005). (b) Modeled particle deposition probability in the respiratory tract (taken from International Commission on Radiological Protection, 1994). Deposition has been modeled assuming an adult breathing through his nose at 25 l/min (light exercise), and exposed to spherical particles with a density of 1 g/cm³.



Many epidemiological and toxicological studies have been undertaken in order to assess health effects of particulate matter. Epidemiology does not allow studying biological mechanisms by which particles influence human health, but bring insight into the relationship between exposure to particulate matter and biological effects (dose-response relationship) (Lippmann and Ito, 2000). Epidemiological studies are numerous, but concern mainly atmospheric particles in urban areas. They usually point out the important role of the particle size, but are not able to determine which fraction is the most relevant to health (Englert, 2004). Over the past 20 years, many toxicological studies have been undertaken *in vivo* (with animals) and *in vitro*, and have brought better insight into the mechanisms by which particulate matter induces adverse health effects. These studies clearly demonstrated that, for particles with the same chemical composition, small particles are much more hazardous than larger ones (Buschini *et al*, 2001; Healey *et al*, 2005). Moreover, according to several studies, particle surface characteristics seem to play a key-role in the interactions with cells and organs (Oberdörster, 2001) and in the formation of reactive radical species (Tao *et al*, 2003).

Due to the adverse health effects of particulate matter, great efforts have been placed onto the assessment of exposure of workers to particles. For that purpose, it is essential to identify the possible sources of particles at the workplace, and to use suitable means for the

characterization of occupational exposure. The presence of particles in ambient air is mainly due to nucleation and condensation of gases, industrial emissions and motor emissions. In conventional technologies used at the workplace, particles may be released by hot processes involving metals or alloys, such as welding (Zimmer, 2002) or laser processing (Boulaud *et al*, 1992), which generate metallic oxides; combustion of fossil fuels in motor vehicles (Wichmann, 2007); mechanical processes (Zimmer and Maynard, 2002). Nowadays, emerging nanotechnologies represent considerable economic stakes and are developing very fast. First studies have been recently undertaken in Switzerland to identify industrial sectors where engineered nanomaterials are in use, in order to assess the number of potentially exposed workers (Schmid and Riediker, 2008). Manufacture processes of these nanomaterials are classified in three main categories (Witschger and Fabriès, 2005b): chemical processes (chemical vapor deposition, liquid-phase reactions), physical processes (evaporation/condensation, laser ablation) and mechanical processes.

The monitoring of particles is much more difficult than for other gaseous pollutants, because their size, concentration, chemical content and shape are very variable. In order to assess occupational exposure to particulate matter, it is important to focus on parameters which are believed to be the most relevant for health. Indeed, there are three metrics which can be used to express the particle concentration: number (expressed as the number of particles per volume unit, usually particle/cm³), surface (particle surface area per volume unit, usually $\mu\text{m}^2/\text{cm}^3$) and mass (particle mass per volume unit, usually $\mu\text{g}/\text{m}^3$). As we already mentioned above, toxicological studies have pointed out the important role played by the particle surface characteristics in adverse health effects, and therefore suggest that the “surface” metric would be more relevant for health. On the other hand, it is also essential to measure the particle mass concentration, because all the regulations and occupational exposure limits (OELs) are based on this metric. However, from a toxicological point of view, this metric would not be sufficient to explain health effects of particulate matter. Indeed, one particle of 10 μm diameter has the same mass as one million particles of 100 nm, and toxicological studies have clearly demonstrated that small particles can be much more hazardous than larger ones (Witschger and Fabriès, 2005a). In addition to the measurement of the particle concentration, it is also essential to study other physico-chemical characteristics in order to assess hazards related to an exposure to particulate matter, such as particle structure (electronic microscopy), electrostatic charges, or chemical contents. It is important to keep in mind that for the measurement of each parameter, many techniques are commercially available. These

techniques are not always based on the same principle of measurement, and therefore results obtained may be significantly different. Thus, during a field campaign, it would be important to use simultaneously two different techniques for the measurement of a chosen parameter in order to check for the accuracy of the results.

1.3 Oxidative stress

Several mechanisms have been proposed to explain the adverse health effects of particulate pollutants. These include inflammation, endotoxin effects, stimulation of capsaicin/irritant receptors, autonomic nervous system activity, pro-coagulant effects, covalent modification of cellular components, and reactive oxygen species (ROS) production (Donaldson *et al*, 2003; Nel *et al*, 2006). Among these, ROS production and the generation of oxidative stress have received the most attention.

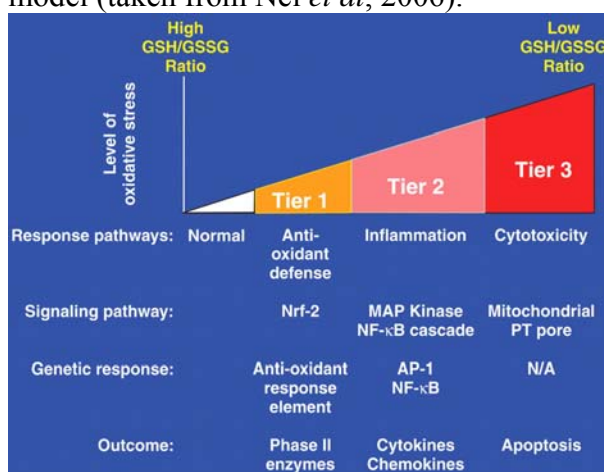
ROS is a collective term that includes both oxygenated radicals and certain non-radicals which are oxidizing agents. The most important oxygen-derived free radicals are superoxide ($O_2^{\bullet-}$), hydroxyl (OH^{\bullet}), peroxy (ROO^{\bullet}) and hydroperoxyl (HO_2^{\bullet}) radicals, while non-radicals include hydrogen peroxide (H_2O_2), hypobromous acid ($HOBr$), hypochlorous acid ($HOCl$), ozone (O_3), molecular singlet oxygen (O_2^1) and peroxynitrite ($ONOO^-$) (Halliwell and Whiteman, 2004). Free radicals can be defined as molecules or molecular fragments containing one or more unpaired electrons in atomic or molecular orbitals (Winterbourn, 1993). This unpaired electron(s) usually gives a considerable degree of reactivity to the free radical. Radicals derived from oxygen represent the most important class of radical species generated in living systems (Liochev and Fridovich, 1994). With the exception of unusual circumstances (ionizing radiation, ultraviolet light, or other forms of high energy exposure), free radicals are produced in cells generally by electron transfer reactions, which can be enzymatically or non-enzymatically mediated. Therefore, these oxidation reactions occur in normal cellular metabolism. In some cases, ROS are produced specifically to serve essential biological functions, whereas in other cases, they represent by-products of metabolic processes (Shen *et al*, 1996).

Under normal coupling conditions in the mitochondrion, ROS are generated at low frequency and are easily neutralized by antioxidant defenses, such as glutathione (GSH) and antioxidant enzymes (Halliwell and Gutteridge, 2007). However, under conditions of excess ROS production, such as may occur in the lung and possibly in the circulatory system during

ambient or occupational nanoparticle exposures (Nel, 2005), the natural antioxidant defenses may be overwhelmed (Halliwell and Gutteridge, 2007). Oxidative stress refers to a state in which GSH is depleted, while oxidized glutathione (GSSG) accumulates (Halliwell and Gutteridge, 2007). Cells respond to this drop in the GSH/GSSG ratio by mounting protective or injurious responses. The GSH/GSSG redox pair not only serves as the principal homeostatic regulator of redox balance but also functions as a sensor that triggers these stress responses that, depending on the rate and level of change in this ratio, could be protective or injurious in nature (Xiao *et al*, 2003).

Using Diesel exhaust particles (DEP) as a model air pollutant, a hierarchical cellular response model has been developed to explain the role of oxidative stress in mediating the biological effects of particles (Li *et al*, 2002). Figure 1.2 shows schematically a three-tier model proposed by Nel *et al* (2006). This three-tier model suggests that low levels of oxidative stress induce protective effects that may yield to

Figure 1.2: Hierarchical oxidative stress model (taken from Nel *et al*, 2006).



more damaging effects at higher levels of oxidative stress. Protective effects (Tier 1) are induced by the transcription nuclear factor erythroid 2-related factor 2 (Nrf2), which regulates the transcriptional activation of more than 200 antioxidant and detoxification enzymes, which are collectively known as the phase 2 response (Li and Nel, 2006). Defects in this protective pathway could determine the susceptibility to particle-induced oxidant injury, for example the exacerbation of airway inflammation and asthma by DEP (Li *et al*, 2003). Thus, it is important to mention that due to the protective Tier 1 response, particle-induced ROS production does not automatically lead to adverse biological outcomes. If these protective responses fail to provide adequate protection, then a further increase in ROS production will result in pro-inflammatory (Tier 2) and cytotoxic (Tier 3) effects (Xiao *et al*, 2003). Pro-inflammatory effects are mediated by the redox-sensitive MAP kinase and NF-κB cascades that are responsible for the expression of cytokines, chemokines, and adhesion molecules, many of which are involved in the inflammatory process of the lung (Li *et al*, 2003; Nel *et al*, 2006). Tier 3 cytotoxic effects, also known as toxic oxidative stress, involve mitochondria, which are capable of releasing pro-apoptotic factors and inducing apoptosis of lung cells

(Hiura *et al*, 2000). Taken together, the hierarchical cellular oxidative stress model provides a mechanistic platform to understand how particles generate adverse health effects.

1.4 Oxidative stress biomarkers

Biomarkers are supposed to reflect changes in biological systems that are related to exposure to xenobiotics or other type of toxic materials (Henderson *et al*, 1989). Usually biomarkers are subdivided into at least three types: biomarkers of exposure, biomarkers of effect, and biomarkers of susceptibility. There are four types of monitoring: environmental monitoring (biomarkers of potential exposure), biological monitoring (biomarkers of exposure and of effect), biological effect monitoring (biomarkers of effect), and health surveillance (biomarkers of effect and medical examination) (Henderson *et al*, 1989). Biological effect monitoring is a step further than measuring solely exposure of an individual by the determination of xenobiotic concentrations in ambient air or even by measuring the internal dose of a compound in blood or urine (Greim *et al*, 1995). A biomarker of effect concerns an assessment of early or late adverse effects of a chemical or another factor on a physiological system, organ or organism. The primary purpose of using biomarkers of effect is surveillance, which is the identification of individuals or a population at risk to adverse health effects, so that preventive measures can be taken. Although a biomarker of effect is usually also related to exposure to a specific chemical, it is generally more closely related to the occurrence of an adverse health effect (Lowry, 1995). An ideal biomarker of effect has at least the following characteristics: high specificity for the effect of interest, reflection of an early effect, easy and inexpensive analysis, medium available by non-invasive sampling techniques, low background level of the biomarker in the body fluid of interest, a well-established relationship between the response of the biomarker and exposure, a well-established relationship between the response of the biomarker and the induced damage.

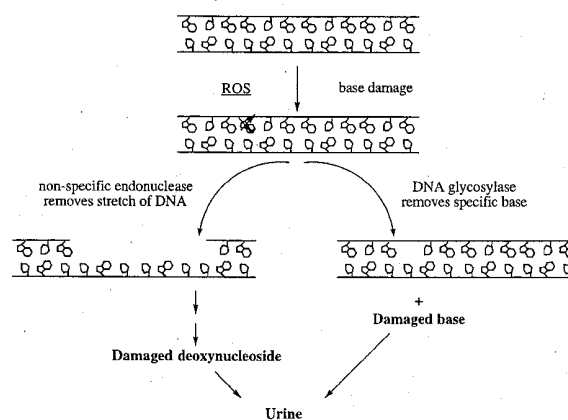
Lipid peroxidation is probably the most extensively investigated process induced by free radicals. The abundant presence of membrane phospholipids at sites where radicals in general and, more specifically, ROS are formed render them easily accessible endogenous targets, rapidly affected by free radicals (de Zwart *et al*, 1999). Especially the group of polyunsaturated fatty acids is highly susceptible to reactions with free radicals. Peroxidation of lipids in fatty acids may lead to a radical chain reaction. Because of these chain reactions, one substrate radical (R^{\bullet}) may result in the formation of many equivalents of lipid peroxides (LOOH). These degenerative propagation reactions in lipid membranes are usually

accompanied by the formation of a wide variety of products, including alkanes and carbonyl compounds. Because some of these products, especially hydroxyalkenals, are toxic by themselves, they may serve as second messengers for radical damage. Products resulting from lipid peroxidation are thus attractive parameters to monitor radical damage.

Protein oxidation products and carbonyl derivatives of proteins may result from oxidative modifications of amino acid side chains, reactive oxygen-mediated peptide cleavage and from reactions with lipid and carbohydrate oxidation products (de Zwart *et al*, 1999). It is now becoming clear that the presence of carbonyl groups in proteins may indicate that the proteins have been subjected to oxidative free radical damage. An increase in protein carbonyl content of tissues is associated with a number of pathological disorders, including rheumatoid arthritis, Alzheimer's disease, respiratory distress syndrome, Parkinson's disease and atherosclerosis.

ROS can attack almost any cellular structure or molecule. However, with respect to aging and cancer, deoxyribo-nucleic acid (DNA) is considered as a major target (Ames and Gold, 1991). ROS may cause DNA-protein cross-links, damage to the deoxyribose-phosphate backbone as well as specific chemical modifications of purine and pyrimidine bases (Dizdaroglu, 1991). Oxidative base modifications may result in mutations, whereas oxidation of deoxyribose moieties may induce base release or DNA strand breaks (Cheng *et al*, 1992). Whereas hydroxyl radicals generate multiple products from all four bases (5-hydroxymethyluracil, 8-hydroxyadenine, thymidine glycol ...), singlet oxygen preferentially modifies guanine by 8-hydroxylation (Dizdaroglu, 1991). Guanine most readily undergoes an oxidative attack, since it possesses the lowest oxidation potential of the four bases. Consequently, the nucleoside 8-hydroxy-2'-deoxyguanosine (8OHdG) is the most often studied biomarker of oxidative DNA damage (Wu *et al*, 2004). *In vivo*, damaged DNA is repaired by endonucleases and glycosylases, liberating deoxynucleotides and bases, respectively (Figure 1.3). Bases are excreted directly in urine, and the deoxynucleotides are

Figure 1.3: Repair of a damaged DNA base by non-specific endonucleases (left) or specific glycosylases (right) (taken from de Zwart *et al*, 1999).



further metabolized to mono-nucleosides before they are excreted into the urine (Fraga *et al*, 1990). The presence of background levels of oxidized nucleotides in urine *in vivo* implies that these processes also occur under non-pathological conditions (Hollstein *et al*, 1984).

1.5 Aim of the research project

According to our knowledge on health effects caused by particulate matter and the oxidative stress process, we formulated two hypotheses for the present research project. Firstly, ultrafine and more generally all particles generate ROS and induce oxidative stress in exposed people. Due to the very reactive nature of ROS, it is only possible to assess the *in vivo* oxidative stress in an indirect way. Compounds produced by reactions of ROS on the DNA or on the lipid bilayer of the cells can be used for that purpose. The presence of such compounds in biological fluids (urine, serum) may indeed be useful markers for monitoring the oxidative stress induced by an exposure to ultrafine particles (such as DEP). Secondly, particle surface characteristics, such as functional groups and surface area, are of prime importance to explain the ROS generation potential of particles.

In order to test these hypotheses, we conducted a field campaign in occupational situations where high levels of particulate matter were expected. During this field campaign, we assessed the exposure of workers to particulate matter, and we collected urine samples of volunteers in order to measure oxidative stress biomarkers. The first hypothesis was verified by testing whether there was any correlation between the exposure to particles at the workplace and the urinary concentration of selected biomarkers. The second hypothesis was verified by testing whether there was any correlation between particle surface characteristics (functional groups, surface area) and urinary concentrations of biomarkers.

Within the framework of this study, we decided to focus on workplaces where many Diesel engines were in use, because DEP is a good “model” for studying health effects of particulate matter and has been the subject of numerous publications related to occupational exposure and health effects. Indeed, DEP consists of fine (<2.5 µm) and ultrafine (<0.1 µm) particles. Collectively, these particles have a large surface area, which makes them an excellent medium for adsorbing organics. Also, their small size makes them highly respirable and they have the potential to reach the deep areas of the lung and even the blood circulation (Wichmann, 2007).

Among the different oxidative stress biomarkers which have been the subject of previous publications, we decided to select 8-hydroxy-2'-deoxyguanosine (8OHdG) as a marker of oxidative DNA damage. Indeed, this compound is by far the most widely studied oxidative adduct in molecular epidemiology studies of increased oxidative DNA damage from occupational exposures, due to its prevalence and relative ease of measurement (Risom *et al*, 2005). It has been estimated that 8OHdG represents about 5% of all oxidative adducts (Beckman and Ames, 1997). We also decided to measure urinary levels of antioxidants, in order to check whether a possible increase of oxidative stress was followed by a biological response of the defense mechanism against oxidative stress (Tier 1 in Figure 1.2).

The present research project deals with several innovative points. The first one is the characterization of occupational exposure to fine/ultrafine particles by measuring simultaneously different metrics (mass, surface area and number). For that purpose, different types of measuring equipment were used during the field campaign, allowing the evaluation and comparison of their response. This has primarily been done for surface related measurements, by simultaneously using a scanning mobility particle sizer (SMPS) and a diffusion charger (DC). The second innovative point is the characterization of several chemical functions present on the particle surface. A Knudsen flow reactor was used for that purpose, and to our knowledge, this is the first time that this technique was used for the surface characterization of ambient particles. Finally, the third innovative point is the combination of both measurements of oxidative stress and antioxidant response.

1.6 Institute for Work and Health

The part of the project related to occupational exposure to particulate matter and assessment of oxidative stress was supervised by the Institute for Work and Health (Lausanne, Switzerland), and undertaken in the Particles and Health Group led by Dr Michael Riediker. This Institute is involved for more than 15 years in the field of occupational exposure and risk assessment of particulate matter. The focal point of their research is the assessment of occupational exposure to particulate matter and other pollutants (Guillemin *et al*, 1992; Riediker *et al*, 2003; Sauvain *et al*, 2003; Imhof, 2008), the measurement of organic (OC) and elemental (EC) carbon (Guillemin *et al*, 1997; Perret *et al*, 1999; Hebisch *et al*, 2003) and of polycyclic aromatic hydrocarbons (PAHs; Sauvain *et al*, 2001; Sauvain *et al*, 2003; Sauvain and Vu Duc, 2004; Huynh *et al*, 2007), the chemical reactivity of particles (Verdannot, 2006; Sauvain *et al*, 2008), and health effects of traffic exposure (Riediker *et al*, 2004). Moreover,

the Institute for Work and Health has become the center of an important European network (NanoImpactNet) coordinated by Dr Michael Riediker and promoting research cooperation in different areas related to nanoparticles (production, exposure, health effects; NanoImpactNet, 2008). Thus, the Institute for Work and Health has a long experience in analytical chemistry of occupational and environmental pollutants, and is internationally recognized in the field of particles, Diesel characterization and associated health effects.

1.7 Swiss Federal Institute of Technology (Air and Soil Pollution Laboratory)

The part of the project related to particle surface characterization was undertaken at the Swiss Federal Institute of Technology (Lausanne, Switzerland), in the Heterogeneous Chemistry Group (Air and Soil Pollution Laboratory) led by Dr Michel J. Rossi. For more than 15 years, the focal point of research of this group is the fundamental and applied study of interfacial reactions occurring on atmospheric particles. Both the development of new experimental techniques as well as their application to environmental problems has been pursued. The main lines of research developed in this group are experimental measurement of the interfacial reactivity and kinetics on mineral dust (Karagulian and Rossi, 2005; Karagulian and Rossi, 2006; Santschi and Rossi, 2006; Karagulian *et al*, 2006), sea salt (Pratte and Rossi, 2006), secondary organic aerosols (Demirdjian and Rossi, 2005) and soot samples (Stadler and Rossi, 2000; Alcala-Jornod *et al*, 2000; Salgado and Rossi, 2002; Salgado Muñoz and Rossi, 2002; Karagulian and Rossi, 2007). Thus, the group led by Dr Michel J. Rossi has acquired a strong experience in the interfacial characterization of model substrates.

1.8 Outline of the thesis

Chapter 2 will present the design of the field campaign, with a description of the population and the workplaces under study. During the field campaign, we assessed the exposure of workers to particulate matter and other pollutants. These results will be presented in Chapter 3 (“Exposure parameters”). After the survey of each sampling site, we measured several functional groups on the surface of particles collected in the field. These results will be discussed in Chapter 4 (“Particle surface characterization”). Urine samples of workers were used to quantify oxidative stress biomarkers (Chapter 5, “Markers of biological effects”). Finally, correlations between exposure to particulate matter and oxidative stress will be discussed in Chapter 6 (“Correlations between oxidative stress and exposure parameters”).

1.9 References

- Alcala-Jornod C., van den Bergh H., Rossi M.J., 2000. Reactivity of NO₂ and H₂O on soot generated in the laboratory: a diffusion tube study at ambient temperature. *Physical Chemistry Chemical Physics*, 2 (24), 5584-5593.
- Ames B.N., Gold L.S., 1991. Endogenous mutagens and the causes of aging and cancer. *Mutation Research/Fundamental and Molecular Mechanisms of Mutagenesis*, 250 (1/2), 3-16.
- Beckman K.B., Ames B.N., 1997. Oxidative decay of DNA. *Journal of Biological Chemistry*, 272 (32), 19633-19636.
- Boulaud D., Chouard J.C., Briand A., Chartier F., Lacour J.L., Mauchien P., Mermet J.M., 1992. Experimental study of aerosol production by laser ablation. *Journal of Aerosol Science*, 23 (suppl. 1), 225-228.
- Buschini A., Cassoni F., Anceschi E., Pasini L., Poli P., Rossi C., 2001. Urban airborne particulate: genotoxicity evaluation of different size fractions by mutagenesis tests on microorganisms and comet assay. *Chemosphere*, 44 (8), 1723-1736.
- Cheng K.C., Cahill D.S., Kasai H., Nishimura S., Loeb L.A., 1992. 8-hydroxyguanine, an abundant form of oxidative DNA damage, causes G → T and A → C substitutions. *Journal of Biological Chemistry*, 267 (1), 166-172.
- Demirdjian B., Rossi M.J., 2005. The surface properties of SOA generated from limonene and toluene using specific molecular probes: exploration of a new experimental technique. *Atmospheric Chemistry and Physics Discussions*, 5, 607-654.
- de Zwart L.L., Meerman J.H.N., Commandeur J.N.M., Vermeulen N.P.E., 1999. Biomarkers of free radical damage applications in experimental animals and in humans. *Free Radical Biology & Medicine*, 26 (1/2), 202-226.
- Dizdaroglu M., 1991. Chemical determination of free radical-induced damage to DNA. *Free Radical Biology & Medicine*, 10 (3/4), 225-242.
- Donaldson K., Stone V., Borm P.J.A., Jimenez L.A., Gilmour P.S., Schins R.P.F., Knaapen A.M., Rahman I., Faux S.P., Brown D.M., MacNee W., 2003. Oxidative stress and calcium signaling in the adverse effects of environmental particles (PM₁₀). *Free Radical Biology & Medicine*, 34 (11), 1369-1382.
- Englert N., 2004. Fine particles and human health - A review of epidemiological studies. *Toxicology Letters*, 149 (1/3), 235-242.

-
- European Standard EN 481, 1993. Workplace atmospheres - Size fractions definitions for measurement of airborne particles. European Committee for Standardization, Bruxelles (Belgium).
 - Fraga C.G., Shigenaga M.K., Park J.-W., Degan P., Ames B.N., 1990. Oxidative damage to DNA during aging: 8-hydroxy-2'-deoxyguanosine in rat organ DNA and urine. *Proceedings of the National Academy of Sciences of the United States of America*, 87 (12), 4533-4537.
 - Greim H., Csanády G., Filser J.G., Kreuzer P., Schwarz L., Wolff T., Werner S., 1995. Biomarkers as tools in human health risk assessment. *Clinical Chemistry*, 41 (12), 1804-1808.
 - Guillemin M.P., Herrera H., Huynh C.K., Droz P.-O., Vu Duc T., 1992. Occupational exposure of truck drivers to dust and polynuclear aromatic hydrocarbons: a pilot study in Geneva, Switzerland. *International Archives of Occupational and Environmental Health*, 63 (7), 439-447.
 - Guillemin M., Cachier H., Chini C., Dabill D., Dahmann D., Diebold F., Fischer A., Fricke H.-H., Groves J.A., Hebisch R., Houpillart M., Israël G., Mattenklott M., Moldenhauer W., Sandino J.P., Schlums C., Sutter E., Tucek E., 1997. International round robin tests on the measurement of carbon in diesel exhaust particulates. *International Archives of Occupational and Environmental Health*, 70 (3), 161-172.
 - Halliwell B., Whiteman M., 2004. Measuring reactive species and oxidative damage in vivo and in cell culture: how should you do it and what do the results mean? *British Journal of Pharmacology*, 142 (2), 231-255.
 - Halliwell B., Gutteridge J.M.C., 2007. Free Radicals in Biology and Medicine (fourth edition). Oxford University Press Inc., New York.
 - Healey K., Lingard J.J.N., Tomlin A.S., Hughes A., White K.L.M., Wild C.P., Routledge M.N., 2005. Genotoxicity of size-fractioned samples of urban particulate matter. *Environmental and Molecular Mutagenesis*, 45 (4), 380-387.
 - Hebisch R., Dabill D., Dahmann D., Diebold F., Geiregat N., Grosjean R., Mattenklott M., Perret V., Guillemin M., 2003. Sampling and analysis of carbon in diesel exhaust particulates - an international comparison. *International Archives of Occupational and Environmental Health*, 76 (2), 137-142.
 - Henderson R.F., Bechtold W.E., Bond J.A., Sun J.D., 1989. The use of biological markers in toxicology. *Critical Reviews in Toxicology*, 20 (2), 65-82.

-
- Hiura T.S., Li N., Kaplan R., Horwitz M., Seagrave J.-C., Nel A.E., 2000. The role of a mitochondrial pathway in the induction of apoptosis by chemicals extracted from Diesel exhaust particles. *Journal of Immunology*, 165 (5), 2703-2711.
 - Hollstein M.C., Brooks P., Linn S., Ames B.N., 1984. Hydroxymethyluracil DNA glycosylase in mammalian cells. *Proceedings of the National Academy of Sciences of the United States of America*, 81 (13), 4003-4007.
 - Huynh C.K., Vu Duc T., Deygout F., Le Coutaller P., Surmont F., 2007. Identification and quantification of PAH in bitumen by GC-ion-trap MS and HPLC-fluorescent detectors. *Polycyclic Aromatic Compounds*, 27 (2), 107-121.
 - Imhof C., 2008. Risk assessment in laboratories handling nano-objects at EPFL. Master thesis, Swiss Federal Institute of Technology (Lausanne, Switzerland) and Institute for Work and Health (Lausanne, Switzerland).
 - International Commission on Radiological Protection, 1994. Publication 66: Human respiratory tract model for radiological protection. Oxford, Pergamon: Elsevier Science Ltd.
 - Kampa M., Castanas E., 2008. Human health effects of air pollution. *Environmental Pollution*, 151 (2), 362-367.
 - Karagulian F., Rossi M.J., 2005. The heterogeneous chemical kinetics of NO₃ on atmospheric mineral dust surrogates. *Physical Chemistry Chemical Physics*, 7 (17), 3150-3162.
 - Karagulian F., Rossi M.J., 2006. The heterogeneous decomposition of ozone on atmospheric mineral dust surrogates at ambient temperature. *International Journal of Chemical Kinetics*, 38 (6), 407-419.
 - Karagulian F., Santschi C., Rossi M.J., 2006. The heterogeneous chemical kinetics of N₂O₅ on CaCO₃ and other atmospheric mineral dust surrogates. *Atmospheric Chemistry and Physics*, 6, 1373-1388.
 - Karagulian F., Rossi M.J., 2007. Heterogeneous chemistry of the NO₃ free radical and N₂O₅ on decane flame soot at ambient temperature: reaction products and kinetics. *Journal of Physical Chemistry A*, 111 (10), 1914-1926.
 - Li N., Kim S., Wang M., Froines J., Sioutas C., Nel A., 2002. Use of a stratified oxidative stress model to study the biological effects of ambient concentrated and diesel exhaust particulate matter. *Inhalation Toxicology*, 14 (5), 459-486.

-
- Li N., Hao M., Phalen R.F., Hinds W.C., Nel A.E., 2003. Particulate air pollutants and asthma: a paradigm for the role of oxidative stress in PM-induced adverse health effects. *Clinical Immunology*, 109 (3), 250-265.
 - Li N., Nel A.E., 2006. Role of the Nrf2-mediated signaling pathway as a negative regulator of inflammation: implications for the impact of particulate pollutants on asthma. *Antioxidants & Redox Signaling*, 8 (1/2), 88-98.
 - Liochev S.I., Fridovich I., 1994. The role of $O_2^{\cdot-}$ in the production of HO^{\cdot} : in vitro and in vivo. *Free Radical Biology & Medicine*, 16 (1), 29-33.
 - Lippmann M., Ito K., 2000. Contributions that epidemiological studies can make to the search for a mechanistic basis for the health effects of ultrafine and larger particles. *Philosophical Transactions of the Royal Society A: Mathematical, Physical & Engineering Sciences*, 358 (1775), 2787-2797.
 - Lowry L.K., 1995. Role of biomarkers of exposure in the assessment of health risks. *Toxicology Letters*, 77 (1/3), 31-38.
 - Maynard A.D., Kuempel E.D., 2005. Airborne nanostructured particles and occupational health. *Journal of Nanoparticle Research*, 7 (6), 587-614.
 - NanoImpactNet, 2008. <http://www.nanoimpactnet.eu/>.
 - Nel A., 2005. Air-pollution related illness: effects of particles. *Science*, 308 (5723), 804-806.
 - Nel A., Xia T., Mädler L., Li N., 2006. Toxic potential of materials at the nanolevel. *Science*, 311 (5761), 622-627.
 - Oberdörster G., 2001. Pulmonary effects of inhaled ultrafine particles. *International Archives of Occupational and Environmental Health*, 74 (1), 1-8.
 - Oberdörster G., Oberdörster E., Oberdörster J., 2005. Nanotoxicology: an emerging discipline evolving from studies of ultrafine particles. *Environmental Health Perspectives*, 113 (7), 823-839.
 - Perret V., Huynh C.K., Droz P.-O., Vu Duc T., Guillemin M., 1999. Assessment of occupational exposure to diesel fumes - Parameter optimisation of the thermal coulometric measurement method for carbon. *Journal of Environmental Monitoring*, 1 (4), 367-372.
 - Pratte P., Rossi M.J., 2006. The heterogeneous kinetics of HOBr and HOCl on acidified sea salt and model aerosol at 40-90% relative humidity and ambient temperature. *Physical Chemistry Chemical Physics*, 8 (34), 3988-4001.

-
- Riediker M., Williams R., Devlin R., Griggs T., Bromberg P., 2003. Exposure to particulate matter, volatile organic compounds, and other air pollutants inside patrol cars. *Environmental Science & Technology*, 37 (10), 2084-2093.
 - Riediker M., Cascio W.E., Griggs T.R., Herbst M.C., Bromberg B.A., Neas L., Williams R.W., Devlin R.B., 2004. Particulate matter exposure in cars is associated with cardiovascular effects in healthy young men. *American Journal of Respiratory and Critical Care Medicine*, 169 (8), 934-940.
 - Risom L., Møller P., Loft S., 2005. Oxidative stress-induced DNA damage by particulate air pollution. *Mutation Research/Fundamental and Molecular Mechanisms of Mutagenesis*, 592 (1/2), 119-137.
 - Salgado M.S., Rossi M.J., 2002. Flame soot generated under controlled combustion conditions: heterogeneous reaction of NO₂ on hexane soot. *International Journal of Chemical Kinetics*, 34 (11), 620-631.
 - Salgado Muñoz M.S., Rossi M.J., 2002. Heterogeneous reactions of HNO₃ with flame soot generated under different combustion conditions: reaction mechanism and kinetics. *Physical Chemistry Chemical Physics*, 4 (20), 5110-5118.
 - Santschi C., Rossi M.J., 2006. Uptake of CO₂, SO₂, HNO₃ and HCl on calcite (CaCO₃) at 300 K: mechanism and the role of adsorbed water. *Journal of Physical Chemistry A*, 110 (21), 6789-6802.
 - Sauvain J.-J., Vu Duc T., Huynh C.K., 2001. Development of an analytical method for the simultaneous determination of 15 carcinogenic polycyclic aromatic hydrocarbons and polycyclic aromatic nitrogen heterocyclic compounds - Application to diesel particulates. *Fresenius' Journal of Analytical Chemistry*, 371 (7), 966-974.
 - Sauvain J.-J., Vu Duc T., Guillemin M., 2003. Exposure to carcinogenic polycyclic aromatic compounds and health risk assessment for diesel-exhaust exposed workers. *International Archives of Occupational and Environmental Health*, 76 (6), 443-455.
 - Sauvain J.-J., Vu Duc T., 2004. Approaches to identifying and quantifying polycyclic aromatic hydrocarbons of molecular weight 302 in diesel particulates. *Journal of Separation Science*, 27 (1/2), 78-88.
 - Sauvain J.-J., Deslarzes S., Riediker M., 2008. Nanoparticle reactivity toward dithiothreitol. *Nanotoxicology*, 2 (3), 121-129.
 - Schmid K., Riediker M., 2008. Use of nanoparticles in Swiss industry: a targeted survey. *Environmental Science & Technology*, 42 (7), 2253-2260.

-
- Shen H.-M., Shi C.-Y., Shen Y., Ong C.-N., 1996. Detection of elevated reactive oxygen species level in cultured rat hepatocytes treated with aflatoxin B₁. *Free Radical Biology & Medicine*, 21 (2), 139-146.
 - Stadler D., Rossi M.J., 2000. The reactivity of NO₂ and HONO on flame soot at ambient temperature: the influence of combustion conditions. *Physical Chemistry Chemical Physics*, 2 (23), 5420-5429.
 - Tao F., Gonzalez-Flecha B., Kobzik L., 2003. Reactive oxygen species in pulmonary inflammation by ambient particulates. *Free Radical Biology & Medicine*, 35 (4), 327-340.
 - U.S. National Aeronautics and Space Administration, 2007. Earth Fact Sheet. <http://nssdc.gsfc.nasa.gov/planetary/factsheet/earthfact.html>.
 - U.S. National Aeronautics and Space Administration. Fact Sheet “What are aerosols?”. <http://terra.nasa.gov/FactSheets/Aerosols/>. Website visited on October 6th, 2008.
 - Verdannet P., 2006. Evaluation in vitro de la réactivité de particules fines et ultrafines. Master thesis, Swiss Federal Institute of Technology (Lausanne, Switzerland) and Institute for Work and Health (Lausanne, Switzerland).
 - Wichmann H.-E., 2007. Diesel exhaust particles. *Inhalation Toxicology*, 19 (suppl. 1), 241-244.
 - Winterbourn C.C., 1993. Superoxide as an intracellular radical sink. *Free Radical Biology & Medicine*, 14 (1), 85-90.
 - Witschger O., Fabriès J.-F., 2005a. Particules ultra-fines et santé au travail - 1) Caractéristiques et effets potentiels sur la santé. INRS - Hygiène et Sécurité du Travail, Cahiers de notes documentaires, ND 2227, 199, 21-35.
 - Witschger O., Fabriès J.-F., 2005b. Particules ultra-fines et santé au travail - 2) Sources et caractérisation de l'exposition. INRS - Hygiène et Sécurité du Travail, Cahiers de notes documentaires, ND 2228, 199, 37-54.
 - Wu L.L., Chiou C.-C., Chang P.-Y., Wu J.T., 2004. Urinary 8-OHdG: a marker of oxidative stress to DNA and a risk factor for cancer, atherosclerosis and diabetics. *Clinica Chimica Acta*, 339 (1/2), 1-9.
 - Xiao G.G., Wang M., Li N., Loo J.A., Nel A.E., 2003. Use of proteomics to demonstrate a hierarchical oxidative stress response to Diesel exhaust particle chemicals in a macrophage cell line. *Journal of Biological Chemistry*, 278 (50), 50781-50790.
 - Zimmer A.T., 2002. The influence of metallurgy on the formation of welding aerosols. *Journal of Environmental Monitoring*, 4 (5), 628-632.

-
- Zimmer A.T., Maynard A.D., 2002. Investigation of the aerosols produced by a high-speed, hand-held grinder using various substrates. *Annals of Occupational Hygiene*, 46 (8), 663-672.

Chapter 2 - Design of the field campaign

2.1 Ethics Committee

Before the start of each scientific research project involving the participation of volunteers, it is necessary to obtain the agreement of an Ethics Committee. For that purpose, a complete file including a questionnaire intended for volunteers and a description of the project was submitted to the Ethics Committee of the Faculty of Biology and Medicine (University of Lausanne). The questionnaire (in French) is given in Annex. It was mainly prepared to collect information on possible confounding factors, which are known or suspected to play a role in oxidative stress (cigarette smoke, food habits, diseases, drug intake) and which may influence results obtained for biological effects. The Ethics Committee gave its agreement for this research project on October 7th 2005.

2.2 Sampling sites

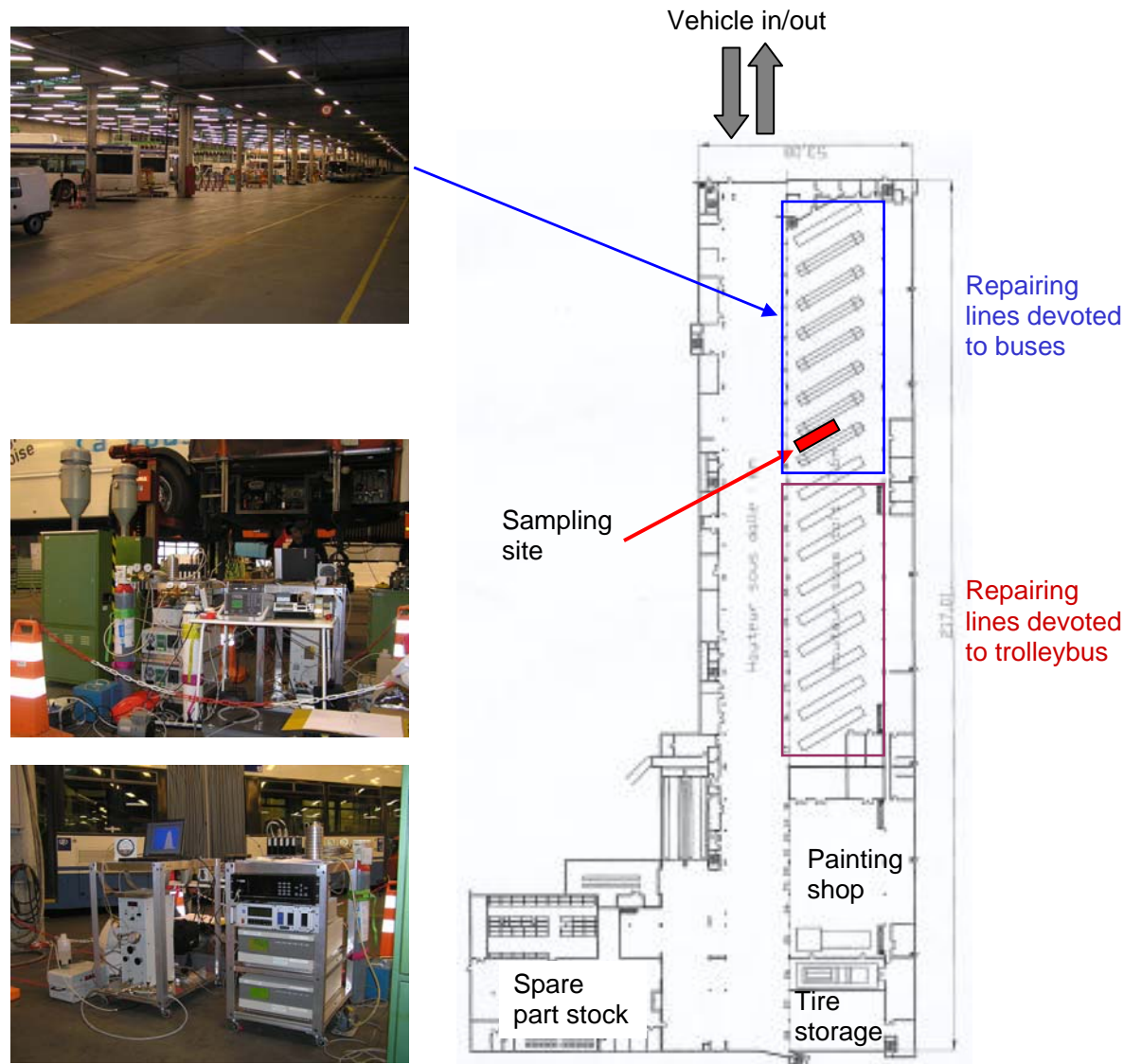
In order to have the best chances to measure significant biological effects due to an exposure to Diesel exhaust particles (DEP), we tried to select occupational situations where many Diesel engines were used, preferably in closed or underground areas. We decided to conduct the field campaign in bus depots, which were expected to correspond to occupational environments with high levels of DEP. We selected three bus depots, named hereafter “bus depot 1”, “bus depot 2” and “bus depot 3”, and samplings took place in mechanical yards, where buses were maintained and repaired. Moreover, in December 2006, we had the opportunity to survey a metro construction site, where rails were installed in a new metro line. Activities at this workplace were very different, especially through installation of rails, welding, and use of gasoline engines. These activities were expected to produce different types of particles compared to bus depots, and thus we thought it would be interesting to compare exposure parameters between the bus depots and the metro construction site. Each sampling site was surveyed during two consecutive days immediately after week-ends (Mondays and Tuesdays). Indeed, we supposed that after two days without exposure to DEP or other pollutants at the workplace, the oxidative stress status of workers would correspond to basic levels on Monday morning before starting work. This sample was thus considered as the reference for each volunteer. We also considered that a sampling over a two-day period was sufficient for this kind of study, since previous papers reported that biological markers

increased in urine samples already 12 hours after an exposure to pollutants (Suzuki *et al*, 1995). A description of the sampling sites is given in Table 2.1.

Table 2.1: List and description of the sampling sites surveyed during the field campaign.

Sampling sites	Date	Time	Description of the sampling sites
Bus depot 1	27/28.03.2006 daytime	07h00 – 16h00	Mechanical yard: repair and maintenance of buses and trolleybuses
Bus depot 2	22/23.05.2006 daytime	07h00 – 16h00	Mechanical yard: repair and maintenance of buses
Bus depot 2	22/23.05.2006 night time	18h00 – 02h00	Nearby a track used by all the buses and trams to join their respective parking place
Bus depot 3	06/07.06.2006 daytime	06h00 – 15h30	Mechanical yard: repair and maintenance of buses and trolleybuses
Bus depot 3	06/07.06.2006 night time	18h00 – 01h00	Maintenance yard: cleaning and fuel filling of buses and trolleybuses
Metro construction site	11/12.12.2006 daytime	10h30 – 18h00 (11.12) 07h00 – 17h00 (12.12)	Nearby the track where rails were installed
Bus depot 2	12/13.02.2007 daytime	07h00 – 16h00	Mechanical yard: repair and maintenance of buses

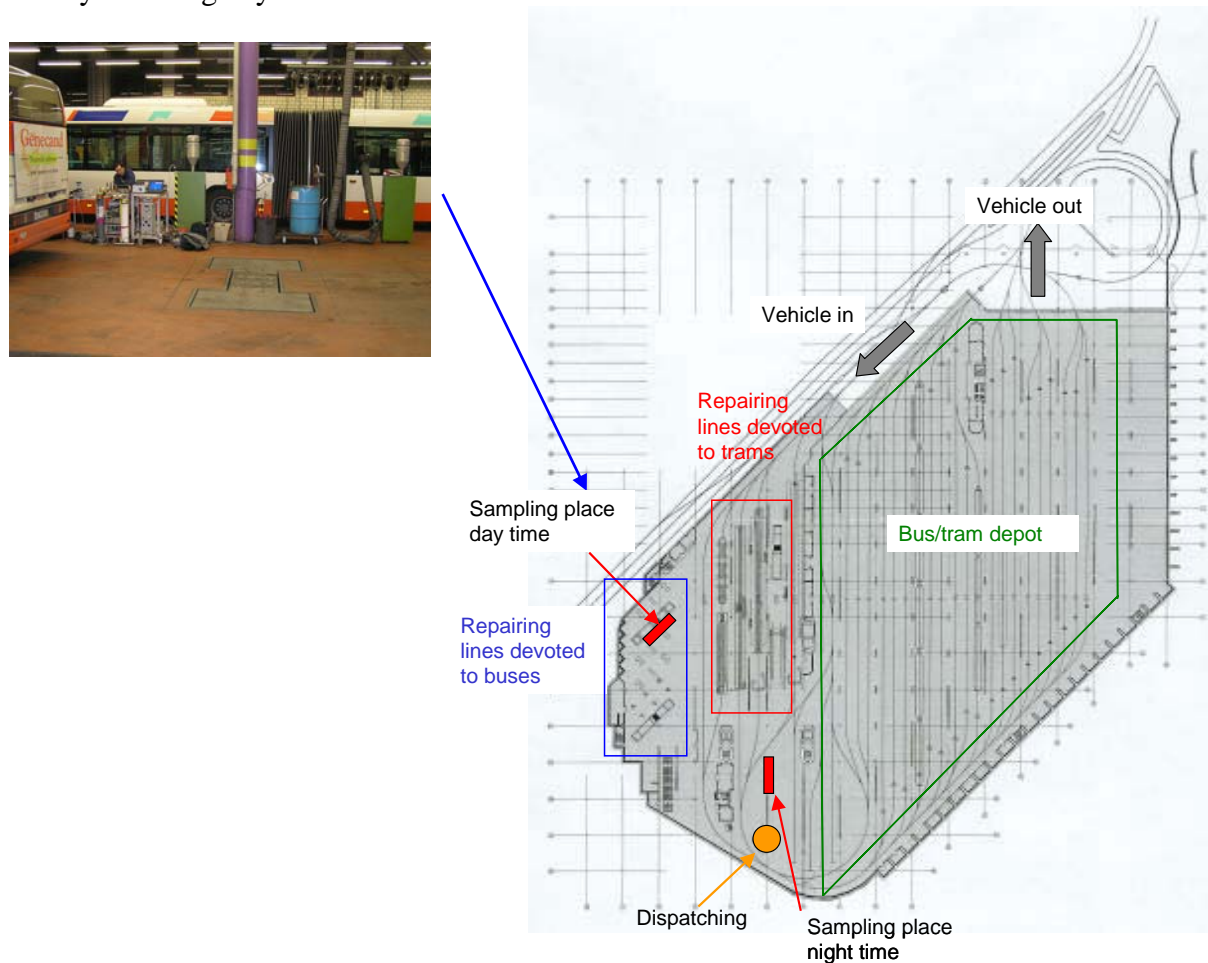
Bus depot 1 corresponds to a mechanical yard (hall of approximately 69'000 m³) devoted to engine repair, coach building and painting, vehicle maintenance. Figure 2.1 displays the drawing of this hall with the sampling site. The vehicle fleet to be repaired consisted of Diesel buses (mainly without particle filters), gas-powered buses and trolleybuses. Ventilation ducts were available to collect and to discard emissions from the exhaust pipe during motor testing outside the hall. We have observed that such equipment was used sometimes. This hall was also used as spare part depot, leading to entrance and exit of heavy duty lorries. Forklifts were in use in order to bring heavy spare parts or to displace trolleybuses for example. The exposure was assessed during two consecutive days, from March 27th to 28th 2006, from around 07h00 to 16h00.

Figure 2.1: Drawing and pictures of the sampling site in bus depot 1.

Bus depot 2 (Figure 2.2) corresponds to a mechanical yard (hall of approximately 140'000 m³) in direct connection to a bus and tram depot. Main activities during the day were engine reparation and vehicle maintenance. As for bus depot 1, a ventilation system was available for exhaust emission collection. The vehicles which circulated inside this hall consisted mainly of Diesel buses (60% of them equipped with particle filters) and trams. The exposure was assessed from around 07h00 to 16h00 during two consecutive days in summer (May 22nd and 23rd, 2006) and in winter (February 12th and 13th, 2007) at the same sampling sites. In order to assess the exposure of night workers, the sampling equipment was displaced to another site in the same bus depot (see Figure 2.2) at the end of the afternoon. Night activities in this hall were mainly devoted to dispatching entering vehicles to their parking place in the depot. Workers were mainly located around this place. The sampling was undertaken in the night of

May 22nd and 23rd 2006, from about 18h00 to 02h00, but we did not survey this site anymore when we came back to this bus depot in February 2007. The activities of the workers were mainly related to the maintenance of trams/vehicles: control and occasionally filling the emergency brake system, washing vehicles (observed only during May 22nd night time). The sampling site during night time was influenced by stop and go emissions from bus/trams near the dispatching place.

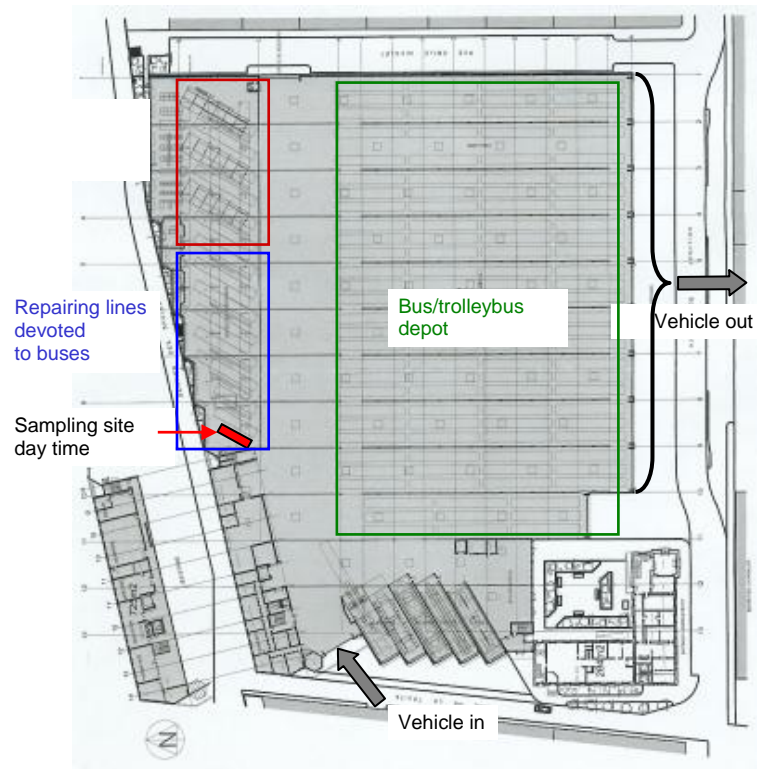
Figure 2.2: Plan of the sampling sites in bus depot 2, and picture of the sampling site surveyed during daytime.



Bus depot 3 was surveyed during daytime on June 6th and 7th 2006 from 06h00 to 15h30. It was similar to bus depot 2, corresponding to a mechanical yard mixed with a bus depot, but the hall was smaller (estimated to approximately 100'000 m³). The vehicle fleet was composed of trolleybuses and Diesel buses. As for bus depot 1, trolleybuses used their gasoline emergency engine in order to reach the repairing places in the mechanical yard. The sampling site was located near bus repairing lines (see Figure 2.3), and was influenced by the

displacement of buses/trolleybuses, motor testing after reparation, oil change, air filters replacements. As for bus depot 1, ventilation system for collecting exhaust emissions was available. At the end of the afternoon, the sampling equipment was displaced to a maintenance yard, where workers were present only during night shifts. Particle sampling in this maintenance yard was undertaken on June 6th and 7th 2006 from about 18h00 to 01h00. At the end of their service time, and before going to their depot place, buses and trolleybuses had to be controlled for maintenance, and eventually to be directed toward the mechanical yard for reparation if technical problems were encountered during the service. Thus, the activities of workers in this site were mainly washing and refilling buses with Diesel fuel. For trolleybuses, graphite contacts allowing electricity flow between aerial electrical lines and vehicles were controlled and changed when necessary also in this site.

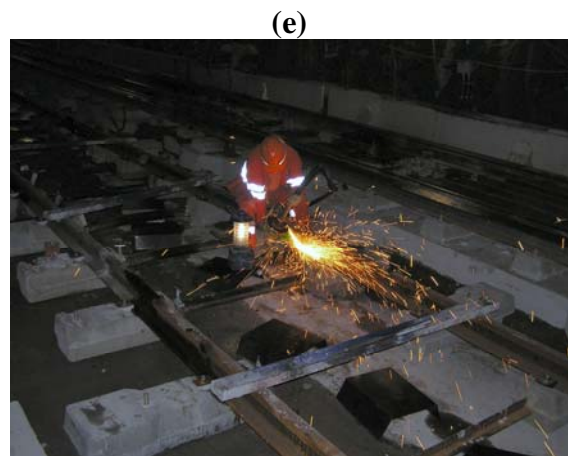
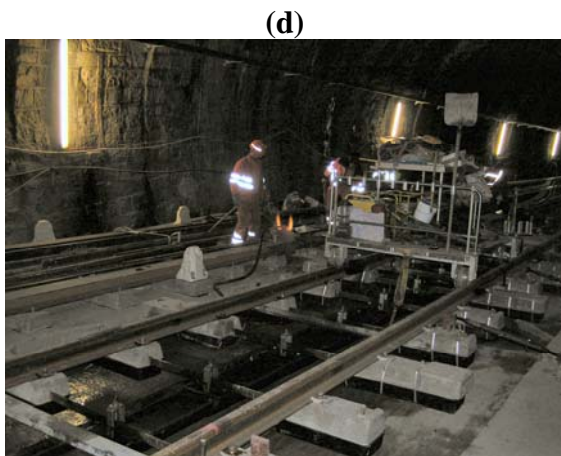
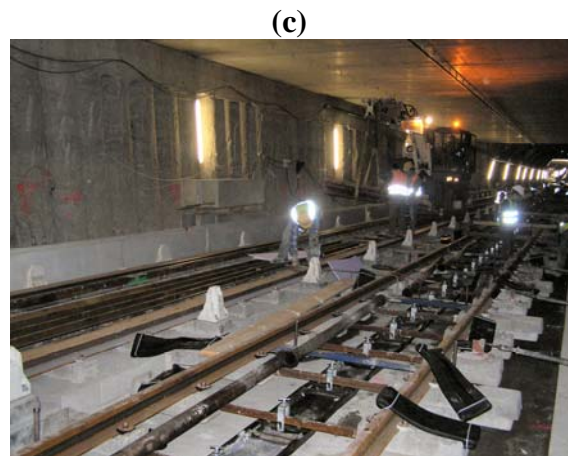
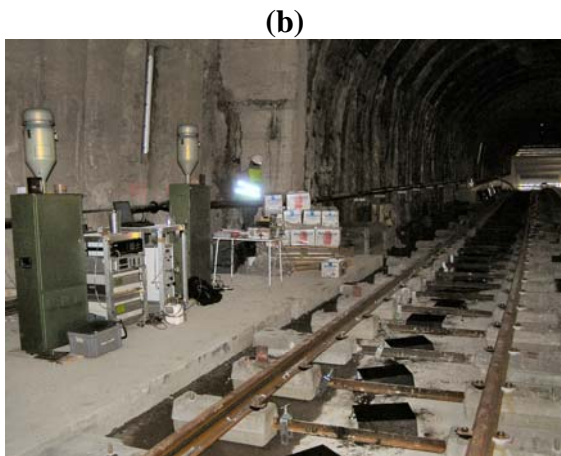
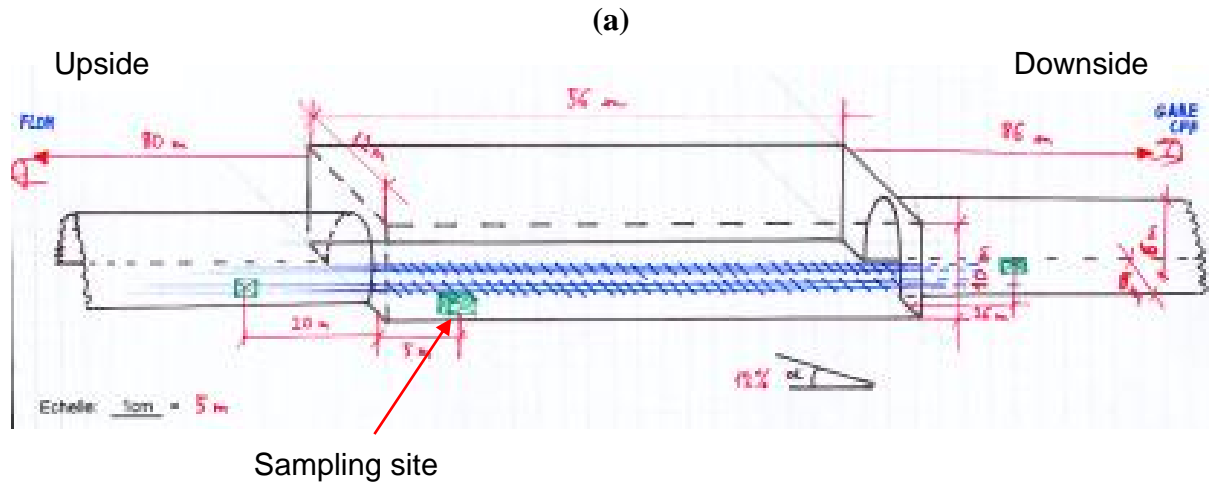
Figure 2.3: Plan of the sampling site surveyed in bus depot 3 during daytime.



The metro construction site is described in Figure 2.4. The main activities were installation of rails for a metro underground system. The main activities related to particle emission were boring concrete, welding, screwing the rails with gasoline screwers, grinding down metallic parts, displacement of a crane and some heavy duty vehicle. The bored tube had a natural slope estimated at 12%. A relatively high natural air flow (0.8 ± 0.2 m/s) was present during the sampling, flowing from bottom to the top of the slope. The sampling site was thus mainly affected by the downstream activities. The exposure was assessed during two consecutive

days, from 10h30 to 18h00 on December 11th 2007, and from 07h00 to 17h00 on December 12th 2007.

Figure 2.4: Drawing (a) and pictures ((b) and (c)) of the metro construction site. Examples of activities in this sampling site: welding of the rails (d), and grinding down of the rails (e).



2.3 Population under study

A total of 40 volunteers participated in the study. Two scientists involved in the present research project were also included as volunteers. One of them volunteered at each sampling site, and was surveyed five times. All the volunteers had to fill in the above-mentioned questionnaire (see Paragraph 2.1, “Ethics Committee”) in order to assess possible confounding factors which may influence results obtained on biological effects. One of the volunteers (worker “M8”) did not fill in the questionnaire, and therefore his smoking status and personal information is unknown. We decided to include him in results obtained for the total population, but we did not take him into account when workers were classified into their respective smoking status (smokers, non-smokers or former smokers). Due to the low number of participants, no exclusion factor was established. All the workers who accepted to participate in the research project were taken into account. Table 2.2 gathers the list of volunteers with sampling sites, dates and personal information.

Table 2.2: Complete list of volunteers with sampling sites, dates and personal information.

Worker	Workplace	Date	Status	Age	Height [m]	Weight [kg]	BMI	Miscellaneous
L 01	Bus depot 1	27/28.03.2006 day	smoker	58	1.82	63	19.0	Respiratory disease, drug and vitamin intake.
L 02	Bus depot 1	27/28.03.2006 day	non-smoker	49	1.84	84	24.8	
L 03	Bus depot 1	27/28.03.2006 day	former smoker	36	1.79	89	27.8	Rheumatism, exposed to engine exhaust during week-end.
L 04	Bus depot 1	27/28.03.2006 day	former smoker	52	1.82	74	22.3	
L 05	Bus depot 1	27/28.03.2006 day	non-smoker	34	1.77	70	22.3	Respiratory disease
L 06	Bus depot 1	27/28.03.2006 day	former smoker	34	1.88	103	29.1	
L 07	Bus depot 1	27/28.03.2006 day	non-smoker	45	1.98	85	21.7	Exposed to gasoline engine exhaust during week-end
G 01 EU	Bus depot 2	22/23.05.2006 day	non-smoker	45	1.85	84	24.5	Rheumatism, respiratory disease.
G 02 EU	Bus depot 2	22/23.05.2006 day	smoker	29	1.70	57	19.7	
G 03 EU	Bus depot 2	22/23.05.2006 day	smoker	51	1.80	92	28.4	Rheumatism, cardiovascular disease, drug intake.
G 04 EU	Bus depot 2	22/23.05.2006 day	non-smoker	25	1.82	78	23.5	Vitamin intake
G 05 EU	Bus depot 2	22/23.05.2006 day	non-smoker	45	1.98	85	21.7	
G 06 EU	Bus depot 2	22/23.05.2006 night	non-smoker	40	1.71	81	27.7	Exposed to barbecue fumes on Day 2 at noon
G 07 EU	Bus depot 2	22/23.05.2006 night	smoker	35	1.70	90	31.1	
G 08 EU	Bus depot 2	22/23.05.2006 night	former smoker	57	1.68	72	25.5	Cardiovascular disease
G 09 EU	Bus depot 2	22/23.05.2006 night	former smoker	55	1.82	74	22.3	Rheumatism, respiratory disease, exposed to dust during week-end.
G 10 EU	Bus depot 2	22/23.05.2006 night	former smoker	39	1.83	106	31.7	Rheumatism, exposed to barbecue fumes during week-end.
G 11 EU	Bus depot 2	22/23.05.2006 night	smoker	46	1.78	84	26.5	
G 12 EU	Bus depot 3	06/07.06.2006 day	non-smoker	44	1.84	93	27.5	
G 13 EU	Bus depot 3	06/07.06.2006 day	former smoker	54	1.65	70	25.7	Rheumatism, drug and vitamin intake.
G 14 EU	Bus depot 3	06/07.06.2006 day	smoker	45	1.75	70	22.9	Respiratory disease, drug and vitamin intake, exposed to barbecue fumes during week-end.
G 15 EU	Bus depot 3	06/07.06.2006 day	non-smoker	45	1.98	85	21.7	
G 16 EU	Bus depot 3	06/07.06.2006 night	former smoker	46	1.73	87	29.1	Respiratory disease, drug intake
G 17 EU	Bus depot 3	06/07.06.2006 night	smoker	N/A	1.80	72.5	22.4	Respiratory disease, worked during week-end.
M1	Metro construction site	11/12.12.2006 day	non-smoker	25	1.86	90	26.0	Drug intake
M2	Metro construction site	11/12.12.2006 day	smoker	49	1.78	80	25.2	Respiratory disease, drug intake, exposed to engine exhaust during week-end.
M3	Metro construction site	11/12.12.2006 day	smoker	34	1.83	93	27.8	
M4	Metro construction site	11/12.12.2006 day	non-smoker	27	1.77	84	26.8	Respiratory disease, exposed to engine exhaust and welding fumes during week-end.
M5	Metro construction site	11/12.12.2006 day	smoker	34	1.80	90	27.8	Respiratory disease, exposed to dust during week-end.
M6	Metro construction site	11/12.12.2006 day	smoker	26	1.81	88	26.9	
M7	Metro construction site	11/12.12.2006 day	non-smoker	45	1.98	85	21.7	
M8	Metro construction site	11/12.12.2006 day	N/A	N/A	N/A	N/A	N/A	
G 02 HU	Bus depot 2	12/13.02.2007 day	smoker	30	1.70	57	19.7	
G 03 HU	Bus depot 2	12/13.02.2007 day	smoker	52	1.80	92	28.4	Rheumatism, cardiovascular disease, drug intake.
G 04 HU	Bus depot 2	12/13.02.2007 day	non-smoker	26	1.82	78	23.5	Vitamin intake
G 05 HU	Bus depot 2	12/13.02.2007 day	non-smoker	46	1.98	85	21.7	
G 06 HU	Bus depot 2	12/13.02.2007 day	non-smoker	41	1.71	81	27.7	
G 08 HU	Bus depot 2	12/13.02.2007 day	former smoker	58	1.68	72	25.5	Cardiovascular disease
G 10 HU	Bus depot 2	12/13.02.2007 day	former smoker	40	1.83	106	31.7	Rheumatism
G 18 HU	Bus depot 2	12/13.02.2007 day	non-smoker	33	1.65	79	29.0	Drug intake

N/A: not available.

No differences could be observed between the different sites for age and body mass index (BMI) (ANOVA with Bonferonni post hoc test). No differences were observed between smokers, former smokers and non-smokers, for age and BMI, as presented in Table 2.3.

Table 2.3: Characteristics of the studied population.

Variables	All subjects	Non-smokers	Former smokers	Smokers
Gender				
Male	40 ^a	16	10	13
Female	0	0	0	0
Age, year (mean \pm SD)	41.1 \pm 10.3	38.4 \pm 8.6	47.1 \pm 9.2	39.8 \pm 11.8
BMI, kg/m² (mean \pm SD)	25.3 \pm 3.4	24.5 \pm 2.6	27.1 \pm 3.4	25.1 \pm 3.9
Alcohol consumption				
Never	9	5	3	1
Less than 1 glass/day	28	11	7	10
1-3 glass(es)/day	2	0	0	2
More than 3 glasses/day	0	0	0	0
Meat consumption				
Never	0	0	0	0
1-3 time(s)/week	23	10	6	7
Once/2 meals	15	6	4	5
At every meal	1	0	0	1
Fruit consumption				
Never	3	0	1	2
Less than 1 fruit/day	12	7	0	5
1-2 fruit(s)/day	19	9	4	6
More than 2 fruits/day	5	0	5	0
Drug intake				
Yes	9	2	2	5
No	30	14	8	8
Vitamin intake				
Yes	5	2	1	2
No	34	14	9	11
Sport (hours/week \pm SD)	2.3 \pm 1.7	1.8 \pm 1.5	2.1 \pm 1.2	3.3 \pm 2.0
Heart diseases				
Yes	4	0	2	2
No	35	16	8	11
Pulmonary diseases				
Yes	10	3	2	5
No	29	13	8	8
Kidney failure				
Yes	0	0	0	0
No	39	16	10	13
Articulation problems				
Yes	9	2	5	2
No	30	14	5	11
Years of employment (mean \pm SD)	10.0 \pm 9.2	6.5 \pm 8.8	16.3 \pm 6.4	9.5 \pm 9.5

^a One volunteer (worker “M8”) did not fill the questionnaire, and therefore his personal information is unknown. SD: standard deviation.

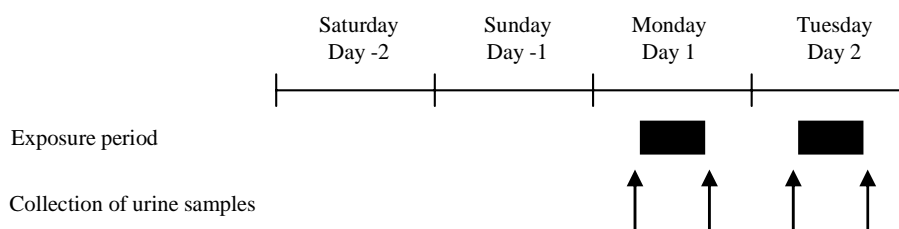
Except for workers at the metro construction site, for which employment in the company lasted less than 2 years in average, volunteers enrolled in this study have worked as mechanical technicians in the same company during an average of 12 years. Smokers

corresponded to people smoking on average 20 cigarettes per day. Former smokers reported to have stopped smoking for a minimum of 2 years (average of 12 years).

2.4 Biological fluids sampling

As mentioned before, a sampling over a two-day period was undertaken in each bus depot. Spot urine samples were collected before and after the shift on Monday and Tuesday. Urine samples of Monday morning before the shift were considered as control due to the fact that volunteers were not working during the week-end, and those of Tuesday evening at the end of shift corresponded to a two-day exposure. Figure 2.5 shows the timeline of interventions during a sampling campaign.

Figure 2.5: Timeline of interventions during a sampling campaign.



A plastic bottle was given to each volunteer on Friday before the sampling campaign, and all workers were asked to collect a specimen on Monday morning before going to work. On Monday morning, upon installing the personal pumps, we collected the urine samples. Before Monday evening at the end of the shift, we gave to each volunteer two plastic bottles, the first one to collect the Monday end of the shift urine, and the second one to collect the Tuesday morning before the shift urine. Finally, we gave them another plastic bottle on Tuesday for the last urine collection at the end of shift. Each urine sample was stored in a cold box (4°C) at the workplace. At the end of the sampling day, each urine sample was mixed, separated into 20 aliquots of 4 ml, and stored at -25°C until analysis. Each biological parameter was determined in one of these aliquots. The collection of before shift urine for volunteers of the metro construction site was not complete and was more difficult to achieve.

2.5 Measurements and analysis

During the field campaign in the bus depots, several parameters were measured using stationary and personal samplings, in order to assess the exposure of workers to particulate matter and other pollutants. After the survey of each sampling site, particles collected on suitable filters were analyzed at the Swiss Federal Institute of Technology using a Knudsen

flow reactor, in order to quantify functional groups on the particle surface. Urine samples of workers were used to quantify oxidative stress biomarkers at the Institute for Work and Health. Finally, correlations between exposure parameters measured at the workplace and the evolution of the oxidative stress status of volunteers over a two-day period of shift were studied.

2.6 Reference

- Suzuki J., Inoue Y., Suzuki S., 1995. Changes in the urinary excretion level of 8-hydroxyguanine by exposure to reactive oxygen-generating substances. *Free Radical Biology & Medicine*, 18 (3), 431-436.

Chapter 3 - Exposure parameters

3.1 Introduction

Epidemiological studies have demonstrated that exposure to particulate matter (PM) is associated with adverse health effects, such as cancer (Steenland *et al*, 1998), cardiovascular (Peters *et al*, 2001) and respiratory (Delfino, 2002) diseases. Due to the toxicity of particulate matter, many studies have been undertaken to assess exposure to particles in various environments (urban areas, workplaces). Emphasis has been placed onto occupational situations, because several workplaces contain important sources of particles, leading to acute health hazards for exposed workers. The most frequently studied workplaces are closed or underground areas, where vehicles or Diesel engines are in use, such as garages, tunnels or construction sites. Table 3.1 gathers selected studies where exposure to particulate matter in several workplaces was assessed. We notice that people working in mining (Dahmann *et al*, 2007) and tunnel construction (Bakke *et al*, 2001) are exposed to very high levels of particles, at least ten times higher than other closed or underground areas.

Table 3.1: Selected studies where occupational exposure to Diesel exhaust particles (DEPs) and other fine particulate matters was assessed.

Working environment	Sampling type	Parameter	n	Mean (\pm SD) [$\mu\text{g}/\text{m}^3$]	Authors
Potash mining	Personal	Respirable dust	557	1570 (\pm 1520)	Dahmann <i>et al</i> , 2007
Heavy and highway construction	Personal	Respirable dust	261	Range 104 - 803	Woskie <i>et al</i> , 2002
Heavy and highway construction	Personal	Elemental carbon	261	Range 5 - 31	
Heavy and highway construction	Personal	Organic carbon	261	Range 30 - 91	
Tunnel construction	Personal	Respirable dust	151	1200 (\pm 2400)	Bakke <i>et al</i> , 2001
Tunnel construction	Personal	Elemental carbon	8	160 (\pm 2.2)	
Tunnel construction	Personal	PM _{2.5}	6	231 (\pm 2)	
Tunnel construction	Personal	Elemental carbon	6	87 (\pm 3)	Lewné <i>et al</i> , 2007
Garage (Diesel)	Personal	PM _{2.5}	20	42 (\pm 3)	
Garage (Diesel)	Personal	Elemental carbon	20	11 (\pm 3)	
Bus garage/repair	Personal	Respirable dust	41	267	Groves and Cain, 2000
Bus garage/repair	Personal	Elemental carbon	53	39	
Bus garage/repair	Personal	Organic carbon	53	109	
Bus depot	Stationary	PM ₄	2	40 (\pm 20)	Sauvain <i>et al</i> , 2003
Bus depot	Stationary	Elemental carbon	2	5 (\pm 1)	
Bus depot	Stationary	Organic carbon	2	13 (\pm 1)	
Bus repair garage	Personal	Elemental carbon	50	14 (\pm 3)	Seshagiri and Burton, 2003
Depots with Diesel fork lift trucks	Stationary	Respirable dust	76	Range <80 - 179	Wheatley and Sadhra, 2004
Depots with Diesel fork lift trucks	Stationary	Elemental carbon	79	Range 7 - 55	
Depots with Diesel fork lift trucks	Stationary	Organic carbon	79	Range 11 - 69	
Bus garage	Stationary	Elemental carbon	35	4 (\pm 1)	Ramachandran <i>et al</i> , 2005
Trucking company	Personal	PM _{2.5}	32	48 (\pm 24)	Lee <i>et al</i> , 2005
Trucking company	Personal	Elemental carbon	32	3 (\pm 4)	
Trucking company	Personal	Organic carbon	32	29 (\pm 21)	
Highway Patrol troopers	Personal	PM _{2.5}	10	23 (\pm 11)	Riediker <i>et al</i> , 2003
Taxi drivers	Personal	PM ₁₀	39	26 (\pm 17)	Lewné <i>et al</i> , 2006
Bus drivers	Personal	PM ₁₀	42	44 (\pm 25)	
Lorry drivers	Personal	PM ₁₀	40	57 (\pm 26)	

SD: standard deviation.

In such studies, several parameters are usually monitored, such as the particle concentration within a selected range of diameter (usually PM_{2.5} or PM₁₀, particulate matter with aerodynamic diameter smaller than 2.5 and 10 µm, respectively), the particle size distribution, and complementary information about some specific pollutants, such as metals or polycyclic aromatic hydrocarbons (PAHs). Each of these parameters may provide information on the particle toxicity and on health hazards in the case of exposure.

The monitoring of PM_{2.5} or PM₁₀ takes into account all the sources of particles at the workplace. As already mentioned in Chapter 1, the difference of the aerodynamic diameter between PM_{2.5} and PM₁₀ has an important incidence on health due to different behaviors during inhalation into the lung. Indeed, small particles have a high probability to penetrate deeply into the lungs and to reach alveolar regions, while coarse particles (PM_{10-2.5}) usually deposit in the naso-pharyngeal region (Maynard and Kuempel, 2005). Several studies pointed out increased health hazards in the smaller particle size fraction. For instance, it has been shown that the PM_{2.5} or smaller size fractions exerted higher induction of oxidative DNA damage than the coarse fraction (Hsiao *et al*, 2000; Buschini *et al*, 2001; Healey *et al*, 2005). Therefore, the monitoring of the particle size distribution is also of prime importance to assess health hazards.

The overall composition of particles is also one of the fundamental topics in the field of environmental chemistry. Great efforts have been spent on the investigation of the particulate carbonaceous fraction, since this element accounts for up to 50% of the particle mass concentration (Park *et al*, 2001). The total carbon (TC) content includes elemental (EC) and organic (OC) carbon. EC is predominantly a primary pollutant emitted directly during incomplete combustion of fossil and carbonaceous fuels, and is usually used as a surrogate of Diesel exhaust particles (DEPs). Indeed, approximately 75% of typical DEP are constituted of EC, depending on engine conditions (U.S. Environmental Protection Agency, 2002). OC has both primary and secondary origins. Primary OC is mainly formed during combustion processes, while secondary OC is formed in the atmosphere via gas-to-particle conversion processes of volatile organic compounds (VOCs). Carbonaceous fraction of particulate matter gathers hundreds of compounds, including alkanes, alkenes, aromatics, PAHs, oxygenated compounds (including aldehydes, ketones and carboxylic acids), amino compounds, and nitrates (Schlesinger *et al*, 2006). Among these compounds, PAHs have been widely studied, because they exhibit a wide range of toxic effects, and some of them are carcinogenic

(Flowers *et al*, 2002). In addition to the carbonaceous fraction, the measurement of the particulate metal content has also been the subject of many studies, since the toxicity of metals has been clearly demonstrated (Costa and Dreher, 1997; Knaapen *et al*, 2002; Okeson *et al*, 2003).

Within the framework of the present study, we intended to focus on the respirable fraction of particulate matter. Even if many authors use PM_{2.5} as the respirable fraction, we decided to follow the European norm EN 481, which is the legal reference for occupational situations and considers PM₄ as the respirable fraction (European Standard EN 481, 1993). It should be stressed that the Swiss law requires Diesel particle filters (DPFs) for Diesel engines in underground areas (Suva, 2003). As already mentioned in Chapter 1, the particle mass concentration, expressed in $\mu\text{g}/\text{m}^3$, has always to be measured in this kind of field campaign, because all the regulations and the occupational exposure limits (OELs) concerning particulate matter have been defined using this metric. However, from a toxicological point of view, the measurement of the particle surface concentration, expressed in $\mu\text{m}^2/\text{cm}^3$, seems also relevant for health. Since a definitive consensus has not been proposed so far for the use of the correct metric, we decided to measure the particle concentration using three metrics (number, surface area and mass).

We also wanted to take into account the presence of gaseous pollutants which are known or suspected to play a role in oxidative stress: nitrogen oxides (NO_x) and ozone (O₃). NO_x, which is the sum of nitrogen monoxide (NO) and nitrogen dioxide (NO₂), is emitted from motor vehicles, and is among the most prominent air pollutants. Due to its higher toxicity, NO₂ is very often monitored in occupational situations where motor vehicles are used. It is interesting to notice that NO has contradictory effects in physiology. On one hand, NO is an endogenous messenger involved in numerous physiological processes, such as regulation of cardiovascular function, memory formation, defense mechanism against oxidative stress (Miranda *et al*, 2000). Therefore, appropriate levels of NO are important in normal physiology. But on the other hand, exposure to sustained levels of NO has been implicated in adverse health effects, such as cancer or stroke (Pacher *et al*, 2007). Moreover, high concentrations of NO may also induce the formation of reactive compounds, which initiate oxidative stress (Beckman *et al*, 1990). Due to high levels of NO_x expected in the bus depots and the role of these compounds in oxidative stress, we thought it was important to monitor NO_x concentrations during the field campaign. O₃ is a major component of air pollution,

mainly formed by photochemical reactions of nitrogen oxides with VOCs or carbon monoxide. Previous studies have shown an association between exposure to O₃ and oxidative stress (Servais *et al*, 2005; Foucaud *et al*, 2006). This pollutant is a strong oxidant exerting its biological action either by direct reaction with target molecules, or by generating reactive oxygen species (ROS) which result in its biological effects and its toxicity. Due to its role in oxidative stress, it was important to monitor this pollutant in the bus depots.

The aim of the present chapter is to describe measurements of several exposure parameters and particle sampling methodologies conducted in the bus depots.

3.2 Material and methods

The most accurate method to assess the exposure of workers to pollutants at the workplace is to use measurement equipment worn by each worker during the whole period of shift. Such sampling methods were technically impossible within the framework of this study. Therefore, we measured all the exposure parameters using stationary samplings by installing the equipment as near as possible to the workers. Only three parameters (PM₄, OC and EC) were measured using both stationary and personal samplings, in order to check whether results obtained with stationary equipment were representative of the real exposure of each worker.

3.2.1 *Stationary sampling*

PM₄. We used different sampling systems to collect PM₄. First, we used several stationary pumps (MSA Company, model Escort Elf Pump; SKC Inc., models 224-XR and Leland Legacy) connected to a sampling head equipped with cyclones (Casella or Dorr-Olivier). Air flow was set at 2 l/min for MSA Escort Elf and SKC 224-XR pumps, and at 10 l/min for SKC Leland Legacy pump. At least duplicate sampling was achieved at all workplaces. The air flow was controlled at least at the beginning and at the end of the sampling using a flow meter (BIOS International Corp., model DryCal DC-Lite). When flow differed of more than 5%, sampling was considered as doubtful. Plasma pre-treated quartz filters (Whatmann QM-A) were used. These filters were conditioned at least 24 hours at constant humidity (60±10%) and ambient temperature before weighing. After sampling, the filters were conditioned again in the same glove box and weighed. These filters were used to determine the PM₄ concentration in the air, and the OC and EC content of the sampled particles (see below). The mean PM₄ concentration was calculated by dividing the particle mass deposited on the filter by the total volume of air which passed through the filter during the whole period of sampling

(approximately eight hours, during the period of shift). This method implies that all the particles contained in this volume of air are retained by the filter with an efficiency of 100%, which is actually not the case.

Moreover, we used two high volume samplers (Digitel, model DH 77) with sampling head of impactor type allowing PM₄ sampling. The air flow was set at 580 l/min, and controlled at least twice during the sampling day. Both high volume samplers were equipped with quartz filters (Whatman; QM-A, 20x23 cm sheets, 1851865) of 15 cm diameter beforehand silanized with dichlorodimethylsilane. At the end of the sampling, the filters of 15 cm diameter were cut into five smaller filters of 4.7 cm diameter, and immediately put into a desiccator filled with argon. These filters of 4.7 cm diameter were used for surface probing (see Chapter 4), and one of the pierced filters of 15 cm diameter was used for the determination of particulate metal content (see below). The complete procedure for the preparation of the silanized quartz filters and the PM₄ sampling using the high-volume samplers will be presented in detail and discussed in Chapter 4.

OC and EC. The determination of OC and EC content of the particles was achieved by coulometric analysis (Strohlein Instruments, model 702) of the quartz filters used for PM₄ sampling, according to a method accredited by the Swiss Federal Office of Metrology (METAS). The measurement consists of a two-stage analysis. In the first stage, the quartz filter is heated to 800°C under a stream of nitrogen. Organics adsorbed on the particles are vaporized and catalytically converted to CO₂, which is then adsorbed into barium perchlorate. A pH change of the electrolytic cell takes place, and the current needed to maintain the pH is recorded. The current result is converted into the mass of carbon in the vaporized organic substances, and refers to OC. Particles remaining after the first stage are heated again to 800°C, but this time under oxygen. Under these conditions, the remaining carbon is oxidized to CO₂, and quantified again in the coulometer. This addresses the EC content. Finally, results obtained for OC and EC were corrected by subtraction of a blank filter, and the mean concentration of OC and EC was calculated by dividing the mass of carbon (OC or EC) by the total volume of air which passed through the filter during the period of sampling. As for the PM₄ concentration, this method implies that all the particles are retained by the filter.

Particulate metal content. Iron (Fe), copper (Cu) and manganese (Mn) were determined on the collected PM₄ (high volume sampling system). The determination was done following a

METAS-accredited method. The filter was digested in fluoridric acid, followed with a treatment in aqua reggia ($\frac{2}{3}$ HCl + $\frac{1}{3}$ HNO₃). After dilution in water, the metal content of the digested solution was analyzed using an atomic absorption spectrometer (Perkin Elmer, model HGA 700). Results obtained for each sample were corrected by subtraction of a blank filter, and the mean concentration of particulate metal concentration was calculated by dividing the mass of metal (Fe, Cu or Mn) by the total volume of air which passed through the filter during the period of sampling.

Particle size distribution. A scanning mobility particle sizer (SMPS; TSI Inc., model 3934) was used to monitor the particle size distribution. It consisted of a differential mobility analyzer (DMA; TSI Inc, model 3071) coupled to a condensation particle counter (CPC; TSI Inc, model 3022). The apparatus used a bipolar charger in the DMA to charge particles to a known charge distribution. Particles were then sorted according to their size by crossing an electrical field in the DMA, and they were finally counted by the CPC. The aerosol sampling flow was set at 0.3 l/min, and the sheath flow at 3 l/min. An impactor of 0.0508 cm diameter was installed at the inlet of the SMPS in order to remove particles larger than 1 μ m. Data were collected using Aerosol Instrument Manager Software for SMPS (TSI Inc; release version 8.1.0.0, 2007). The software was set to measure particle size distribution in the range 15 to 750 nm, with a scanning time of 150 seconds. One scan was recorded every 3 minutes during eight hours of shift. The “multiple charge correction” option was activated to enable a mathematical correction for particles whose mobility was affected due to multiple charges. The “diffusion loss correction” option was not available for our SMPS model. Therefore, we used results obtained by Reineking and Porstendörfer (1986), who determined diffusion losses for the same SMPS model, and we corrected manually our particle size distributions on Microsoft Office Excel 2003 to take into account diffusion losses. A third important correction usually used with SMPS measurements concerns the mobility of nanoparticle aggregates (Lall and Friedlander, 2006; Lall *et al*, 2006). The “nanoparticle aggregate mobility analysis” module was not available on our version of the software, and therefore we did not take into account this correction. Particle size distribution recorded by the software was then used to calculate the total number, mass and surface area of particles comprised in the range 15 to 750 nm. For the determination of particle mass, the density was set at 1.8 g/cm³. For the calculation of the particle surface area, the software considers each particle as a sphere, and uses the formula for the surface of a sphere ($S = 4 \cdot \pi \cdot r^2$). The SMPS was regularly

calibrated by atomization of solutions containing latex polymers (Duke Scientific Corp) of known size (80 and 300 nm).

In addition to the SMPS, a diffusion charging (DC) particle sensor (Matter Engineering AG, model LQ1-DC) was also used to monitor the particle surface area. This apparatus measures the total active surface area of particles, which is the total surface area available to be involved in interactions with surrounding ions. Ions are produced by a corona discharge, and attach themselves to the surface of the particles. The charged aerosol particles are then collected on an electrically insulated filter. The electric charge is finally converted to a DC voltage signal in an electrometer amplifier. The instrument was calibrated by Matter Engineering AG before each use in the field.

Particle mass distribution. The mass size distribution was determined using an Andersen type cascade impactor (Andersen Inc.; model 2000, nine stages) connected to a pump set at 28 l/min. Nine size ranges could be determined: >11 μm ; 7-11 μm ; 4.7-7 μm ; 3.3-4.7 μm ; 2.1-3.3 μm ; 1.1-2.1 μm ; 0.7-1.1 μm ; 0.4-0.7 μm ; <0.4 μm . The sampling flow was controlled at least twice during sampling. Particles were collected on glass microfiber filters (Whatman 934 AH; Maidstone, GB). These nine filters were conditioned and weighed as described for PM₄ sampling. Then, an “in house” DOS-based software written in Qbasic was used to smooth the particle mass distribution obtained from the nine size bins.

NO_x concentrations. A direct reading instrument (Monitor Labs Inc, model ML 9841A) was used to monitor NO_x concentrations at the workplaces. The principle of use of the NO_x analyzer is based on the chemiluminescence of NO₂. NO is first determined following Reactions 3.1 and 3.2:



The amount of emitted photons is proportional to the NO concentration in the air, and is measured using a photomultiplier, which transforms light flux into an electrical signal. In order to determine NO₂, it has first to be reduced into NO with a molybdenum-based catalyst (Reaction 3.3). Then, the quantification of the total NO follows the same principle as before. Every 5 seconds, the equipment switches between NO and NO_x determination, and the NO₂

concentration is calculated by the difference between these two values. The instrument was calibrated before each sampling measurement by using different air sources with known NO concentrations. For that purpose, we diluted on the field NO 40 ppm (Carbagas, Gümligen; mixture 40 ppm NO 30, rest N₂ 60, 10 liters, 150 bar) with air (Carbagas; controlled air, 30 liters, 200 bar) to obtain different NO concentrations between 0 and 1000 ppb. The calibration was achieved with zero air (controlled air cleaned through two tubes filled with activated charcoal and a third one filled with silicagel) and a 1000 ppb NO concentration. The linearity of the calibration curve was checked by measuring the response at three intermediate NO concentrations (250, 500 and 750 ppb).



Reaction 3.3

Ozone concentrations. An ultra-violet (UV) photometer (Monitor Labs Inc, model ML 9810) was used to monitor ozone concentrations at the workplaces. Air was pumped continuously and filtered using a Teflon filter in order to remove all particles which could interfere with the measurement. Air was then conducted to a chamber irradiated with an UV light (254 nm), either directly or by crossing a MnO₂ filter which destroys selectively ozone. The ozone concentration was calculated by the difference between the amount of UV absorbed by air and the one absorbed by air without ozone. The apparatus was calibrated at the sampling site using an ozone generator (Horiba Ltd). The calibration was achieved with zero air (controlled air cleaned through two tubes filled with activated charcoal and a third one filled with silicagel) and a 100 ppb ozone concentration. The linearity of the calibration curve was checked by measuring the response at three intermediate ozone concentrations (25, 50 and 75 ppb).

Temperature and relative humidity. The temperature and the relative humidity were monitored at each sampling site using an Ecolog standard sensor (Elpro-Buchs AG, model TH1).

3.2.2 Personal sampling

PM₄, OC and EC. Each volunteer in the bus depot wore a personal pump for PM₄ sampling (the same equipment as for stationary sampling) during the whole period of shift. Particles collected with these personal pumps were used for the determination of daily mean PM₄, OC and EC concentrations, following the same procedure as for stationary sampling.

3.2.3 Statistical analyses

Statistical analyses were performed using SYSTAT for Windows, version 10.2. The comparison between smokers and non-smokers for personal samplings was tested by the non-parametric Mann-Whitney U-test. Both groups were considered as significantly different when $p < 0.05$. The Spearman's rank correlation coefficient was used to test the correlation between results obtained using different instruments, as well as the correlation between stationary and personal samplings. Correlations were considered significant when $p < 0.05$.

3.3 Results and discussion

3.3.1 Stationary sampling

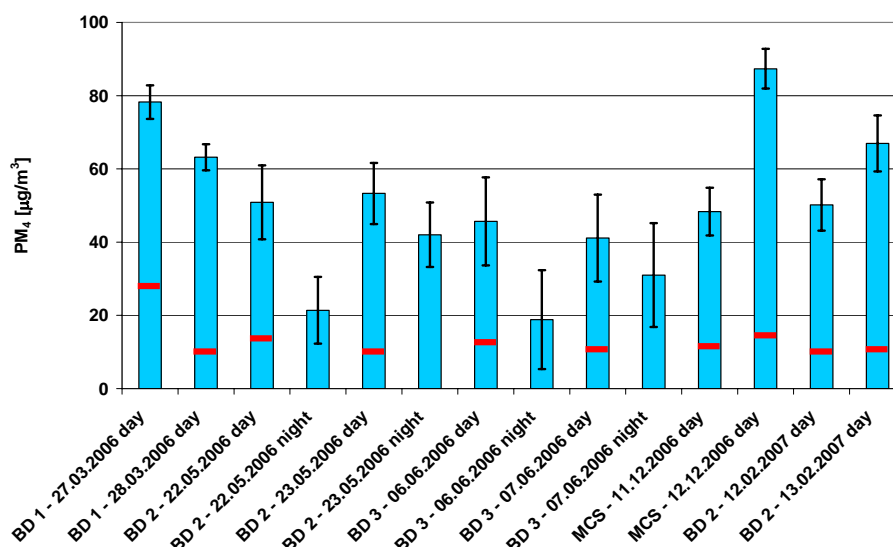
PM₄. Figure 3.1 presents mean PM₄ concentrations over an 8-hour period of shift measured in the sampling sites, and numerical values are given in Annex. Values were comprised between 41 and 87 $\mu\text{g}/\text{m}^3$ during daytime, while PM₄ levels measured during night time were lower (between 19 and 42 $\mu\text{g}/\text{m}^3$) due to reduced activities of workers in the bus depots. The highest PM₄ concentration (87 $\mu\text{g}/\text{m}^3$) was measured at the metro construction site on 12.12.2006 daytime, due to intense welding activities near our equipment. Previous studies undertaken in the same kind of workplace reported very variable results. PM₄ levels measured in the present study are comparable to those obtained by Lewné *et al* (2007) for workers exposed to Diesel exhaust in bus garages, where mean value of PM_{2.5} was 42 (± 3) $\mu\text{g}/\text{m}^3$ (see Table 3.1). On the other hand, higher concentrations of particulate matter have also been reported in previous studies, like in that of Groves and Cain (2000). They conducted a survey of exposure to Diesel exhaust in several workplaces, including bus garages and maintenance depots. The concentrations of respirable dust in these workplaces were much higher (mean value for 41 personal samplings: 267 $\mu\text{g}/\text{m}^3$). The low concentrations of PM₄ measured in the sampling sites in the present study may cause some difficulties to relate exposure to Diesel exhaust and biological effects (oxidative stress). Figure 3.1 also shows daily mean PM₄ concentrations in urban/traffic sites of the same cities and the same days as the field campaign. These values were estimated using official measurements of PM₁₀, either by the Swiss National Air Pollution Monitoring Network (NABEL), or by cantonal offices for environmental protection. The calculation was carried out using Equation 3.1:

$$\text{PM}_4 \text{ estimated} = 0.8 \cdot \text{PM}_{10} \text{ measured}$$

Equation 3.1

We notice that the PM_4 background levels of outdoor air were not negligible, when considering the exposure of workers. They contributed to $24 (\pm 7) \%$ of the total PM_4 level measured in the workplaces.

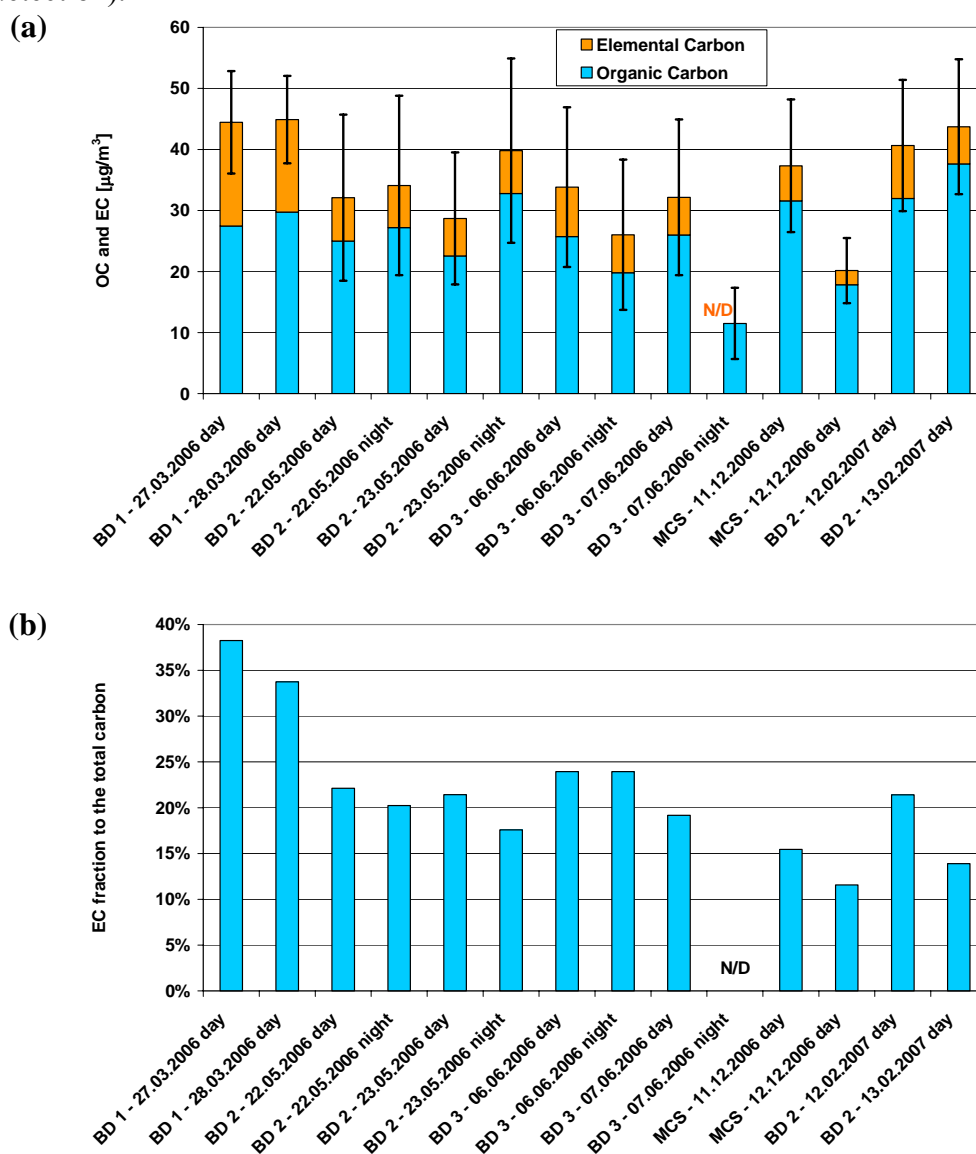
Figure 3.1: Mean PM_4 concentrations over an 8-hour period of shift. Error bars: uncertainty due to the measurement. Horizontal red bars: daily mean PM_4 concentrations in the same city (urban/traffic site) and the same day, estimated using official measurements of PM_{10} (Equation 3.1); values for night time are not available. BD: bus depot. MCS: metro construction site.



OC and EC. Figure 3.2(a) gathers mean OC and EC concentrations over an 8-hour period of shift measured in the sampling sites (numerical values in Annex). We notice that the total carbon (TC), which is the sum of OC and EC, was mainly comprised in the range of $30\text{--}45 \mu g/m^3$, and was roughly uniform in the different workplaces. The highest TC concentration ($45 \mu g/m^3$) was observed in the bus depot 1 during both sampling days, while TC level below $20 \mu g/m^3$ was observed once. We also notice that during night time, TC concentrations were a bit lower due to reduced activities. By comparing data collected for TC and PM_4 , we notice that the contribution of TC to PM_4 was approximately $77 (\pm 36) \%$. This ratio is similar to that given by Lee *et al* (2005) for a field campaign conducted in different trucking companies. We also notice that the TC concentration at the metro construction site on 12.12.2006 daytime was rather low, while the PM_4 level was the highest of all workplaces. This is due to the fact that welding generally produces metallic rather than carbonaceous particles. Figure 3.2(b) shows the EC fraction to the total carbon concentrations in the sampling sites. Results indicate that the particulate EC contribution was in the range of 10–40%. Since EC is well known as an

indicator of Diesel engine exhaust emissions, a high EC fraction of the total carbonaceous particles means a high contribution from Diesel emissions.

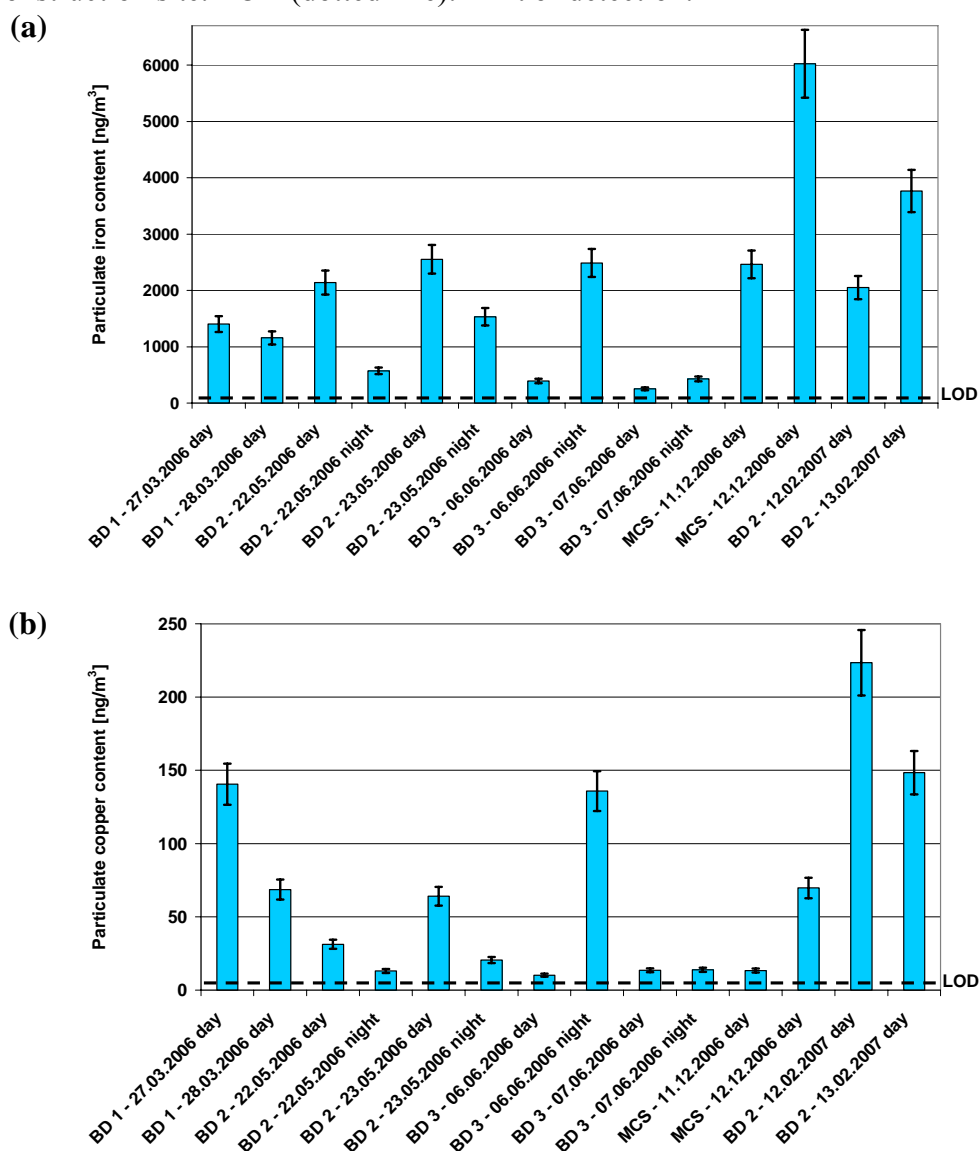
Figure 3.2: (a) Mean organic and elemental carbon concentrations over an 8-hour period of shift. (b) Elemental carbon fraction to the total carbon (OC+EC). Error bars in (a): uncertainty due to the analytical method. BD: bus depot. MCS: metro construction site. N/D: not detected (below the limit of detection).

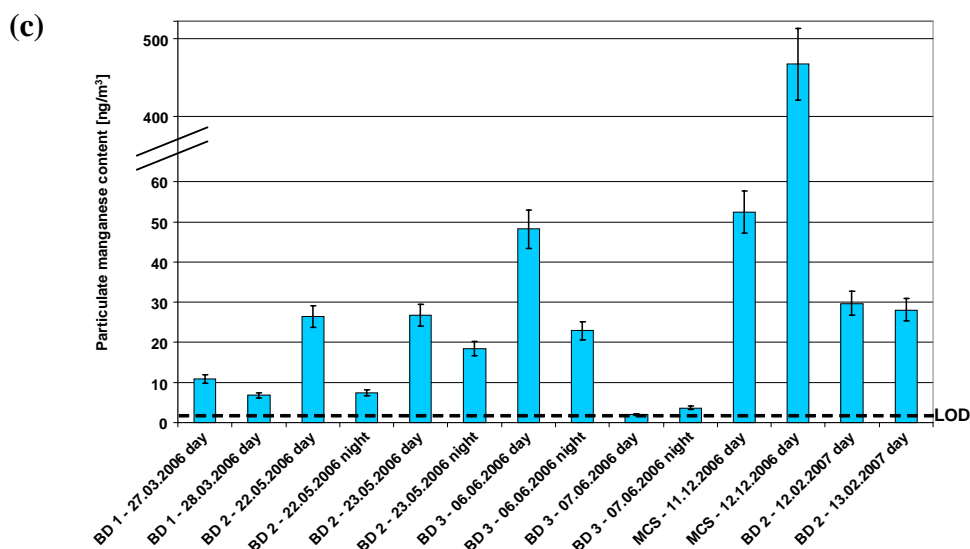


Particulate metal content. Figure 3.3 shows iron (Fe), copper (Cu) and manganese (Mn) content of particles sampled in the workplaces (numerical values in Annex). For each workplace, the order of metal concentration was Fe>Cu>Mn. The only exceptions were observed at the bus depot 3 on 06.06.2006 daytime and at the metro construction site on both sampling days, where particulate manganese content was higher than that for copper.

However, we already noticed that activities of workers at the metro construction site were very different (welding). Results obtained for the three metals were very variable according to the sampling site. Previous papers (Valavanidis *et al*, 2005; Basha *et al*, 2007) confirmed the trend observed in the present study for particulate iron, copper and manganese content. Moreover, many other studies (Costa and Dreher, 1997; Heal *et al*, 2005) pointed out that iron is a major component of particulate matter.

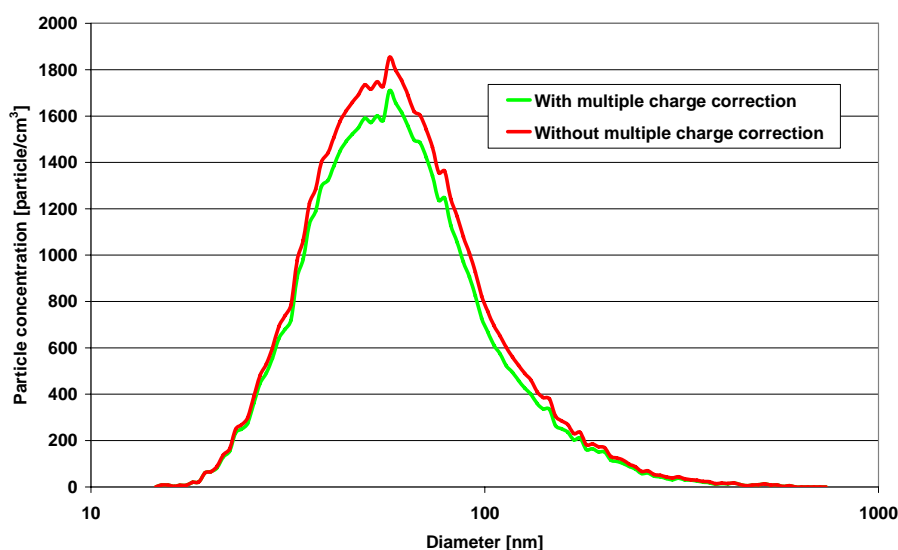
Figure 3.3: Particulate iron (a), copper (b) and manganese (c) content. Error bars: uncertainty due to the analytical method. BD: bus depot. MCS: metro construction site. LOD (dotted line): limit of detection.





Particle size distribution. The particle size distribution in the sub-micron range was measured using a SMPS. This apparatus is widely used for laboratory purposes as well as for field measurements. For more than 20 years, experiments have been carried out to check the accuracy of the measurements with the SMPS. So far, three main phenomena have been pointed out, leading to important errors: particle multiple charge, diffusion loss and the mobility of nanoparticle aggregates. The first phenomenon, the particle multiple charge, is due to the fact that the software assumes a particle has only one charge. If a particle has more than one charge, it will be incorrectly binned into a smaller sized particle range. The activation of the “multiple charge correction” option turns on an internal algorithm that attempts to correct the sample data for the effects of the multiple charged particles. Figure 3.4 shows the influence of the multiple charge correction on the particle size distribution. The effects of the multiple charged particles are usually more pronounced for particles larger than 100 nm. Since particles in the workplaces were mainly below 100 nm, this multiple charge correction did not change significantly particle size distributions (less than 10% difference in the particle number concentration).

Figure 3.4: Influence of the multiple charge correction on the particle size distribution.



The second phenomenon, the diffusion loss, is due to the fact that after a collision with a surface, particles adhere due to van der Waals force, electrostatic force and surface tension. If particles diffuse to the wall of their measurement flow path, there will be diffusion losses, and the measured size distribution will underestimate the particle number. Since diffusion is the primary transport mechanism for particles smaller than 100 nm, diffusion losses are more pronounced for small particles. A “diffusion correction” option was available in our software, but this option was designed to be used with another SMPS model. Therefore, we used results obtained by Reineking and Porstendörfer (1986), who measured diffusion losses with our model of SMPS, and we corrected manually our particle size distributions on Microsoft Office Excel 2003 to take into account diffusion losses. Figure 3.5(a) shows the particle penetration into our model of SMPS (Reineking and Porstendörfer, 1986). This graph indicates that for a particle size larger than 100 nm, more than 90% of the particles which enter into the DMA are counted by the CPC, and therefore less than 10% of these particles are lost in the flow path. On the contrary, diffusion loss becomes very important for particles smaller than 50 nm. Figure 3.5(b) shows the influence of the diffusion loss correction on the particle size distribution. This correction leads not only to higher number concentrations, but also to a shift of the mode towards smaller particle sizes. Since particles in the workplaces were mainly below 100 nm, the difference of size distributions was important, with a 20% increase in the particle number concentration. It should be stressed that the corrections shown in Figures 3.4 and 3.5(b) only apply to these examples, and may be totally different for other size distributions.

Figure 3.5: (a) Particle penetration into the SMPS (TSI Inc., model 3934), adapted from Reineking and Porstendörfer (1986). (b) Influence of the diffusion loss correction on the particle size distribution.

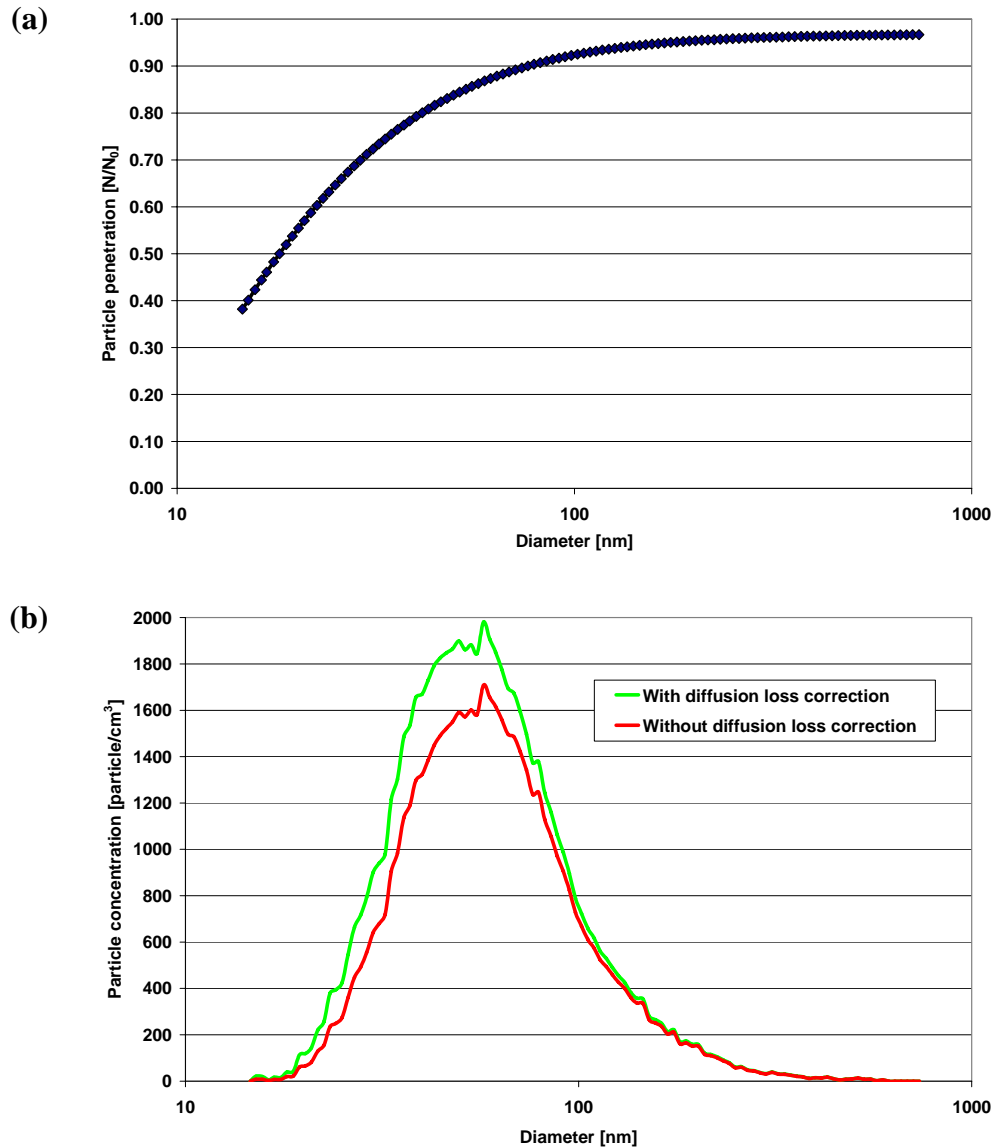
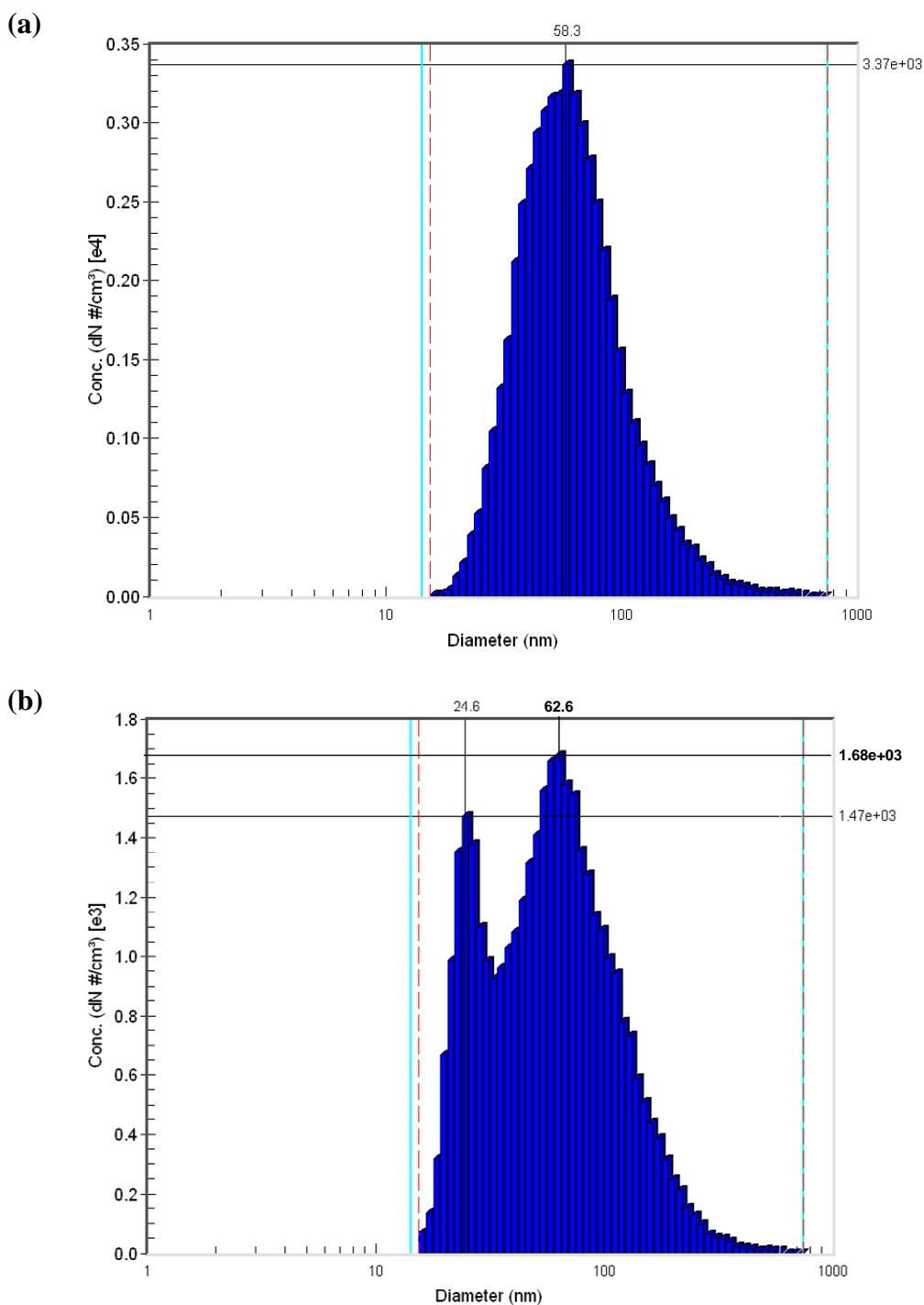


Figure 3.6 shows two examples of particle size distributions measured in the workplaces. According to the activities of workers and the passage of vehicles near the equipment, the particle concentrations and the size distributions were very variable. Figure 3.6(a) is a typical size distribution obtained without significant activity near the equipment, and may be considered as a “background”. We notice that the mode was at 58 nm, and that particles were mainly smaller than 100 nm. Figure 3.6(b) is a particle size distribution which was recorded immediately after the passage of a bus near the SMPS. We notice the presence of a second mode at 25 nm, due to the contribution of freshly emitted soot, which is usually very small. These primary soot particles are quickly agglomerated to form larger particles, and thus the

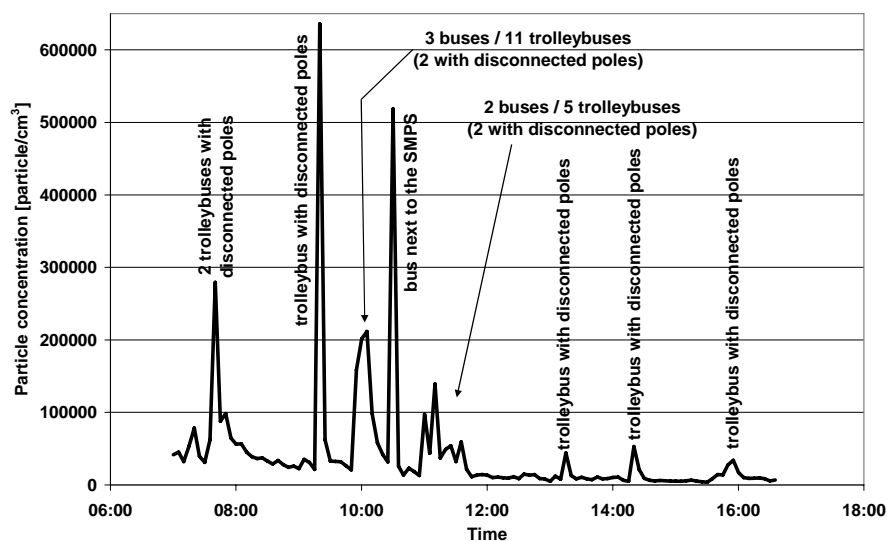
peak at 25 nm disappears already in the following scan recorded three minutes after that of Figure 3.6(b).

Figure 3.6: Two examples of particle size distributions measured using a SMPS. **(a)** Typical particle size distribution measured in the bus depot 3 (06.06.2006 at 7h55) without significant activity near the SMPS. **(b)** Particle size distribution recorded immediately after the passage of a bus near the SMPS in the bus depot 3 (06.06.2006 at 7h05). Resolution: 32 channels/decade.



Particle size distributions shown in Figure 3.6 allow calculating the total number of particles comprised in the range of 15-750 nm. Figure 3.7 shows an example of the particle concentrations measured during a whole period of shift. According to the activities of workers and the passage of vehicles near the equipment, peaks corresponding to important release of particles may be observed. We noticed that the most important sources of particles were buses and trolleybuses with disconnected poles, especially in the morning when the bus fleet leaved the depot. The only exception was the metro construction site on 12.12.2006 daytime, where particles were mainly emitted by welding activities. It is interesting to notice that when buses equipped with particle filters passed near the SMPS, no increase of particle concentration was observed. However, previous studies showed the presence of small particles (smaller than 40 nm) after the filters, due to homogeneous nucleation (Burtcher, 2005). This phenomenon was perhaps too slow to distinguish these particles from those coming from other sources.

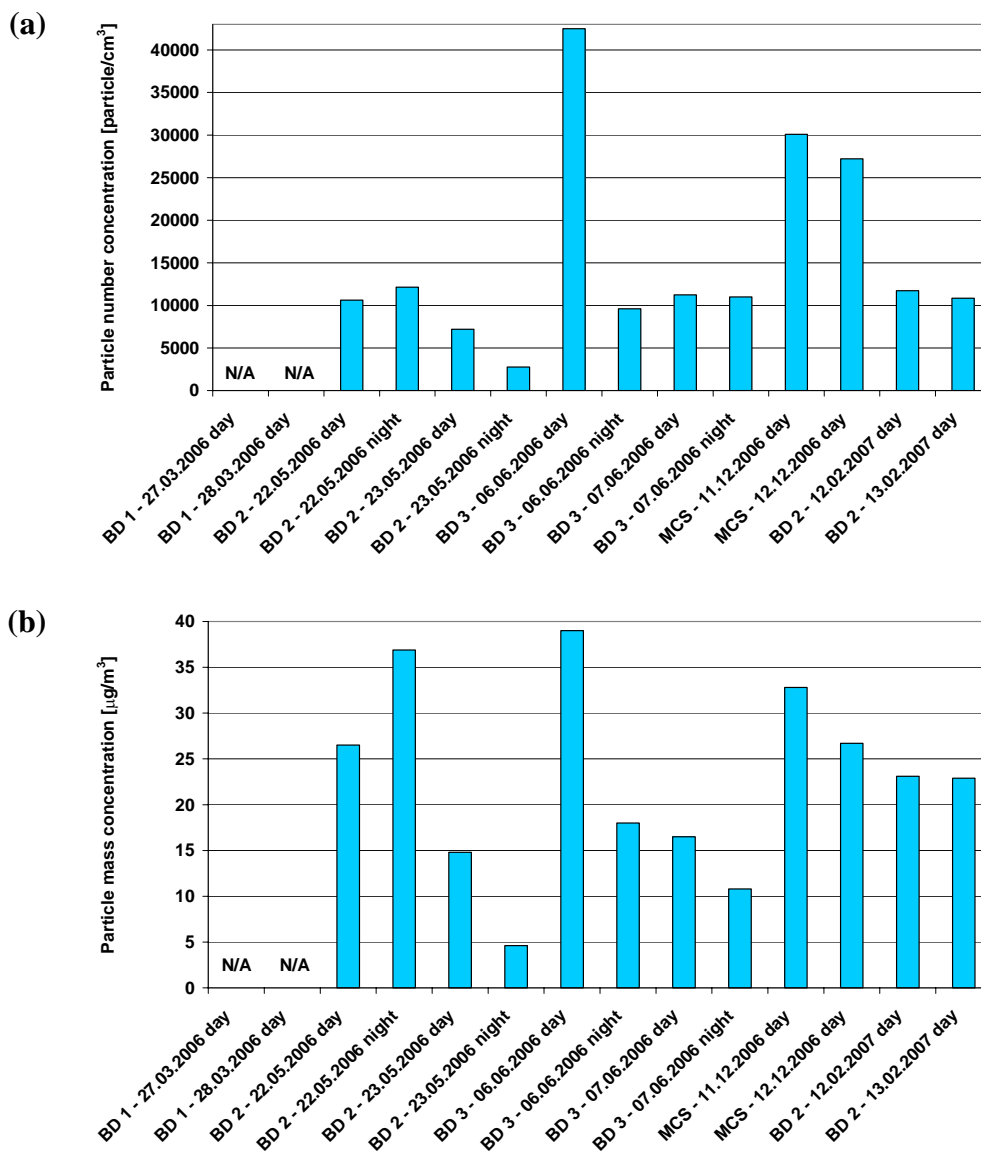
Figure 3.7: Example of particle number concentrations monitored using a SMPS at the bus depot 3 (06.06.2006, daytime). One scan was recorded every three minutes during the whole period of shift.

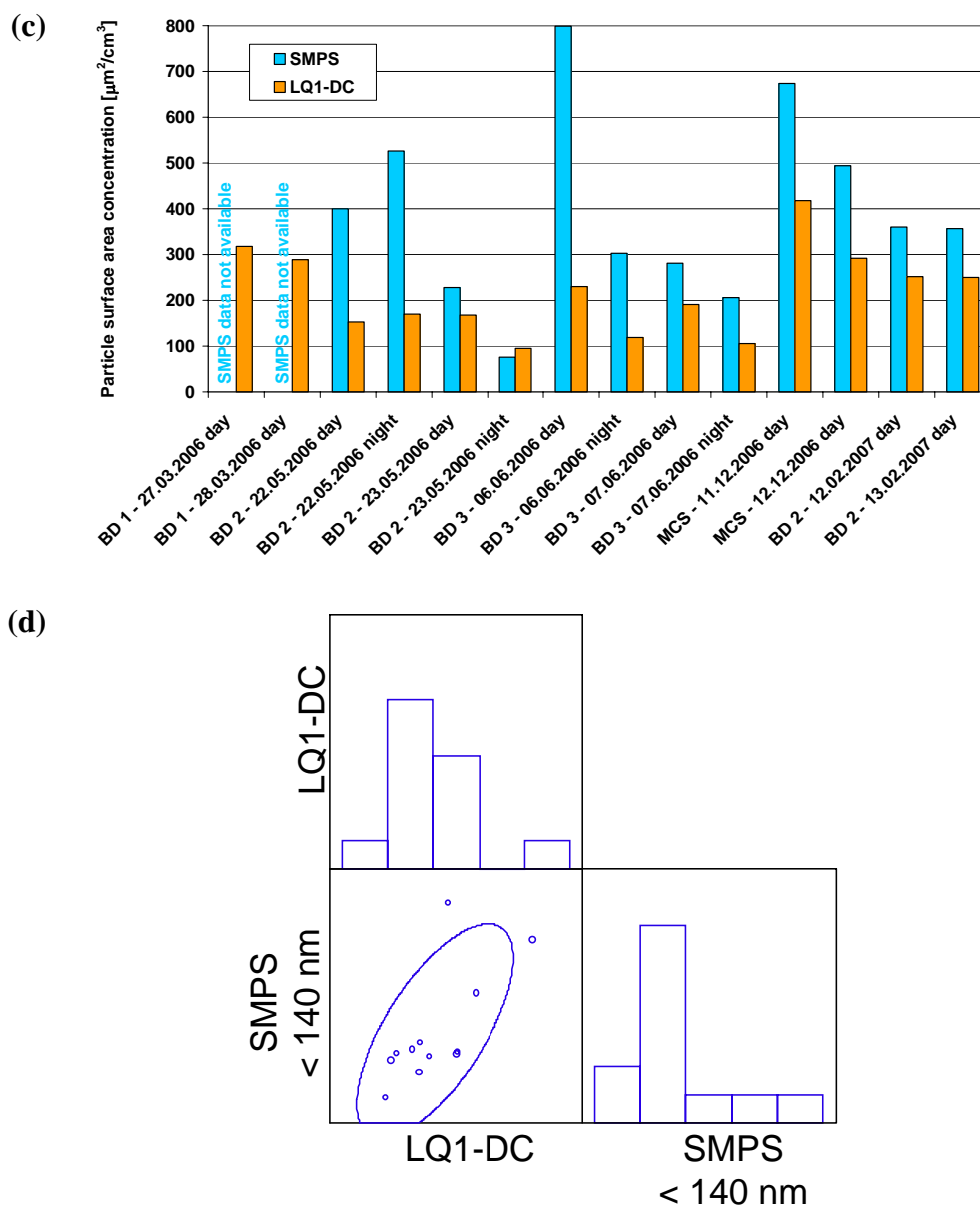


In addition to the number, particle size distributions (Figure 3.6) allow calculating particle mass and surface area. These results are gathered in Figure 3.8 (numerical values in Annex). Moreover, results obtained for the surface area are compared to those obtained using the LQ1-DC. The particle number concentrations (Figure 3.8(a)) in the sampling sites were lower than expected for this kind of workplace. Indeed, the particle concentration was approximately 10'000 particles/cm³ in most of the sampling sites, and exceeded 25'000 particles/cm³ only three times. For the determination of the particle mass (Figure 3.8(b)), we decided to set the density at 1.8 g/cm³. Ambient particle densities reported in the literature range from 1.5 to 1.9

g/cm³ (Kuhlbusch *et al*, 2004). The determination of the particle mass using the SMPS may be correct for particles of a known chemical composition, for which the density is known or estimated. However, it may be subject to important errors in the case of a complex mixture of particles, for which the composition is not known. According to the presence of organic compounds or metallic particles in the sampling sites, the density may vary, leading to important errors in the calculation of the particle mass. For the calculation of the particle surface area (Figure 3.8(c), the software considers each particle as a sphere, and uses the formula for the surface of a sphere ($S = 4 \cdot \pi \cdot r^2$). We are aware that this approximation may also lead to errors according to the shape of the particles. Figure 3.8(c) shows that the particle surface areas measured using the SMPS were systematically higher than those measured with the LQ1-DC, except for one case (bus depot 2, 23.05.2006 night time). This difference is due to the fact that the principle of measurement is not the same for both apparatuses. Indeed, the SMPS measures the mobility diameter of particles in an electrical field, while the LQ1-DC measures the active surface area of particles, which is the total surface area available to be involved in interactions with surrounding compounds. As mentioned earlier, the SMPS was set to monitor particle size distribution in the range 15 to 750 nm, but the apparatus is more efficient for particles smaller than 300 nm. The response of the LQ1-DC has been found to be proportional to the active surface area in the range of 30-150 nm (Jung and Kittelson, 2005). The detection efficiency of the apparatus is below 80% for particles larger than 100 nm, and falls with increasing particle size. Thus, results measured using the LQ1-DC are lower than those obtained with the SMPS, because the diffusion charger is efficient in a smaller range of particle size. According to Figure 3.8(d), if we take into account particles smaller than 140 nm in results obtained with the SMPS, the correlation between both instruments is satisfactory ($p < 0.05$ with the Spearman's rank correlation coefficient; $R^2 = 0.4643$).

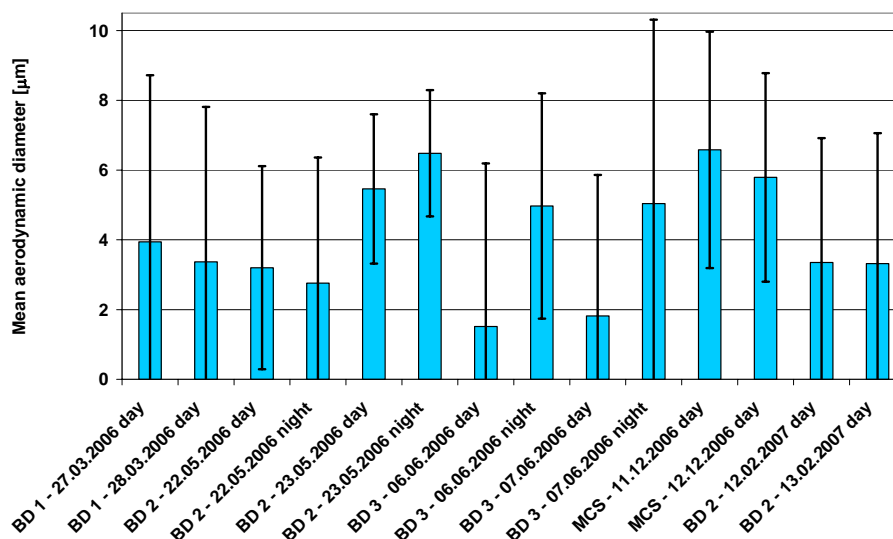
Figure 3.8: Mean particle number (a), mass (b) and surface area (c) concentrations over an 8-hour period of shift, measured using the SMPS (also with LQ1-DC for the surface area). (d) Correlation between particle surface areas measured using LQ1-DC and SMPS. For the SMPS, only particles smaller than 140 nm were taken into account in this plot. $p < 0.05$ with the Spearman's rank correlation coefficient. BD: bus depot. MCS: metro construction site. N/A: not available.





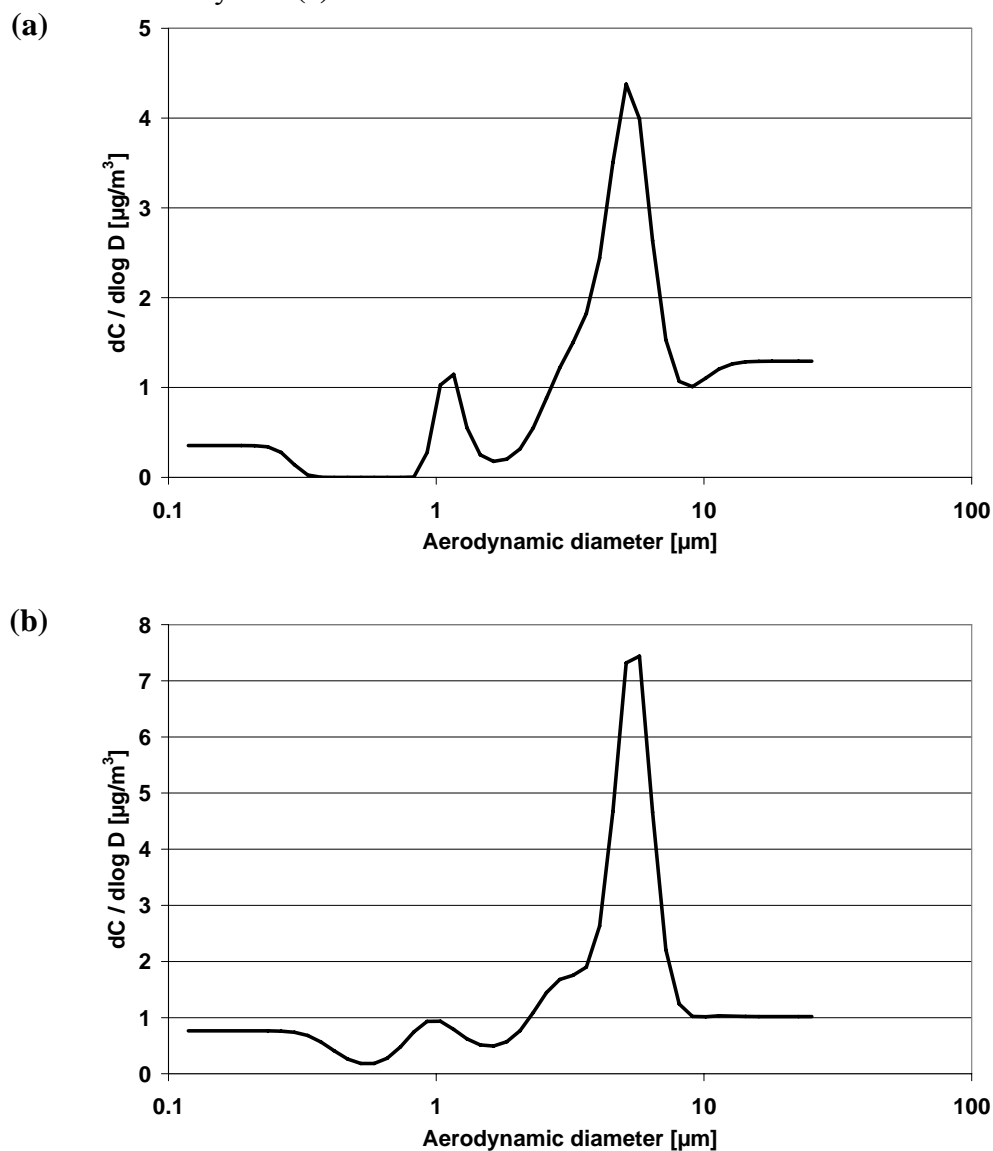
Particle mass distribution. Figure 3.9 presents mean aerodynamic diameters of the particles collected in the different sampling sites (numerical values in Annex). We observed a mean aerodynamic diameter smaller for bus depot 3 (06/07.06.2006, daytime) compared to the others. On the other hand, coarse particles were clearly present in the metro construction site, mean aerodynamic diameter being approximately $6 \mu\text{m}$ on both days.

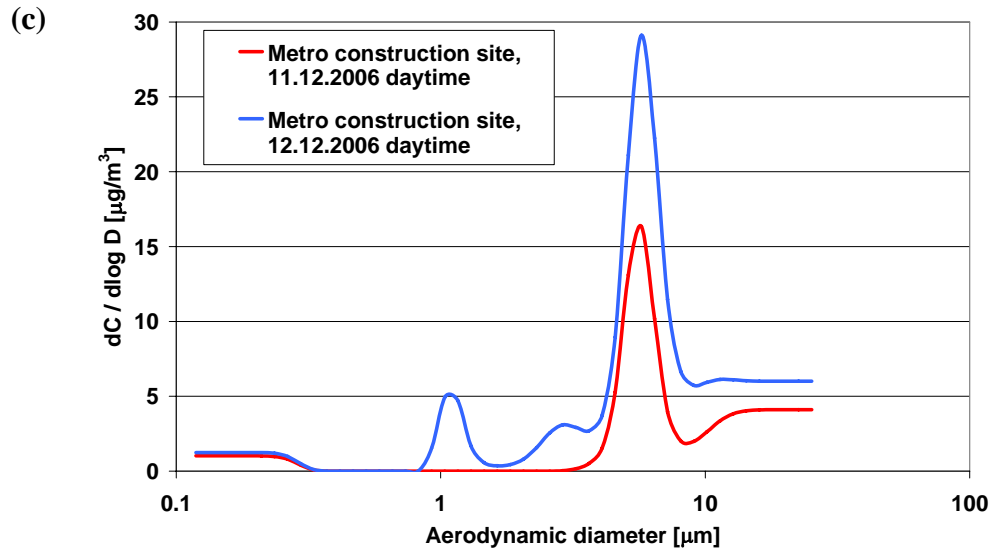
Figure 3.9: Mean aerodynamic diameter of particles, determined using the Andersen type cascade impactor. Error bars: standard deviation. BD: bus depot. MCS: metro construction site.



All surveyed sampling sites presented complex mass size distribution with at least two to three modes: one coarse mode was centered at around 6-7 μm , and one fine mode at around 1 μm (example: Figure 3.10(a)). In some cases, a shoulder at around 2-3 μm was also present (example: Figure 3.10(b)). It is interesting to observe that a very similar mass size distribution of particulate matter was present throughout all the sites surveyed. For the metro construction site, welding activities, which generate small-size particles, are clearly seen on 12.12.2006 daytime with the contribution at 1 μm , when compared with the size distribution obtained on 11.12.2006 daytime (Figure 3.10(c)).

Figure 3.10: Examples of particulate mass size distribution determined using the Andersen type cascade impactor at the bus depot 2 on 06.06.2006 night time (a), on 13.02.2007 daytime (b) and at the metro construction site on 11/12.12.2006 daytime (c).





NO_x and ozone concentrations. Figure 3.11(a) shows mean NO_x concentrations over an 8-hour period of shift measured in the sampling sites (numerical values in Annex), while NO₂ contributions to NO_x are reported in Figure 3.11(b). We notice that NO_x levels were comprised between 100 and 1000 ppb, and that values were very variable according to the sampling site. This range of NO_x level was not a surprise for this kind of workplace, with the presence of tens of motor vehicles, since nitrogen oxides are known to be produced by combustion processes.

Figure 3.11: (a) Mean NO_x concentrations over an 8-hour period of shift. **(b)** NO₂ contribution to NO_x. Error bars in **(a)**: uncertainty due to the measurement. BD: bus depot. MCS: metro construction site. N/A: not available.

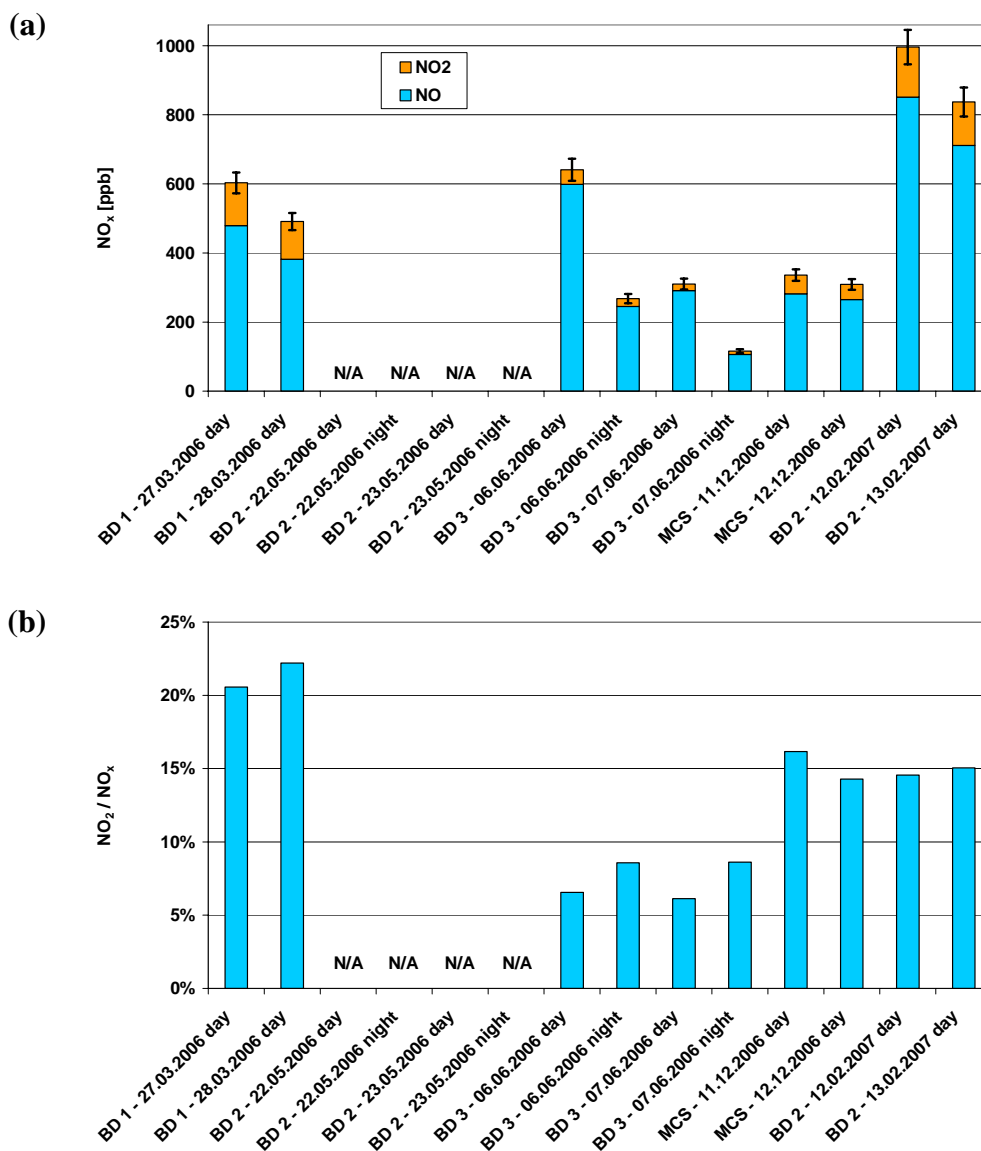
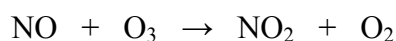
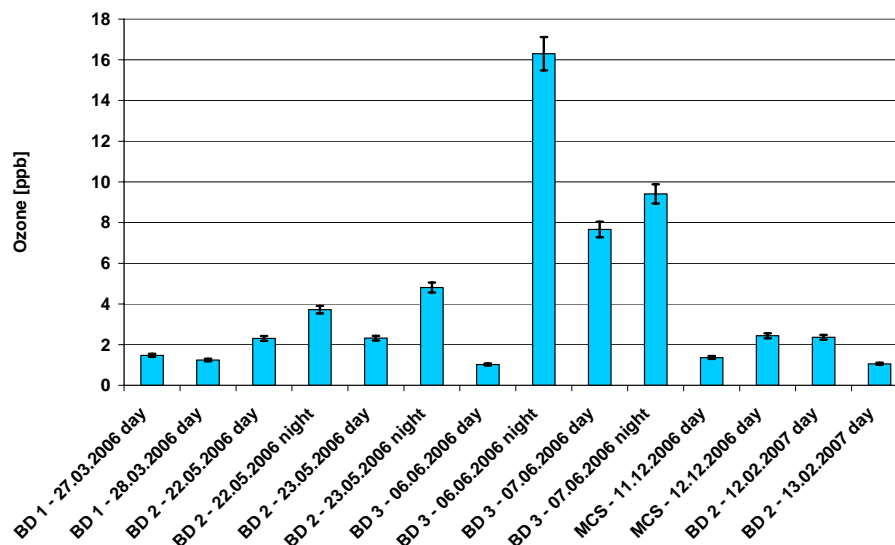


Figure 3.12 shows mean ozone concentrations over an 8-hour period of shift measured in the bus depots (numerical values in Annex). As a consequence of the high levels of NO_x, ozone concentrations were negligible. Indeed, the presence of NO immediately destroys ozone according to Reaction 3.4:



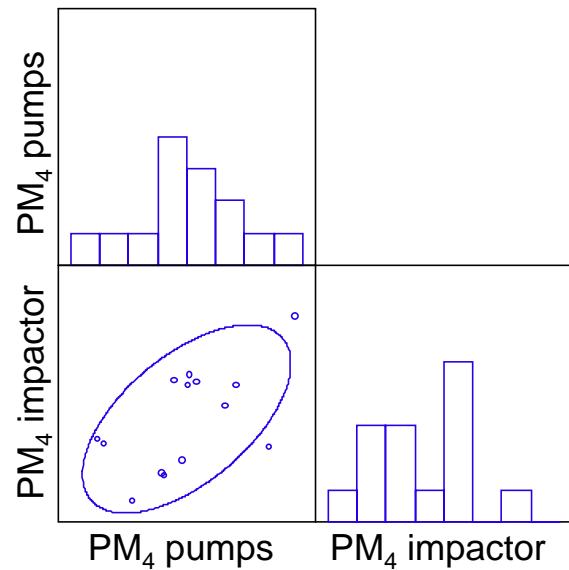
Reaction 3.4

Figure 3.12: Mean ozone concentrations over an 8-hour period of shift. Error bars: uncertainty due to the measurement. BD: bus depot. MCS: metro construction site.



Consistency of the results. During the field campaign, we had the opportunity to use several instruments to measure the same parameter. An important task was to check the robustness of these measurements by testing the correlation between results obtained with different instruments. We already mentioned above that results obtained for the particle surface area using the SMPS and the LQ1-DC were well correlated. We can also compare results obtained for PM_4 using stationary pumps and the Andersen type cascade impactor. For the Andersen impactor, we took into account the six filters which collected particles smaller than $4 \mu m$. Figure 3.13 shows the correlation between both instruments. The Spearman's rank correlation coefficient indicates that results obtained using stationary pumps and the Andersen impactor were well correlated ($p < 0.05$; $R^2 = 0.3469$).

Figure 3.13: Correlation between results obtained for PM₄ using stationary pumps and the Andersen type cascade impactor. For the Andersen impactor, the six filters which collected particles smaller than 4 µm were taken into account in this plot. $p < 0.05$ with the Spearman's rank correlation coefficient.



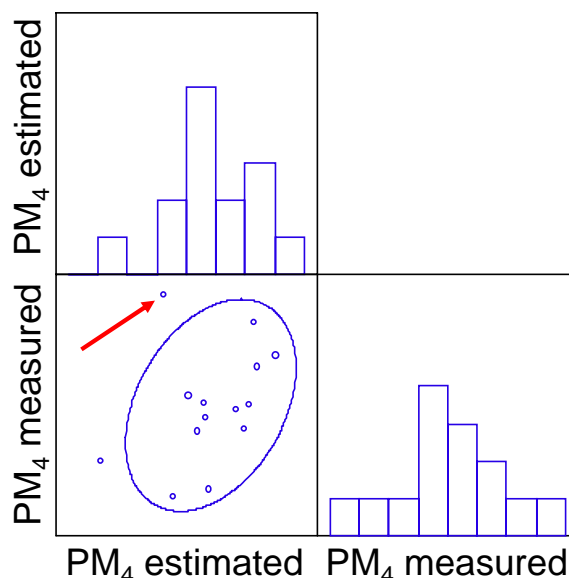
PM₄ concentrations measured using stationary pumps can also be compared to results of OC, EC and metal ions (iron, copper and manganese). If we consider that carbon and metal ions have an important contribution to the total mass of PM₄, we can use Equation 3.2 to estimate the concentration of PM₄:

$$\text{PM}_4 (\text{estimated}) = (1.4 \cdot \text{OC}) + \text{EC} + \text{Fe} + \text{Cu} + \text{Mn} \quad \text{Equation 3.2}$$

Figure 3.14 shows the correlation between results obtained for PM₄ using personal pumps (PM₄ measured) and Equation 3.2 (PM₄ estimated). This plot shows that for one of the workplaces (metro construction site, 12.12.2006 daytime; red arrow in Figure 3.14), the PM₄ concentration calculated using Equation 3.2 was very underestimated compared to that measured using stationary pumps. We already mentioned above that the activities of workers that day consisted mainly of welding of rails, which produces a lot of metallic particles. Therefore, it is possible that the Equation 3.2 does not take into account metallic species produced during welding activities. If we do not take into account this result, the Spearman's rank correlation coefficient obtained for the remaining workplaces indicates that results obtained for PM₄ using stationary pumps and those estimated with the Equation 3.2 were well correlated ($p < 0.05$; $R^2 = 0.4295$). Nevertheless, despite this satisfactory correlation, we also notice that in three cases (bus depot 2, 22/23.05.2006 night time; bus depot 3, 06.06.2006 night time), the sum of total carbon (OC and EC) and metal ions was higher than PM₄ concentrations measured using stationary pumps. Actually, these results are impossible and indicate a lack of accuracy in the analysis of one of these parameters. We notice that this

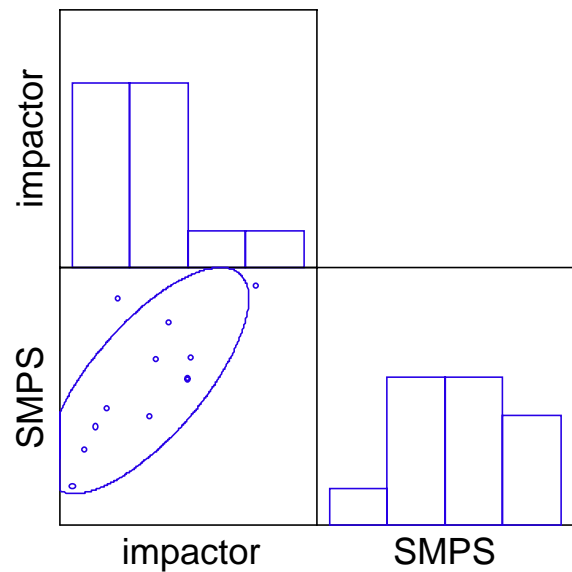
excess of carbon and metal ions compared to PM₄ was observed during night time measurements, when the concentration of PM₄ was low. This can explain the uncertainty of the results obtained for these samples.

Figure 3.14: Correlation between results obtained for PM₄ using stationary pumps (PM₄ measured) and those estimated with OC, EC and metal ions (PM₄ estimated, Equation 3.2). Red arrow: result for the metro construction site (12.12.2006, daytime). $p < 0.05$ with the Spearman's rank correlation coefficient, if we do not take into account the result indicated by the red arrow.



Finally, we can compare results obtained for particle mass concentrations using the SMPS and the Andersen type cascade impactor. For the Andersen impactor, we took into account the three filters which collected particles smaller than 750 nm, in order to focus on the same size range than the SMPS. Figure 3.15 shows the correlation between both instruments. The Spearman's rank correlation coefficient indicated that results obtained using the SMPS and the Andersen impactor were very well correlated ($p < 0.01$; $R^2 = 0.5254$). It is important to remind that the particle mass concentrations using the SMPS were calculated by fixing the particle density to 1.8 g/cm^3 . The excellent correlation between the SMPS and the Andersen impactor suggests that the choice of the particle density was correct, and that this density was not very variable, depending on the workplace.

Figure 3.15: Correlation between results obtained for the particle mass concentrations using the SMPS and the Andersen type cascade impactor. For the Andersen impactor, the three filters which collected particles smaller than 750 nm were taken into account in this plot. $p < 0.01$ with the Spearman's rank correlation coefficient.

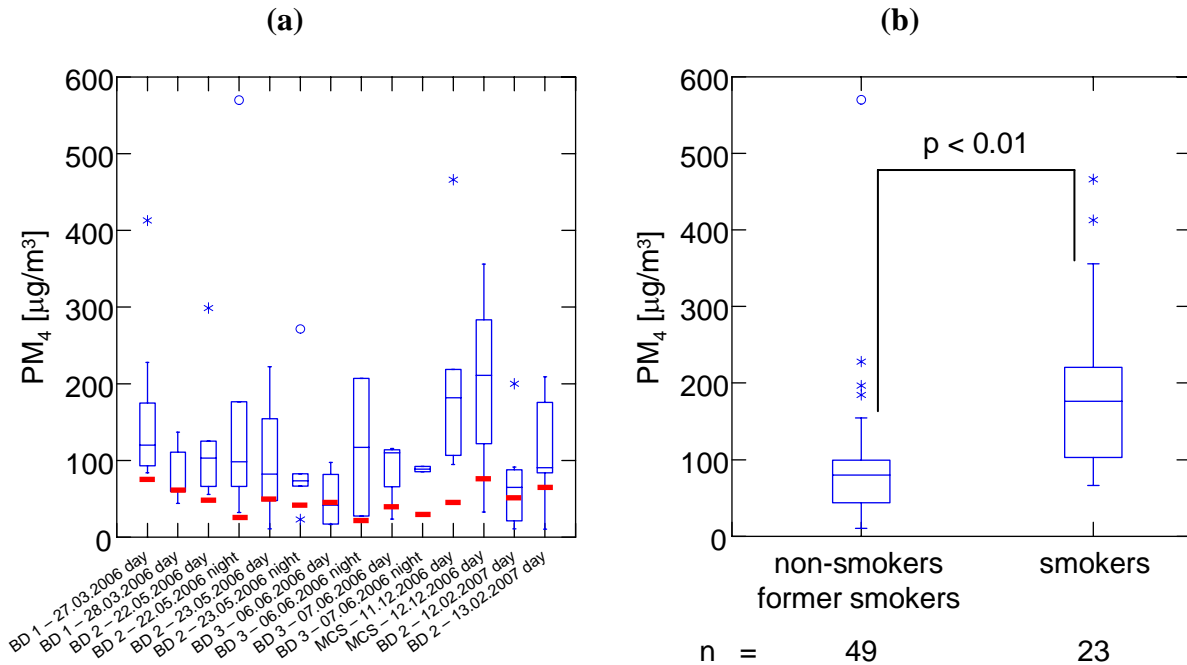


In summary, the correlations that we found between the different instruments stress the good quality of the results obtained for exposure parameters.

3.3.2 Personal sampling

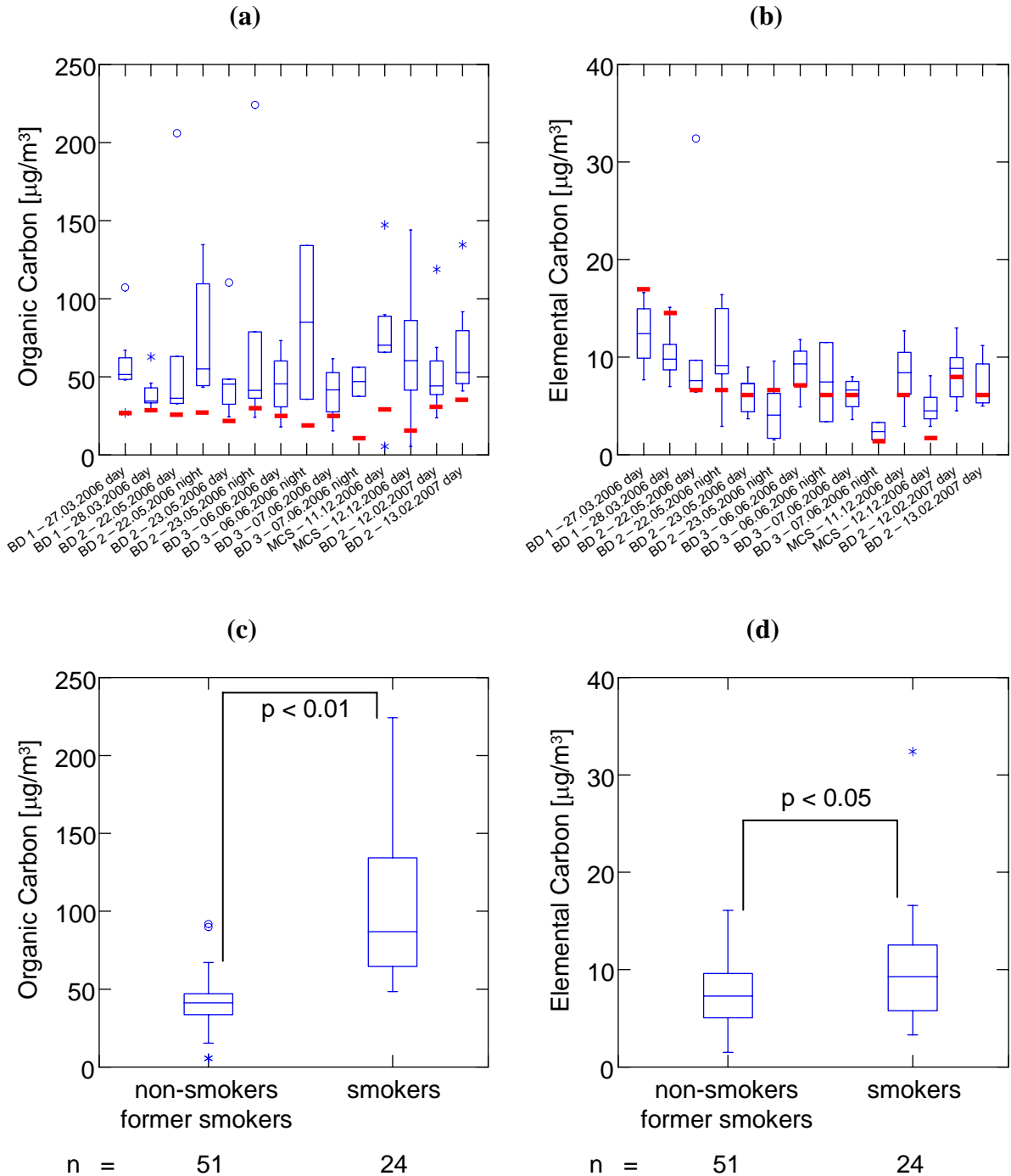
PM₄. Figure 3.16 shows results obtained for PM₄ concentrations with personal samplings (numerical values in Annex). Figure 3.16(a) indicates that PM₄ levels were in general higher for personal samplings than those measured with stationary samplings. This result was expected, since workers were usually closer to the particle sources than the equipment used for stationary sampling. Previous similar studies also pointed out higher levels of particulate matter for personal samplings than for stationary samplings (Groves and Cain, 2000; Lee *et al*, 2005). Figure 3.16(b) shows that smokers were as expected exposed to much higher levels of PM₄ than non-smokers/former smokers. The medians of smokers and non-smokers/former smokers were statistically different ($p < 0.01$ with Mann-Whitney U-test).

Figure 3.16: Box plots of mean PM₄ concentrations over an 8-hour period of shift, measured on personal samples. Results are shown according to sampling sites and dates (a), or to smoking status (b). For each box plot, the central horizontal line marks the median. Boxes show the range within which the central 50% of the values fall, while whiskers contain top and bottom 25% of the values. Asterisks mark outside values ($1.5 \cdot$ previous value), and empty circles mark far outside values ($3 \cdot$ previous value). Horizontal red lines in (a) correspond to stationary samplings. BD: bus depot. MCS: metro construction site.



OC and EC. Figure 3.17 gathers results obtained for OC and EC concentrations with personal samplings (numerical values in Annex). We notice that OC levels were in general higher for personal samplings than those measured with stationary samplings (Figures 3.17(a)), and that smokers were exposed to higher OC concentrations than non-smokers/former smokers ($p < 0.01$ with Mann-Whitney U-test; Figure 3.17(c)). This is exactly the same trend as that observed with PM₄ concentrations, and was also pointed out by previous studies (Groves and Cain, 2000; Lee *et al*, 2005). EC concentrations were also higher for smokers than for non-smokers/former smokers ($p < 0.05$ with Mann-Whitney U-test; Figure 3.17(d)), but we notice in Figure 3.17(b) that EC concentrations measured on personal pumps were comparable to those measured with stationary samplings. A similar trend was observed only in the study of Groves and Cain (2000), while Lee *et al* (2005) measured higher EC levels on personal pumps than on stationary pumps. Our results are certainly due to the fact that workers were not located near the main source of EC. Indeed, EC is considered as a surrogate for Diesel exhaust particles and was mainly generated by the passage of vehicles, not by the activities of workers. Moreover, these results could imply that the EC concentration may be considered as rather homogeneously distributed throughout the workplace.

Figure 3.17: Box plots of mean organic ((a) and (c)) and elemental ((b) and (d)) carbon concentrations over an 8-hour period of shift, measured on personal samples. Results are shown according to sampling sites and dates ((a) and (b)), or to smoking status ((c) and (d)). For each box plot, the central horizontal line marks the median. Boxes show the range within which the central 50% of the values fall, while whiskers contain top and bottom 25% of the values. Asterisks mark outside values ($1.5 \cdot$ previous value), and empty circles mark far outside values ($3 \cdot$ previous value). Horizontal red lines in (a) and (b) correspond to stationary samplings. BD: bus depot. MCS: metro construction site.



3.3.3 Comparison between stationary and personal samplings

As mentioned earlier, we wanted to check whether it was possible to extrapolate the exposure of each worker with results obtained with stationary samplings. The possible associations between stationary and personal samplings for three parameters (PM₄, OC and EC) were tested by using the non-parametric Spearman test. The obtained Spearman's rank correlation coefficients are given in Table 3.2. An outlier for personal PM₄ was removed from this analysis (worker "G 06 EU", bus depot 2, 22.05.2006 night time). This volunteer presented a very high personal PM₄ exposure for one day (570 µg/m³). We attribute this high exposure to the fact that he was responsible for refilling the emergency brake tank of trams with sand and could thus have been exposed to high concentrations of particle dust. The association is significant between stationary and personal samplings for EC, while it is significant for PM₄ only when considering non-smokers and former smokers, and without taking into account workers of the metro construction site. On the other hand, no association between fixed and personal data is observed for OC. This result suggests that workers were exposed to organic compounds that were not determined with fixed samplings due to their specific activities. Thus, these data indicate that it is not easy to extrapolate stationary concentrations to personal ones.

Table 3.2: Spearman's rank correlation matrix between stationary and personal samplings for PM₄, OC and EC.

Parameter	Population	PM ₄ stationary	OC stationary	EC stationary
PM ₄ personal	All	0.132 (n=73)		
	Non-smokers/former smokers	0.289 (n=48 ^a)		
	Non-smokers/former smokers, without MCS	0.389 (n=45 ^a) *		
OC personal	All		0.094 (n=76)	
	Non-smokers/former smokers		0.293 (n=51)	
	Non-smokers/former smokers, without MCS		0.280 (n=46)	
EC personal	All			0.462 (n=76) *
	Non-smokers/former smokers			0.569 (n=51) *
	Non-smokers/former smokers, without MCS			0.572 (n=46) *

MCS: metro construction site.

^a without one outlier (worker "G 06 EU", bus depot 2, 22.05.2006 night time).

* significant correlation (p<0.05).

3.3.4 Summary

Table 3.3 gathers results obtained for stationary and personal samplings. This table confirms that all parameters were lower than the OELs.

Table 3.3: Summary of results obtained for exposure parameters in the workplaces with stationary and personal samplings, and corresponding occupational exposure limits (OELs) for Switzerland (data valid in 2007; Suva, 2007).

Instrument	Parameter	Stationary sampling	Personal sampling	Min – Max	OEL
Personal pumps	PM ₄	50 (±20) [µg/m ³]	121 (±104) [µg/m ³]	<10 - 570.0 [µg/m ³]	3000 [µg/m ³]
Coulomat	Organic Carbon	26 (±7) [µg/m ³]	61 (±40) [µg/m ³]	7.0 - 224.2 [µg/m ³]	
	Elemental Carbon	7 (±4) [µg/m ³]	8 (±5) [µg/m ³]	<1 - 32.4 [µg/m ³]	100 [µg/m ³]
	Total Carbon	34 (±9) [µg/m ³]	69 (±43) [µg/m ³]	<8 - 238.4 [µg/m ³]	
	EC/TC	21 (±8) [%]	14 (±7) [%]	2.1 - 37.4 [%]	
Atomic absorption spectrometer	Iron	1944 (±1556) [ng/m ³]			1'000'000 [ng/m ³]
	Copper	69 (±68) [ng/m ³]			100'000 [ng/m ³]
	Manganese	54 (±120) [ng/m ³]			500'000 [ng/m ³]
Scanning mobility particle sizer	PM _{0.7} number	15579 (±11496) [# /cm ³]			
	PM _{0.7} mass	23 (±10) [µg/m ³]			
	PM _{0.7} surface area	392 (±204) [µm ² /cm ³]			
LQ1-DC	Particle surface area	218 (±92) [µm ² /cm ³]			
Direct reading instrument	O ₃	4 (±4) [ppb]			100 [ppb]
Direct reading instrument	NO	421 (±235) [ppb]			24'000 [ppb]
	NO ₂	70 (±51) [ppb]			3'000 [ppb]
	NO _x	490 (±277) [ppb]			
	NO ₂ /NO _x	13 (±6) [%]			

Results for stationary and personal samplings: mean (± standard deviation).

3.4 Conclusion

All the exposure parameters measured in the workplaces were lower than the OELs valid in Switzerland. Results obtained for PM₄, OC and EC indicate that occupational exposure to particulate matter was rather low. It is possible that these low levels of particulate matter are not sufficient to induce significant or measurable biological effects. Moreover, we noticed that many parameters were very variable according to the sampling sites.

Several instruments were simultaneously used to measure the same parameter. The correlation between results obtained using different apparatuses is satisfactory, stressing the good quality of the measurements during the field campaign. Nevertheless, the correlation between stationary and personal samplings indicates that it is not so easy to extrapolate the exposure of each worker with results obtained with stationary samplings.

3.5 References

- Bakke B., Stewart P., Ulvestad B., Eduard W., 2001. Dust and gas exposure in tunnel construction work. *American Industrial Hygiene Association (AIHA) Journal*, 62 (4), 457-465.
- Basha S., Gaur P.M., Thorat R.B., Trivedi R.H., Mukhopadhyay S.K., Anand N., Desai S.H., Mody K.H., Jha B., 2007. Heavy metal content of suspended particulate matter at world's largest ship-breaking yard, Alang-Sosiya, India. *Water, Air and Soil Pollution*, 178 (1/4), 373-384.
- Beckman J.S., Beckman T.W., Chen J., Marshall P.A., Freeman B.A., 1990. Apparent hydroxyl radical production by peroxynitrite: implications for endothelial injury from nitric oxide and superoxide. *Proceedings of the National Academy of Sciences of the United States of America*, 87 (4), 1620-1624.
- Burtscher H., 2005. Physical characterization of particulate emissions from diesel engines: a review. *Journal of Aerosol Science*, 36 (7), 896-932.
- Buschini A., Cassoni F., Anceschi E., Pasini L., Poli P., Rossi C., 2001. Urban airborne particulate: genotoxicity evaluation of different size fractions by mutagenesis tests on microorganisms and comet assay. *Chemosphere*, 44 (8), 1723-1736.
- Costa D.L., Dreher K.L., 1997. Bioavailable transition metals in particulate matter mediate cardiopulmonary injury in healthy and compromised animal models. *Environmental Health Perspectives*, 105 (suppl. 5), 1053-1060.
- Dahmann D., Monz C., Sönksen H., 2007. Exposure assessment in German potash mining. *International Archives of Occupational and Environmental Health*, 81 (1), 95-107.
- Delfino R.J., 2002. Epidemiologic evidence for asthma and exposure to air toxics: linkages between occupational, indoor, and community air pollution research. *Environmental Health Perspectives*, 110 (suppl. 4), 573-589.
- European Standard EN 481, 1993. Workplace atmospheres - Size fractions definitions for measurement of airborne particles. European Committee for Standardization, Bruxelles (Belgium).
- Flowers L., Rieth S.H., Coglianò V.J., Foureman G.L., Hertzberg R., Hofmann E.L., Murphy D.L., Nesnow S., Schoeny R.S., 2002. Health assessment of polycyclic aromatic hydrocarbon mixtures: current practices and future directions. *Polycyclic Aromatic Compounds*, 22 (3/4), 811-821.

-
- Foucaud L., Bennasroune A., Klestadt D., Laval-Gilly P., Falla J., 2006. Oxidative stress induction by short term exposure to ozone on THP-1 cells. *Toxicology in Vitro*, 20 (1), 101-108.
 - Groves J., Cain J.R., 2000. A survey of exposure to Diesel engine exhaust emissions in the workplace. *Annals of Occupational Hygiene*, 44 (6), 435-447.
 - Heal M.R., Hibbs L.R., Agius R.M., Beverland I.J., 2005. Total and water-soluble trace metal content of urban background PM₁₀, PM_{2.5} and black smoke in Edinburgh, UK. *Atmospheric Environment*, 39 (8), 1417-1430.
 - Healey K., Lingard J.J.N., Tomlin A.S., Hugues A., White K.L.M., Wild C.P., Routledge M.N., 2005. Genotoxicity of size-fractionated samples of urban particulate matter. *Environmental and Molecular Mutagenesis*, 45 (4), 380-387.
 - Hsiao W.L.W., Mo Z.-Y., Fang M., Shi X.-M., Wang F., 2000. Cytotoxicity of PM_{2.5} and PM_{2.5-10} ambient air pollutants assessed by the MTT and the Comet assays. *Mutation Research/Genetic Toxicology and Environmental Mutagenesis*, 471 (1/2), 45-55.
 - Jung H., Kittelson D.B., 2005. Characterization of aerosol surface instruments in transition regime. *Aerosol Science and Technology*, 39 (9), 902-911.
 - Knaapen A.M., Shi T., Borm P.J.A., Schins R.P.F., 2002. Soluble metals as well as the insoluble particle fraction are involved in cellular DNA damage induced by particulate matter. *Molecular and Cellular Biochemistry*, 234/235 (1), 317-326.
 - Kuhlbusch T.A.J., Neumann S., Fissan H., 2004. Number size distribution, mass concentration, and particle composition of PM₁, PM_{2.5}, and PM₁₀ in bag filling areas of carbon black production. *Journal of Occupational and Environmental Hygiene*, 1 (10), 660-671.
 - Lall A.A., Friedlander S.K., 2006. On-line measurement of ultrafine aggregate surface area and volume distributions by electrical mobility analysis: I. Theoretical analysis. *Journal of Aerosol Science*, 37 (3), 260-271.
 - Lall A.A., Seipenbusch M., Rong W., Friedlander S.K., 2006. On-line measurement of ultrafine aggregate surface area and volume distributions by electrical mobility analysis: II. Comparison of measurements and theory. *Journal of Aerosol Science*, 37 (3), 272-282.
 - Lee B.-K., Smith T.J., Garshick E., Natkin J., Reaser P., Lane K., Lee H.K., 2005. Exposure of trucking company workers to particulate matter during the winter. *Chemosphere*, 61 (11), 1677-1690.

-
- Lewné M., Nise G., Lind M.-L., Gustavsson P., 2006. Exposure to particles and nitrogen dioxide among taxi, bus and lorry drivers. *International Archives of Occupational and Environmental Health*, 79 (3), 220-226.
 - Lewné M., Plato N., Gustavsson P., 2007. Exposure to particles, elemental carbon and nitrogen dioxide in workers exposed to motor exhaust. *Annals of Occupational Hygiene*, 51 (8), 693-701.
 - Maynard A.D., Kuempel E.D., 2005. Airborne nanostructured particles and occupational health. *Journal of Nanoparticle Research*, 7 (6), 587-614.
 - Miranda K.M., Espey M.G., Wink D.A., 2000. A discussion of the chemistry of oxidative and nitrosative stress in cytotoxicity. *Journal of Inorganic Biochemistry*, 79 (1/4), 237-240.
 - Okeson C.D., Riley M.R., Fernandez A., Wendt J.O.L., 2003. Impact of the composition of combustion generated fine particles on epithelial cell toxicity: influences of metals on metabolism. *Chemosphere*, 51 (10), 1121-1128.
 - Pacher P., Beckman J.S., Liaudet L., 2007. Nitric oxide and peroxynitrite in health and disease. *Physiological Reviews*, 87 (1), 315-424.
 - Park S.S., Kim Y.J., Fung K., 2001. Characteristics of PM_{2.5} carbonaceous aerosol in the Sihwa industrial area, South Korea. *Atmospheric Environment*, 35 (4), 657-665.
 - Peters A., Dockery D.W., Muller J.E., Mittleman M.A., 2001. Increased particulate air pollution and the triggering of myocardial infarction. *Circulation*, 103 (23), 2810-2815.
 - Ramachandran G., Paulsen D., Watts W., Kittelson D., 2005. Mass, surface area and number metrics in diesel occupational exposure assessment. *Journal of Environmental Monitoring*, 7 (7), 728-735.
 - Reineking A., Porstendörfer J., 1986. Measurements of particle loss functions in a Differential Mobility Analyzer (TSI, model 3071) for different flow rates. *Aerosol Science and Technology*, 5 (4), 483-486.
 - Riediker M., Williams R., Devlin R., Griggs T., Bromberg P., 2003. Exposure to particulate matter, volatile organic compounds, and other air pollutants inside patrol cars. *Environmental Science & Technology*, 37 (10), 2084-2093.
 - Sauvain J.-J., Vu Duc T., Guillemin M., 2003. Exposure to carcinogenic polycyclic aromatic compounds and health risk assessment for diesel-exhaust exposed workers. *International Archives of Occupational and Environmental Health*, 76 (6), 443-455.

-
- Schlesinger R.B., Kunzli N., Hidy G.M., Gotschi T., Jerrett M., 2006. The health relevance of ambient particulate matter characteristics: coherence of toxicological and epidemiological inferences. *Inhalation Toxicology*, 18 (2), 95-125.
 - Servais S., Boussouar A., Molnar A., Douki T., Pequignot J.M., Favier R., 2005. Age-related sensitivity to lung oxidative stress during ozone exposure. *Free Radical Research*, 39 (3), 305-316.
 - Seshagiri B., Burton S., 2003. Occupational exposure to Diesel exhaust in the Canadian federal jurisdiction. *American Industrial Hygiene Association (AIHA) Journal*, 64 (3), 338-345.
 - Steenland K., Deddens J., Stayner L., 1998. Diesel exhaust and lung cancer in the trucking industry: exposure-response analyses and risk assessment. *American Journal of Industrial Medicine*, 34 (3), 220-228.
 - Suva, 2003. Utilisation de systèmes de filtres à particules sur les chantiers souterrains. AS 457.f, Lucerne (Switzerland).
 - Suva, 2007. Valeurs limites d'exposition aux postes de travail 2007. 1903.f, Lucerne (Switzerland).
 - U.S. Environmental Protection Agency, 2002. Health assessment document for Diesel engine exhaust. EPA/600/8-90/057F, Washington DC.
 - Valavanidis A., Vlahoyianni T., Fiotakis K., 2005. Comparative study of the formation of oxidative damage marker 8-hydroxy-2'-deoxyguanosine (8-OHdG) adduct from the nucleoside 2'-deoxyguanosine by transition metals and suspensions of particulate matter in relation to metal content and redox reactivity. *Free Radical Research*, 39 (10), 1071-1081.
 - Wheatley A.D., Sadhra S., 2004. Occupational exposure to Diesel exhaust fumes. *Annals of Occupational Hygiene*, 48 (4), 369-376.
 - Woskie S.R., Kalil A., Bello D., Virji M.A., 2002. Exposure to quartz, Diesel, dust, and welding fumes during heavy and highway construction. *American Industrial Hygiene Association (AIHA) Journal*, 63 (4), 447-457.

Chapter 4 - Particle surface characterization

4.1 Introduction

The presence of anthropogenic particulate matter in the atmosphere is nowadays considered to be a major environmental problem. Indeed, exposure to PM₁₀ and PM_{2.5} (particulate matter with an aerodynamic diameter smaller than 10 and 2.5 µm, respectively) is associated with a range of adverse health effects, including cancer (Bhatia *et al*, 1998), respiratory (Neuberger *et al*, 2004) and cardiovascular (Pope *et al*, 2004) diseases. So far, several mechanisms have been proposed to explain harmful effects of particulate matter. According to the most probable hypotheses, particle surface characteristics (chemical reactivity, surface area) are of prime importance for the understanding of the toxicity of particulate matter (Brown *et al*, 2001). Surface chemistry is important, because it controls the molecular and cellular interactions with the critical parts of the respiratory-tract components, such as lung lining fluid and different cells. Therefore, physico-chemical characteristics of the particle surface impacting the lung may affect the initial physiological responses, and thus control the downstream effects. For instance, the presence of several components adsorbed on particles, such as metal ions (Park *et al*, 2006) and organics (Mauderly and Chow, 2008), has been found to generate reactive oxygen species (ROS), and thereby cause oxidative stress in biological systems.

Moreover, particles are involved in atmospheric processes, and suspected to play a role in global climate change (Finlayson-Pitts and Pitts, 2000). They are able to scatter incoming solar radiation and, in some cases, to absorb it as well, converting absorbed energy to heat, and therefore contributing to the warming of the troposphere. Particles are also involved in the formation of clouds, and may affect the concentration of atmospheric trace gases by heterogeneous chemical reactions (Cwiertny *et al*, 2008).

Over the past 10 years, great efforts have been placed onto the surface characterization of particulate matter. So far, experiments have been carried out mainly by means of different spectroscopic methods. X-ray photoelectron spectroscopy (XPS; Qi *et al*, 2006), Fourier transform infra-red (FT-IR; Fermo *et al*, 2006) and Raman (Sze *et al*, 2001) have been often used to investigate carbonaceous and inorganic particles, but these techniques do not focus

exclusively on the gas-particle interface. Near-edge X-ray absorption fine structure (NEXAFS) spectroscopy is an emerging tool in the surface characterization of carbonaceous particles (Braun, 2005). C (1s) NEXAFS spectra have the advantage to present molecular fingerprints allowing to distinguish various kinds of carbonaceous particles, such as graphite or Diesel soot. Electron energy loss spectroscopy (EELS) is a related technique which has been widely used in the analysis of carbonaceous particles (Chen *et al*, 2005), often in association with transmission electron microscopy (TEM). However, these electron spectroscopies are hampered by low to modest energy resolution, as well as a limited sensitivity for surface species.

The Knudsen flow reactor represents an alternative technique that allows the characterization of surface functional groups present on particulate matter. This method is based on a heterogeneous chemical reaction between a gas-phase probe molecule and a specific functional group on the surface of a sample. Over the past 15 years, this technique has been used especially in the field of atmospheric chemistry. Heterogeneous reactions have been investigated on different kinds of particle surrogates, such as soot (Stadler and Rossi, 2000; Alcala-Jornod *et al*, 2000; Salgado and Rossi, 2002; Salgado Muñoz and Rossi, 2002; Karagulian and Rossi, 2007), mineral dust (Ullerstam *et al*, 2003; Karagulian and Rossi, 2005; Karagulian and Rossi, 2006; Santschi and Rossi, 2006; Karagulian *et al*, 2006) or sea salt (Rossi, 2003; Pratte and Rossi, 2006). Even if the present titration reactions are undertaken in the gas-phase, we surmise that the particle surface composition will not significantly change when the particle is immersed into a liquid, such that the results of the present approach may still give useful clues for solution studies. An advantage of this technique over spectroscopic methods is that kinetic data and the identification of reaction products may be obtained. On the other hand, the identification of surface functional groups is indirect and afforded by the chemical reactivity of the surface in terms of surface composition. The results may be difficult to interpret because of several possible competing reactions.

Within the framework of the present project, the Knudsen flow reactor technique was used to measure functional groups present on the surface of particles sampled in the workplaces. A study was first undertaken to test the reactivity of several probe gases towards laboratory-generated aerosols. Preliminary work had already been performed by Demirdjian and Rossi (2005), who tested the reactivity of four probe gases towards several laboratory-generated

aerosols. We have extended this work in order to find other probe gases allowing the quantification of additional functional groups present on the particle surface, especially those which are suspected to play a role in adverse health effects of particulate matter (metal ions, acids). In the second part of the study, we sampled ambient fine and ultrafine particles during the field campaign in bus depots, and investigated surface functional groups of these samples. The kinetics of titration reactions were also measured to obtain further information on the reactivity of particulate matter. After the field campaign, we had the opportunity to participate in the NANOTOX project, coordinated by Francelyne Marano (University Paris VII). The aim of this project was to study the toxicity of different types of nanoparticles (carbonaceous particles, titanium dioxide) by means of *in vitro* assays. Within the framework of this project, we analyzed several samples using the Knudsen flow reactor in order to provide information on the particle surface, allowing a better understanding of the surface characteristics involved in the toxicity of the particles. These results will also be presented in this chapter.

4.2 Material and methods

4.2.1 *Knudsen flow reactor*

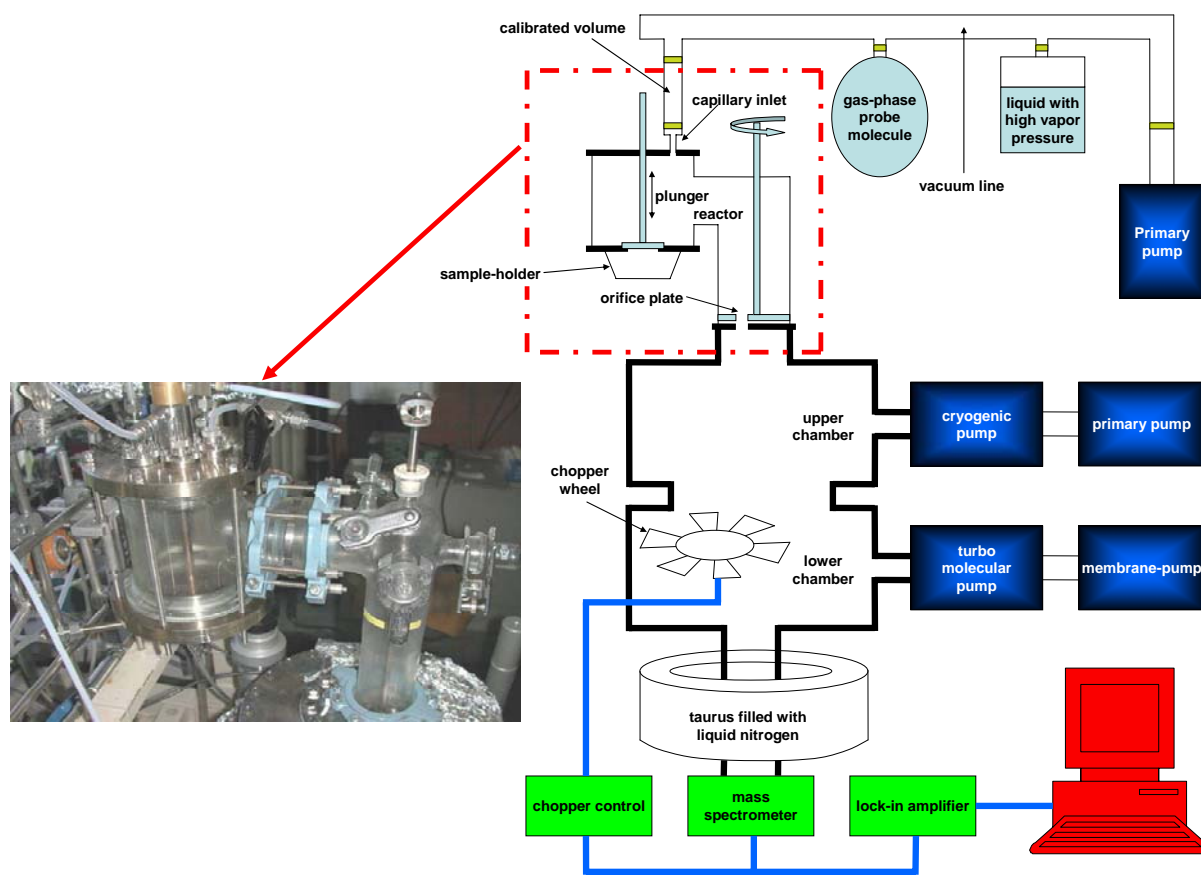
The Knudsen flow reactor is used for heterogeneous chemical reactions between a gas-phase probe molecule and a solid-phase sample. For each type of functional group present on the aerosol surface (such as carbonyl, acidic, basic, or oxidizable groups), the interaction of a suitable titrant molecule is studied. The type and number of probe molecules taken up by the sample, the mass and surface area of which have previously been measured, reveals the type and number of functional groups present on the surface of the sample.

The experimental setup of the Knudsen flow reactor is shown in Figure 4.1, the parameter setting in Table 4.1 and a typical raw data of a titration experiment in Figure 4.2(a). The reactor is maintained under high vacuum (up to 10^{-6} mbar) by means of a cryogenic (Leybold Vakuum GmbH, model COOLVAC 1500) and a turbo-molecular (Varian Vacuum Technologies, model Turbo-V 550) pump. Prior to every titration experiment, the content of the sample-holder is pumped during a few minutes, in order to obtain the same pressure as in the reactor. Water and light volatile compounds adsorbed onto particles may be removed during this step. The vacuum line is filled with a probe gas, coming either from a pure gas or from a liquid, the vapor pressure of which is high enough to sustain a constant flow into the reactor. Then the inlet valve is opened in order to set a constant molecular flow of gas through the reactor, from the capillary inlet to the quadrupole mass spectrometer (MS; Balzers AG,

model QMG 421-4). Once a steady state flow is reached, the plunger isolating the sample chamber from the plenum of the reactor is lifted in order to expose the sample to the gas. If a heterogeneous reaction occurs between the probe gas and the surface functional groups, a part of the gas will be taken up by the sample, and the MS signal will quickly decrease, as shown in Figure 4.2(a). Once all the functional groups on the surface of the sample have reacted with the gas (saturation of the gas uptake), the MS signal will come back to its initial value. The number of gas-phase probe molecules taken up by the sample is then calculated using Equation 4.1.

$$\text{Uptake} = S_{\text{area}} \cdot K_{\text{calibr}} \quad \text{Equation 4.1}$$

where S_{area} [V·s] is the integrated surface area of the MS signal (see hatched curve in Figure 4.2(a)), and K_{calibr} [molecule/V·s] the calibration constant (Figure 4.2(b)). The calibration constant K_{calibr} is measured for each probe gas and orifice diameter by filling the calibrated volume of the vacuum line (Figure 4.1) with different pressures of probe gas, and by measuring for each pressure the molecular flow rate and the MS signal (Figure 4.2(b)). The slope of the curve corresponds to K_{calibr} . Finally, the number of gas-phase probe molecules taken up by the sample (determined using Equation 4.1) is divided either by the particle mass (molecule/mg, see Sub-chapter 4.2.4 “Particle mass”) or by the particle surface area (molecule/cm², see Sub-chapter 4.2.5 “Particle size distribution”).

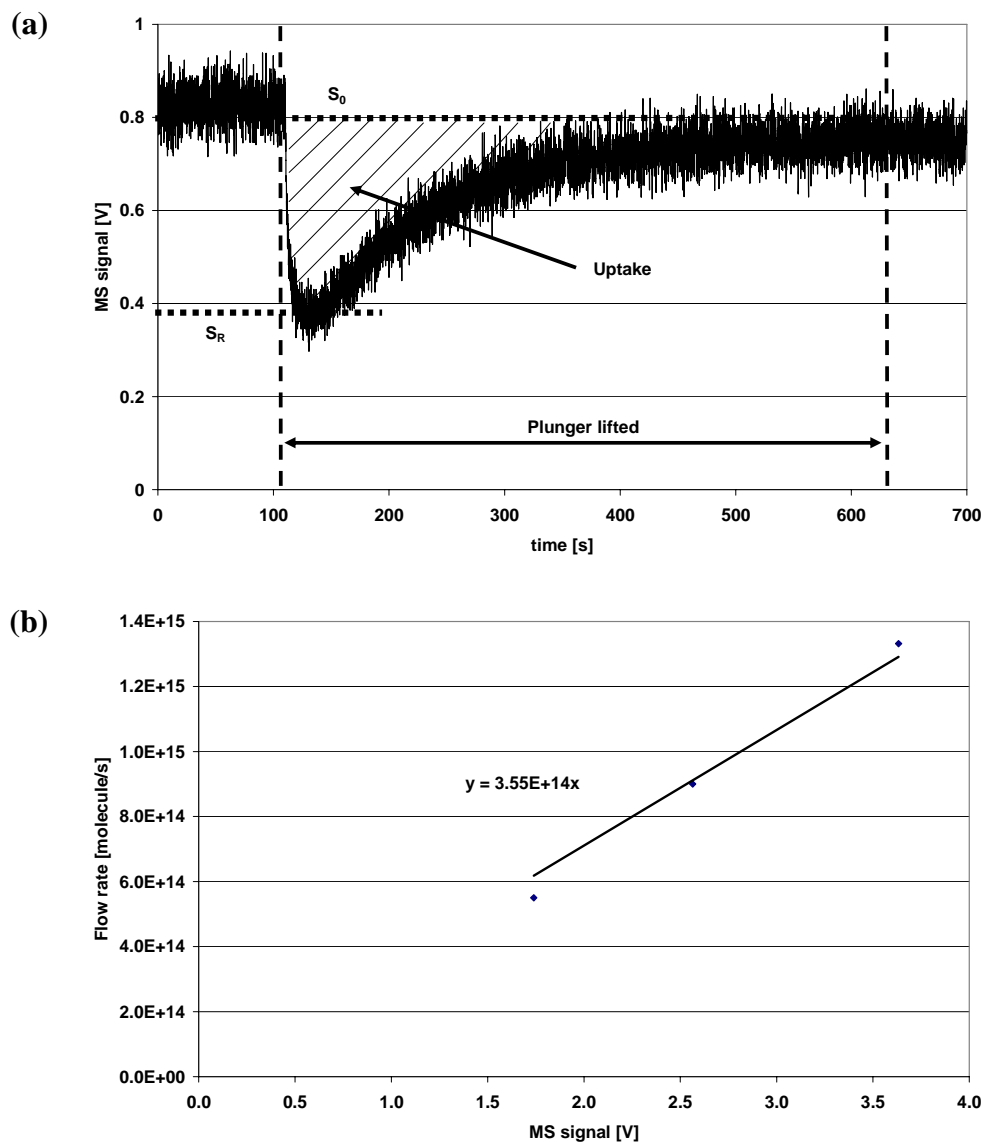
Figure 4.1: Schematic drawing of the Knudsen flow reactor, and photograph of the reactor.**Table 4.1:** Parameters of the Knudsen flow reactor.

Parameter	Value
Volume of the reactor	$V = 1830 \text{ [cm}^3\text{]}$
Estimated surface area of the reactor	$S = 1300 \text{ [cm}^2\text{]}$
Geometric surface area of the samples	$A_s = 17.3 \text{ [cm}^2\text{]}$
Escape orifice diameter	$\varnothing = 1 \text{ [mm]}$
Calibrated volume in the vacuum line	$42 \text{ [cm}^3\text{]}$
Chopper frequency	225 [Hz]
Concentration of gas-phase probes in the reactor	$1 \cdot 10^{13} \text{ to } 5 \cdot 10^{13} \text{ [molecule/cm}^3\text{]}$
Molecular flow rate of gas-phase probes	$2 \cdot 10^{14} \text{ to } 1 \cdot 10^{15} \text{ [molecule/s]}$
Escape rate constant	$k_{\text{esc}} = 0.01 \cdot \sqrt{T/MW} \text{ [s}^{-1}\text{]}$
Fragments monitored with the mass spectrometer	$m/z \text{ } 58 \text{ (N(CH}_3\text{)}_2\text{(CH}_2\text{)}^+)$ for $\text{N(CH}_3\text{)}_3$ $m/z \text{ } 33 \text{ (NH}_2\text{OH}^+)$ for NH_2OH $m/z \text{ } 45 \text{ (COOH}^+)$ for CF_3COOH $m/z \text{ } 36 \text{ (HCl}^+)$ for HCl $m/z \text{ } 48 \text{ (O}_3^+)$ for O_3 $m/z \text{ } 46 \text{ (NO}_2^+)$ for NO_2

T: temperature [K]

MW: molecular weight [g/mol]

Figure 4.2: (a) Typical raw data of a titration experiment using the Knudsen flow reactor. Sample: aerosols collected in bus depot 2 (23.05.2006, daytime) on silanized quartz fiber filter. Probe gas: HCl. m/z : 36. S_0 : MS signal at steady state. S_R : MS signal immediately after the beginning of the reaction. (b) Example of a calibration curve obtained for the determination of K_{calibr} . Probe gas: $\text{N}(\text{CH}_3)_3$. \varnothing : 1 mm. K_{calibr} = slope of the curve, which is forced through zero.



4.2.2 Probe gases

Prior to the field campaign, the reactivity of several probe gases was tested using laboratory-generated aerosols. During their preliminary work performed in our laboratory, Demirdjian and Rossi (2005) tested the reactivity of four probe gases: trimethylamine ($\text{N}(\text{CH}_3)_3$), hydroxylamine (NH_2OH), ozone (O_3) and nitrogen dioxide (NO_2) on laboratory-generated aerosols collected on a Teflon filter. Within the framework of the present study, we evaluated several additional probe gases, and decided to select $\text{N}(\text{CH}_3)_3$, NH_2OH , O_3 , NO_2 , trifluoroacetic acid (CF_3COOH) and hydrochloric acid (HCl).

Table 4.2 shows reactions which were generally expected to occur between these six probes and the particle surface at the conditions of the Knudsen flow reactor. Indeed, heterogeneous reactions were studied at ambient temperature, the residence time of the gas-phase probe molecules in the reactor was comprised between 20 seconds and 1 minute, and their concentration in the reactor was low (in the range of $1 \cdot 10^{13}$ to $5 \cdot 10^{13}$ molecule/ cm^3). Thus, a reaction may be observed using this technique only if it occurs at ambient temperature, and if the kinetics is fast enough to enable a reaction during the residence time of the probe gas in the reactor. This has led to the choice of allowed reactions displayed on the left of Table 4.2, whereas the reactions on the right were rejected based on the above criteria.

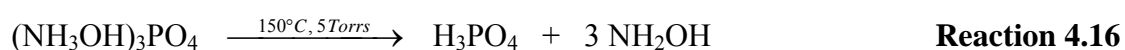
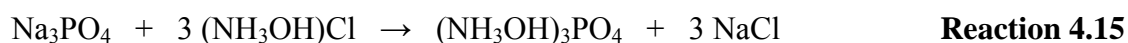
Table 4.2: List of different chemical reactions during the titration experiments in the Knudsen flow reactor under the given experimental conditions.

Probes	Probable reactions occurring at the conditions of the Knudsen flow reactor	Reactions not expected to occur at the conditions of the Knudsen flow reactor
N(CH ₃) ₃	Reaction 4.1: acid-base reaction (Hossain <i>et al</i> , 2004) $\text{H}^+-\text{A}^- + \text{H}_3\text{C}-\text{N}(\text{CH}_3)_3 \longrightarrow \text{A}^- \cdot \text{H}_3\text{C}-\text{N}^+(\text{CH}_3)_3$ Reaction 4.2: metal complexation (Guilbault and Billedeau, 1971) $\text{M}^{n+} + x \text{N}(\text{CH}_3)_3 \longrightarrow [\text{M}(\text{N}(\text{CH}_3)_3)_x]^{n+}$	
NH ₂ OH	Reaction 4.3: addition (Jencks, 1959) $\text{R}'-\text{C}(=\text{O})-\text{R}'' + \text{NH}_2\text{OH} \longrightarrow \text{R}'-\text{C}(\text{N}=\text{OH})-\text{R}'' + \text{H}_2\text{O}$	Reaction 4.4: Hydroamination (Beauchemin <i>et al</i> , 2008) $\text{R}'-\text{C}(\text{R}'')=\text{C}(\text{R}''')-\text{R}'''' + \text{NH}_2\text{OH} \xrightarrow[\text{> 10 h}]{\text{T > 100}^\circ\text{C}} \text{R}'-\text{C}(\text{H})(\text{NH}_2\text{OH})-\text{C}(\text{R}''')-\text{R}''''$
CF ₃ COOH	Reaction 4.5: acid-base reaction $\text{B} + \text{F}_3\text{C}-\text{C}(=\text{O})\text{OH} \longrightarrow \text{F}_3\text{C}-\text{C}(=\text{O})\text{O}^- \cdot \text{B}-\text{H}^+$	
HCl	Reaction 4.6: acid-base reaction $\text{B} + \text{HCl} \longrightarrow \text{B}-\text{H}^+ \cdot \text{Cl}^-$	Reaction 4.7: addition (Raley <i>et al</i> , 1948) $\text{R}'-\text{C}(\text{R}'')=\text{C}(\text{R}''')-\text{R}'''' + \text{HCl} \xrightarrow[\text{peroxide}]{\text{hv or}} \text{R}'-\text{C}(\text{H})(\text{Cl})-\text{C}(\text{R}''')-\text{R}''''$ Reaction 4.8: (Landini <i>et al</i> , 1974) $\text{R}-\text{OH} + \text{HCl} \xrightarrow[\text{catalyst}]{105^\circ\text{C} / 30 \text{ h}} \text{R}-\text{Cl} + \text{H}_2\text{O}$
O ₃	Reaction 4.9: ozonolysis (Horie and Moortgat, 1998) $\text{R}'-\text{C}(\text{R}'')=\text{C}(\text{R}''')-\text{R}'''' + \text{O}_3 \longrightarrow \text{R}'-\text{C}(=\text{O})-\text{R}'' + \text{Criegee intermediates}$	Reaction 4.10: ozonation (Cohen <i>et al</i> , 1975) $\text{R}'-\text{C}(\text{R}'')-\text{H} + \text{O}_3 \longrightarrow \text{R}'-\text{C}(\text{R}'')-\text{OH}$ Reaction 4.11: ozonation (Bachman and Strawn, 1968) $\text{R}'-\text{C}(\text{R}'')-\text{NH}_2 + \text{O}_3 \longrightarrow \text{R}'-\text{C}(\text{R}'')-\text{NO}_2$ Reaction 4.12: ozonation (Erickson <i>et al</i> , 1969) $\text{R}'-\text{C}(\text{R}'')=\text{N}-\text{R}''' + \text{O}_3 \longrightarrow \text{R}'-\text{C}(\text{R}'')=\text{O} + \text{O}=\text{N}-\text{R}'''$ Reaction 4.13: (Klein and Steinmetz, 1975) $\text{R}-\text{C}_6\text{H}_5 + \text{O}_3 \longrightarrow \text{R}-\text{COOH} + \text{C}_6\text{H}_6$
NO ₂	Reaction 4.14: redox reaction (Stadler and Rossi, 2000) $\text{NO}_2 + \{\text{C}-\text{H}\}_{\text{RED}} \longrightarrow \text{HONO} + \{\text{C}\}_{\text{OX}}$	

N(CH₃)₃ (Sigma-Aldrich Chemie GmbH, Buchs, Switzerland; purum, ≥99.0%, Fluka 92251) is a strong base in the gas phase, as measured by its proton affinity (PA = 942 kJ/mol, compared to 854 kJ/mol for NH₃; Jolly, 1991), and is designed to probe strong as well as weak Lewis acids according to Reaction 4.1 of Table 4.2. In addition to carboxylic groups,

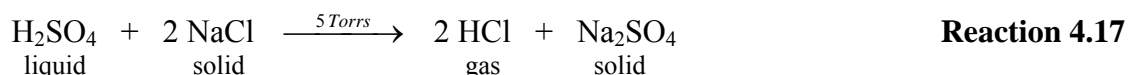
there are other acidic groups that may contribute to the acidity of organic compounds, such as acidic oxides on combustion aerosol particles that have been extensively studied in the past (Hofmann and Ohlerich, 1950; Boehm and Diehl, 1962; Boehm *et al*, 1964; Boehm, 1966). $\text{N}(\text{CH}_3)_3$ is also known to form stable complexes with transition metal ions (Reaction 4.2 of Table 4.2).

NH_2OH is expected to specifically react with carbonyl functions to form oximes (Reaction 4.3 of Table 4.2), if catalytic amounts of organic acids are present as the reaction is acid- or base-catalyzed (Roberts and Caserio, 1977). Owing to the heterogeneous nature of the reaction under the present conditions, the reaction may also occur with carbonyl groups other than those of aldehydes and ketones. Thus, amides, organic acids, acid anhydrides and other carbonyl-bearing species may in principle also contribute to the reactivity towards NH_2OH . NH_2OH is also known to be involved in redox reactions (Davis *et al*, 1951) and in the complexation of several metal ions (Cheng *et al*, 1994). It may also react as a base, but its proton affinity ($\text{PA} = 803 \text{ kJ/mol}$; Jolly, 1991) indicates that NH_2OH is a much weaker base than $\text{N}(\text{CH}_3)_3$ ($\text{PA} = 942 \text{ kJ/mol}$; Jolly, 1991). NH_2OH was prepared by thermal decomposition of tertiary hydroxylammonium phosphate (Reactions 4.15 and 4.16) according to the method of Schenk (1963).



Two acids of different strength, CF_3COOH and HCl , were used to quantify basic sites. CF_3COOH tends to react with basic sites according to Reaction 4.5 of Table 4.2, while HCl is expected to react according to Reaction 4.6 of Table 4.2. Regarding the acidity, HCl is a far stronger acid than CF_3COOH in solution, but this trend is opposite in the gas-phase. Because of the absence of solvent effects in the gas-phase, acid-base properties of organic compounds are indeed different from solution acidities. The gas-phase acidity of a compound AH is determined by the enthalpy change of deprotonation ($\Delta_f\text{H}^\circ_{\text{deprot}}$), according to the reaction $\text{AH} \rightarrow \text{A}^- + \text{H}^+$. $\Delta_f\text{H}^\circ_{\text{deprot}}$ of CF_3COOH is 1351 kJ/mol (Cumming and Kebarle, 1978), while that of HCl is 1395 kJ/mol (Trainham *et al*, 1987). This means that CF_3COOH needs less enthalpy to undergo deprotonation, and therefore is a stronger acid in the gas-phase than HCl . We surmise that gas-phase acidities/basicities are more applicable than solution values in the

present context, because species adsorbed on a surface do not undergo extensive solvation after charge separation compared to aqueous solution. CF₃COOH was commercially available (Sigma-Aldrich Chemie GmbH, Buchs, Switzerland; purum, Fluka 91700), while HCl was prepared by a reaction between sulfuric acid (H₂SO₄) and sodium chloride (NaCl) according to Reaction 4.17. The reaction was achieved at ambient temperature under vacuum, and HCl was condensed in a balloon maintained in liquid nitrogen.



O₃ is a strong oxidizing probe, and was chosen to quantify oxidizable sites. The main expected reaction is the ozonolysis of carbon-carbon double bonds (Reaction 4.9 of Table 4.2), whereas it decomposes on metal oxide surfaces (Dhandapani and Oyama, 1997). Oxidation of alcohols and aldehydes to carboxylic acids is too slow to be observed using this technique. O₃ was prepared daily by corona discharge in pure oxygen by means of an ozone generator (Fischer Technology, model 502), and was condensed in a vessel filled with silica gel and maintained in a cold methanol bath (-80°C) in order to control the vapor pressure.

NO₂ is also an oxidizing probe, but less so than O₃. Its reactivity towards carbonaceous particles has been widely studied (Tabor *et al*, 1993; Tabor *et al*, 1994; Gerecke *et al*, 1998; Alcala-Jornod *et al*, 2000; Stadler and Rossi, 2000; Salgado and Rossi, 2002), and the main expected reaction corresponds to the oxidation of reduced carbonaceous sites (Reaction 4.14 of Table 4.2). NO₂ is expected to react quickly with carbonaceous samples generated under reducing flame conditions, while oxidized samples would not undergo further oxidation upon exposure to the NO₂ probe. Therefore, the reactivity of NO₂ is expected to be a good indicator of the oxidation state of the surface of the carbonaceous particles. NO₂ was purchased from Carbogas (Gümligen, Switzerland).

4.2.3 Samples

Samples analyzed using the Knudsen flow reactor can be classified into different groups, according to their chemical composition and their origin. Secondary organic aerosols (SOA), inorganic particles, carbonaceous particles and titanium dioxide (TiO₂) samples were either commercially available or generated in the laboratory under controlled conditions, while samples of ambient particles were collected during the field campaign in the bus depots.

Laboratory-generated aerosols. In preliminary work, Demirdjian and Rossi (2005) tested the reactivity of probe gases towards several laboratory-generated aerosols. Their titration experiments were carried out on two SOA samples (limonene and toluene) and on one flame soot sample (toluene). In anticipation of the sampling campaign, we chose to carry out titration experiments on three different types of aerosol surrogates for particulate matter expected in bus depots. We used limonene SOA as a surrogate for organic aerosols, $\text{Pb}(\text{NO}_3)_2$ and $\text{Cd}(\text{NO}_3)_2$ as surrogates for soluble metal ions.

Limonene SOA was obtained by oxidation of limonene 145 (Sigma-Aldrich Chemie GmbH, Buchs, Switzerland; purum, Fluka 89188) in the presence of ozone. A flow of limonene vapor in air (250 ml/min), ozone (3 ml/min), dry air (30 ml/min) and wet air (150 ml/min) was admitted into a reactor (volume = 480 cm³), and the outlet of the reactor was linked to a denuder coated with potassium iodide (KI) in order to destroy excess ozone. Under these conditions, the relative humidity in the reactor was 37%. Limonene SOA was finally collected on a Teflon membrane filter (Millipore AG, Volketswil, Switzerland; Fluoropore membrane filter, 0.22 µm, Ø 47 mm, FGLP04700) located immediately after the KI denuder. The yield of limonene SOA Y_{SOA} was calculated using Equation 4.2:

$$Y_{\text{SOA}} = \frac{M_{\text{SOA}}}{F \cdot MW_{\text{lim}} \cdot \Delta t} \quad \text{Equation 4.2}$$

where M_{SOA} [g] is the gravimetrically-determined mass of limonene SOA collected on the Teflon filter, F [mol/h] the flow rate of limonene into the reactor, MW_{lim} [g/mol] the molecular weight of limonene, and Δt [h] the duration of SOA generation.

Lead (II) nitrate ($\text{Pb}(\text{NO}_3)_2$; Merck AG, Dietikon, Switzerland; GR for analysis ACS, 107398) and cadmium (II) nitrate ($\text{Cd}(\text{NO}_3)_2$) particles were obtained by atomization of the salt solution in water (2 g/l). We used a constant output atomizer (TSI Inc., model 3076), and the aerosols were dried after flowing in a stream of filtered air across two diffusion dryers (TSI Inc., model 3062) filled with silica gel and connected in series. Under these conditions, the relative humidity after passage across both diffusion dryers was 5%. Particles were also collected on a Teflon membrane filter.

Carbonaceous particles. We analyzed three samples manufactured by Evonik Degussa GmbH (FS 101, Printex 60 and FW 2), two hexane soot samples that we produced with a co-flow burner under two different combustion conditions (rich and lean flame) and two Diesel soot samples. Except for the case of one of the Diesel soot samples, all the carbonaceous particles were produced under controlled conditions, and had very different physico-chemical properties depending on the production method and conditions. These compounds were chosen in anticipation of the sampling campaign in the bus depots, where we expected high levels of particles generated by combustion due to the operation of many gasoline and Diesel engines.

FS 101, Printex 60 and FW 2 are produced by three different processes, and therefore their physico-chemical properties are very different. Table 4.3 gathers technical data provided by Evonik Degussa GmbH (Frankfurt/Main, Germany). FS 101 is characterized by a rather large average primary particle size, a very low BET (Brunauer/Emmett/Teller) surface area and a neutral pH value. Printex 60, which is produced by the “furnace black” process, is characterized by a higher BET surface area and an alkaline pH, presumably due to the presence of basic oxides on the surface. Finally, FW 2 underwent an oxidative post-treatment using NO₂, ozone or other oxidants, significantly increasing acidic surface groups. Therefore, FW 2 has a high BET surface area and its pH is low.

Table 4.3: Technical data of carbonaceous particles manufactured by Evonik Degussa GmbH (brochure “Pigment blacks - Technical Data Europe”, 2008).

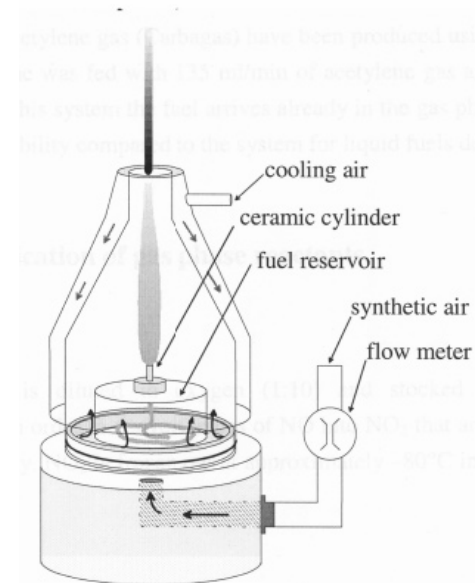
Properties	FS 101	Printex 60	FW 2 ^a
Type	Lamp black	Regular colour furnace	High colour gas
Volatile matter at 950°C [%]	-	1	16.5
pH value	7.5	10	2.5
BET surface area [m ² /g]	20	115	460
Average primary particle size [nm]	95	21	13

^a FW 2 sample was acquired in the 1990s. Values reported in this Table refer to data published at that time (the BET value for the surface area has changed since then).

A small co-flow burner (Figure 4.3) was used to produce soot samples under controlled conditions. The burner consists of a diffusion flame fed by a controlled stream of air. The fuel is transported by capillarity across a cotton wick, which is topped by a Pyrex disc (Verrerie de Carouge SARL, Carouge, Switzerland). The fuel flow is controlled by the use of Pyrex discs of different porosity. Hexane soot was obtained using this device at two operating conditions, namely rich flame and lean flame. A rich flame refers to a high fuel/air ratio, and was obtained by using a Pyrex disc with porosity in the range of 41-100 µm and an air flow rate of

1.375 l/min. On the contrary, the lean flame has a lower fuel/air ratio, and was obtained using a Pyrex disc with porosity in the range of 11-16 μm and an air flow rate of 1.75 l/min. The flame soot was directly deposited onto a glass Petri dish of 4 cm inner diameter (ID) and weighed gravimetrically, typically several mg. In order to distinguish hexane soot from a rich and a lean flame, we used the products of the heterogeneous reaction of NO_2 on the corresponding soot as a discriminating feature. The criterion between a rich and lean hexane flame was the exclusive HONO production resulting from the heterogeneous reaction on soot from the rich and NO generation from the lean flame (Stadler and Rossi, 2000). In order to control the quality of soot on a routine basis, frequent checks using the Knudsen flow reactor were performed.

Figure 4.3: Schematic drawing of the co-flow burner used to produce hexane soot (taken from Alcalá-Jornod and Rossi, 2004).



Two Diesel soot samples were also investigated using the Knudsen flow reactor. First, a commercially available certified Diesel particulate matter (SRM 2975) was purchased from the National Institute of Standards and Technology (NIST). This standard reference material (SRM) was collected from a Diesel engine of a heavy duty industrial forklift. Secondly, during the field campaign in the bus depot 2 (22/23.05.2006), we recovered Diesel soot deposited in a Diesel particle filter (DPF) of a heavy duty urban bus engine. This soot sample stayed for a long time in the particle filter, and was expected to be highly oxidized due to a long exposure to the exhaust gas, especially to NO_x . This sample is called hereafter “Diesel BD 2”. For both Diesel soot samples, a few milligrams of powder were weighed on a teflonized Petri dish and installed in the sample-holder of the Knudsen flow reactor.

Titanium dioxide (TiO_2). TiO_2 samples were analyzed within the framework of the NANOTOX project. TiO_2 is an insoluble white powder that is manufactured worldwide in large quantities for use in a wide range of applications, such as paint, cosmetics, plastics, and some foods. For a long time, this compound has been considered as toxicologically inert, but experimental studies undertaken with animals suggested possible carcinogenic effects and pulmonary lesions due to TiO_2 . Since then, toxicological and epidemiological studies have

been undertaken in order to assess health hazards due to an exposure to TiO₂. According to the latest results, the International Agency for Research on Cancer (IARC) has classified TiO₂ in group 2B: possibly carcinogenic to human (International Agency for Research on Cancer, 2008).

Two TiO₂ samples were purchased from Sigma-Aldrich Chemie GmbH (Buchs, Switzerland): TiO₂ anatase (637254, hereafter called “TiO₂ 15”) and TiO₂ mixture of rutile and anatase (634662, hereafter called “TiO₂ 50”). TiO₂ 15 and TiO₂ 50 had primary particle diameters of 15 and 25-75 nm. TiO₂ P25, an often used catalyst support of technical significance, was purchased from Evonik Degussa GmbH (Frankfurt/Main, Germany). TiO₂ 15, TiO₂ 50 and TiO₂ P25 contained 98, 65 and 80-90% (w/w) anatase balanced by rutile. For the three TiO₂ samples, a few milligrams of powder were weighed on a teflonized Petri dish and installed in the sample-holder of the Knudsen flow reactor.

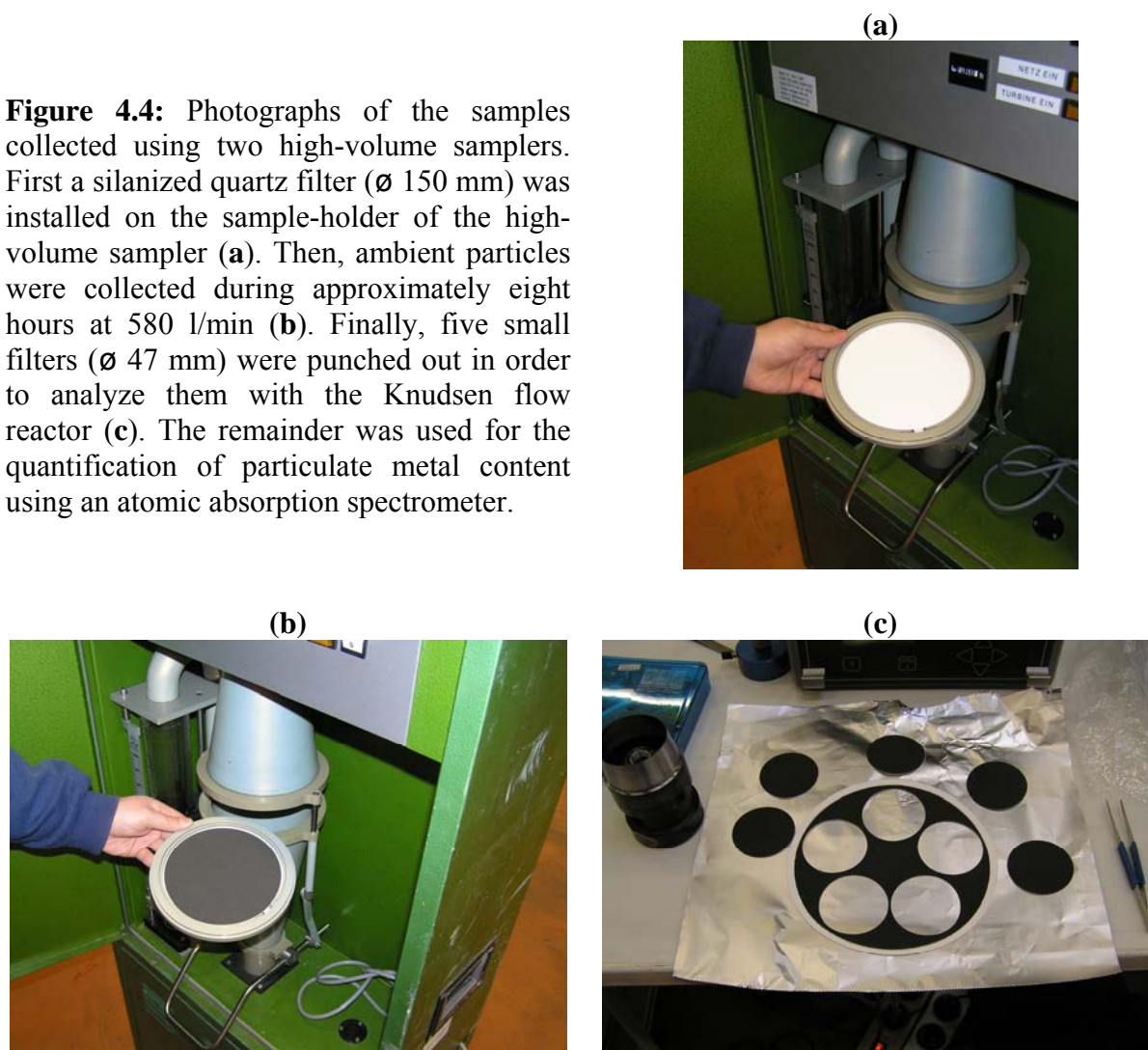
Ambient particles. Ambient particles were collected in the bus depots on filters using two high-volume samplers (Digitel, model DH 77). Filters used during the sampling had to allow the passage of considerable air flows across the high-volume samplers (580 l/min), and at the same time they had to be chemically inert towards the probe gases used in the Knudsen flow reactor. We evaluated several filter types and passivation methods, and decided to use quartz microfiber filters, after chemical passivation with a reactive silane reagent in order to decrease their reactivity towards the probe gases.

We first cut filters of 150 mm diameter and several filters of 47 mm diameter for the blanks from quartz microfiber sheets (Whatman; QM-A, 20x23 cm sheets, 1851865). These filters were cleaned in a solution of chromic acid for four hours, and were washed seven times with tap water and three times with bidistilled water. The filters were then dried at 150°C during two hours, and were left overnight in a solution of 20% dichlorodimethylsilane (Acros Organics, distributor in Switzerland: Chemie Brunschwig AG, Basel; 99+%, 11331-0010) in toluene inside a desiccator, in order to avoid evaporation of toluene and reaction of the silane with air moisture. The following day, the filters were washed three times with toluene and once with distilled methanol, and were finally dried at 120°C during one hour. It should be stressed that prior to the field campaign, the efficiency of eight silanes (dichlorodimethylsilane, dichlorodiphenylsilane, chlorotrimethylsilane,

dimethyloctadecylchlorosilane, dichloromethyloctadecylsilane, dichlorodiethylsilane and dichloromethylphenylsilane) had been tested before choosing dichlorodimethylsilane.

After the preparation of the filters, ambient particles were sampled in each bus depot using two high-volume samplers located side by side (Figure 4.4(a)). Particles were collected on silanized quartz microfiber filters of 150 mm diameter at an air flow of 580 l/min during approximately eight hours for each day of sampling (Figure 4.4(b)). An impactor was installed above the filter-holder in order to remove particles larger than 4 μm . Immediately after sampling, the filters of 150 mm diameter were cut into five smaller filters of 47 mm diameter (Figure 4.4(c)) using a device specially designed for that purpose, in order to avoid artefacts due to filter handling. The filters were then stored in a desiccator filled with argon until the analysis with the Knudsen flow reactor, in order to avoid oxidation of the particle surface between the sampling and the analysis. This experimental setup allowed for a total of ten small filters of 47 mm diameter to be used for surface chemical titration using the Knudsen flow reactor. The remainder was used for the quantification of particulate metal content using an atomic absorption spectrometer (see Chapter 3).

Figure 4.4: Photographs of the samples collected using two high-volume samplers. First a silanized quartz filter (\varnothing 150 mm) was installed on the sample-holder of the high-volume sampler (a). Then, ambient particles were collected during approximately eight hours at 580 l/min (b). Finally, five small filters (\varnothing 47 mm) were punched out in order to analyze them with the Knudsen flow reactor (c). The remainder was used for the quantification of particulate metal content using an atomic absorption spectrometer.



4.2.4 Particle mass

The particle mass deposited on the filters was measured by gravimetry using an analytical balance (Mettler Toledo, model AT 201). For the laboratory-generated aerosols, the Teflon filters were weighed before and after aerosol generation. For the field campaign, five small filters of 47 mm diameter coming from a single high-volume sampler and five blanks, which had been silanized in the same batch, were let to stabilize overnight at constant relative humidity and temperature. Then all the filters were weighed, and the particle mass deposited on the filters was calculated by subtracting the average mass of the blanks from the loaded filters.

4.2.5 Particle size distribution

A scanning mobility particle sizer (SMPS) was used to monitor the particle size distribution and surface area of the laboratory-generated aerosols (limonene SOA, $\text{Pb}(\text{NO}_3)_2$ and

$\text{Cd}(\text{NO}_3)_2$). This equipment and the conditions were already presented in Chapter 3. We also calculated the geometric standard deviation (σ_g), in order to provide an indication of the particle dispersion. σ_g was calculated according to Equation 4.3:

$$\ln \sigma_g = \sqrt{\frac{\sum_{i=m}^n N_i (\ln d_i - \ln d_g)^2}{N - 1}} \quad \text{Equation 4.3}$$

where m is the first channel, n the last channel, N_i [particle/cm³] the concentration within the channel i , d_i [nm] the midpoint diameter for size channel i , d_g [nm] the geometric mean diameter, and N [particle/cm³] the total concentration.

The normalization of the titration results of carbonaceous particles (FS 101, Printex 60, FW 2, hexane soot, SRM 2975 and Diesel BD 2) and TiO_2 samples was performed using the values of the BET surface area specified by the manufacturer rather than the measured particle size distributions based on mobility diameters. We stress that the specific surface area calculated using the SMPS and that measured by the BET technique may be significantly different. Indeed, the mobility measurement considers each particle as a sphere, while the N_2 adsorption used in the BET technique allows taking into account the shape and the porosity of the particles. This may lead to a significantly higher value of the specific surface area determined by the BET technique, which may be considered as an upper limit to the surface area determined by the effective mobility diameter. Therefore, we may not directly compare the surface area of samples for which the BET value was used with that of the aerosol samples measured using the SMPS.

For the field campaign, further equipment had to be added for aerosol characterization, because the upper size limit of the SMPS was fixed at 750 nm, while the high-volume samplers were set to collect particles up to 4 μm (PM_{10}). In order to take into account the particle fraction between 750 nm and 4 μm , we used in addition an Andersen type cascade impactor, which has also been presented in Chapter 3. At each sampling site, the Andersen impactor was installed next to the high-volume samplers, and the sampling was performed simultaneously. The particle mass deposited on each filter stage was measured gravimetrically, and the four stages corresponding to sizes between 700 nm and 4.7 μm were used to calculate the missing particle surface area when using the SMPS. The particle mass

was converted into surface area using the surface/volume ratio and an estimated mass density of 1.8 g/cm³. Finally, data collected with the SMPS (for particles smaller than 750 nm) and the Andersen impactor (for particles in the range 750 nm to 4 µm) at each sampling site were combined to determine the size distribution of all PM₄ samples collected using the high-volume samplers. Calculations indicated that approximately 10 to 30% of the total PM₄ surface area was due to particles in the size range 750 nm to 4 µm. Therefore the use of the Andersen impactor was necessary to correct data obtained from the SMPS by adding the missing surface area. We are aware of the approximation due to the transfer of this correction factor obtained from an aerodynamic (Andersen impactor) to a mobility measurement (SMPS). However, we deem this difference to be less than 10%.

Moreover, it should be stressed that the use of the high-volume samplers at a high flow rate (580 l/min) could promote the agglomeration of particles on the filters. Unfortunately, we did not have the opportunity to use electron microscopy to observe particles collected in the field. Thus, it was impossible to assess the agglomeration state of the samples. This information may be important for results obtained with the Knudsen flow reactor, since agglomeration reduces the particle surface area available for gas probing. Therefore, results obtained for aerosols collected in the field are perhaps underestimated.

4.2.6 Kinetics of heterogeneous titration reactions

Besides the quantification of surface functional groups on particulate matter, we also measured the uptake kinetics of reactions between aerosols and probe gases, in order to obtain further information about the reactivity of the collected particulate matter. The kinetic parameter studied within the framework of this project was the initial uptake coefficient γ_0 , which corresponds to the probability that a collision between a probe gas and a sample leads to a chemical reaction just after opening the sample compartment. The γ_0 value can range from 0, which corresponds to no reaction, to 1, when each collision between the probe gas and the sample leads to an uptake of the probe gas. For the case of γ_0 equal to 1, the reaction will be saturated very quickly. The uptake coefficient γ_0 was calculated using Equation 4.4:

$$\gamma_0 = \frac{k_{\text{uni}}}{\omega}$$

Equation 4.4

where k_{uni} [s^{-1}] is the first order rate constant for the uptake reaction, and ω [s^{-1}] the collision frequency of a molecule with the geometric surface area of a sample. k_{uni} was calculated using Equation 4.5:

$$k_{\text{uni}} = \left(\frac{S_0}{S_R} - 1 \right) \cdot k_{\text{esc}} \quad \text{Equation 4.5}$$

where S_0 [V] is the MS signal at steady state, and S_R [V] the MS signal immediately after the beginning of the reaction, as shown on Figure 4.2(a). k_{esc} [s^{-1}] is the escape rate constant of the probe gas from the reactor, and is measured experimentally. Finally, in order to calculate γ_0 in Equation 4.4, ω was determined as follows:

$$\omega = \left(\frac{\bar{c}}{4 \cdot V} \right) \cdot A_s \quad \text{Equation 4.6}$$

where \bar{c} [cm/s] is the mean velocity of the gas-phase probe molecule, V [cm^3] the volume of the reactor, and A_s [cm^2] the geometric surface area of the sample. Further information on kinetic parameters can be found in Caloz *et al* (1997).

4.2.7 Statistical analyses

Statistical analyses were performed using SYSTAT for Windows, version 10.2. The Spearman's rank correlation coefficient was used to test the correlation between reaction kinetics and uptakes of probe gases in the Knudsen flow reactor. Correlations were considered significant when $p < 0.05$.

4.3 Results and discussion

Table 4.4 shows results of particle surface probing for laboratory-generated aerosols, carbonaceous aerosols and TiO_2 samples. The first three entries (limonene SOA, $\text{Pb}(\text{NO}_3)_2$ and $\text{Cd}(\text{NO}_3)_2$) correspond to samples collected on filters, while the other samples have been investigated in powder form. The number of gas-phase probe molecules taken up by the samples was divided either by the particle mass (**a**), or by the particle surface area (**b**) as discussed above. In order to facilitate the comparison between these values, we also calculated the approximate number of molecules per cm^2 forming a complete molecular

monolayer on the particle surface using the density of each probe (c). For each result given in Table 4.4, the combined uncertainty due to the measurements of the mass, surface area and probe gas uptake has been calculated. The limit of detection was calculated for each probe gas by the average of the combined uncertainty of each sample.

Table 4.4: Titration experiments on laboratory-generated aerosols, carbonaceous aerosols and TiO₂ samples using the Knudsen flow reactor.

Samples	BET surface	N(CH ₃) ₃	NH ₄ OH	CF ₃ COOH	HCl	O ₃	NO ₂
		1 monolayer : 3.5 · 10 ¹⁴ [# /cm ²]	1 monolayer : 7.8 · 10 ¹⁴ [# /cm ²]	1 monolayer : 4.0 · 10 ¹⁴ [# /cm ²]	1 monolayer : 7.3 · 10 ¹⁴ [# /cm ²]	1 monolayer : 7.4 · 10 ¹⁴ [# /cm ²]	1 monolayer : 7.1 · 10 ¹⁴ [# /cm ²]
		limit of detection : 1.7 · 10 ¹⁴ [# /mg] 2.2 · 10 ¹² [# /cm ²]	limit of detection : 4.1 · 10 ¹⁶ [# /mg] 1.4 · 10 ¹⁴ [# /cm ²]	limit of detection : 9.2 · 10 ¹³ [# /mg] 1.1 · 10 ¹² [# /cm ²]	limit of detection : 7.4 · 10 ¹⁴ [# /mg] 4.8 · 10 ¹² [# /cm ²]	limit of detection : 7.2 · 10 ¹⁴ [# /mg] 2.8 · 10 ¹² [# /cm ²]	limit of detection : 1.3 · 10 ¹⁵ [# /mg] 1.6 · 10 ¹² [# /cm ²]
limonene SOA		(a) 1.7 (±0.1) · 10 ¹⁵ (b) 1.3 (±0.1) · 10 ¹³ (c) 3.7%	(a) 5.6 (±0.4) · 10 ¹⁷ (b) 3.9 (±0.3) · 10 ¹⁵ (c) 500.0%	(a) 2.6 (±0.2) · 10 ¹⁵ (b) 1.1 (±0.2) · 10 ¹³ (c) 2.8%	not detected	(a) 9.0 (±0.8) · 10 ¹⁵ (b) 5.7 (±0.5) · 10 ¹³ (c) 7.7%	not detected
Pb(NO ₃) ₂		(a) 1.5 (±0.2) · 10 ¹⁵ (b) 1.6 (±0.2) · 10 ¹³ (c) 4.6%	(a) 1.3 (±0.1) · 10 ¹⁷ (b) 1.6 (±0.1) · 10 ¹⁵ (c) 205.1%	(a) 5.2 (±0.4) · 10 ¹⁴ (b) 8.2 (±0.7) · 10 ¹² (c) 2.1%	(a) 1.3 (±0.1) · 10 ¹⁶ (b) 2.0 (±0.1) · 10 ¹⁴ (c) 27.0%	not detected	not tested
Cd(NO ₃) ₂		(a) 8.1 (±1.6) · 10 ¹⁴ (b) 7.3 (±1.4) · 10 ¹² (c) 2.1%	(a) 8.6 (±0.7) · 10 ¹⁷ (b) 6.3 (±0.5) · 10 ¹⁵ (c) 807.7%	(a) 1.3 (±0.1) · 10 ¹⁵ (b) 2.2 (±0.2) · 10 ¹³ (c) 5.5%	(a) 1.0 (±0.1) · 10 ¹⁷ (b) 9.0 (±0.8) · 10 ¹⁴ (c) 121.6%	not detected	not tested
FS 101	20 [m ² /gr]	(a) 5.8 (±1.4) · 10 ¹⁴ (b) 2.9 (±0.7) · 10 ¹² (c) 0.83%	not detected	(a) 1.8 (±0.2) · 10 ¹⁵ (b) 9.2 (±1.0) · 10 ¹² (c) 2.3%	not detected	(a) 7.3 (±0.6) · 10 ¹⁷ (b) 3.7 (±0.3) · 10 ¹⁵ (c) 500.0%	(a) 2.0 (±0.2) · 10 ¹⁵ (b) 9.8 (±0.8) · 10 ¹² (c) 1.4%
Printex 60	115 [m ² /gr]	(a) 1.5 (±0.3) · 10 ¹⁵ (b) 1.3 (±0.2) · 10 ¹² (c) 0.37%	not detected	(a) 4.0 (±0.4) · 10 ¹⁵ (b) 3.5 (±0.3) · 10 ¹² (c) 0.88%	not detected	(a) 6.4 (±0.7) · 10 ¹⁶ (b) 5.6 (±0.6) · 10 ¹³ (c) 7.6%	(a) 7.4 (±0.6) · 10 ¹⁵ (b) 6.4 (±0.5) · 10 ¹² (c) 0.90%
FW 2	460 [m ² /gr]	(a) 2.4 (±0.2) · 10 ¹⁷ (b) 5.2 (±0.5) · 10 ¹³ (c) 14.9%	(a) 4.4 (±0.4) · 10 ¹⁷ (b) 9.6 (±0.8) · 10 ¹³ (c) 12.3%	(a) 4.5 (±0.5) · 10 ¹⁶ (b) 9.9 (±1.1) · 10 ¹² (c) 2.5%	not detected	(a) 4.4 (±0.4) · 10 ¹⁷ (b) 9.6 (±0.8) · 10 ¹³ (c) 13.0%	(a) 4.1 (±0.3) · 10 ¹⁶ (b) 8.9 (±0.8) · 10 ¹² (c) 1.3%
hexane rich flame	48.9 [m ² /gr]	(a) 1.8 (±0.1) · 10 ¹⁵ (b) 3.6 (±0.3) · 10 ¹² (c) 1.0%	(a) 2.1 (±0.2) · 10 ¹⁷ (b) 4.4 (±0.3) · 10 ¹⁴ (c) 56.4%	(a) 1.8 (±0.2) · 10 ¹⁵ (b) 3.8 (±0.3) · 10 ¹² (c) 0.95%	(a) 9.0 (±0.5) · 10 ¹⁵ (b) 1.8 (±0.1) · 10 ¹³ (c) 2.4%	(a) 9.5 (±0.8) · 10 ¹⁷ (b) 1.9 (±0.2) · 10 ¹⁵ (c) 256.8%	(a) 2.6 (±0.2) · 10 ¹⁶ (b) 5.2 (±0.4) · 10 ¹³ (c) 7.3%
hexane lean flame	74.3 [m ² /gr]	(a) 2.8 (±0.2) · 10 ¹⁵ (b) 3.7 (±0.3) · 10 ¹² (c) 1.1%	(a) 3.3 (±0.3) · 10 ¹⁷ (b) 4.5 (±0.4) · 10 ¹⁴ (c) 57.7%	(a) 3.2 (±0.3) · 10 ¹⁵ (b) 4.3 (±0.4) · 10 ¹² (c) 1.1%	(a) 3.1 (±0.2) · 10 ¹⁵ (b) 4.2 (±0.2) · 10 ¹² (c) 0.57%	(a) 2.0 (±0.2) · 10 ¹⁸ (b) 2.7 (±0.2) · 10 ¹⁵ (c) 364.9%	(a) 1.9 (±0.2) · 10 ¹⁶ (b) 2.5 (±0.2) · 10 ¹³ (c) 3.5%
SRM 2975	91 [m ² /gr]	(a) 4.9 (±0.5) · 10 ¹⁶ (b) 5.3 (±0.5) · 10 ¹³ (c) 15.1%	(a) 1.3 (±0.1) · 10 ¹⁸ (b) 1.5 (±0.1) · 10 ¹⁵ (c) 192.3%	not detected	(a) 2.4 (±1.3) · 10 ¹⁵ (b) 2.6 (±1.5) · 10 ¹² (c) 0.35%	(a) 8.3 (±0.7) · 10 ¹⁵ (b) 9.1 (±0.8) · 10 ¹² (c) 1.2%	(a) 3.2 (±0.3) · 10 ¹⁵ (b) 3.5 (±0.3) · 10 ¹² (c) 0.49%
Diesel BD 2	53.1 [m ² /gr]	(a) 3.1 (±0.3) · 10 ¹⁶ (b) 5.8 (±0.6) · 10 ¹³ (c) 16.6%	(a) 1.4 (±0.1) · 10 ¹⁸ (b) 2.6 (±0.2) · 10 ¹⁵ (c) 333.3%	not detected	(a) 4.6 (±0.4) · 10 ¹⁶ (b) 8.7 (±0.7) · 10 ¹³ (c) 11.8%	(a) 1.3 (±0.1) · 10 ¹⁷ (b) 2.5 (±0.2) · 10 ¹⁴ (c) 33.8%	(a) 1.3 (±0.1) · 10 ¹⁶ (b) 2.4 (±0.2) · 10 ¹³ (c) 3.4%
TiO ₂ 15 nm	210 [m ² /gr]	(a) 1.4 (±0.1) · 10 ¹⁷ (b) 6.6 (±0.6) · 10 ¹³ (c) 18.9%	(a) 2.7 (±0.2) · 10 ¹⁸ (b) 1.1 (±0.1) · 10 ¹⁵ (c) 141.0%	(a) 1.1 (±0.1) · 10 ¹⁷ (b) 5.3 (±0.5) · 10 ¹³ (c) 13.3%	(a) 3.9 (±0.2) · 10 ¹⁷ (b) 1.9 (±0.1) · 10 ¹⁴ (c) 25.7%	(a) 1.9 (±0.3) · 10 ¹⁶ (b) 9.1 (±1.3) · 10 ¹² (c) 1.2%	no reaction
TiO ₂ 50 nm	21.4 [m ² /gr]	(a) 3.2 (±0.3) · 10 ¹⁶ (b) 1.5 (±0.2) · 10 ¹⁴ (c) 42.9%	(a) 1.5 (±0.1) · 10 ¹⁸ (b) 7.0 (±0.6) · 10 ¹⁵ (c) 897.4%	(a) 1.2 (±0.2) · 10 ¹⁶ (b) 5.7 (±0.9) · 10 ¹³ (c) 14.3%	(a) 3.9 (±0.2) · 10 ¹⁷ (b) 1.8 (±0.1) · 10 ¹⁵ (c) 243.2%	(a) 7.1 (±1.9) · 10 ¹⁵ (b) 3.3 (±0.9) · 10 ¹³ (c) 4.5%	no reaction
TiO ₂ P25	50 [m ² /gr]	(a) 6.4 (±0.6) · 10 ¹⁶ (b) 1.3 (±0.1) · 10 ¹⁴ (c) 37.1%	(a) 3.9 (±0.3) · 10 ¹⁸ (b) 7.7 (±0.6) · 10 ¹⁵ (c) 987.2%	(a) 1.1 (±0.2) · 10 ¹⁶ (b) 2.3 (±0.4) · 10 ¹³ (c) 5.8%	(a) 1.4 (±0.1) · 10 ¹⁷ (b) 2.8 (±0.2) · 10 ¹⁴ (c) 37.8%	(a) 6.4 (±0.5) · 10 ¹⁶ (b) 1.3 (±0.1) · 10 ¹⁴ (c) 17.6%	no reaction

(a) Number of gas-phase probe molecules taken up per mg of aerosol [molecule/mg];

(b) Number of gas-phase probe molecules taken up per cm² of aerosol [molecule/cm²];

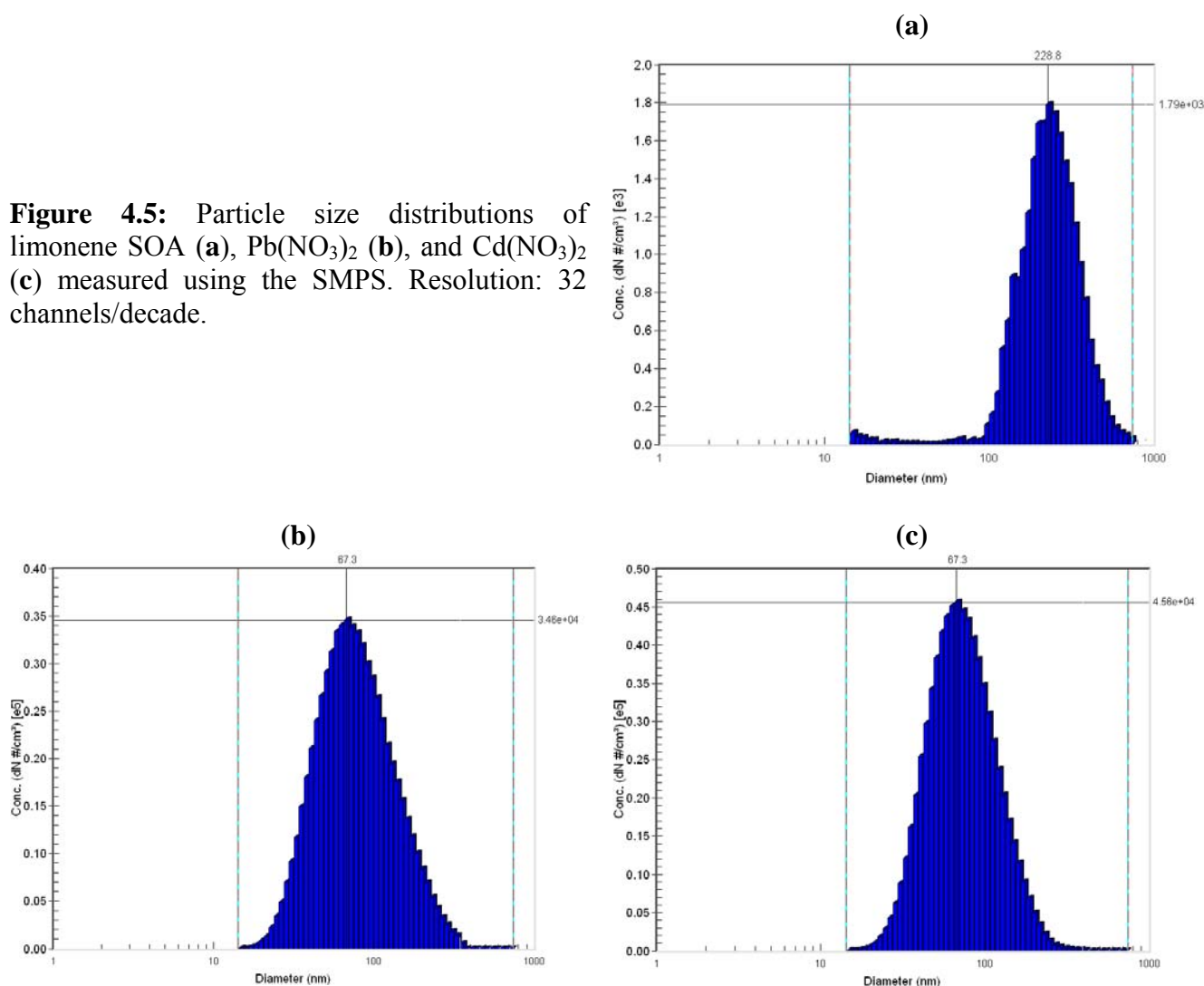
(c) % of a complete molecular monolayer.

Values between brackets: combined uncertainty due to the measurements of the mass, surface area and probe gas uptake.

“not detected”: results below the limit of detection in both units (molecule/mg and molecule/cm²).

4.3.1 Laboratory-generated aerosols

Figure 4.5 shows a few examples of particle size distributions measured using the SMPS. We notice that laboratory-generated aerosols have systematically a single mode, and follow a perfect log-normal distribution. Inorganic particles ($\text{Pb}(\text{NO}_3)_2$ and $\text{Cd}(\text{NO}_3)_2$) obtained by atomization have a mode at approximately 67 nm (Figures 4.5(b) and 4.5(c)), while typical diameters of limonene SOA were much larger (more than 200 nm in Figure 4.5(a)), certainly because of particle agglomeration during the generation of SOA in the reactor. The geometric standard deviations (σ_g) were 1.58 for limonene SOA, and 1.75 for inorganic particles. We note that the used equipment did not allow checking whether particles larger than 750 nm were generated. According to the particle size distributions shown in Figure 4.5, we make the assumption that the contribution to the total surface area of particles larger than 750 nm is small.



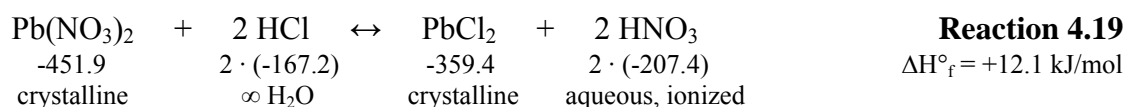
The yield of limonene SOA, calculated using Equation 4.2, indicated that only 2% of the limonene used for SOA generation was converted into SOA and collected on the Teflon filter. In contrast, the yield was much higher (55%) in the previous study of Demirdjian and Rossi (2005). Actually, the present limonene SOA sample and that of Demirdjian and Rossi (2005) were not generated under the same conditions. The main difference between both conditions was the residence time of limonene in the reactor, which was approximately 2 minutes for the conditions of Demirdjian and Rossi (2005), and 1 minute under the present conditions. This difference explains the low yield obtained under the present conditions. Moreover, previous publications highlighted reduced yields due to deposition and loss of particles to the walls of the reactors (Shilling *et al*, 2008).

Table 4.4 indicates that the surface of limonene SOA and inorganic particles contain acidic sites interacting with $\text{N}(\text{CH}_3)_3$, corresponding to 2-5% of a monolayer. The reactivity toward limonene SOA may be due to the presence of Lewis acidic functional groups, while the reactivity toward $\text{Pb}(\text{NO}_3)_2$ and $\text{Cd}(\text{NO}_3)_2$ may be due to the formation of stable complexes (Guilbault and Billedeau, 1971).

NH_2OH reacted to a large extent with all the samples. This result indicates the presence of an important amount of carbonyl functions on the surface of limonene SOA. However, reactions with $\text{Pb}(\text{NO}_3)_2$ and $\text{Cd}(\text{NO}_3)_2$ are more surprising. These reactions might be due to the complexation of metal ions by hydroxylamine. The number of NH_2OH taken up corresponded to several molecular monolayers (up to eight monolayers for $\text{Cd}(\text{NO}_3)_2$). This suggests that during the time scale of a titration experiment (approximately 10 minutes), subsurface reactions with NH_2OH , or diffusion exchange and subsequent reaction of carbonyl compounds from within the bulk of the aerosol with NH_2OH may take place, akin to the NH_2OH reaction with limonene SOA (Demirdjian and Rossi, 2005).

Of both acidic probes which were used to quantify basic sites on the particle surface, the uptake of HCl was higher than for CF_3COOH on $\text{Pb}(\text{NO}_3)_2$ and $\text{Cd}(\text{NO}_3)_2$. CF_3COOH is a stronger acid in the gas-phase, and therefore was expected to react with more basic sites, even with the weakest ones. Thus the extensive reaction of HCl in comparison to CF_3COOH may not be explained exclusively on the basis of gas-phase acidities. Enthalpy changes of these reactions have been calculated using thermodynamic data (Wagman *et al*, 1982), and may provide an explanation for these changes. However, thermodynamic data for trifluoroacetic

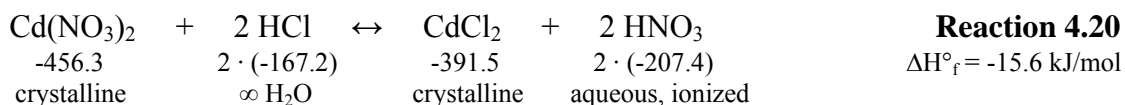
acid and trifluoroacetates are not available in the literature. Therefore we used the analogous values given for acetic acid and acetates. For instance in the case of $\text{Pb}(\text{NO}_3)_2$, results indicate that the reaction with HCl is less endothermic (Reaction 4.19: $\Delta H^\circ_f = +12.1$ kJ/mol) than that with CH_3COOH (Reaction 4.18: $\Delta H^\circ_f = +45.3$ kJ/mol), and therefore should be favored during the titration experiment in the Knudsen flow reactor.



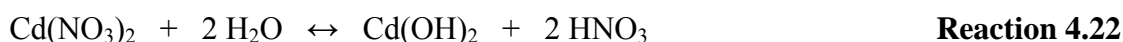
Ozone reacted only with limonene SOA (7.7% of a complete molecular monolayer, Table 4.4). However, in preliminary study (Demirdjian and Rossi, 2005; DR), limonene SOA had not reacted with O_3 . The results for limonene SOA presented here suggest the presence of incomplete oxidation. This could be related to a shorter residence time of limonene in the reactor, or to a lower O_3 concentration in the reactor. Thus, limonene SOA obtained under the present conditions was less oxidized than that generated by DR. This may explain the difference in reactivity observed between both samples. Indeed, if limonene SOA is more oxidized, then more acidic sites and carbonyl functions will be expected. This is confirmed for the uptakes of $\text{N}(\text{CH}_3)_3$ and NH_2OH . Indeed, the uptake of $\text{N}(\text{CH}_3)_3$ corresponds to 5.0% of a monolayer for the DR sample, as compared to 3.7% for the present sample, confirming the presence of a higher number of acidic sites on the surface of the DR limonene SOA. For the surface densities of carbonyl functions, the uptake of NH_2OH corresponded to more than 31 monolayers for the DR sample, and five monolayers for the present sample, thus confirming a higher content of carbonyl functions for the DR sample.

Table 4.4 indicates that the reactivities of $\text{Pb}(\text{NO}_3)_2$ and $\text{Cd}(\text{NO}_3)_2$ towards all probe gases, except for the case of the non-interacting ozone, are significantly different from each other, although the oxidation state of the metal ion and the conditions used to generate these particles were the same. For the reactivity towards HCl, chemical thermodynamic properties of the Reactions 4.19 and 4.20 indicate that the reaction of HCl with $\text{Cd}(\text{NO}_3)_2$ is exothermic (Reaction 4.20: $\Delta H^\circ_f = -15.6$ kJ/mol), while that with $\text{Pb}(\text{NO}_3)_2$ is endothermic (Reaction 4.19: $\Delta H^\circ_f = +12.1$ kJ/mol). Therefore, Reaction 4.20 should be favored over Reaction 4.19,

which explains why the uptake of HCl is higher for $\text{Cd}(\text{NO}_3)_2$ ($9.0 \cdot 10^{14}$ molecule/ cm^2) than for $\text{Pb}(\text{NO}_3)_2$ ($2.0 \cdot 10^{14}$ molecule/ cm^2).



On the other hand, we can not exclude the formation of hydroxides during the generation of inorganic aerosols, according to Reactions 4.21 and 4.22. In this case, nitric acid (HNO_3) would evaporate, while $\text{Pb}(\text{OH})_2$ (Reaction 4.21) and $\text{Cd}(\text{OH})_2$ (Reaction 4.22) could be collected on the Teflon filters and react with HCl or CF_3COOH in the Knudsen flow reactor. Thus, it is possible that during the generation of inorganic aerosols, a mixture of nitrates and hydroxides is produced and collected on the Teflon filters.



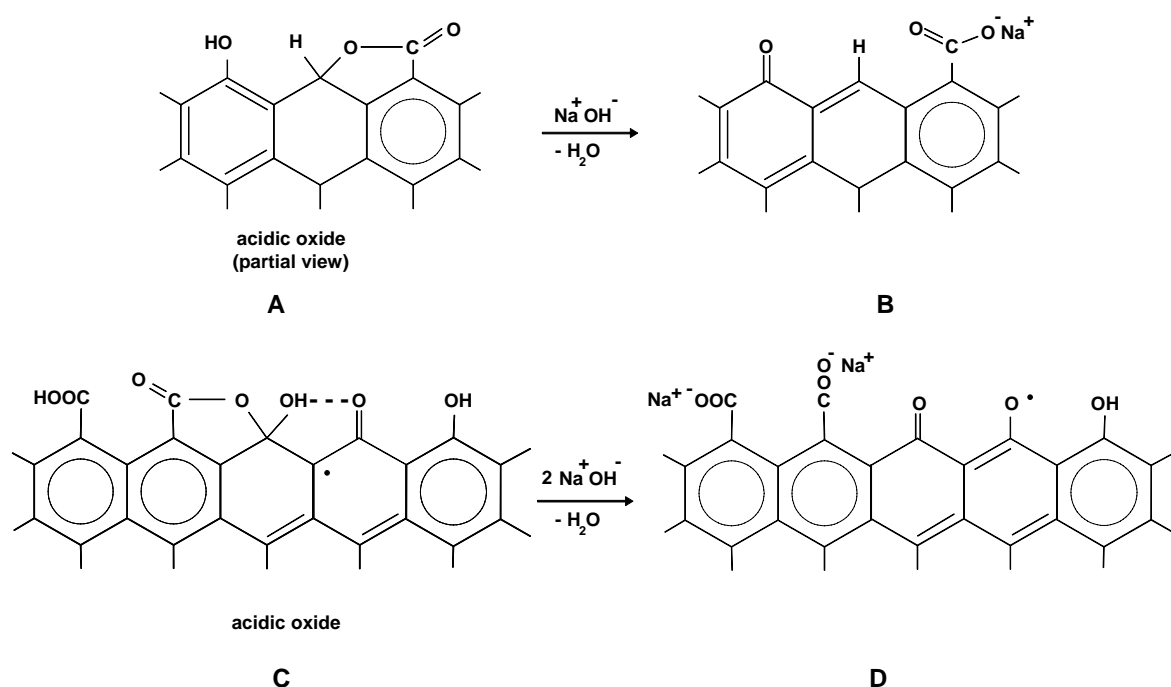
Boehm and Voll (1970) reported that basic oxides on the surface of amorphous carbon have more affinity towards CH_3COOH than HCl. Table 4.4 indicates a selectivity of limonene SOA for CF_3COOH over HCl uptake. Therefore, we assume that the generation of limonene SOA leads to the formation of basic oxides on the SOA surface.

4.3.2 Carbonaceous particles

Results obtained for $\text{N}(\text{CH}_3)_3$ (Table 4.4) reveal a significant presence of Lewis acidic functional groups among all investigated carbonaceous nanoparticles. We suspect the presence of carboxylic groups generated in the combustion process to be similar to the occurrence of mono- and dicarboxylic acids resulting from photooxidation processes of biogenic hydrocarbons that end up as SOA (Jacobson *et al*, 2000; Larsen *et al*, 2001; Liu *et al*, 2004; Lanz *et al*, 2008). In addition, combustion aerosols may contain acidic oxides (Figure 4.6), a subgroup of interfacial oxides on carbon, that have been detected on suitably activated amorphous carbon through heat treatment in the presence of dry oxygen (Hofmann and Ohlerich, 1950; Boehm *et al*, 1964; Boehm, 1994). Some of these acidic oxides may be the precursors of surface carboxylic groups in the presence of water vapour. In fact, Boehm *et al* (1964) detected four different acidic surface groups, classified from I to IV. Group I and II are identified as being a more and a less (lactone) acidic carboxylic group, respectively, with

group III and IV being a phenolic and carbonyl group, respectively. Figures 4.6(A) and 4.6(B) present a molecular model for groups I and II before and after reaction with a base, whereas Figures 4.6(C) (lactol) and 4.6(D) display the complete molecular model with all four groups before and after reaction with a base. These models are consistent with all chemical reactions occurring in solution which enable the identification of the surface functional groups present on activated charcoal or amorphous carbon. By analogy we conclude that the interfacial reaction of gas phase $\text{N}(\text{CH}_3)_3$ proceeds similarly to the reaction of NaOH with the acidic oxides in solution in view of the large proton affinity of $\text{N}(\text{CH}_3)_3$.

Figure 4.6: Carbonaceous surface acidic oxide neutralization.



A closer look at the results for $\text{N}(\text{CH}_3)_3$ in Table 4.4 reveals low uptakes (approximately 1% of a formal monolayer) for the amorphous carbon samples FS 101 and Printex 60, as well as for the hexane flame soot, both rich and lean flame. In contrast, uptakes of $\text{N}(\text{CH}_3)_3$ are high for FW 2, on the order of a factor of ten larger than the foregoing akin to the “aged” Diesel soot samples SRM 2975 and Diesel BD 2. According to the manufacturer’s specifications, the amorphous carbon FW 2 has been postoxidized using either HNO_3 or H_2O_2 , which would explain the increased uptakes of $\text{N}(\text{CH}_3)_3$ values compared to the other two samples, namely FS 101 and Printex 60. We take note that the “aged” Diesel soot samples SRM 2975 and Diesel BD 2 have an increased amount of acidic surface functional groups, indicating the high degree of oxidation of the surface of these samples. Based on these different studies, the

general apparent sequence for the $\text{N}(\text{CH}_3)_3$ reactivity on different carbonaceous aerosol is the following:

“aged” Diesel soot (SRM 2975 and Diesel BD 2) and amorphous carbon FW 2 > amorphous carbon Printex 60; FS 101; lean and rich hexane soot.

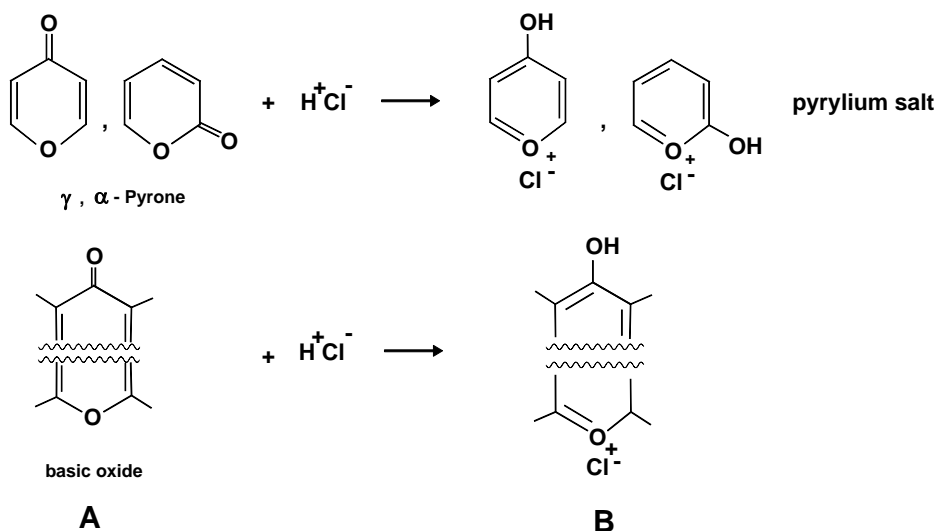
The uptakes of NH_2OH for the carbonaceous substrates displayed in Table 4.4 are significant and are at variance with the results of Demirdjian and Rossi (2005) for toluene soot from a diffusion flame. Of note is that the used co-flow burners for both toluene and hexane soot are of very similar design and operated under near identical flow conditions so that we expected soot of comparable properties (Stadler and Rossi, 2000; Alcalá-Jornod and Rossi, 2004). The amorphous carbon samples all show a low reactivity towards oxime formation upon NH_2OH exposure, whereas the aged Diesel particulate samples SRM 2975 and Diesel BD 2 show a high reactivity towards oxime formation. Both hexane flame soot samples lie in-between the Diesel soot models and the amorphous carbons inasmuch as reaction with NH_2OH is concerned which is noteworthy in view of our previous results on toluene flame soot which resulted in low values. Printex 60 again shows the lowest reactivity and qualifies for a carbon substrate with a low number of surface functional groups. Owing to the fact that oxime formation is general acid catalyzed (Roberts and Caserio, 1977), the differential reactivity of the present carbonaceous samples may either be attributed to the availability or mobility of the acid or to the number of available carbonyl groups at the interface. The elucidation of this aspect of surface titration must await further experiments as is the question regarding the types of surface carbonyl groups that are able to undergo oxime formation in addition to aldehydes and ketones. At this moment we rule out significant surface oxime formation by carboxylic groups because of the low uptakes of $\text{N}(\text{CH}_3)_3$ displayed in Table 4.4. These data suggest a surface density of carboxylic groups of less than a factor of ten with respect to the carbonyl groups.

An additional potential ambiguity concerns the basic nature of both NH_2OH and $\text{N}(\text{CH}_3)_3$, the former being a very much weaker base compared to the latter in both the gas phase (PA) as well as in solution (pK_a). If the uptakes of NH_2OH were due to the basicity alone, one would expect a smaller value than that for $\text{N}(\text{CH}_3)_3$ compared to hydroxylamine. In fact, just the opposite is true by factors of several up to ten, which points to a very limited involvement of the (weak) basicity of NH_2OH in its titration reaction. An obvious exception is that of FW 2

which has a large number of oxidized surface sites owing to its postoxidation treatment. We therefore tend to attribute the high reactivity of the aerosol surface towards NH_2OH to oxime formation according to Reaction 4.3 of Table 4.2, aldehydes and ketones being the sole carriers of oxime formation.

Acidic probe gases such as HCl and CF_3COOH interact with interfacial Lewis base sites B: whose molecular identity is not known *a priori*. Reactions 4.5 and 4.6 of Table 4.2 display the expected acid-base reactions with the generation of the acid-base complex or salt. It is noteworthy that HCl is a weaker acid than CF_3COOH in the gas phase, in contrast to aqueous solution where solvating effects predominate (Jolly, 1991). Owing to the smaller proton affinity compared to Cl^- (1350 vs 1395 kJ/mol), CF_3COO^- is less basic than Cl^- . Therefore, the gas phase acidity of the conjugate acid HCl is lower than that of CF_3COOH . The basic sites may be embodied by basic oxides whose existence on combustion aerosol particles and associated reactivity has been extensively documented in the past (Hofmann and Ohlerich, 1950; Boehm and Voll, 1970; Voll and Boehm, 1970; Voll and Boehm, 1971a; Voll and Boehm, 1971b). The basicity does not need to be centered on a N-containing base such as an amino group or pyridine, rather it may be located on O-containing “bases” or basic oxides such as displayed in Figure 4.7. Indeed, relevant acid-base reactions of α - and γ -pyrones that serve as model compounds for the basic oxides with HCl and CF_3COOH lead to pyrylium salts upon neutralization (Figure 4.7). In addition to the fact that certain carbonaceous substrates do not interact with either CF_3COOH or HCl (see Table 4.4), the reactivities of the acidic probe gases with the basic oxides are in general lower than for the corresponding basic $\text{N}(\text{CH}_3)_3$ probe. According to Table 4.4, SRM 2975 and Diesel BD 2 soot do not react with CF_3COOH whereas all three amorphous carbons FS 101, Printex 60 and FW 2 do. For the HCl probe, the inverse is true: FS 101, Printex 60 and FW 2 do not interact, whereas both SRM 2975 and Diesel BD 2 abundantly react with HCl .

Figure 4.7: Carbonaceous surface basic oxide neutralization. The wavy line indicates that both O-functionalities are not required to be part of the same aromatic ring system but may be separated by one or several aromatic rings.



Basic oxides are generated when amorphous carbon is heated under dry conditions to 900°C and subsequently exposed to a humid atmosphere at ambient temperature. Depending on specific combustion conditions such as temperature, richness of flame and residence time, it is not inconceivable that certain amorphous carbons may accumulate basic oxides on their surface. Boehm and Voll (1970) have found that acetic acid (CH_3COOH) is taken up on basic oxides located on the surface of amorphous carbon in quantities larger by a factor of three to six compared to HCl . We attribute this to charge delocalization in the acetate compared to the chloride ion thus rendering it more nucleophilic than acetate. The rate of the reverse Reactions 4.5 and 4.6 (Table 4.2) will therefore be faster for Cl^- than for CH_3COO^- , favoring the equilibrium towards the acid-base complex (salt) for acetate compared to chloride. In other words, the reaction kinetics of $\text{CH}_3\text{COO}^- + \text{H}^+ \rightarrow \text{CH}_3\text{COOH}$ is slower than $\text{Cl}^- + \text{H}^+ \rightarrow \text{HCl}$ owing to charge delocalization in the acetate anion. This will affect the equilibrium in Reactions 4.5 and 4.6 (Table 4.2) in agreement with the results of Boehm and Voll (1970). We therefore take the ratio $\text{uptake}_{\text{CF}_3\text{COOH}}/\text{uptake}_{\text{HCl}} > 1$ as a strong indication for the presence of basic oxides on the surface of these carbonaceous aerosol particles which does not preclude the presence of additional types of Lewis bases on the substrate at the same time. Of course, we make the assumption that the behaviour of CH_3COOH is expected to be similar to CF_3COOH as far as charge delocalization in the anion is concerned.

Considering the above ratio from data displayed in Table 4.4, we conclude that all the investigated amorphous carbons, namely FS 101, Printex 60 and FW 2 and to a lesser extent hexane soot from a lean flame apparently contain basic oxides on their surface. Diesel BD 2 soot is noteworthy for its high uptake of HCl in that it can bind significant amounts of HCl compared to all other substrates, perhaps with the exception of soot from a rich hexane flame. This Diesel soot, however, may have interacted with both the hot engine exhaust as well as with the atmosphere by virtue of its location in a DPF that may be exposed intermittently to the atmosphere and therefore to atmospheric bases such as ammonia. Moreover, the same substrate also contains a large number of acidic sites (see Table 4.4) in just about equal numbers. This shows that a soot surface may contain a large number of Lewis base as well as acidic surface functional groups that act independently of each other. A last remark concerns Printex 60 soot that once again shows a low number of basic sites compared to all other samples. In the end, the present titration technique does not give detailed molecular information on the sites reacting with both CF_3COOH and HCl. However, the ratio $\text{uptake}_{\text{CF}_3\text{COOH}}/\text{uptake}_{\text{HCl}}$ reveals precious information on the possible presence of pyrone structures. Moreover, the structure and identity of the remaining basic sites preferentially reacting with HCl remain to be elucidated in the future.

O_3 is a stronger oxidizer than NO_2 , therefore the extent of interaction of an oxidizable substrate with ozone will usually be larger than with NO_2 (see Table 4.4). The reaction product of O_3 on carbonaceous aerosol particles is O_2 (Stephens *et al*, 1986) and of NO_2 either HONO and/or NO (Gerecke *et al*, 1998), depending on the nature of the adsorbed organic phase. Olefins are practically the only hydrocarbons that quickly react with O_3 in gas phase ozonolysis reactions, the products and mechanism of which are well established (Finlayson-Pitts and Pitts, 2000). In contrast, reactions of gas-phase polycyclic aromatic hydrocarbons (PAHs) with O_3 are slow, except in cases where part of the hydrocarbon retains an olefinic character, such as for example in azulene, acenaphthylene and indene (Atkinson and Aschmann, 1988; Atkinson *et al*, 1992; Kwok *et al*, 1997; Reisen and Arey, 2002). In contrast, the reaction rate constant for the reaction of O_3 with PAH's adsorbed on SiO_2 , graphite or Diesel soot is larger by two-to-three orders of magnitude compared to the corresponding reaction of gas phase PAH's (Kahan *et al*, 2006; Perraudin *et al*, 2007a; Perraudin *et al*, 2007b; Kwamena *et al*, 2007) when the disappearance of the PAH in the presence of O_3 is monitored. The fundamental reason for this discrepancy is unclear at the moment, but it may be related to the nature of the adsorption site on the carbonaceous

substrate. A significant fraction, namely up to 70% of the PAH's adsorbed on graphite and amorphous carbon resists oxidative decay in the presence of O_3 , whereas the decay is quantitative for PAH's adsorbed on SiO_2 (Perraudin *et al*, 2007a). A similar situation holds for reactions of NO_2 with PAH's adsorbed on Diesel soot and silica, the competitive kinetics of which with OH free radical has been studied by Perraudin *et al* (2005) and by Esteve *et al* (2006). Slower by four orders of magnitude compared to OH, the NO_2 /PAH reaction retains some structure-specific aspects but is deemed not to be of any atmospheric importance.

Concerning the interaction with O_3 and NO_2 , both types of hexane flame soot generated in the laboratory from a diffusion flame have a functional group density larger by at least a factor of ten compared to all other carbonaceous substrates. In going from a rich to a lean hexane flame, the result for NO_2 displayed in Table 4.4 is as expected, that is the uptake of NO_2 for the rich flame soot is larger by a factor of two compared to the lean flame soot. We assume that a rich flame generates an adsorbed organic phase that is less oxidized, hence interacts to a larger extent with NO_2 . In contrast, when considering the analogous results for O_3 as a probe gas interacting with hexane flame soot the ordering is inversed with values differing by only 50%. Therefore, the reactivity of both hexane flame soots towards O_3 is apparently very similar. The SRM 2975 as well as all three amorphous carbon samples have low uptakes of NO_2 , indicating their advanced state of surface oxidation, in contrast to hexane flame soot that may be characterized by a fairly reduced surface owing to the fact that we deal with carbonaceous particles, the atmospheric aging of which has not yet set in. An obvious exception is the Diesel BD 2 sample that apparently retains its reducing power despite its age, sample history and number of carboxylic groups based on $N(CH_3)_3$ uptake (see Table 4.4). In keeping with the relative oxidizing power of O_3 vs NO_2 , the uptakes of O_3 are larger by a factor of ten or more compared to NO_2 for the corresponding substrates.

4.3.3 TiO_2 particles

Titanium dioxide (TiO_2) has both surface $-OH$ groups as well as Lewis acid, but no Brönsted acid sites that undergo reaction with either Brönsted or Lewis bases (Busca *et al*, 1985). The Lewis acid character of pure TiO_2 is preserved upon adsorption of heavy-metal oxides such as Fe_2O_3 (Larrubia *et al*, 2001). Wet-chemical titration of anatase TiO_2 aqueous suspensions indicated a continuous spectrum of the amphiphilic nature of surface OH-groups in TiO_2 spanning the range from strongly acidic to basic OH groups (Flaig-Baumann *et al*, 1970). Numerous N-containing compounds such as NH_3 , N_2H_4 and NH_2OH preferentially interact

with Lewis acid sites in view of the confirmed absence of Brönsted acidity in pure anatase TiO_2 (Busca *et al*, 1985). However, when TiO_2 contains contaminants such as SiO_2 , significant Brönsted acidity may result. Taking on a slightly different viewpoint, Boehm (1994) has stated that the density of acidic and basic OH-groups in TiO_2 (including TiO_2 P25) is roughly balanced. Assuming TiO_2 to be pure, it appears that $\text{N}(\text{CH}_3)_3$ directly interacts with TiO_2 as a Lewis acid akin to ammonia and NH_2OH (Ramis *et al*, 2000). The existing literature data point to the fact that ammonia, and by analogy $\text{N}(\text{CH}_3)_3$, may be oxidized at higher temperatures via hydrazine-type intermediates to N_2 , whereas NH_2OH will be oxidized to NO in a competing mechanism (Larrubia *et al*, 2001), hence the technological importance of TiO_2 . However, these reactions do not take place under the present conditions.

NH_2OH strongly interacts with Lewis acid sites of pure TiO_2 (anatase) despite the fact that it is a much weaker base than ammonia. Both the pK_a in aqueous solution as well as the gas phase proton affinity PA are larger for NH_3 than for NH_2OH (Jolly, 1991): $\text{pK}_a(\text{NH}_3) = 9.25$, $\text{pK}_a(\text{NH}_2\text{OH}) = 5.96$; $\text{PA}(\text{NH}_3) = 854 \text{ kJ/mol}$, $\text{PA}(\text{NH}_2\text{OH}) = 803 \text{ kJ/mol}$. $\text{N}(\text{CH}_3)_3$ is an even stronger base than NH_3 both in the gas phase as well as in aqueous solution: $\text{PA}(\text{N}(\text{CH}_3)_3) = 942 \text{ kJ/mol}$, $\text{pK}_a(\text{N}(\text{CH}_3)_3) = 9.81$. This indicates that NH_2OH specifically interacts with Lewis acid sites of TiO_2 in agreement with the fact that pure TiO_2 is not a strong Brönsted acid (Busca *et al*, 1985).

A look at Table 4.4 reveals a significant uptake of both $\text{N}(\text{CH}_3)_3$ and even more so of NH_2OH at ambient temperature on all three TiO_2 samples. A very efficient reaction of NH_2OH occurs on approximately up to ten formal monolayers of the TiO_2 substrate, at least for two of the investigated substrates, namely TiO_2 P25 and TiO_2 50. This means that NH_2OH may undergo a reaction with deeper layers of TiO_2 . In addition, the most reactive sample towards NH_2OH , TiO_2 P25, has been shown to contain traces of SiO_2 (Busca *et al*, 1985), the Brönsted activity of which may contribute somewhat to its high reactivity towards NH_2OH . The present data also indicate that $\text{N}(\text{CH}_3)_3$ and NH_2OH uptake is the smallest for TiO_2 with a high anatase content (TiO_2 15) compared to a TiO_2 with a lower anatase content such as TiO_2 50. However, the anatase content given by the manufacturer *a priori* addresses the bulk composition which nevertheless does not preclude a systematic variation of the interface with the composition of the bulk. Under the present reaction conditions both N-containing compounds adsorb on the TiO_2 substrate until saturation with no observable products evolved at ambient temperature. We emphasize that NH_2OH apparently specifically reacts with the

TiO₂ matrix, in contrast to combustion aerosol where the probe gas primarily interacts with aldehydes and ketones that are presumably part of the adsorbed organic phase of the carbonaceous aerosol. A last remark concerns the lack of uptake of gas phase CO₂ with TiO₂ 15 and TiO₂ 50 which is in stark contrast to the significant interaction of HCO₃⁻ with aqueous suspensions of TiO₂ P25 (Flaig-Baumann *et al*, 1970). Although not systematically used as a surface probe in the present investigation, we earmark the behaviour of CO₂ towards the TiO₂ samples as an important difference between gas phase and condensed phase reactivity.

As shown in Table 4.4, both acidic probes substantially interact with all three TiO₂ samples despite the fact that its Lewis acid character is well established (Busca *et al*, 1985). Apparently, TiO₂ has the ability to bind acidic probe gases on basic sites akin to combustion aerosol particles. Compared to the carbonaceous substrates, uptakes of CF₃COOH and HCl are large and of the same order of magnitude, except for TiO₂ 50 that has a ten times higher uptake of HCl. In view of the fact that the generic TiO₂ surface is a Lewis rather than a Brönsted acid (Busca *et al*, 1985), we propose to explain the fairly uniform reactivity towards CF₃COOH and HCl with the presence of surface hydroxyl groups that act as basic sites in agreement with results obtained by Flaig-Baumann *et al* (1970). The obvious exception, namely the titration of TiO₂ 50 by a large amount of HCl, may be due to the suspected formation of an oxychloride, the presence of which will have to be investigated in future experiments. Titration experiments in aqueous suspension of TiO₂ P25 reveal a strong adsorption of acetic acid, but none with strong mineral acids such as HCl and HClO₄ (Flaig-Baumann *et al*, 1970). A look at Table 4.4 shows that this trend is not borne out in the gas phase where there is even a slight preference for HCl adsorption compared to CF₃COOH. This is another example where the previous results on solution surface titration are significantly different from the gas phase. With this change in differential reactivity of CF₃COOH vs HCl, the absence of any interaction of TiO₂ with gas phase NO₂ (see below) and the lack of CO₂ reaction, we have several examples of a change in reactivity of probe gases between the gas- and the condensed phase.

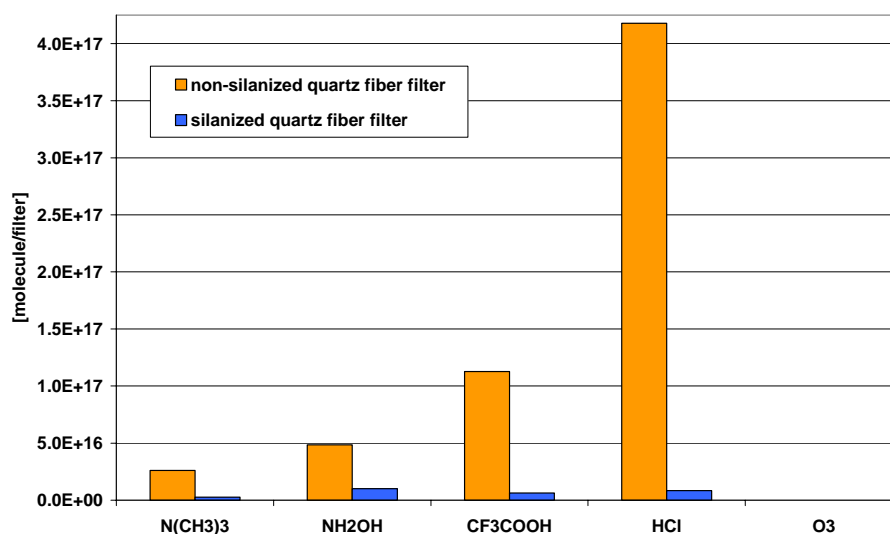
TiO₂ does not interact with NO₂ in the gas phase, but reacts with gas phase O₃, most probably resulting in non-catalytic decomposition of ozone and generating O₂ (Bulanin *et al*, 1995; Oyama, 2000; Radakrishnan and Oyama, 2001). O₃ reacts as a Lewis base and forms an adduct with TiO₂ owing to its Lewis acid character. In contrast, it was reported that TiO₂ P25 reacted with NO₂ in solution to surface nitrate whose infra-red (IR) absorption has been

identified (Flaig-Baumann *et al*, 1970). Owing to the absence of significant amounts of adsorbed H_2O , this reaction is thought to be a surface variant of the well-known disproportionation reaction leading to nitrate and nitrite. The absence of a reaction in the gas phase as opposed to aqueous suspension is an additional example where gas- and condensed phase results differ (see above). The O_3 uptake on TiO_2 is non-catalytic because the reaction ceases after saturation, which would not be the case if O_3 decomposition were catalytic. In addition, O_2 generation also ceases after saturation of the O_3 uptake on TiO_2 . No systematic trend between the anatase and rutile phase could be detected when considering the relative reactivities of all probe gases as expressed by their uptakes. This is perhaps not too surprising as the specific structure is a property of the bulk of the particle whereas the present titration scheme specifically addresses the surface composition and structure.

4.3.4 Aerosols collected in the field

Prior to the field campaign, we had to ascertain that the silanized quartz fiber filters were chemically sufficiently inert towards the used probe gases. Figure 4.8 shows the reactivity of silanized and non-silanized quartz fiber filters towards all used probe gases. Results indicate that the silanization of filters decreased their reactivity up to 50 times for HCl , which was the most reactive probe. We therefore considered silanized quartz fiber filters as suitable filters for the field campaign.

Figure 4.8: Uptake measurements of probe gases on silanized and non-silanized quartz fiber filters using the Knudsen flow reactor. Units: number of gas-phase probe molecules taken up per filter of 47 mm diameter.

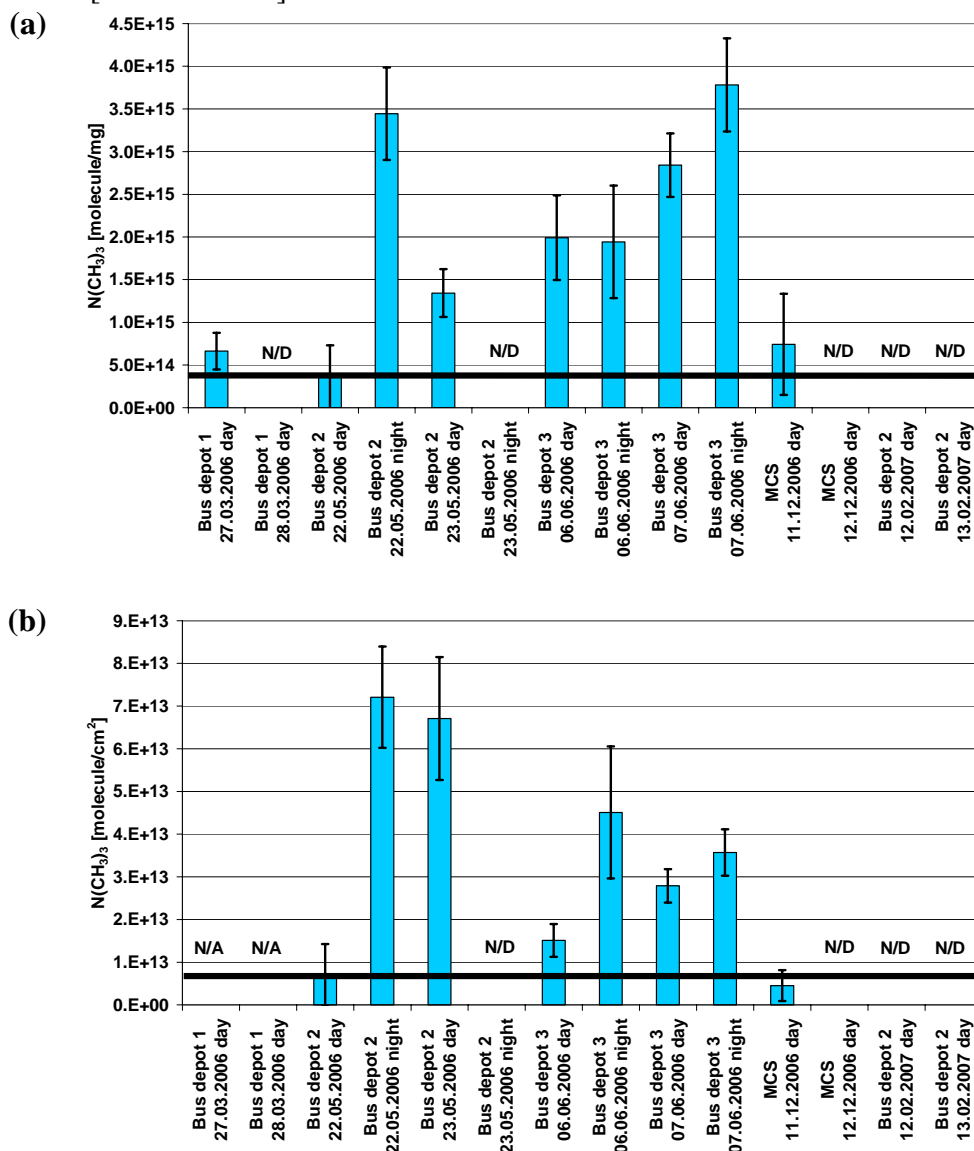


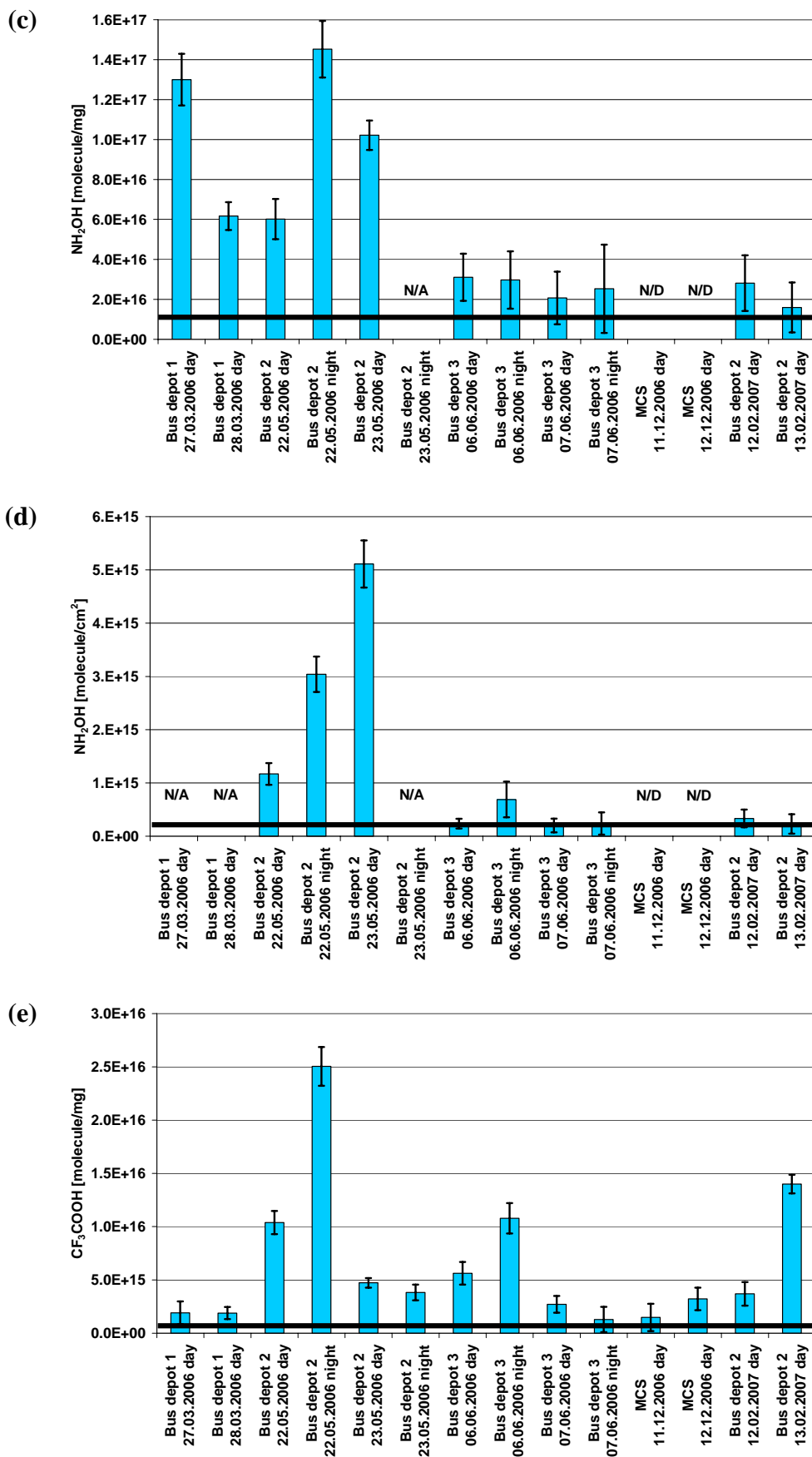
Particle size distributions measured using the SMPS in the workplaces were already discussed in Chapter 3. Compared to laboratory-generated aerosols, particle size distributions showed a very large variability during the period of shift in the workplaces, depending on the activities of workers and the passage of vehicles near the SMPS. In general, particles were smaller than 100 nm, and had one or two modes.

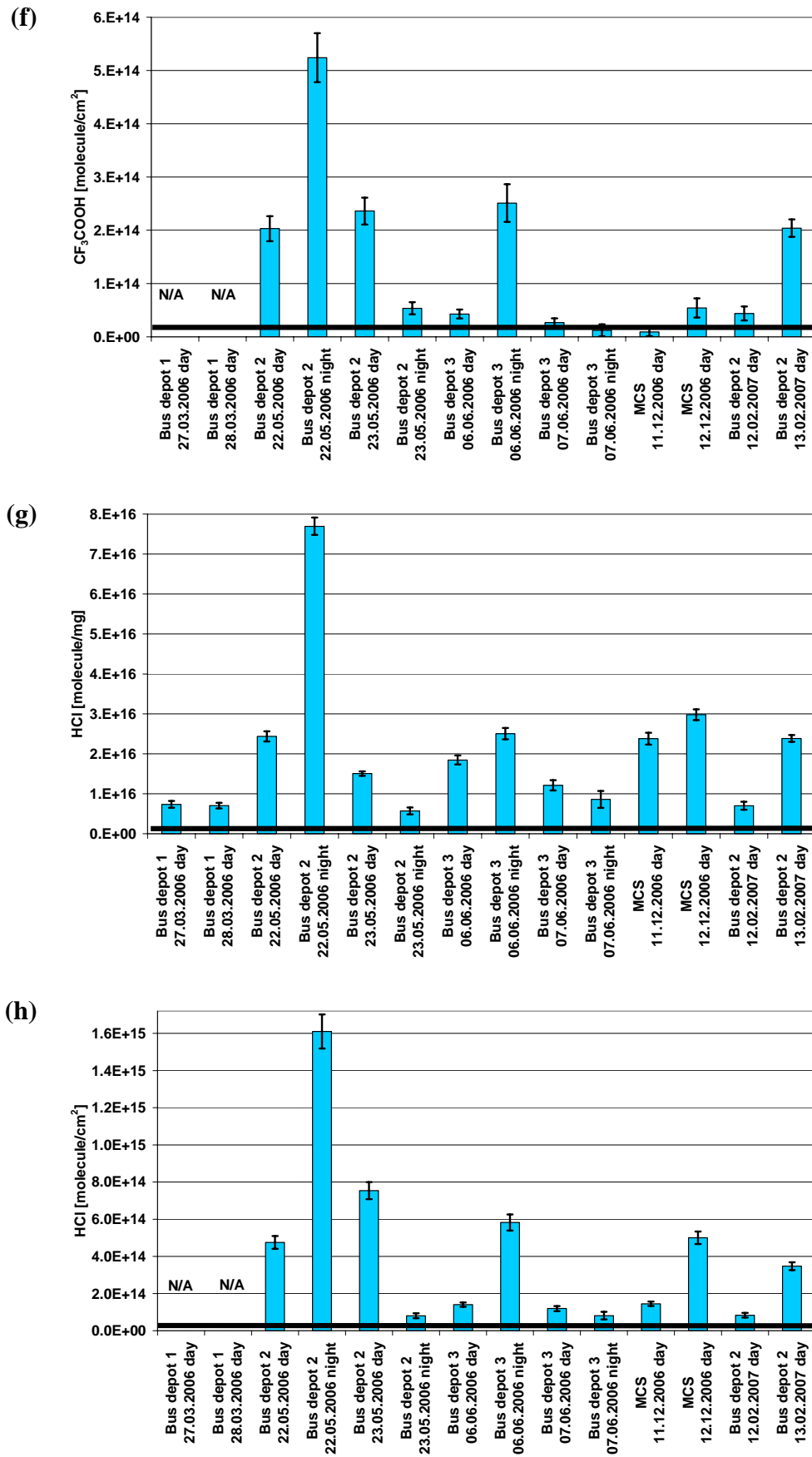
Figure 4.9 shows the uptake of probe gases on aerosols collected in the field, while numerical values are given in Annex. These results were obtained by first subtracting each sample by a blank which had been silanized in the same batch. Then, the number of gas-phase probe molecules taken up by the whole sample was divided by the particle mass (molecule/mg; Figure 4.9(a, c, e, g, i)). In order to determine the density of functional groups on the particle surface (molecule/cm²; Figure 4.9(b, d, f, h, j)), the number of gas-phase probe molecules taken up by the whole sample was divided by the particle surface area.

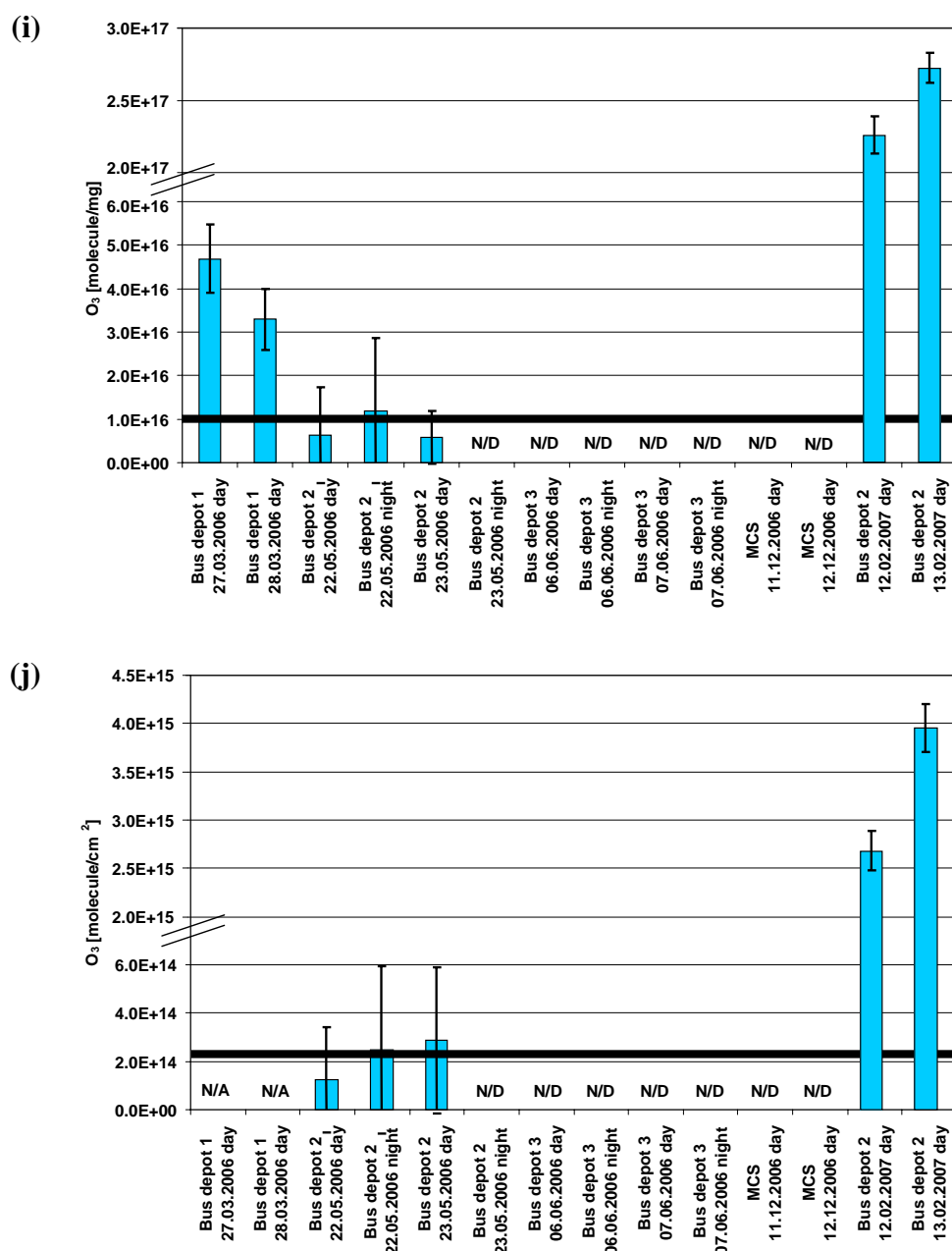
Figure 4.9: Uptake measurements of $\text{N}(\text{CH}_3)_3$ (**a** and **b**), NH_2OH (**c** and **d**), CF_3COOH (**e** and **f**), HCl (**g** and **h**), and O_3 (**i** and **j**) on aerosols collected in the workplaces using the Knudsen flow reactor. Results: mean values of duplicates. Error bars: combined uncertainty due to the measurement of the mass, surface area and probe-gas uptake. Horizontal bold line: limit of detection. MCS: metro construction site. N/A: not available. N/D: not detected (below the limit of detection).

(**a, c, e, g, i**): Number of gas-phase probe molecules taken up per mg of aerosol [molecule/mg],
 (**b, d, f, h, j**): Number of gas-phase probe molecules taken up per cm^2 of aerosol [molecule/ cm^2].









In Figure 4.9, results expressed as the number of probe molecules taken up per particle mass do not show the same detailed trends as those expressed according to the particle surface area. In order to obtain insight on a molecular level into the reactivity of the particle surface, we base the following discussion on results expressed as the number of probe molecules taken up per unit of particle surface area (molecule/cm²). This choice is motivated by previous studies, which pointed out the importance of the surface reactivity to the toxicity of nanoparticles (Warheit *et al*, 2007) and to the ability of particulate matter to adsorb a wide variety of compounds (proteins, surfactant components) in the lung (Kendall *et al*, 2004).

In Figure 4.9, the surface reactivity of the collected aerosols showed a large variability according to the workplace and the season. Indeed, the difference of probe gas uptake between the most reactive and the less reactive sample could reach a factor of 100. These differences may be due to various activities of the workers in the bus depots, and also to the background of outdoor air. Moreover, almost all the samples reacted with the five probe gases, which indicate that the particle surface is multi-functional, with the simultaneous presence of antagonistic functional groups on the same particle, such as acids and bases.

There were several similarities between laboratory-generated aerosols and aerosols collected in the field. First, the uptake of NH_2OH on all samples was very large. As with the laboratory-generated aerosols, these results indicate the presence of an important amount of carbonyl functions on the particle surface. This result is in agreement with previous studies, which also suggested that carbonyl functions are significant constituents of ambient particulate matter (Reff *et al.*, 2005). Moreover, Figures 4.9(f) and 4.9(h) indicate that HCl reacted to a larger extent compared to CF_3COOH with all the samples. As discussed for carbonaceous aerosol samples, particulate matter sampled in all the bus depots seems to contain a low amount of basic oxides similar to α/γ pyrone structures. On the other hand, of all the studied samples (laboratory-generated aerosols as well as aerosols collected in the field), limonene SOA is the only one to have a higher selectivity towards CF_3COOH (2.8% of a monolayer, Table 4.4) than towards HCl (less than 0.5% of a monolayer, which corresponds to the limit of detection for HCl ; Table 4.4). This result suggests that limonene SOA is perhaps not a good surrogate for organic aerosols in bus depots.

Figures 4.9(b) and 4.9(j) show that aerosols collected in the field present anticorrelated reactivities towards $\text{N}(\text{CH}_3)_3$ and O_3 . Indeed, particulate matter sampled in the bus depot 2 on February 2007 reacted strongly with O_3 (Figure 4.9(j)), but not with $\text{N}(\text{CH}_3)_3$ (Figure 4.9(b)). On the other hand, particulate matter sampled on May and June 2006 reacted with $\text{N}(\text{CH}_3)_3$ (Figure 4.9(b)), while reactions with O_3 were near the limit of detection ((Figure 4.9(j)). This suggests that during summer, particulate matter underwent photo-oxidation, which generated carboxylic acids and increased the oxidation state of the organic aerosol. The presence of carboxylic acids on particulate matter in summer explains the reactivity of these samples towards $\text{N}(\text{CH}_3)_3$, while the very weak reactions with O_3 is due to the fact that such a high oxidation status hinders further oxidation by the O_3 probe. On the contrary, photo-oxidation does not occur in winter, and therefore compounds adsorbed on the particulate matter sampled

on February 2007 were in a reduced state. These samples did not react with $\text{N}(\text{CH}_3)_3$ because of the absence of carboxylic acids, while they underwent oxidation by O_3 . This observation points out the influence of the background of outdoor air on the results, because photo-oxidation usually does not occur in an indoor environment. These observations are in agreement with results obtained by previous studies (Kawamura and Ikushima, 1993), which also noticed higher levels of acids in particulate matter during summer.

The uptake of probe gases on aerosols collected in the field was in general of the same order of magnitude as laboratory-generated aerosols and as the most oxidized carbonaceous samples. The reactivity of samples containing organics (aerosols collected in the field, limonene SOA and SRM 2975) towards $\text{N}(\text{CH}_3)_3$, NH_2OH and O_3 may be explained by the degree of partial oxidation, while that towards HCl and CF_3COOH is mainly explained by the presence of basic sites including basic oxides. However, due to the very complex mixture of aerosols collected in the field, we are unable to express the observed reactivity in terms of fractions of model or laboratory aerosol present in ambient particles.

4.3.5 Kinetics of heterogeneous titration reactions

According to Equations 4.4 and 4.6, the geometric surface area of the samples (A_s) is necessary to calculate the uptake coefficient γ_0 of the titration reactions. This parameter is easily known for aerosols collected in the field, because aerosols are deposited homogeneously on the whole geometric surface area of the filters (see photographs in Figure 4.4). However, the determination of the geometric surface area is more difficult for powders, because these samples are spreaded on the surface of a Petri dish without filling the whole surface area of the support. Moreover, the spread of the powders on the surface of the Petri dish is variable depending on the sample, and therefore we can not easily compare the values of γ_0 determined for the powders.

The uptake coefficients γ_0 of the titration reactions for laboratory-generated aerosols, carbonaceous and TiO_2 samples are shown in Table 4.5. These values have been calculated by assessing that the samples filled a quarter of the geometric surface area of the Petri dish. Reactions with γ_0 smaller than 10^{-4} may be considered as slow, while those higher than 10^{-3} as fast. For carbonaceous as well as for TiO_2 samples, we notice that the fastest reactions occurred generally with samples having the largest BET surface area: FW 2 in the case of

carbonaceous particles, and TiO₂ 15 nm for titanium dioxide samples. This trend stresses the importance of the surface area in the reactivity, and maybe also in the toxicity of particles.

Table 4.5: Uptake coefficient γ_0 of heterogeneous chemical reactions between probe gases and aerosol samples in the Knudsen flow reactor.

	N(CH ₃) ₃	NH ₂ OH	CF ₃ COOH	HCl	O ₃	NO ₂
limonene SOA	$2.5 (\pm 0.1) \cdot 10^{-4}$	$2.4 (\pm 0.4) \cdot 10^{-3}$	$7.1 (\pm 0.6) \cdot 10^{-5}$	not detected	$4.7 (\pm 0.4) \cdot 10^{-4}$	not detected
Pb(NO₃)₂	$3.5 (\pm 0.2) \cdot 10^{-4}$	$2.0 (\pm 0.3) \cdot 10^{-4}$	$2.9 (\pm 0.2) \cdot 10^{-3}$	$5.8 (\pm 0.2) \cdot 10^{-2}$	not detected	not tested
Cd(NO₃)₂	$9.9 (\pm 0.6) \cdot 10^{-5}$	$2.0 (\pm 0.3) \cdot 10^{-4}$	$1.8 (\pm 0.1) \cdot 10^{-3}$	$6.3 (\pm 0.2) \cdot 10^{-4}$	not detected	not tested
FS 101	$7.8 (\pm 0.4) \cdot 10^{-4}$	not detected	$7.9 (\pm 0.6) \cdot 10^{-3}$	not detected	$1.1 (\pm 0.1) \cdot 10^{-2}$	$3.8 (\pm 0.3) \cdot 10^{-4}$
Printex 60	$9.9 (\pm 0.6) \cdot 10^{-4}$	not detected	$2.2 (\pm 0.2) \cdot 10^{-2}$	not detected	$1.0 (\pm 0.1) \cdot 10^{-1}$	$1.8 (\pm 0.2) \cdot 10^{-3}$
FW 2	$4.3 (\pm 0.2) \cdot 10^{-2}$	$4.4 (\pm 0.7) \cdot 10^{-2}$	$1.6 (\pm 0.1) \cdot 10^{-2}$	not detected	$1.1 (\pm 0.1) \cdot 10^{-1}$	$5.8 (\pm 0.5) \cdot 10^{-3}$
hexane rich flame	$8.4 (\pm 0.5) \cdot 10^{-5}$	$4.2 (\pm 0.7) \cdot 10^{-4}$	$3.6 (\pm 0.3) \cdot 10^{-4}$	$2.0 (\pm 0.1) \cdot 10^{-4}$	$1.6 (\pm 0.1) \cdot 10^{-3}$	$2.8 (\pm 0.2) \cdot 10^{-3}$
hexane lean flame	$8.7 (\pm 0.5) \cdot 10^{-5}$	$1.5 (\pm 0.3) \cdot 10^{-3}$	$2.9 (\pm 0.2) \cdot 10^{-3}$	$1.7 (\pm 0.1) \cdot 10^{-4}$	$2.4 (\pm 0.2) \cdot 10^{-2}$	$2.5 (\pm 0.2) \cdot 10^{-3}$
SRM 2975	$2.4 (\pm 0.1) \cdot 10^{-2}$	$1.5 (\pm 0.3) \cdot 10^{-2}$	not detected	$2.9 (\pm 0.1) \cdot 10^{-3}$	$5.8 (\pm 0.5) \cdot 10^{-4}$	$6.3 (\pm 0.5) \cdot 10^{-4}$
Diesel BD 2	$1.3 (\pm 0.1) \cdot 10^{-2}$	$2.1 (\pm 0.4) \cdot 10^{-2}$	not detected	$1.3 (\pm 0.1) \cdot 10^{-2}$	$1.0 (\pm 0.1) \cdot 10^{-2}$	$1.4 (\pm 0.1) \cdot 10^{-3}$
TiO₂ 15 nm	$2.5 (\pm 0.1) \cdot 10^{-1}$	$8.4 (\pm 1.4) \cdot 10^{-2}$	$5.5 (\pm 0.4) \cdot 10^{-2}$	$1.4 (\pm 0.1) \cdot 10^{-1}$	$1.0 (\pm 0.1) \cdot 10^{-3}$	not detected
TiO₂ 50 nm	$6.5 (\pm 0.4) \cdot 10^{-3}$	$1.5 (\pm 0.3) \cdot 10^{-2}$	$1.0 (\pm 0.1) \cdot 10^{-2}$	$1.9 (\pm 0.1) \cdot 10^{-2}$	$6.4 (\pm 0.5) \cdot 10^{-4}$	not detected
TiO₂ P25	$4.5 (\pm 0.3) \cdot 10^{-2}$	$5.9 (\pm 1.0) \cdot 10^{-2}$	$3.5 (\pm 0.3) \cdot 10^{-2}$	$1.5 (\pm 0.1) \cdot 10^{-1}$	$1.5 (\pm 0.1) \cdot 10^{-3}$	not detected

Values between brackets: standard deviation of duplicates.

Table 4.6 shows the uptake coefficient γ_0 of the titration reactions for aerosols collected in the field. All the aerosol samples reacted fairly slowly with N(CH₃)₃, which points to the presence of organic carboxylic rather than mineral acids. Except for the last aerosol sample collected on 13.02.2007 daytime, NH₂OH reacted roughly at a uniform rate with all aerosol samples with γ_0 being on the order of 10^{-4} . Moreover, all aerosol samples consistently reacted faster with HCl than with CF₃COOH ($\gamma_0(\text{HCl}) > \gamma_0(\text{CF}_3\text{COOH})$). We also notice that O₃ reacted very fast with all the samples, γ_0 being on the order of 10^{-3} . A look at the corresponding uptakes shown in Figure 4.9 indicates that there is no apparent relationship between the kinetics (Table 4.6) and uptakes (Figure 4.9). This observation is confirmed by the Spearman's rank correlation coefficients shown in Table 4.7. According to this table, kinetics and uptakes were correlated only in the case of CF₃COOH, while available data for O₃ are not sufficient to assert that there is a correlation. This suggests that, except for the case of CF₃COOH, the kinetic behavior is different for different kinds of particles using the same probe. This may reflect a different reaction mechanism for probe uptake for the same class of particles. However, the ability of aerosols collected in the field to undergo fast redox reactions with O₃ and slow acid-base reactions with N(CH₃)₃ is an interesting outcome of this study, regarding the health effects of particulate matter. Indeed, the quantification of surface functional groups may not be sufficient to explain the reactivity of particulate matter if the kinetics is very slow. For instance, if the particle surface is characterized by a high content of

acidic sites, the slow kinetics may prevent excessive damages in biological systems due to acid-base reactions, and therefore will reduce the adverse health effects of particulate matter.

Table 4.6: Uptake coefficient γ_0 of heterogeneous chemical reactions between probe gases and aerosols collected in the field.

	$\text{N}(\text{CH}_3)_3$	NH_2OH	CF_3COOH	HCl	O_3
Bus depot 1 27.03.2006 day	$7.6 (\pm 1.1) \cdot 10^{-5}$	$1.9 (\pm 0.4) \cdot 10^{-4}$	$7.8 (\pm 1.0) \cdot 10^{-5}$	$1.1 (\pm 0.2) \cdot 10^{-4}$	$2.0 (\pm 0.1) \cdot 10^{-3}$
Bus depot 1 28.03.2006 day	not detected	$2.3 (\pm 0.7) \cdot 10^{-4}$	$1.0 (\pm 0.1) \cdot 10^{-4}$	$1.7 (\pm 0.2) \cdot 10^{-4}$	$2.6 (\pm 0.2) \cdot 10^{-3}$
Bus depot 2 22.05.2006 day	$7.4 (\pm 0.4) \cdot 10^{-5}$	$2.4 (\pm 0.2) \cdot 10^{-4}$	$2.0 (\pm 0.4) \cdot 10^{-4}$	$4.3 (\pm 0.3) \cdot 10^{-4}$	$1.0 (\pm 0.1) \cdot 10^{-3}$
Bus depot 2 22.05.2006 night	$1.0 (\pm 0.1) \cdot 10^{-4}$	$3.3 (\pm 0.1) \cdot 10^{-4}$	$4.1 (\pm 0.4) \cdot 10^{-4}$	$1.6 (\pm 0.1) \cdot 10^{-3}$	$1.2 (\pm 0.1) \cdot 10^{-3}$
Bus depot 2 23.05.2006 day	$9.1 (\pm 0.3) \cdot 10^{-5}$	$4.6 (\pm 0.1) \cdot 10^{-4}$	$2.0 (\pm 0.1) \cdot 10^{-4}$	$4.3 (\pm 0.1) \cdot 10^{-4}$	$1.5 (\pm 0.2) \cdot 10^{-3}$
Bus depot 2 23.05.2006 night	not detected	not available	$1.0 (\pm 0.1) \cdot 10^{-4}$	$1.5 (\pm 0.1) \cdot 10^{-4}$	not detected
Bus depot 3 06.06.2006 day	$5.2 (\pm 0.1) \cdot 10^{-5}$	$3.0 (\pm 0.4) \cdot 10^{-4}$	$9.7 (\pm 1.1) \cdot 10^{-5}$	$1.4 (\pm 0.1) \cdot 10^{-4}$	not detected
Bus depot 3 06.06.2006 night	$6.2 (\pm 0.5) \cdot 10^{-5}$	$2.0 (\pm 0.6) \cdot 10^{-4}$	$1.2 (\pm 0.1) \cdot 10^{-4}$	$1.6 (\pm 0.1) \cdot 10^{-4}$	not detected
Bus depot 3 07.06.2006 day	$7.9 (\pm 0.7) \cdot 10^{-5}$	$1.4 (\pm 0.1) \cdot 10^{-4}$	$7.3 (\pm 0.1) \cdot 10^{-5}$	$9.2 (\pm 0.3) \cdot 10^{-5}$	not detected
Bus depot 3 07.06.2006 night	$1.1 (\pm 0.1) \cdot 10^{-4}$	$1.4 (\pm 0.3) \cdot 10^{-4}$	$5.0 (\pm 0.2) \cdot 10^{-5}$	$5.4 (\pm 0.1) \cdot 10^{-5}$	not detected
Metro construction site 11.12.2006 day	$8.5 (\pm 0.1) \cdot 10^{-5}$	not detected	$8.2 (\pm 0.5) \cdot 10^{-5}$	$1.5 (\pm 0.2) \cdot 10^{-4}$	not detected
Metro construction site 12.12.2006 day	not detected	not detected	$1.1 (\pm 0.1) \cdot 10^{-4}$	$2.1 (\pm 0.1) \cdot 10^{-4}$	not detected
Bus depot 2 12.02.2007 day	not detected	$7.5 (\pm 1.5) \cdot 10^{-4}$	$4.2 (\pm 0.6) \cdot 10^{-3}$	$4.5 (\pm 0.8) \cdot 10^{-3}$	$3.6 (\pm 0.3) \cdot 10^{-3}$
Bus depot 2 13.02.2007 day	not detected	$1.5 (\pm 0.1) \cdot 10^{-3}$	$1.4 (\pm 0.1) \cdot 10^{-2}$	$1.8 (\pm 0.3) \cdot 10^{-2}$	$3.3 (\pm 0.5) \cdot 10^{-3}$

Values between brackets: standard deviation of duplicates.

Table 4.7: List of Spearman's rank correlation coefficients between uptake coefficient γ_0 and number of probe gases taken up by the samples collected in the workplaces (molecule/mg or molecule/cm²). For each probe gas, only reactions above the limit of detection were taken into account.

	Uptake [molecule/mg]	Uptake [molecule/cm ²]
$\gamma_0 (\text{N}(\text{CH}_3)_3)$	0.467 (n = 9)	0.429 (n = 8)
$\gamma_0 (\text{NH}_2\text{OH})$	0.055 (n = 11)	0.233 (n = 9)
$\gamma_0 (\text{CF}_3\text{COOH})$	0.741 ** (n = 14)	0.741 ** (n = 12)
$\gamma_0 (\text{HCl})$	0.337 (n = 14)	0.498 (n = 12)
$\gamma_0 (\text{O}_3)$	0.821 * (n = 7)	0.900 (n = 5)

* : $p < 0.05$

** : $p < 0.01$

4.4 Conclusion

In this chapter, we report the use of a novel method allowing the quantitative characterization of functional groups on the surface of particulate matter. As opposed to spectroscopic methods usually used for this kind of measurement, the Knudsen flow reactor provides an alternative approach, focusing on the chemical reactivity of particulate matter. The sensitivity of the method allowed detecting less than 1% of a molecular monolayer of surface functional groups.

The work undertaken on laboratory-generated aerosols allowed the selection of five different probe gases for the titration of important functional groups, such as acids, bases, carbonyl functions and oxidizable sites.

In the second part of this work, the Knudsen flow reactor was successfully used for the first time to study aerosols collected in the field. Results showed important differences in surface functional groups, depending on sampling sites, season, particle sources, activities of workers and background of outdoor air. The particle surface in bus depots was usually characterized by a high content of carbonyl functions, and showed a high degree of partial oxidation. However, because of the extensive variability of the particle surface in the different bus depots, we are unable to give a description of the surface of typical ambient fine and ultrafine particles. The ability of almost all samples to react with the five probe gases indicates that the surface of particulate matter is multi-functional, with the simultaneous presence of antagonistic functional groups which do not undergo internal chemical reactions, such as acid-base neutralization. The measurement of kinetic parameters for aerosols collected in the field indicated that redox reactions of oxidizable sites on the particle surface were fast, while reactions of acidic sites on particulate matter towards $\text{N}(\text{CH}_3)_3$ were rather slow.

Additional work has still to be performed in order to find probe gases allowing the quantification of other functional groups. In particular, it would be important to find probe gases reacting specifically with metal ions and oxidizing agents, because these classes of compounds are suspected to play a central role in health effects of particulate matter.

4.5 References

- Alcala-Jornod C., van den Bergh H., Rossi M.J., 2000. Reactivity of NO₂ and H₂O on soot generated in the laboratory: a diffusion tube study at ambient temperature. *Physical Chemistry Chemical Physics*, 2 (24), 5584-5593.
- Alcala-Jornod C., Rossi M.J., 2004. Chemical kinetics of the interaction of H₂O vapor with soot in the range 190 K ≤ T ≤ 300 K: a diffusion tube study. *Journal of Physical Chemistry A*, 108 (48), 10667-10680.
- Atkinson R., Aschmann S.M., 1988. Kinetics of the reactions of acenaphthene and acenaphthylene and structurally-related aromatic compounds with OH and NO₃ radicals, N₂O₅ and O₃ at 296 ± 2 K. *International Journal of Chemical Kinetics*, 20 (7), 513-539.
- Atkinson R., Arey J., Aschmann S.M., 1992. Gas-phase reactions of azulene with OH and NO₃ radicals and O₃ at 298 ± 2 K. *International Journal of Chemical Kinetics*, 24 (5), 467-480.
- Bachman G.B., Strawn K.G., 1968. Ozone oxidation of primary amines to nitroalkanes. *Journal of Organic Chemistry*, 33 (1), 313-315.
- Beauchemin A.M., Moran J., Lebrun M.-E., Séguin C., Dimitrijevic E., Zhang L., Gorelsky S.I., 2008. Intermolecular Cope-type hydroamination of alkenes and alkynes. *Angewandte Chemie International Edition*, 47 (8), 1410-1413.
- Bhatia R., Lopipero P., Smith A.H., 1998. Diesel exhaust exposure and lung cancer. *Epidemiology*, 9 (1), 84-91.
- Boehm H.P., Diehl E., 1962. Untersuchung an Säuren Oberflächenoxyden des Kohlenstoffs. *Zeitschrift für Elektrochemie*, 66 (8/9), 642-647.
- Boehm H.P., Diehl E., Heck W., Sappok R., 1964. Oberflächenoxyde des Kohlenstoffs. *Angewandte Chemie*, 76 (17), 742-751.
- Boehm H.P., 1966. Funktionelle Gruppen an Festkörper-Oberflächen. *Angewandte Chemie*, 78 (12), 617-628.
- Boehm H.P., Voll M., 1970. Basische Oberflächenoxide auf Kohlenstoff - I. Adsorption von Säuren. *Carbon*, 8 (2), 227-240.
- Boehm H.P., 1994. Some aspects of the surface chemistry of carbon blacks and other carbons. *Carbon*, 32 (5), 759-769.
- Braun A., 2005. Carbon speciation in airborne particulate matter with C (1s) NEXAFS spectroscopy. *Journal of Environmental Monitoring*, 7 (11), 1059-1065.

-
- Brown D.M., Wilson M.R., MacNee W., Stone V., Donaldson K., 2001. Size-dependant proinflammatory effects of ultrafine polystyrene particles: a role for surface area and oxidative stress in the enhanced activity of ultrafines. *Toxicology and Applied Pharmacology*, 175 (3), 191-199.
 - Bulanin K.M., Lavalley J.C., Tsyganenko A.A., 1995. Infrared study of ozone adsorption on TiO₂ (anatase). *Journal of Physical Chemistry*, 99 (25), 10294-10298.
 - Busca G., Saussey H., Saur O., Lavalley J.C., Lorenzelli V., 1985. FT-IR characterization of the surface-acidity of different titanium-dioxide anatase preparations. *Applied Catalysis*, 14 (1/3), 245-260.
 - Caloz F., Fenter F. F., Tabor K. D., Rossi M. J., 1997. Paper I: Design and construction of a Knudsen-cell reactor for the study of heterogeneous reactions over the temperature range 130-750 K: performances and limitations. *Review of Scientific Instruments*, 68 (8), 3172-3179.
 - Chen Y., Shah N., Braun A., Huggins F.E., Huffman G.P., 2005. Electron microscopy investigation of carbonaceous particulate matter generated by combustion of fossil fuels. *Energy & Fuels*, 19 (4), 1644-1651.
 - Cheng T.-Y., Ponce A., Rheingold A.L., Hillhouse G.L., 1994. Hydroxylamine, hydrazine, and diazene as unidentate ligands in osmium and ruthenium complexes. *Angewandte Chemie International Edition in English*, 33 (6), 657-659.
 - Cohen Z., Keinan E., Mazur Y., Varkony T.H., 1975. Dry ozonation - a method for stereoselective hydroxylation of saturated compounds on silica gel. *Journal of Organic Chemistry*, 40 (14), 2141-2142.
 - Cumming J.B., Kebarle P., 1978. Summary of gas phase measurements involving acids AH - Entropy changes in proton transfer reactions involving negative ions - Bond dissociation energies D(AH) and electron affinities EA(A). *Canadian Journal of Chemistry*, 56 (1), 1-9.
 - Cwiertny D.M., Young M.A., Grassian V.H., 2008. Chemistry and photochemistry of mineral dust aerosol. *Annual Review of Physical Chemistry*, 59, 27-51.
 - Davis P., Evans M.G., Higginson W.C.E., 1951. Some oxidation-reduction reactions of hydroxylamine. *Journal of the Chemical Society*, 2563-2567.
 - Demirdjian B., Rossi M.J., 2005. The surface properties of SOA generated from limonene and toluene using specific molecular probes: exploration of a new experimental technique. *Atmospheric Chemistry and Physics Discussions*, 5, 607-654.

-
- Dhandapani B., Oyama S.T., 1997. Gas phase ozone decomposition catalysts. *Applied Catalysis B: Environmental*, 11 (2), 129-166.
 - Erickson R.E., Andrusis P.J. Jr, Collins J.C., Lungle M.L., Mercer G.D., 1969. Mechanism of ozonation reactions - IV. Carbon-nitrogen double bonds. *Journal of Organic Chemistry*, 34 (10), 2961-2966.
 - Esteve W., Budzinski H., Villenave E., 2006. Relative rate constants for the heterogeneous reactions of NO₂ and OH radicals with polycyclic aromatic hydrocarbons adsorbed on carbonaceous particles - Part 2: PAHs adsorbed on diesel particulate exhaust SRM 1650a. *Atmospheric Environment*, 40 (2), 201-211.
 - Fermo P., Piazzalunga A., Vecchi R., Valli G., Ceriani M., 2006. A TGA/FT-IR study for measuring OC and EC in aerosol samples. *Atmospheric Chemistry and Physics*, 6, 255-266.
 - Finlayson-Pitts B.J., Pitts J.N., 2000. Chemistry of the upper and lower atmosphere - Theory, experiments, and applications. Academic Press, San Diego.
 - Flaig-Baumann R., Herrmann M., Boehm H.P., 1970. Über die Chemie der Oberfläche des Titandioxids - III. Reaktionen der basischen Hydroxylgruppen auf der Oberfläche. *Zeitschrift für Anorganische und Allgemeine Chemie*, 372 (3), 296-307.
 - Gerecke A., Thielmann A., Gutzwiller L., Rossi M.J., 1998. The chemical kinetics of HONO formation resulting from heterogeneous interaction of NO₂ with flame soot. *Geophysical Research Letters*, 25 (13), 2453-2456.
 - Guilbault G.G., Billedeau S.M., 1971. Gas phase reactions of trimethylamine and transition metal salts. *Journal of Inorganic & Nuclear Chemistry*, 33 (5), 1411-1415.
 - Hofmann U., Ohlerich G., 1950. Oberflächenchemie des Kohlenstoffs. *Angewandte Chemie*, 62 (1), 16-21.
 - Horie O., Moortgat G.K., 1998. Gas-phase ozonolysis of alkenes - Recent advances in mechanistic investigations. *Accounts of Chemical Research*, 31 (7), 387-396.
 - Hossain M.Z., Machida S.-I., Nagao M., Yamashita Y., Mukai K., Yoshinobu J., 2004. Highly selective surface Lewis acid-base reaction: trimethylamine on Si(100)c(4x2). *Journal of Physical Chemistry B*, 108 (15), 4737-4742.
 - International Agency for Research on Cancer, 2008. Overall evaluations of carcinogenicity to humans. <http://monographs.iarc.fr/ENG/Classification/crthgr02b.php>.
 - Jacobson M.C., Hansson H.C., Noone K.J., Charlson R.J., 2000. Organic atmospheric aerosols: review and state of the science. *Reviews of Geophysics*, 38 (2), 267-294.

-
- Jencks W. P., 1959. Studies on the mechanism of oxime and semicarbazone formation. *Journal of the American Chemical Society*, 81 (2), 475-481.
 - Jolly W.L., 1991. Modern Inorganic Chemistry. 2nd edition, McGraw Hill, New York.
 - Kahan T.F., Kwamena N.-O.A., Donaldson D.J., 2006. Heterogeneous ozonation kinetics of polycyclic aromatic hydrocarbons on organic films. *Atmospheric Environment*, 40 (19), 3448-3459.
 - Karagulian F., Rossi M.J., 2005. The heterogeneous chemical kinetics of NO₃ on atmospheric mineral dust surrogates. *Physical Chemistry Chemical Physics*, 7 (17), 3150-3162.
 - Karagulian F., Rossi M.J., 2006. The heterogeneous decomposition of ozone on atmospheric mineral dust surrogates at ambient temperature. *International Journal of Chemical Kinetics*, 38 (6), 407-419.
 - Karagulian F., Santschi C., Rossi M.J., 2006. The heterogeneous chemical kinetics of N₂O₅ on CaCO₃ and other atmospheric mineral dust surrogates. *Atmospheric Chemistry and Physics*, 6, 1373-1388.
 - Karagulian F., Rossi M.J., 2007. Heterogeneous chemistry of the NO₃ free radical and N₂O₅ on decane flame soot at ambient temperature: reaction products and kinetics. *Journal of Physical Chemistry A*, 111 (10), 1914-1926.
 - Kawamura K., Ikushima K., 1993. Seasonal changes in the distribution of dicarboxylic acids in the urban atmosphere. *Environmental Science & Technology*, 27 (10), 2227-2235.
 - Kendall M., Brown L., Trought K., 2004. Molecular adsorption at particle surfaces: a PM toxicity mediation mechanism. *Inhalation Toxicology*, 16 (suppl. 1), 99-105.
 - Klein H., Steinmetz A., 1975. Umsetzung Adsorbierter Aromaten mit Ozon. *Tetrahedron Letters*, 48, 4249-4250.
 - Kwamena N.-O.A., Staikova M.G., Donaldson D.J., George I.J., Abbatt J.P.D., 2007. Role of the aerosol substrate in the heterogeneous ozonation reactions of surface-bound PAHs. *Journal of Physical Chemistry A*, 111 (43), 11050-11058.
 - Kwok E.S.C., Atkinson R., Arey J., 1997. Kinetics of the gas-phase reactions of indan, indene, fluorene, and 9,10-dihydroanthracene with OH radicals, NO₃ radicals, and O₃. *International Journal of Chemical Kinetics*, 29 (4), 299-309.
 - Landini D., Montanari F., Rolla F., 1974. Conversion of primary alcohols to alkyl chlorides using aqueous hydrochloric acid in the presence of phase-transfer catalysts. *Synthesis*, 37-38.

-
- Lanz V.A., Alfara M.R., Baltensperger U., Buchmann B., Hueglin C., Szidat S., Wehrli M.N., Wacker L., Weimer S., Caseiro A., Puxbaum H., Prevot A.S.H., 2008. Source attribution of submicron organic aerosols during wintertime inversions by advanced factor analysis of aerosol mass spectra. *Environmental Science & Technology*, 42 (1), 214-220.
 - Larrubia M.A., Ramis G., Busca G., 2001. An FT-IR study of the adsorption and oxidation of N-containing compounds over Fe₂O₃-TiO₂ SCR catalysts. *Applied Catalysis B: Environmental*, 30 (1/2), 101-110.
 - Larsen B.R., Di Bella D., Glasius M., Winterhalter R., Jensen N.R., Hjorth J., 2001. Gas-phase OH oxidation of monoterpenes: gaseous and particulate products. *Journal of Atmospheric Chemistry*, 38 (3), 231-276.
 - Liu X., Mason M., Krebs K., Sparks L., 2004. Full-scale chamber investigation and simulation of air freshener emissions in the presence of ozone. *Environmental Science & Technology*, 38 (10), 2802-2812.
 - Mauderly J.L., Chow J.C., 2008. Health effects of organic aerosols. *Inhalation Toxicology*, 20 (3), 257-288.
 - Neuberger M., Schimek M.G., Horak F. Jr, Moshhammer H., Kundi M., Frischer T., Gomiseck B., Puxbaum H., Hauck H., AUPHEP-Team, 2004. Acute effects of particulate matter on respiratory diseases, symptoms and functions: epidemiological results of the Austrian Project on Health Effects of Particulate Matter (AUPHEP). *Atmospheric Environment*, 38 (24), 3971-3981.
 - Oyama S.T., 2000. Chemical and catalytic properties of ozone. *Catalysis Reviews: Science and Engineering*, 42 (3), 279-322.
 - Park S., Nam H., Chung N., Park J.-D., Lim Y., 2006. The role of iron in reactive oxygen species generation from diesel exhaust particles. *Toxicology in Vitro*, 20 (6), 851-857.
 - Perraudin E., Budzinski H., Villenave E., 2005. Kinetic study of the reactions of NO₂ with polycyclic aromatic hydrocarbons adsorbed on silica particles. *Atmospheric Environment*, 39 (35), 6557-6567.
 - Perraudin E., Budzinski H., Villenave E., 2007a. Kinetic study of the reactions of ozone with polycyclic aromatic hydrocarbons adsorbed on atmospheric model particles. *Journal of Atmospheric Chemistry*, 56 (1), 57-82.
 - Perraudin E., Budzinski H., Villenave E., 2007b. Identification and quantification of ozonation products of anthracene and phenanthrene adsorbed on silica particles. *Atmospheric Environment*, 41 (28), 6005-6017.

-
- Pigment Blacks - Technical Data Europe, 2008. Evonik Degussa GmbH, Frankfurt/Main, Germany.
 - Pope C.A. III, Burnett R.T., Thurston G.D., Thun M.J., Calle E.E., Krewski D., Godleski J.J., 2004. Cardiovascular mortality and long-term exposure to particulate air pollution: epidemiological evidence of general pathophysiological pathways of disease. *Circulation*, 109 (1), 71-77.
 - Pratte P., Rossi M.J., 2006. The heterogeneous kinetics of HOBr and HOCl on acidified sea salt and model aerosol at 40-90% relative humidity and ambient temperature. *Physical Chemistry Chemical Physics*, 8 (34), 3988-4001.
 - Qi J.H., Feng L.J., Li X.G., Zhang M.P., 2006. An X-ray photoelectron spectroscopy study of elements on the surface of aerosol particles. *Journal of Aerosol Science*, 37 (2), 218-227.
 - Radhakrishnan R., Oyama S.T., 2001. Ozone decomposition over manganese oxide supported on ZrO₂ and TiO₂: a kinetic study using *in situ* laser Raman spectroscopy. *Journal of Catalysis*, 199 (2), 282-290.
 - Raley J.H., Rust F.F., Vaughan W.E., 1948. Some free radical reactions of hydrogen chloride. *Journal of the American Chemical Society*, 70 (8), 2767-2770.
 - Ramis G., Larrubia M.A., Busca G., 2000. On the chemistry of ammonia over oxide catalysts: Fourier transform infrared study of ammonia, hydrazine and hydroxylamine adsorption over iron-titania catalyst. *Topics in Catalysis*, 11/12 (1/4), 161-166.
 - Reff A., Turpin B.J., Porcja R.J., Giovannetti R., Cui W., Weisel C.P., Zhang J., Kwon J., Alimokhtari S., Morandi M., Stock T., Maberti S., Colome S., Winer A., Shendell D., Jones J., Farrar C., 2005. Functional group characterization of indoor, outdoor, and personal PM_{2.5}: results from RIOPA. *Indoor Air*, 15 (1), 53-61.
 - Reisen F., Arey J., 2002. Reactions of hydroxyl radicals and ozone with acenaphthene and acenaphthylene. *Environmental Science & Technology*, 36 (20), 4302-4311.
 - Roberts J.D., Caserio M.C., 1977. Basic Principles of Organic Chemistry, 2nd edition. W.A. Benjamin Inc., Menlo Park, CA.
 - Rossi M.J., 2003. Heterogeneous reactions on salts. *Chemical Reviews*, 103 (12), 4823-4882.
 - Salgado M.S., Rossi M.J., 2002. Flame soot generated under controlled combustion conditions: heterogeneous reaction of NO₂ on hexane soot. *International Journal of Chemical Kinetics*, 34 (11), 620-631.

-
- Salgado Muñoz M.S., Rossi M.J., 2002. Heterogeneous reactions of HNO_3 with flame soot generated under different combustion conditions: reaction mechanism and kinetics. *Physical Chemistry Chemical Physics*, 4 (20), 5110-5118.
 - Santschi C., Rossi M.J., 2006. Uptake of CO_2 , SO_2 , HNO_3 and HCl on calcite (CaCO_3) at 300 K: mechanism and the role of adsorbed water. *Journal of Physical Chemistry A*, 110 (21), 6789-6802.
 - Schenk P.W., 1963. Hydroxylammonium salts and Hydroxylamine, in: Brauer G., Handbook of preparative inorganic chemistry, volume I, 2nd edition. Academic Press, New York, 500-503.
 - Shilling J.E., Chen Q., King S.M., Rosenoern T., Kroll J.H., Worsnop D.R., McKinney K.A., Martin S.T., 2008. Particle mass yield in secondary organic aerosol formed by the dark ozonolysis of α -pinene. *Atmospheric Chemistry and Physics*, 8 (7), 2073-2088.
 - Stadler D., Rossi M.J., 2000. The reactivity of NO_2 and HONO on flame soot at ambient temperature: the influence of combustion conditions. *Physical Chemistry Chemical Physics*, 2 (23), 5420-5429.
 - Stephens S., Rossi M.J., Golden D.M., 1986. The heterogeneous reaction of ozone on carbonaceous surfaces. *International Journal of Chemical Kinetics*, 18 (10), 1133-1149.
 - Sze S.-K., Siddique N., Sloan J.J., Escibano R., 2001. Raman spectroscopic characterization of carbonaceous aerosols. *Atmospheric Environment*, 35 (3), 561-568.
 - Tabor K., Gutzwiller L., Rossi M.J., 1993. The heterogeneous interaction of NO_2 with amorphous carbon. *Geophysical Research Letters*, 20 (14), 1431-1434.
 - Tabor K., Gutzwiller L., Rossi M.J., 1994. Heterogeneous chemical kinetics of NO_2 on amorphous carbon at ambient temperature. *Journal of Physical Chemistry*, 98 (24), 6172-6186.
 - Trainham R., Fletcher G.D., Larson D.J., 1987. One- and two-photon detachment of the negative chlorine ion. *Journal of Physics B: Atomic and Molecular Physics*, 20 (23), L777-L784.
 - Ullerstam M., Johnson M.S., Vogt R., Ljungström E., 2003. DRIFTS and Knudsen cell study of the heterogeneous reactivity of SO_2 and NO_2 on mineral dust. *Atmospheric Chemistry and Physics*, 3, 2043-2051.
 - Voll M., Boehm H.P., 1970. Basische Oberflächenoxide auf Kohlenstoff - II. Stöchiometrie und Kinetik der Bildungsreaktion; termischer Abbau. *Carbon*, 8 (6), 741-752.

-
- Voll M., Boehm H.P., 1971a. Basische Oberflächenoxide auf Kohlenstoff - III. Aktiver Wasserstoff und polare Adsorptionszenter. *Carbon*, 9 (4), 473-480.
 - Voll M., Boehm H.P., 1971b. Basische Oberflächenoxide auf Kohlenstoff - IV. Chemische Reaktionen zur Identifizierung der Oberflächengruppen. *Carbon*, 9 (4), 481-488.
 - Wagman D.D., Evans W.H., Parker V.B., Schumm R.H., Halow I., Bailey S.M., Churney K.L., Nuttall R.L., 1982. The NBS tables of chemical thermodynamic properties - Selected values for inorganic and C1 and C2 organic substances in SI units. *Journal of Physical and Chemical Reference Data*, 11 (suppl. 2), 1-&.
 - Warheit D.B., Webb T.R., Colvin V.L., Reed K.L., Sayes C.M., 2007. Pulmonary bioassay studies with nanoscale and fine-Quartz particles in rats: toxicity is not dependent upon particle size but on surface characteristics. *Toxicological Sciences*, 95 (1), 270-280.

Chapter 5 – Markers of biological effects

5.1 Introduction

Free radicals and other reactive species can either be produced by normal cellular metabolism, or come from exogenous sources. These reactive compounds are usually countered in biological systems by antioxidants. When antioxidant defenses are overloaded and not able anymore to eliminate reactive species, oxidative stress occurs and may cause damages to a wide variety of biomolecules, such as proteins, lipids or deoxyribo-nucleic acid (DNA). Direct measurement of free radicals and reactive species is very difficult because of their short life time. Therefore, the study of oxidative stress in biological systems preferably involves the measurement of biomarkers that reflect damages induced from an attack by reactive species on different cellular structures, such as the DNA, or the lipid bilayer of cell membranes (de Zwart *et al*, 1999).

Over the past 15 years, 8-hydroxy-2'-deoxyguanosine (8OHdG) has been widely used as biomarker of oxidative DNA damage due to an exposure to pollutants or resulting from various illnesses. Table 5.1 gives some examples of such studies. The aim of these studies was usually to compare urinary levels of 8OHdG for a large and homogeneous population exposed to a specific pollutant with those obtained for an unexposed control population. Exposure to fine particles, polycyclic aromatic hydrocarbons (PAHs) and other types of chemical compounds usually leads to a significant increase of urinary levels of 8OHdG. Many studies (Yao *et al*, 2004; Lodovici *et al*, 2005; Hu *et al*, 2006 (a)) pointed out effects of cigarette smoke in urinary levels of 8OHdG. These results indicate that cigarette smoke contains chemical compounds which induce oxidative stress and may be an important confounding factor. Therefore smokers are systematically separated from non-smokers in statistical analyses. In addition to cigarette smoke, other confounding factors have been identified in previous studies, such as body mass index (BMI; Mizoue *et al*, 2006), food habits and alcohol consumption (Irie *et al*, 2005), perceived workload and psychological stress (Irie *et al*, 2001). Moreover, many studies pointed out increased levels of 8OHdG during cancer (Tagesson *et al*, 1995; Cho *et al*, 2006) and other diseases (Akagi *et al*, 2003; Kono *et al*, 2006).

Table 5.1: Non-exhaustive list of studies where 8OHdG was used as biomarker of oxidative stress.

Population	Age	Approach	Matrix	Mean 8OHdG (\pm SD)	Reference
Smokers (n=21)	48.2 \pm 12.5	CE-AD	Urine	23.5 (\pm 21.3) μ g/g creatinine	Yao <i>et al</i> , 2004
Non-smokers (n=21)	30.7 \pm 9.3	CE-AD	Urine	12.6 (\pm 13.2) μ g/g creatinine	
Smokers (n=30)	41 \pm 2.2	HPLC-ECD	Leukocytes	1.98 (\pm 0.47) 8OHdG/10 ⁵ dG	Lodovici <i>et al</i> , 2005
Non-smokers (n=29)	40.3 \pm 2.1	HPLC-ECD	Leukocytes	0.59 (\pm 0.09) 8OHdG/10 ⁵ dG	
Smokers (n=32)	25.4 \pm 7.9	LC-MS/MS	Urine	7.26 (\pm 3.14) μ g/g creatinine	Hu <i>et al</i> , 2006 (a)
Non-smokers (n=35)	23.1 \pm 3.0	LC-MS/MS	Urine	4.69 (\pm 1.70) μ g/g creatinine	
Cancer patients (n=136)	N/A	HPLC-ECD	Urine	2.13 (\pm 1.40) μ mol/mol creatinine	Tagesson <i>et al</i> , 1995
Healthy individuals (n=27)	N/A	HPLC-ECD	Urine	1.11 (\pm 0.62) μ mol/mol creatinine	
Patients with dilated cardiomyopathy (n=56)	53 \pm 12	ELISA	Serum	5.2 (\pm 2.9) ng/ml	Kono <i>et al</i> , 2006
Control subjects (n=20)	50 \pm 12	ELISA	Serum	3.0 (\pm 1.5) ng/ml	
Workers exposed to styrene (n=17)	41.5 \pm 11.5	HPLC-UV-ECD	White blood cells	2.23 (\pm 0.54) 8OHdG/10 ⁵ dG	Marczynski <i>et al</i> , 1997
Control workers (unexposed, n=67)	40.9 \pm 13.1	HPLC-UV-ECD	White blood cells	1.52 (\pm 0.45) 8OHdG/10 ⁵ dG	
Engine room personnel exposed to PAH (n=19)	37	HPLC-ECD	Urine	23.2 nmol/l, adjusted to urine density (min: 18.6, max: 27.8)	Nilsson <i>et al</i> , 2004
Control workers (unexposed, n=33)	43	HPLC-ECD	Urine	18.0 nmol/l, adjusted to urine density (min: 15.2, max: 20.7)	
Workers exposed to arsenic (n=50)	22.7 \pm 2.9	LC-MS/MS	Urine	5.60 (\pm 2.77) μ g/g creatinine	Hu <i>et al</i> , 2006 (b)
Control workers (unexposed, n=40)	22.0 \pm 2.9	LC-MS/MS	Urine	3.35 (\pm 1.63) μ g/g creatinine	
Workers exposed to coke oven emissions (n=47)	39.9 \pm 1.5	HPLC-ECD	Urine	1.9 μ mol/mol creatinine (min: 1.4, max: 15.4)	Liu <i>et al</i> , 2006
Control workers (unexposed, n=31)	38.7 \pm 2.4	HPLC-ECD	Urine	1.3 μ mol/mol creatinine (min: 1.0, max: 4.0)	
Workers exposed to PM _{2.5} , pre-workshift (n=91)	N/A	ELISA	Urine	13.26 (\pm 1.04) μ g/g creatinine	Kim <i>et al</i> , 2004
Workers exposed to PM _{2.5} , post-workshift (n=90)	N/A	ELISA	Urine	15.22 (\pm 0.99) μ g/g creatinine	
People exposed to traffic exhausts (n=47)	N/A	ELISA	Urine	13.3 (\pm 7.1) μ g/g creatinine	Lai <i>et al</i> , 2005
Control population (unexposed, n=24)	N/A	ELISA	Urine	8.4 (\pm 6.2) μ g/g creatinine	
Taxi/moto drivers in a major city (n=35)	N/A	HPLC-UV-ECD	Lymphocyte DNA	2.05 (\pm 1.25) 8OHdG/10 ⁵ dG	Fanou <i>et al</i> , 2006
Village residents (n=6)	N/A	HPLC-UV-ECD	Lymphocyte DNA	1.11 (\pm 0.82) 8OHdG/10 ⁵ dG	

SD: standard deviation.

N/A: not available.

8OHdG is an oxidized by-product of deoxyguanosine, one of the four constituents of DNA.

The molecule comprises a guanine with a hydroxyl group at C₈, and attached to a deoxyribose ring (Figure 5.1(a)). 8OHdG has a molecular mass of 283.24 g/mol, and the molecule is polar due to the presence of hydroxyl and carbonyl functions. Among the four nucleosides involved in the DNA structure, guanosine is the one which has the lowest redox potential. Therefore, in the case of an oxidative stress on DNA, guanosine is preferentially oxidized. This explains why 8OHdG is so widely used to monitor oxidative damages on DNA. Culp *et al* (1989) studied structural and acid-base properties of 8OHdG by means of nuclear magnetic resonance (NMR) spectroscopy (¹³C and ¹⁵N), ultra-violet (UV) absorption and infra-red (IR) spectral analyses. The molecule contains two keto-enol equilibriums, leading to the presence of four possible isomers (Figure 5.1(b)). Among these isomers, 6-8,diketo is the more stable. Acid-base titration indicates the presence of two pK_a values, at respectively pH 8.6 and 11.7. These pK_a values suggest that the molecule remains neutral at acidic and neutral pH, while it undergoes deprotonation at alkaline pH, leading to the formation of a dianion in strong alkali (Figure 5.2). Acid-base properties of 8OHdG are of prime importance for the development of an analytical method, because the pH of urine samples fixes the charge of the molecule

(neutral molecule, anion or dianion), and therefore influences the behavior of the compound during the urine clean-up (by solid-phase extraction [SPE]) and the separation step (by chromatography).

Figure 5.1: Molecular structure (a) and tautomeric forms (b) of 8-hydroxy-2'-deoxyguanosine.

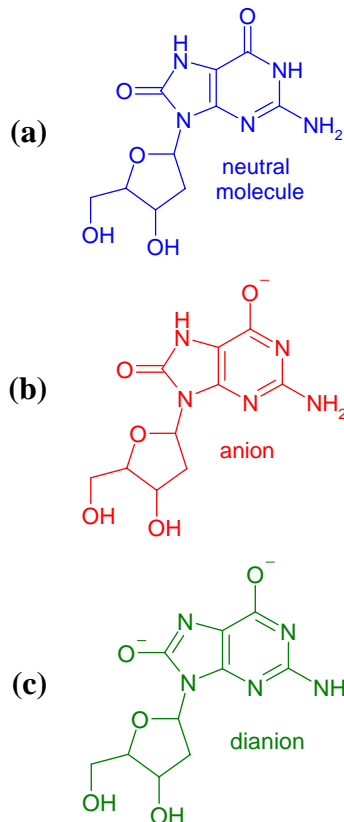
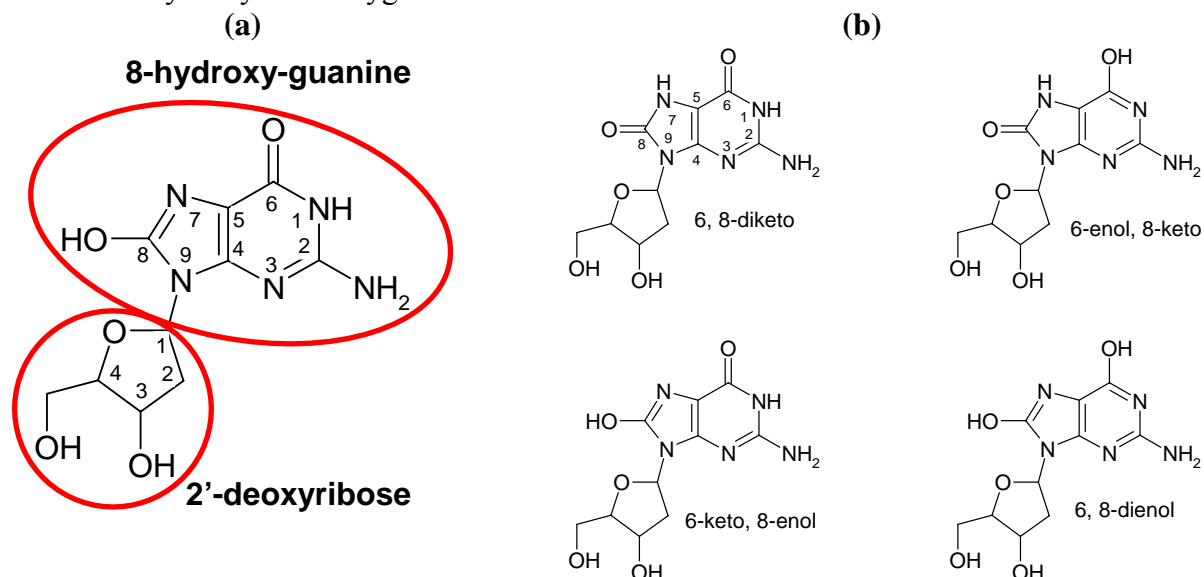
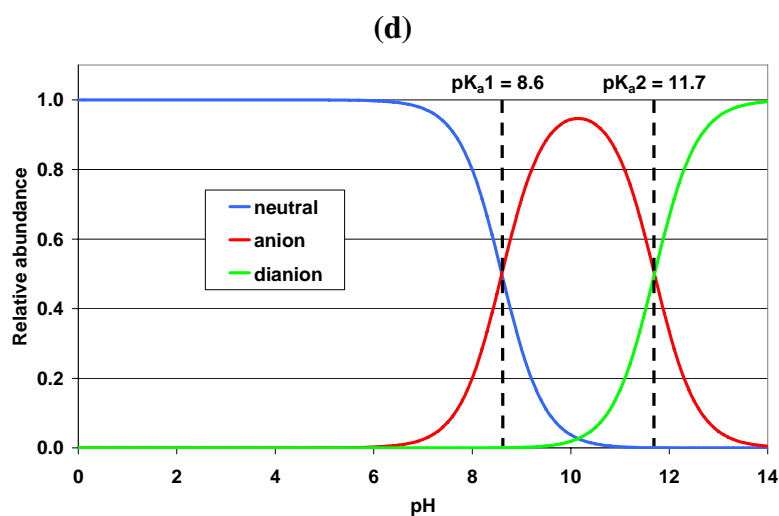


Figure 5.2: Molecular structure of 8OHdG under neutral (a), anionic (b) and dianionic (c) form. Relative abundance of these three forms depending on pH (d).



Over the past 10 years, great efforts have been placed into the development of analytical methodology for 8OHdG. Analytical approaches for the quantification of 8OHdG include separation techniques (high performance liquid chromatography [HPLC], gas chromatography [GC], capillary electrophoresis [CE]), immunoassays, and methods of labeling of nucleotides with radioactive ^{32}P or fluorescent compounds. Table 5.2 gathers various analytical methods recently published, with their respective limit of detection and recovery rate.

Table 5.2: Non-exhaustive list of analytical methods for 8OHdG.

Approach	Matrix	Limit of detection	Recovery rate	Reference
HPLC-ECD	urine	0.9 nM	45.8 %	Germadnik <i>et al</i> , 1997
HPLC-ECD	urine	N/A	90-98 %	Kasai <i>et al</i> , 2001
HPLC-ECD	urine	17.7 nM	74.5 %	de Martinis and Bianchi, 2002
HPLC-ECD	urine	3 nM	71 %	Samcová <i>et al</i> , 2004
HPLC-ECD	urine	80 nM	71 %	Rebelo <i>et al</i> , 2004
HPLC-ECD	urine	17.7 nM	97.2 %	Matayatsuk and Wilairat, 2008
LC-MS/MS	calf thymus DNA	1.25 nM	N/A	Singh <i>et al</i> , 2003
LC-MS/MS	urine	0.71 nM	83.2 %	Sabatini <i>et al</i> , 2005
LC-MS/MS	urine	0.50 nM	81%	Cooke <i>et al</i> , 2006
LC-MS/MS	urine	0.02 nM	99-102 %	Hu <i>et al</i> , 2006 (a)
LC-MS/MS	urine	2 nM	96.4-111.2 %	Malayappan <i>et al</i> , 2007
LC-MS/MS	urine	0.48 nM	99.6-106 %	Crow <i>et al</i> , 2008
GC-MS	urine	2.5 nM	N/A	Lin <i>et al</i> , 2004
GC-MS	urine	0.5 nM	99.37%	Mei <i>et al</i> , 2005
CE-ECD	urine	50 nM	56%	Weiss and Lunte, 2000
CE-ECD	urine	20 nM	87.2%	Mei <i>et al</i> , 2003
CE-UV	urine	1700 nM	N/A	Kvasnikova <i>et al</i> , 2003
ELISA	human DNA	1 per 10^5 dG	78.4%	Yin <i>et al</i> , 1995
ELISA	urine	1.8 nM	N/A	Chiou <i>et al</i> , 2003
ELISA	urine	2.3 nM	N/A	Kim <i>et al</i> , 2004
ELISA	urine	1.77 nM	N/A	Cooke <i>et al</i> , 2006
ELISA	blood	3.5 nM	N/A	Konopka <i>et al</i> , 2007
^{32}P -labelling	calf thymus DNA	1 per $5 \cdot 10^4$ nucleotides	N/A	Randerath <i>et al</i> , 1981
^{32}P -labelling	calf thymus DNA	0.1 per 10^5 dG	32-42 %	Zeisig <i>et al</i> , 1999
^{32}P -labelling	calf thymus DNA	<1.8 per 10^7 nucleotides	55-70 %	Gupta and Arif, 2001

N/A: not available.

One of the most commonly used methods of measuring 8OHdG levels involves HPLC separation with electro-chemical detection (HPLC-ECD). Analyses by HPLC-ECD are often preceded by a clean-up procedure with solid-phase extraction (SPE), in order to remove a maximum of contaminants from the urine matrix. However, recent methodology focuses on simplifying and expediting sample cleanup procedures for urine and reducing artifactual oxidation for DNA digests (Adachi *et al*, 1995; Helbock *et al*, 1998; Hofer and Möller, 2002). These issues have been addressed by employing various SPE columns, immunoaffinity columns, and column-switching techniques (Park *et al*, 1992; Bogdanov *et al*, 1999; Kasai,

2003). The latter methodology captures a fraction corresponding to 8OHdG on the first column, which is then eluted and chromatographically separated on the second column. A number of columns have been used for this technique, including anion and cation exchange and reverse phase columns such as C₈ and C₁₈. The main criticism of HPLC-ECD methods employing multiple column switching techniques is that the timing of the 8OHdG fraction elution changes on different days and is dependent on the sample injected (Kasai, 2003).

Mass spectrometry (MS) coupled with either HPLC or GC has provided a sensitive means of detection for oxidative DNA damage, capable of providing structural information. Unlike HPLC methodology, samples must be converted into volatile derivatives prior to the analysis by GC-MS, a procedure which induces artificial oxidation of the related normal DNA components. Therefore, results obtained by GC/MS are usually overestimated compared to HPLC (Cadet *et al*, 1997). According to Table 5.2, chromatographic methods coupled to MS detection (LC-MS/MS and GC-MS) are so far the most sensitive techniques for the analysis of 8OHdG. This trend has also been observed in previous studies in which the performance of different analytical methods was compared (Cooke *et al*, 2006). Nevertheless, because of the generation of artificial oxidation products in GC/MS methodology, LC-MS/MS remains the most suitable analytical method for 8OHdG.

Capillary electrophoresis (CE) has been applied as a separation approach for the analysis of 8-OHdG as an alternative to HPLC methods, which may involve column switching techniques (Weiss and Lunte, 2000; Mei *et al*, 2003). Greater separation efficiency is expected with CE, which is favorable for 8OHdG analysis in complex biological matrices where interferences may complicate the assay (Yao *et al*, 2004). However, there are inherent disadvantages in CE concerning concentration sensitivity and detection limits, particularly for UV detection. The small volumes used for detection in CE result in lowered concentration sensitivity and reduced limits of detection when compared to HPLC. Sample concentration techniques and sensitive detection modes have been employed for the analysis of 8OHdG using CE. Detection modes used in CE include electro-chemical detector (CE-ECD), UV (CE-UV), and laser-induced fluorescence of the labeled nucleotide.

Enzyme-linked immuno-sorbent assay (ELISA) is based on a reaction between 8OHdG and a monoclonal antibody. Different procedures are used to quantify 8OHdG by ELISA. Usually, the analytical procedure takes place in small plates, and involves a reaction between 8OHdG

and a first monoclonal antibody, followed by an enzyme-labeled secondary antibody. Then, a substrate solution is added in the plate and results in the development of color in proportion to the amount of 8OHdG. The compound is finally quantified by measuring the absorbance of the solution. Recent analytical methods make use of an ELISA kit specially prepared for the analyses of 8OHdG, and manufactured by the Japan Institute for the Control of Aging (JaICA). ELISA allows to measure tens of samples per day, and remains so far the fastest and simplest method. Nevertheless, several publications reported that results obtained by ELISA are overestimated compared to HPLC, because of a lack of selectivity of antibodies, which interact also with other compounds than 8OHdG (Breton *et al*, 2003).

³²P-postlabelling methods involve the incorporation of a radioactive label into nucleotides digested from DNA and the monitoring of radioactivity for quantitative measurement (Randerath *et al*, 1981). Highly sensitive ³²P-postlabelling methods have been developed for the analysis of 8OHdG adducts, measured as monophosphate nucleotides in biological samples (Randerath *et al*, 1981; Zeisig *et al*, 1999; Gupta and Arif, 2001).

Exposure to free radicals has led organisms to develop a series of defense mechanisms. According to the hierarchical oxidative stress model (Li *et al*, 2002; Xiao *et al*, 2003; Nel *et al*, 2006) discussed in Chapter 1, antioxidant response represents the first line of defense against reactive oxygen species (ROS). According to many studies undertaken with animals and humans, exposure to particulate matter induced oxidative stress and inflammation, and was accompanied by an alteration of the antioxidant status (Liu and Meng, 2005; Behndig *et al*, 2006; Delfino *et al*, 2008).

The determination of antioxidants has been widely investigated in the field of human health. Analyses are usually performed by spectrophotometry, fluorescence and chromatography, but these traditional techniques are being replaced by other innovative technologies (Prieto-Simón *et al*, 2008). In this direction, electrochemical biosensors are promising tools, suitable for fast analyses, based on inexpensive instrumentation and simple operation protocols. These biosensors have been developed for the assessment of the antioxidant capacity, based on the ability to counter free radicals. The presence of antioxidants in a sample where radicals are generated involves the decomposition of radicals. Therefore, evaluation of the antioxidant capacity of different compounds can be determined based on the variation of the ROS concentration in the reaction medium. With the aim to assess antioxidant capacity based on

the measurement of $O_2^{\bullet -}$ concentration, two main types of biosensors have been developed, using cytochrome c or super-oxide dismutase (SOD) enzyme. Another method to determine the antioxidant capacity is by measuring the damage produced to DNA by free radicals. In this case, the presence of antioxidants involves a decrease in DNA alterations. Recently, an antioxidant redox sensor was developed by EDEL Therapeutics S.A. (Lausanne, Switzerland). This technique is an electrochemical-based method allowing to measure the level of antioxidants in biological fluids (saliva, serum, urine).

Within the framework of the study in the bus depots, our first task was to develop an analytical method for the quantification of 8OHdG in urine samples. After a first attempt to develop the analytical method by HPLC-ECD, we decided to use a recently acquired LC-MS/MS. An efficient analytical method was successfully developed using this equipment, and used for the quantification of 8OHdG in urine samples of the volunteers during the study in the bus depots. At the same time, we had the opportunity to test the new antioxidant redox sensor, developed by EDEL Therapeutics S.A. We decided to use this technique to analyze urine samples during the study in the bus depots, and to check whether we could correlate the oxidative stress status and the level of antioxidants.

5.2 Material and methods

5.2.1 *Chemicals*

8OHdG (>98%, TLC), water (for HPLC), methanol (CHROMASOLV for HPLC), acetonitrile (CHROMASOLV for HPLC), formic acid (puriss. p. a. eluent additive for LC-MS), KH_2PO_4 (puriss. p.a., anhydrous), picric acid (13 g/l solution) and Discovery DSC-SAX SPE cartridges (500 mg, 3 ml) were purchased from Sigma-Aldrich Chemie GmbH (Buchs, Switzerland). Na_2HPO_4 (anhydrous GR), NaOH and creatinine were purchased from Merck AG (Dietikon, Switzerland); trichloroacetic acid (1.2 M solution) from Roche AG (Rotkreuz, Switzerland); BondElut C_{18}/OH SPE cartridges (500 mg, 3 ml) from Varian Inc (distributor in Switzerland: BioPack Sàrl, Lausanne); and Oasis WCX SPE cartridges (1 ml, 30 mg, 30 μm) from Waters AG (Rapperswil, Switzerland). Prior to use, water was filtered on a Teflon membrane (filter type HV, pore size 0.45 μm) purchased from Millipore AG (Volketswil, Switzerland), while methanol and acetonitrile were distilled and degassed in an ultrasonic cleaner (Branson Ultrasonic Corp., model 5210).

A stock solution of 8OHdG (309.3 μM) was prepared by dissolving 4.38 mg of 8OHdG in 50 ml water, and stored at -25°C . From this, an intermediate stock solution (30.9 μM) was prepared by dilution with water, and also stored at -25°C . Calibration standards (0.9, 1.8, 4.4, 8.8, 17.5, 43.8, 87.6 and 175.2 $\text{pg}/\mu\text{l}$) were prepared weekly by dilution of the intermediate stock solution with water, and stored at $+4^{\circ}\text{C}$.

Urine samples of the workers were collected during the field campaign in the bus depots. Population under study and urine sampling were described in detail in Chapter 2. Two control urine samples were prepared to control the quality of analyses. All these urine samples were vigorously mixed, separated into aliquots of 4 ml, and stored at -25°C until analyses.

5.2.2 Analytical method of urinary 8OHdG by HPLC-ECD

Even if HPLC-ECD is not the most sensitive and selective method (see Table 5.2), we decided to develop an analytical method based on this technique, because the required equipment was already available at the Institute for Work and Health. Two different clean-up procedures were tested.

For the first clean-up procedure, a weak cation exchange SPE cartridge (Oasis WCX) was used. Two solutions were prepared prior to the analyses. A phosphate buffer (25 mM, pH 7) was prepared by dissolving 500 mg of KH_2PO_4 and 2.5 gr of Na_2HPO_4 in 1 l of water. A solution of 20 mM KH_2PO_4 was prepared by dissolving 2.7218 g KH_2PO_4 in 1 l of water. Urine samples were thawed and mixed with an equal volume of phosphate buffer (25 mM, pH 7). Oasis WCX SPE cartridges were first conditioned with 1 ml of methanol, 1 ml of water and 1 ml of phosphate buffer (pH 7). SPE cartridges were then loaded with 1 ml of urine sample. We cleaned with 1 ml of phosphate buffer (pH 7) and 1 ml of acetonitrile. 8OHdG was then eluted with 1 ml of methanol, and SPE cartridges were dried under vacuum. The solvent was evaporated under a stream of nitrogen at 37°C . 8OHdG was finally dissolved in 1 ml of mobile phase for HPLC (96.5% KH_2PO_4 20 mM, 2.5% acetonitrile and 1% methanol), and 50 μl of this solution were injected into HPLC-ECD.

The second clean-up procedure was developed with a combined SPE system constituted of a strong anion exchange (Discovery DSC-SAX) and a hydrophobic (BondElut C_{18}/OH) cartridge. Several solutions were also prepared prior to the analyses. A solution of 5 mM

H₂SO₄ was prepared by diluting 27 µl of H₂SO₄ 98% in 100 ml of water. A phosphate buffer (pH 6.9) was prepared by dissolving 3.549 g Na₂HPO₄ and 3.402 g KH₂PO₄ in 1 l of water. Discovery DSC-SAX SPE cartridges were first conditioned with 4 ml of methanol, 4 ml of H₂SO₄ 5 mM, 4 ml of water and 4 ml of phosphate buffer (pH 6.9). SPE cartridges BondElut C₁₈/OH were conditioned separately with 4 ml of methanol, 4 ml of methanol 15% in phosphate buffer, 4 ml of water and 4 ml of phosphate buffer. Discovery DSC-SAX SPE cartridges were then fixed over BondElut C₁₈/OH, and SPE cartridges were loaded with 1 ml of urine sample and 4 ml of phosphate buffer. Then we removed Discovery DSC-SAX SPE cartridges, and we washed BondElut C₁₈/OH with 4 ml of phosphate buffer (pH 6.9) and 4 ml of methanol 5% in phosphate buffer. 8OHdG and other adsorbed material were finally eluted with 5 ml of methanol 15% in phosphate buffer, and SPE cartridges were dried under vacuum. The samples were concentrated up to approximately 1 ml in a SpeedVac concentrator (Savant, model SVC100H), and the volume of solvent remaining in the tubes after this step was determined by gravimetry, assuming that the entire methanol was removed during the concentration in the SpeedVac and that the density of the remaining solvent was 1 g/ml. 50 µl of the eluat were finally injected into HPLC-ECD.

The separation of 8OHdG was carried out using a HPLC system (Varian Inc, model LC 5000) consisting of a pump for three mobile phases, an AutoSampler (Varian Inc, model 9090), and a ZORBAX Bonus-RP analytical column (length = 250 mm, inner diameter = 4.6 mm, porosity 5 µm; Agilent Technologies, distributor in Switzerland: MSP Friedli & Co, Koeniz) equipped with a guard cartridge (length = 12.5 mm, inner diameter = 4.6 mm, porosity 5 µm; Agilent Technologies). Detection was carried out with an electro-chemical detector (ECD; Hewlett-Packard, model 1049A). For the preparation of the mobile phase, a solution of KH₂PO₄ 20 mM was prepared by dissolving 2.7218 g KH₂PO₄ in 1 l of water. The mobile phase used for isocratic elution of 8OHdG was composed of 96.5% KH₂PO₄ 20 mM, 2.5% acetonitrile and 1% methanol (pH 4.6), and was degassed in an ultrasonic cleaner. Table 5.3 shows parameter settings for HPLC and ECD.

Table 5.3: Parameter settings for HPLC-ECD.

HPLC	Analytical column	ZORBAX Bonus-RP (L=250 mm, ID=4.6 mm, 5 μ m)
	Program mobile phase ^a	isocratic: 0' = 100% A 30' = 100% A
	Flow rate	0.8 ml/min
	Column temperature	30 °C
	Injection volume	50 μ l
ECD	Working electrode	Glassy carbon
	Reference electrode	Ag/AgCl
	Mode	Pretreat
	Potential	+ 0.600 V
	Upper limit	+ 1.000 V
	Lower limit	- 0.600 V
	Response time	4 sec
	Peak width	0.4 min
	Polarity	Oxidation
	Prepare time	2 min
	Stop time	25 min
	Post time	15 min
	Pretreat cycles	80
	Potential 1	+ 1.500 V
	Potential 2	- 1.000 V
	Time 1	500 msec
	Time 2	500 msec
	Time 3	500 msec
	Temperature	30°C

^a solution A = 96.5% KH₂PO₄ 20 mM, 2.5% acetonitrile and 1% methanol (pH 4.6).

Identification of 8OHdG on the chromatograms was based on retention time only. Quantification of 8OHdG in urine was performed by peak-area integration, and by using a six-point calibration curve. For that purpose, we injected external standard solutions of 8OHdG in water in the concentration range of 4.4-175.2 pg/ μ l.

5.2.3 Analytical method of urinary 8OHdG by LC-MS/MS

Prior to the analyses, urine samples were thawed and mixed with an equal volume of bidistilled water. If the urine pH is higher than 7.0, urine samples must be acidified with 20 μ l of HCl 2 M. BondElut C₁₈/OH SPE cartridges were first conditioned with 4 ml of methanol and 4 ml of bidistilled water. SPE cartridges were then loaded with 2 ml of urine sample. We cleaned with 4 ml of bidistilled water and 4 ml of methanol 5% in bidistilled water, in order to remove some interfering compounds. 8OHdG was finally eluted with 7 ml methanol 15% in bidistilled water, and these samples were concentrated up to approximately 1 ml in a SpeedVac concentrator (approximately 6 hours). The volume of solvent remaining in the tubes after this step was determined by gravimetry, assuming that the entire methanol was removed during the concentration in the SpeedVac and that the density of the remaining solvent was 1 g/ml.

20 µl of the samples were injected into a LC-MS/MS system constituted of two pumps (Varian Inc, model ProStar 210), an AutoSampler (Varian Inc, model ProStar 410), a Polaris C-18 analytical column (length = 50 mm, inner diameter = 2 mm, porosity 5 µm), and a tandem mass spectrometer (Varian Inc, model 1200). Two solutions of 0.1% formic acid in water (pH 2.7) and 0.1% formic acid in methanol were degassed in an ultrasonic cleaner, and used for the mobile phase. Table 5.4 gathers parameter settings for HPLC and MS/MS.

Table 5.4: Parameter settings for LC-MS/MS.

<u>HPLC</u>	Analytical column	Polaris C-18 (L=50mm, ID=2mm, 5µm)
	Program mobile phase ^a	0' = 95% A / 5% B 3' = 95% A / 5% B 5' = 30% A / 70% B 10' = 30% A / 70% B 10.1' = 95% A / 5% B 15' = 95% A / 5% B
	Flow rate	0.3 ml/min
	Column temperature	40 °C
	Injection volume	20 µl
<u>MS/MS</u>	Ionization mode	Negative
	Gas	Air
	Housing temperature	65 °C
	Nebulization temperature	290 °C
	Drying gas temperature	250 °C
	Needle tension	- 4500 V
	Shield tension	- 600 V
	Capillary tension	- 68 V
	Ion monitoring in 1 st quadrupole	m/z 282
	Argon collision energy in 2 nd quadrupole	- 19 V for m/z = 282
	Ion monitoring in 3 rd quadrupole	m/z 192

^a solution A = 0.1% formic acid in water (pH 2.7); solution B = 0.1% formic acid in methanol.

Identification of 8OHdG on the chromatograms was based on retention time only. Quantification of 8OHdG in urine was done by peak-area integration, and by using an eight-point calibration curve. For that purpose, we injected external standard solutions of 8OHdG in water in the concentration range of 0.9-175.2 pg/µl. Urinary concentrations of 8OHdG were then adjusted to creatinine (analytical method described below), and the results expressed in terms of µg 8OHdG per g creatinine.

5.2.4 Measurement of urinary creatinine

Urinary analytes may be more or less diluted depending on water intake. In order to take into account this dilution effect between urine samples, concentrations of analytes require adjustment to parameters which have low variability or constant excretion in time, and are only slightly influenced by exogenous factors. Thus, urinary levels of analytes are usually

normalized to 1 g of urinary creatinine or to specific gravity (Carrieri *et al*, 2001). Creatinine is a break-down product of creatine phosphate in muscle and is excreted at a fairly constant rate into urine, while specific gravity depends on the body's hydration and urinary solutes. Creatinine adjustment works well if the analyte behaves similarly to creatinine in the kidney. However, if the analyte is excreted predominantly through passive secretion in the kidney, the analyte secretion will vary with urine flow rate, and creatinine adjustment would not correct for urine concentration/dilution (Barr *et al*, 2005). To our knowledge, no publication has reported clearly the excretion mechanism of 8OHdG in the kidney. Nevertheless, almost all the publications related to the measurement of 8OHdG in urine normalized systematically to creatinine, except for the case of one publication which used specific gravity (Nilsson *et al*, 2004; see Table 5.1). Therefore, we decided to normalize to creatinine.

The analytical method of creatinine is based on the colorimetric determination of the picrate-creatinine complex formed in alkaline condition (Jaffe's method; Jaffe, 1886). Analyses were performed at the Institute for Work and Health according to a METAS-accredited method. Prior to the analysis, several solutions were prepared. A solution of 35 mM picric acid was prepared by diluting 31 ml of picric acid 13 g/l up to 50 ml with water. A solution of 1.6 M NaOH was prepared by dissolving 6.4 g NaOH in 100 ml water. A picric acid/NaOH mixture was then prepared by mixing an equal volume of 35 mM picric acid and 1.6 M NaOH. A standard solution of creatinine was obtained by dissolving 100 mg creatinine in 50 ml water, and by diluting this solution 50 times in water. 0.5 ml of the diluted standard solution was then mixed with 0.5 ml of trichloroacetic acid and 1 ml of picric acid/NaOH mixture. Urine samples were defrosted and diluted 50 times in water. 0.5 ml of diluted urine was then mixed with 0.5 ml of trichloroacetic acid and 1 ml of picric acid/NaOH mixture. The urine sample was then vigorously mixed, incubated at 37°C during 20 min, and analyzed using a spectrophotometer at a wavelength of 520 nm. Urinary concentration of creatinine [mg/l] was calculated using Equation 5.1.

$$[\text{creatinine}] = 50 \cdot 30 \cdot \frac{\text{absorption of urine sample}}{\text{absorption of standard solution}} \quad \text{Equation 5.1}$$

5.2.5 Measurement of urinary antioxidants

We used a novel antioxidant redox sensor, manufactured by EDEL Therapeutics S.A. This technique is an electrochemical-based method allowing to measure the level of antioxidants in biological fluids (saliva, serum, urine). 100 µl of biological fluid are laid down on a chip, and an increasing potential between 0 and +1.2 V (vs Ag/AgCl reference electrode) is applied between two metallic conductors. The current is then recorded; if a compound undergoes a redox reaction within this range of potential, then it will give a contribution to the current. Since potential is increasing from low to high voltage, only antioxidants in their reduced state will be measured by such a method. We used this technique to analyze urine samples during the study in the bus depots.

5.2.6 Statistical analyses

Statistical analyses were performed using SYSTAT for Windows, version 10.2. Analysis of variance (ANOVA) was performed in order to test whether the evolution of urinary levels of 8OHdG, creatinine and antioxidants between Monday morning and Tuesday evening were statistically significant. The differences were considered significant when $p < 0.05$. The comparison of urinary levels of 8OHdG between smokers and non-smokers was tested using the non-parametric Mann-Whitney U-test. Both groups were considered as significantly different when $p < 0.05$. Correlations between 8OHdG, creatinine, and antioxidants were tested using the Spearman's rank correlation coefficient, and were considered significant when $p < 0.05$.

5.3 Results and discussion

5.3.1 Analytical method of urinary 8OHdG by HPLC

Our first attempt to develop an analytical method for 8OHdG was based on a 1-step clean-up procedure, with a weak cation exchange cartridge (Oasis WCX). This sorbent contains carboxylate ions ($-\text{COO}^-$) as well as aliphatic and aromatic groups. During the clean-up procedure, 8OHdG was supposed to be retained by aliphatic and aromatic groups through hydrophobic interactions, while interfering acidic compounds in urine, which are normally deprotonated and negatively charged at the conditions of the analysis (pH 7), are eliminated during this step. The separation by HPLC was then performed using a reverse-phase column (ZORBAX Bonus-RP), which contains polar amid groups incorporated in long alkyl chains. 8OHdG being polar and under neutral form at the pH of the mobile phase (pH 4.6), the molecule is expected to move slowly through the analytical column and to have a high

retention time, due to important interactions with the stationary phase. Detection was carried out using an ECD. This detector applies a constant potential in the mobile phase, and if a charge transfer occurs between an analyte and the electrode at that potential, then it will give a signal proportional to its concentration. The principle of measurement explains the lack of selectivity of this detector, because each chemical compound which undergoes a redox reaction at the selected potential may interfere with 8OHdG. Therefore, 8OHdG must be very well separated from other compounds of the urine matrix to be correctly quantified.

Figure 5.3 shows typical chromatograms obtained with different standard solutions. The retention time for 8OHdG was 21.2 minutes. The shape of the peaks (absence of tailing) and the full width at half maximum (approximately 30 seconds) indicate that the signal obtained under these conditions was satisfactory.

Figure 5.3: Typical chromatograms of standard solutions obtained by HPLC-ECD. Conditions of analysis as described in Table 5.3. **009:** 8.8 pg/ μ l; **018:** 17.5 pg/ μ l; **044:** 43.8 pg/ μ l; **088:** 87.6 pg/ μ l; **175:** 175.2 pg/ μ l.

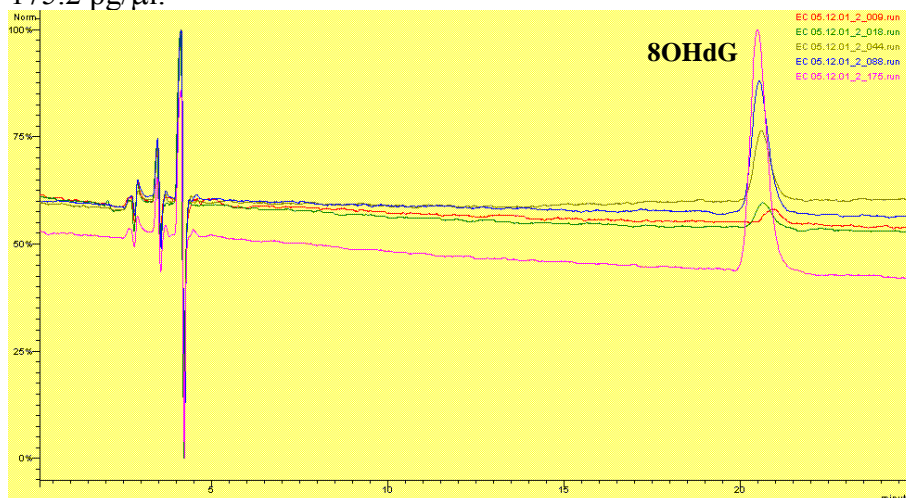
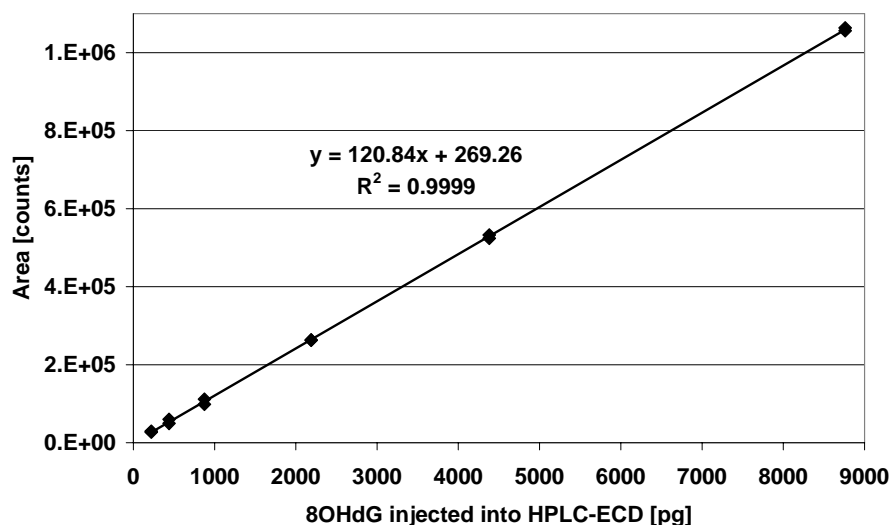


Figure 5.4 shows a six-point calibration curve prepared in duplicate. The calibration curve was found to be linear in the range of 220-8760 pg injected into the HPLC, which corresponds to a concentration range of 4.4-175.2 pg/ μ l (15.5-619.1 nM). An excellent linearity was obtained over the entire concentration range, with a correlation coefficient (R^2) of 0.9999.

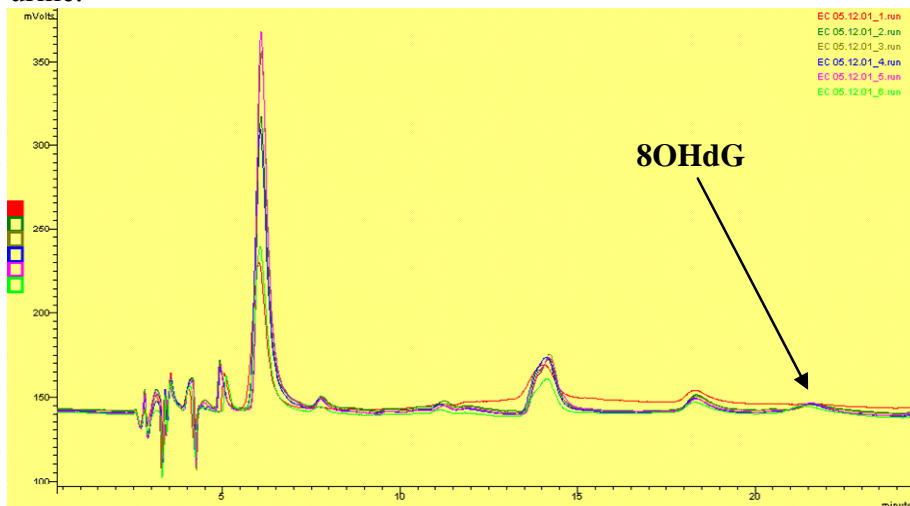
Figure 5.4: Six-point calibration curve measured in duplicates by HPLC-ECD. Conditions of analysis as described in Table 5.3.



The limit of detection was determined by measuring the signal to noise ratio (S/N) for several chromatograms of standard solutions and urine samples. We consider the limit of detection as the concentration of 8OHdG for which $S/N = 3$. The limit of detection was determined to be 1.5 pg/ μ l (5.3 nM) for standard solutions, and 5.0 pg/ μ l (17.7 nM) for urine samples. These values are approximately in the range of previous studies (Table 5.2) which used the same equipment (HPLC-ECD).

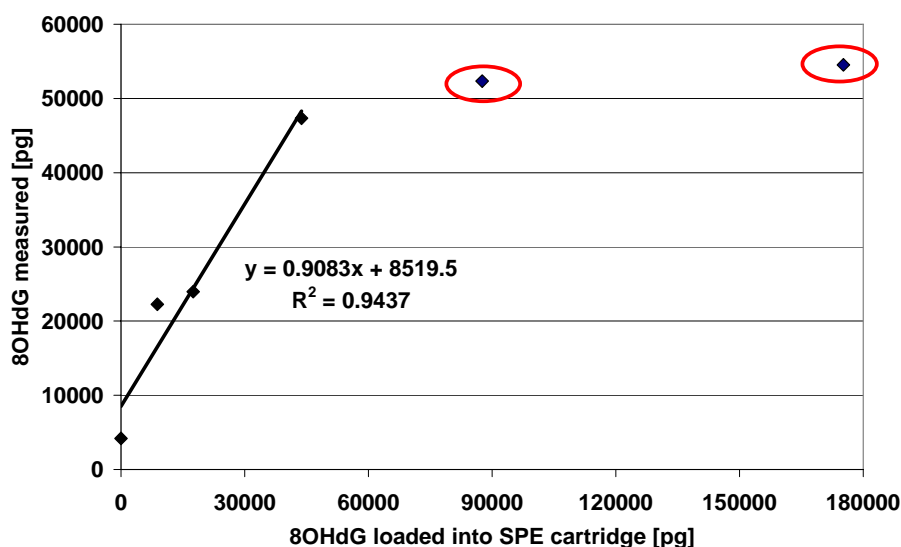
Figure 5.5 shows typical chromatograms of non-spiked and spiked urine samples. We notice that in addition to the peak present at the retention time of 8OHdG observed for standard solutions (21.2 minutes, Figure 5.3), a few other peaks are also present (6.2, 7.8, 14.2 and 18.3 minutes).

Figure 5.5: Typical chromatograms of non-spiked and spiked urine samples. 1-step clean-up by SPE (Oasis WCX), followed by HPLC-ECD. Conditions of analysis as described in Table 5.3. **1:** non-spiked urine; **2:** 8.8 pg/ μ l spiked urine; **3:** 17.5 pg/ μ l spiked urine; **4:** 43.8 pg/ μ l spiked urine; **5:** 87.6 pg/ μ l spiked urine; **6:** 175.2 pg/ μ l spiked urine.



The accuracy of the analytical method was evaluated by measuring the recovery rate of 8OHdG in spiked urines (Figure 5.6). The curve was obtained by performing the analytical method with a known amount of 8OHdG in spiked urines, and by measuring the amount of 8OHdG recovered after the clean-up procedure. The slope of the curve corresponds to the recovery rate, and the y-intercept to the amount of 8OHdG present in the non-spiked urine sample. The recovery rate could not be determined with the curve shown in Figure 5.6, because of a saturation occurring after approximately 60'000 pg injected into the SPE cartridge. If we do not take into account the points surrounded in red (Figure 5.6), the recovery rate will be 90.8%. Nevertheless, the correlation coefficient ($R^2 = 0.9437$) is too low, and suggests the presence of interfering compounds at the same retention time as 8OHdG, which prevents correct integration of the peak. Thus, the good recovery rate obtained in Figure 5.6 may be due to the fact that we took into account not only 8OHdG, but also other compounds having the same retention time and giving a signal with the ECD.

Figure 5.6: Recovery rate of 8OHdG in spiked urine samples. 1-step clean-up by SPE (Oasis WCX), followed by HPLC-ECD. Conditions of analysis as described in Table 5.3. The curve and the equation on the chart do not take into account the points surrounded in red.



The repeatability of the sample injection into HPLC was determined by injecting ten times in a row standard solutions of 8.8 and 87.6 pg/ μ l. Intra-day variability (repeatability) of the analytical method was determined by quantifying five times simultaneously 8OHdG in a standard solution of 43.8 pg/ μ l. Results are gathered in Table 5.5. We notice that solutions with low concentrations of 8OHdG, such as 8.8 pg/ μ l, usually have high standard deviations.

Table 5.5: Precision of the first analytical method by HPLC-ECD.

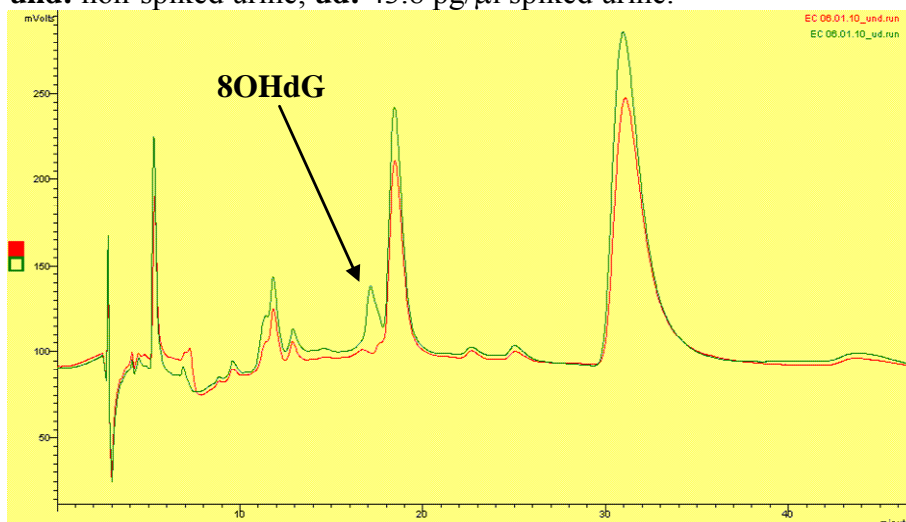
	Samples	Mean measured concentration	Standard deviation
Repeatability of the injection into HPLC	Calibration standard 8.8 pg/ μ l	5.6 pg/ μ l (n=10)	14.2 % (n=10)
	Calibration standard 87.6 pg/ μ l	83.8 pg/ μ l (n=10)	4.5 % (n=10)
Intra-day variability of the analytical method	Calibration standard 43.8 pg/ μ l	20.9 pg/ μ l (n= 5)	11.3 % (n= 5)

In summary, results reported above presented several advantages, such as satisfactory signals for standard solutions and good recovery rate. Nevertheless, the most important problem concerns the bad separation of 8OHdG from interfering compounds of the urine matrix, which prevent to quantify correctly 8OHdG. Moreover, we observed an unusual saturation for high concentrations of 8OHdG in urine (Figure 5.6). Therefore, this analytical method was not suitable for the analysis of 8OHdG in urine samples, and was forsaken.

After the failure of the first analytical method for 8OHdG, we decided to develop a 2-step clean-up procedure, first with a strong anion exchange cartridge (Discovery DSC-SAX) followed by a hydrophobic cartridge (BondElut C₁₈/OH). This procedure was supposed to remove a maximum of contaminants from the urine samples before the analysis by HPLC, and therefore to limit interferences due to the urine matrix. Discovery DSC-SAX contains a polymerically bonded quarternary amine that remains positively charged at all pH levels, and was supposed to retain weaker anions, such as deprotonated carboxylic acids, while 8OHdG under its neutral form was not retained by the SPE cartridge. The second SPE cartridge contains C₁₈-OH groups, which retain chemical compounds mainly by hydrophobic interactions. The presence of hydroxyl groups improves the interaction with polar compounds by means of hydrogen bridges. The separation of 8OHdG was then performed by HPLC-ECD under the same conditions as for the first analytical method (Table 5.3), even if several tests were performed to improve the separation of 8OHdG (gradient of the mobile phase, flow rate, column temperature).

Figure 5.7 shows chromatograms of non-spiked and spiked urine samples. The retention time of 8OHdG was slightly shorter than for the previous analytical method (17.2 minutes, instead of 21.2 minutes), because we tested a different column temperature that day (50°C, instead of 30°C). Peaks at 19 and 32 minutes have a larger area for the spiked urine sample, because during the concentration of samples in the SpeedVac concentrator, the spiked urine sample was slightly more concentrated than the non-spiked one. We notice that the peak corresponding to 8OHdG was difficult to integrate, because of the presence of an interfering peak at 19 minutes.

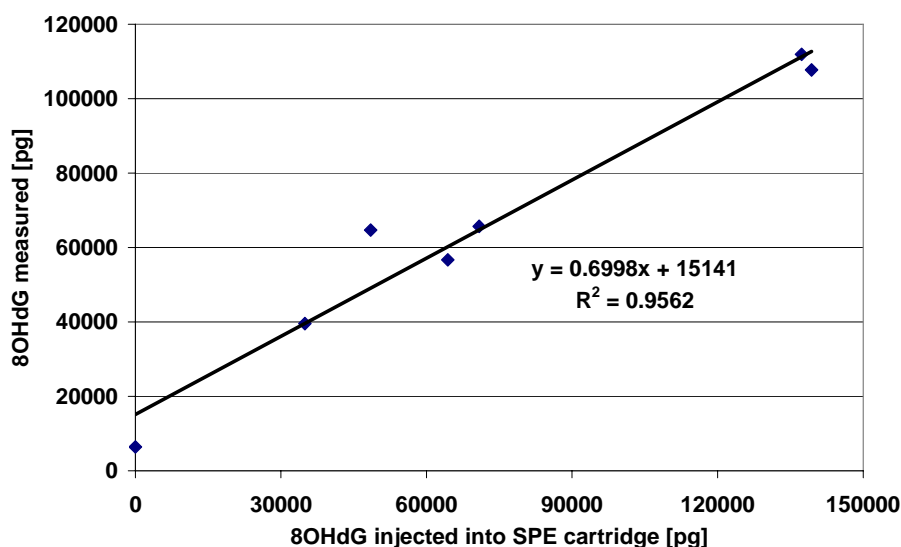
Figure 5.7: Typical chromatograms of non-spiked and spiked urine samples. 2-step clean-up by SPE (Discovery DSC-SAX, BondElut C₁₈/OH), followed by HPLC-ECD. Conditions of analysis as described in Table 5.3, except for the column temperature (50°C). **und:** non-spiked urine; **ud:** 43.8 pg/μl spiked urine.



The limit of detection was determined as previously by measuring the S/N ratio for several chromatograms of urine samples. For standard solutions, the limit of detection was the same as for the first analytical method (1.5 pg/μl, 5.3 nM), since analyses with HPLC-ECD were performed with the same parameter settings. The limit of detection was determined to be 5.0 pg/μl (17.7 nM) for urine samples. This value is approximately in the range of previous studies (Table 5.2) which used the same equipment (HPLC-ECD).

The accuracy of the analytical method was evaluated by measuring the recovery rate of 8OHdG in spiked urine samples (Figure 5.8), as previously described. The recovery rate (70.0%) was satisfactory, but the correlation coefficient ($R^2 = 0.9562$) was too low, as for the first analytical method. This result points out the difficulty to integrate correctly the peak of 8OHdG, because of a bad separation from other interfering compounds of the urine matrix.

Figure 5.8: Recovery rate of 8OHdG in spiked urine samples. 2-step clean-up by SPE (Discovery DSC-SAX, BondElut C₁₈/OH), followed by HPLC-ECD. Conditions of analysis as described in Table 5.3, except for the column temperature (50°C).



Intra-day variability was determined by quantifying three times simultaneously 8OHdG in several samples (one standard solution and two spiked urine samples). Results are gathered in Table 5.6. We notice that 43.8 pg/μl spiked urine sample shows high standard deviation, although it is a concentrated solution.

Table 5.6: Precision of the second analytical method by HPLC-ECD.

	Samples	Mean measured concentration	Standard deviation
Intra-day variability of the analytical method	Standard solution 43.8 pg/μl	36.4 pg/μl (n=3)	4.7 % (n=3)
	Spiked urine 43.8 pg/μl	44.1 pg/μl (n=3)	22.6 % (n=3)
	Spiked urine 87.6 pg/μl	68.7 pg/μl (n=3)	10.2 % (n=3)

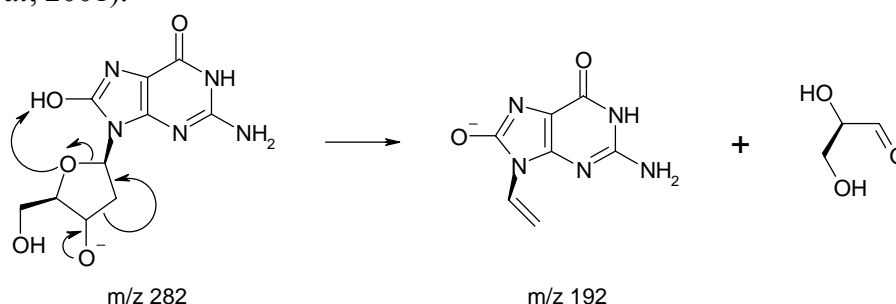
In summary, this second method also presents weak points which prevent us to use it routinely for the analysis of 8OHdG in urine. Indeed, 8OHdH is not well separated from other contaminants on the chromatograms, and the integration of the peak corresponding to 8OHdG is prevented by these interfering compounds.

5.3.2 Analytical method of urinary 8OHdG by LC/MS-MS

After the failure of the analytical method by HPLC, we took advantage of the acquirement of a new LC-MS/MS to develop the analytical method using this technique. The tandem mass spectrometer is constituted of 3 quadrupoles. The first one is set to monitor a single ion, the second one induces a fragmentation of the compounds by collision with argon (collision-

induced dissociation, CID), and the last one is also set to monitor a single ion. This detection method is much more selective than ECD, and allows to resolve the problems due to interfering compounds that we encountered with the previous analytical methods. Figure 5.9 shows a proposed fragmentation pathway of 8OHdG during negative ion electrospray tandem mass spectrometry (Hua *et al*, 2001). Negative ionization induces the loss of a proton to give an ion of m/z 282. The deprotonated molecule was then fragmented in the second quadrupole, and the most abundant fragment ion observed had a m/z 192.

Figure 5.9: Proposed fragmentation pathway of 8OHdG during negative ion electrospray tandem mass spectrometry with CID (Hua *et al*, 2001).



Some chromatograms obtained with calibration standards are shown in Figure 5.10. The retention time is 2.4 minutes, and the full width at half maximum is approximately 8 seconds.

Figure 5.10: Typical chromatograms of standard solutions, obtained by LC-MS/MS. Conditions of analysis as described in Table 5.4.

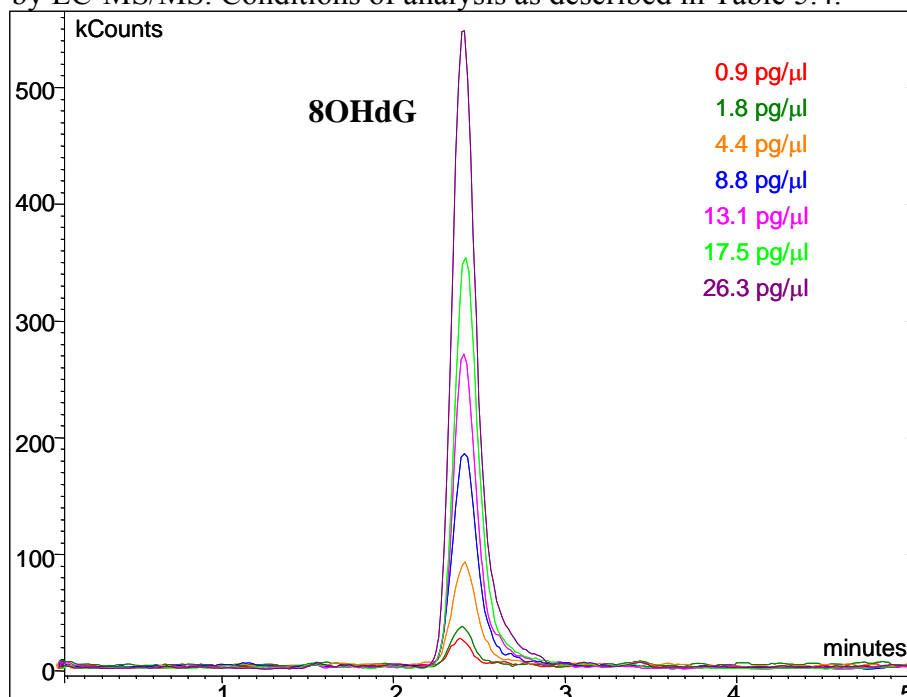
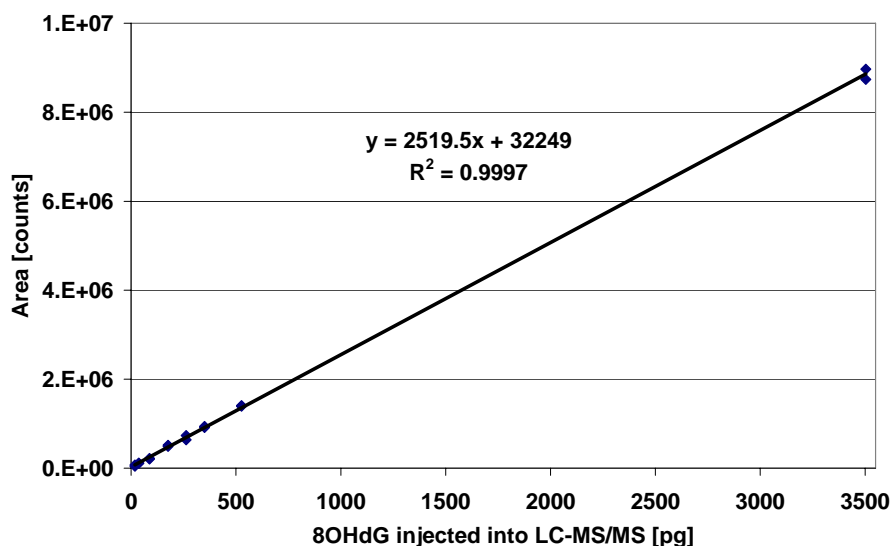


Figure 5.11 shows an eight-point calibration curve prepared in duplicate. The calibration curve was found to be linear in the range of 18-3500 pg injected into LC-MS/MS, which corresponds to a concentration range of 0.9-175.2 pg/ μ l (3.2-619.1 nM). This linearity range fits with values of urinary 8OHdG reported in previous studies.

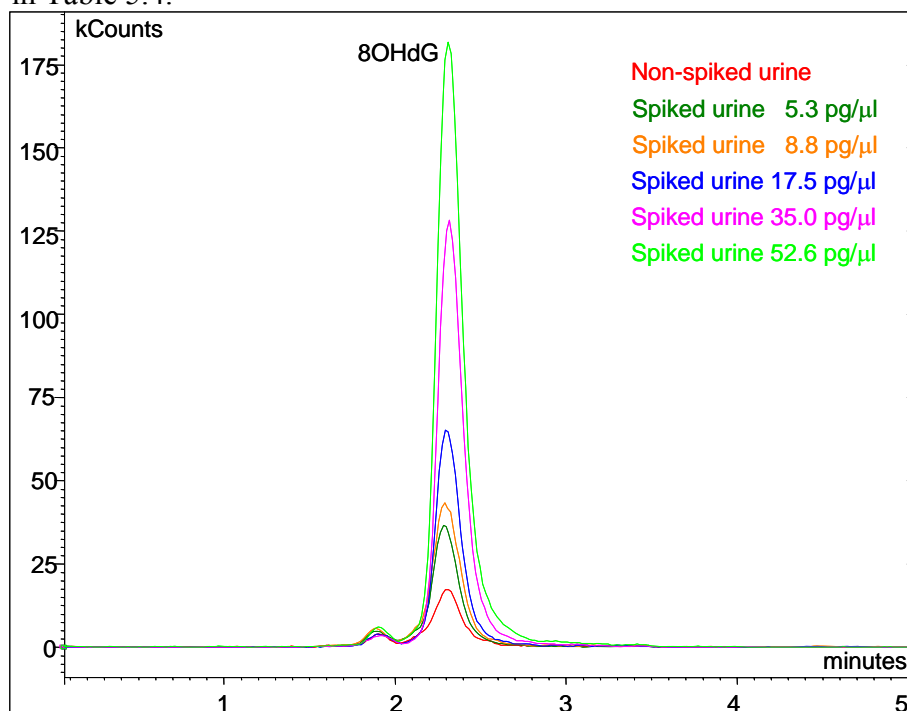
Figure 5.11: Eight-point calibration curve measured in duplicates by LC-MS/MS. Conditions of analysis as described in Table 5.4.



The limit of detection was determined as previously by measuring the S/N ratio for several chromatograms of calibration standards and spiked urines. The limit of detection was determined to be 0.35 ± 0.07 pg/ μ l (1.24 ± 0.24 nM) ($n=5$) for calibration standards, and 1.04 ± 0.39 pg/ μ l (3.67 ± 1.39 nM) ($n=5$) for urine samples. Even if more sensitive methods have been previously published (Table 5.2), the sensitivity of the present analytical method is good enough to detect easily levels of 8OHdG usually present in urine samples. Moreover, if urinary levels of 8OHdG are very low in some samples, this analytical method presents the advantage of enabling to concentrate samples using the SpeedVac concentrator, and therefore to compensate for low concentrations of 8OHdG.

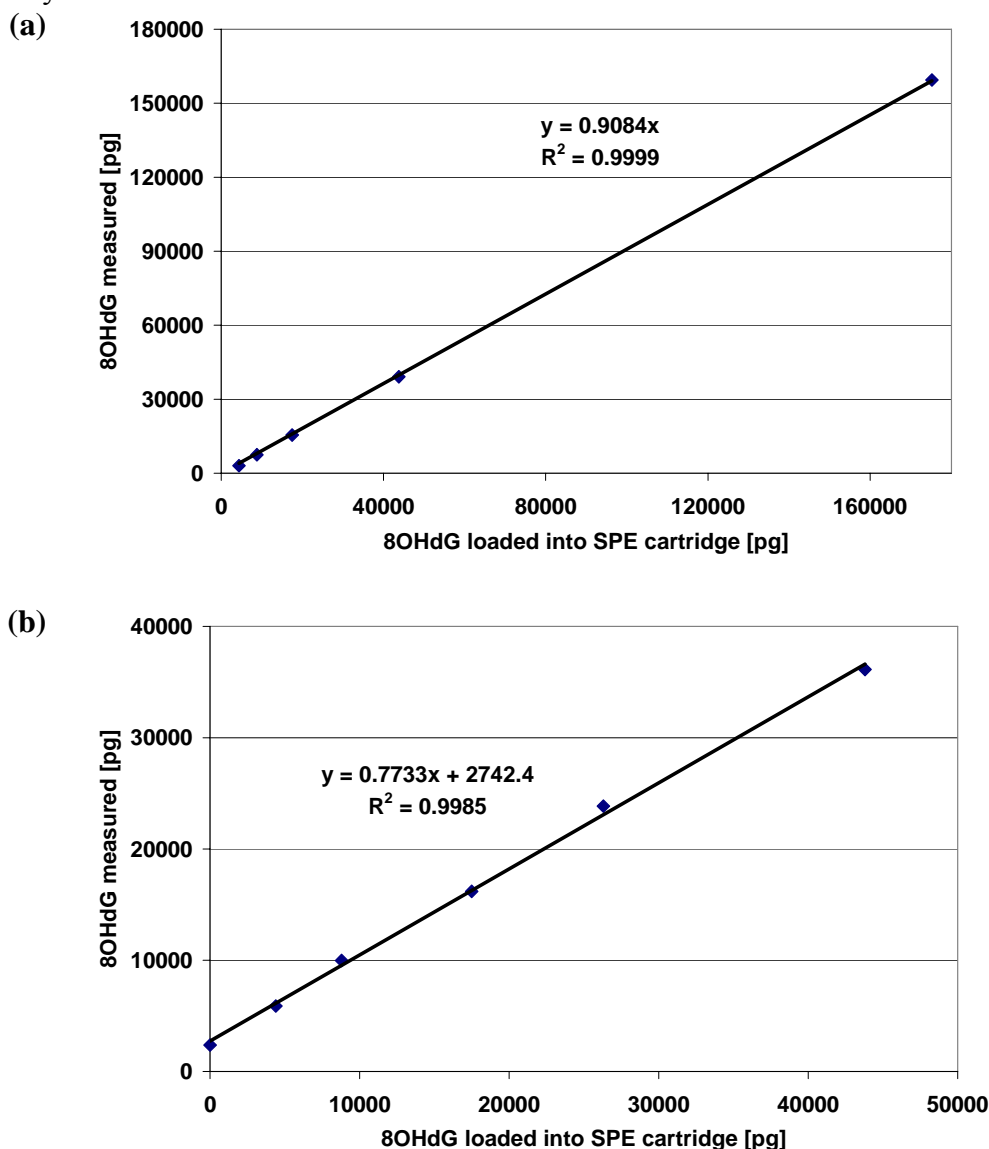
Chromatograms obtained with non-spiked and spiked urine samples are shown in Figure 5.12. A first peak is present after 1.9 minute. This peak has the same area for all the spiked urines, and therefore can not be related to 8OHdG. Chromatograms show that this first peak is well separated from 8OHdG, and therefore its presence is not inconvenient for the integration of 8OHdG.

Figure 5.12: Typical chromatograms of non-spiked and spiked urine samples, obtained by LC-MS/MS. Conditions of analysis as described in Table 5.4.



The accuracy of the analytical method was evaluated by measuring the recovery rate for calibration standards and spiked urines several times. Figure 5.13 shows examples of curves obtained for the recovery rate of 8OHdG in standard solutions and urine samples. During the analyses of standard solutions, 95.8 (± 6.2) % ($n=6$) of 8OHdG loaded into the SPE cartridge were recovered (Figure 5.13(a)), while 73.4 (± 11.8) % ($n=5$) were recovered from urine samples (Figure 5.13(b)). These values are comparable to those reported in the literature, in the case of analytical methods involving a clean-up procedure by SPE. In the latest publications (Malayappan *et al*, 2007; Crow *et al*, 2008), urine samples were directly injected into HPLC or LC-MS without any clean-up procedure, which allows to reach a recovery rate of almost 100%. However, we preferred to avoid such methods, because the analytical column might be quickly damaged by particles and sediments contained in urine samples.

Figure 5.13: Examples of curves obtained for the recovery rate of 8OHdG in standard solutions (a) and in spiked urine samples (b). 1-step clean-up procedure (BondElut C₁₈/OH), followed by LC-MS/MS. Conditions of analysis as described in Table 5.4.



The precision of the measurement using the LC-MS/MS was determined by injecting ten times in a row standard solutions of 4.4 and 43.8 pg/μl. Intra-day variability (repeatability) was determined by measuring six times during the same day non-spiked and spiked urine samples. Inter-day variability (reproducibility) was determined by quantifying 8OHdG in two different urine samples which were previously divided into aliquots. Each day, one aliquot was analyzed. Results are gathered in Table 5.7. According to these results, inter-day variability (reproducibility) seems to be the weakest point of this analytical method.

Table 5.7: Precision of the analytical method by LC-MS/MS.

	Samples	Mean measured concentration	Standard deviation
Repeatability of the injection into LC-MS/MS	Standard solution 4.4 pg/μl	4.3 pg/μl (n=10)	5.2 % (n=10)
	Standard solution 43.8 pg/μl	42.0 pg/μl (n=10)	3.3 % (n=10)
Intra-day variability of the analytical method	Non-spiked urine	5.2 pg/μl (n= 6)	8.2 % (n= 6)
	Spiked urine 10.5 pg/μl	9.8 pg/μl (n= 6)	3.0 % (n= 6)
Inter-day variability of the analytical method	Control urine N° 1	3.7 pg/μl (n=14)	39.5 % (n=14)
	Control urine N° 2	3.8 pg/μl (n=10)	14.3 % (n=10)

In summary, the analytical method developed with the LC-MS/MS is selective and sensitive enough to quantify 8OHdG in urine. Moreover, the use of the SpeedVac concentrator is an important advantage of this method, because it allows to quantify 8OHdG in all the samples, even if the concentration of 8OHdG is very low. The recovery rate and the repeatability are also satisfactory, whereas reproducibility is the weakest point of this analytical method.

5.3.3 Summary of the analytical methods

Table 5.8 summarizes the different results obtained for the three analytical methods. The LC-MS/MS was five times more sensitive than the HPLC-ECD, as indicated by the limit of detection. The main problem of both analytical methods using the HPLC-ECD was the bad separation of 8OHdG from interfering compounds of the urine matrix, which prevented the quantification of 8OHdG. This problem also questions results obtained for the recovery rates, since interfering compounds would also be taken into account in the quantification of 8OHdG when using HPLC-ECD. Finally, concerning the other available data, we notice that the repeatability (intra-day variability) for urine samples was also better with LC-MS/MS than with HPLC-ECD. Therefore, according to these considerations, we decided to use the analytical method developed with the LC-MS/MS to analyze urine samples collected during the field campaign in bus depots.

Table 5.8: Summary of the data related to the robustness of the three analytical methods of urinary 8OHdG.

	1-step clean-up HPLC-ECD	2-step clean-up HPLC-ECD	1-step clean-up LC-MS/MS
Linearity (standard solutions)	4.4-175.2 pg/μl ^a		0.9-175.2 pg/μl
Limit of detection (standard solutions)	1.5 pg/μl ^a		0.35 (±0.07) pg/μl
Limit of detection (urine samples)	5.0 pg/μl	5.0 pg/μl	1.04 (±0.39) pg/μl
Recovery rate (standard solutions)	N/A	N/A	95.8 (±6.2)% (mean value for the range of 4'400-175'200 pg)
Recovery rate (urine samples)	90.8% (mean value for the range of 0-43'800 pg) ^b	70.0 % (mean value for the range of 0-139'400 pg)	73.4 (±11.8)% (mean value for the range of 0-43'800 pg)
Injection into chromatography (standard solutions)	14.2% (8.8 pg/μl) ^a 4.5% (87.6 pg/μl) ^a		5.2% (4.4 pg/μl) 3.3% (43.8 pg/μl)
Intra-day variability (standard solutions)	11.3% (43.8 pg/μl)	4.7% (43.8 pg/μl)	N/A
Intra-day variability (urine samples)	N/A	22.6% (43.8 pg/μl) 10.2% (87.6 pg/μl)	8.2% (non spiked) 3.0% (10.5 pg/μl)
Inter-day variability (standard solutions)	N/A	N/A	N/A
Inter-day variability (urine samples)	N/A	N/A	39.5% (sample 1) 14.3% (sample 2)

^a These results were obtained using only the HPLC-ECD (without clean-up procedure). Therefore, they are the same for both analytical methods.

^b Saturation observed for higher amounts of 8OHdG loaded into SPE cartridge.

N/A: not available

5.3.4 Levels of urinary 8OHdG for workers in bus depots

The analytical method developed with the LC-MS/MS was used to measure concentrations of 8OHdG in urine samples of workers during the field campaign. Four urine samples of each volunteer (day 1 before the shift, day 1 after the shift, day 2 before the shift, day 2 after the shift) were analyzed on the same day in order to avoid inter-day variability. The quality of the analyses was checked each day by analyzing non-spiked and spiked (8.8 pg/μl) control urine. Table 5.9 gathers concentrations of 8OHdG measured each day for control urines and the recovery rate. If results obtained above for recovery rate during validation were satisfactory, we were very surprised to notice that during the analyses of urine samples of volunteers, recovery rates measured for control urines were by far lower and very variable according to the date.

Table 5.9: Detailed results obtained for the reproducibility (inter-day variability) of the analytical method by LC-MS/MS. Recovery rate refers to spiked urine (8.8 pg/μl).

Sample	Date	[8OHdG] [pg/μl]	Recovery rate
Control urine N° 1	11.10.2006	2.88	59.7%
	25.10.2006	4.01	65.4%
	26.10.2006	3.69	33.1%
	31.10.2006	3.57	53.0%
	10.11.2006	7.79	34.5%
	14.11.2006	3.90	28.7%
	15.11.2006	2.35	36.8%
	17.11.2006	3.16	48.4%
	22.11.2006	3.48	40.6%
	23.11.2006	3.34	51.4%
	24.04.2007	1.60	25.8%
	01.05.2007	5.36	40.1%
	03.05.2007	3.05	27.8%
	03.05.2007	3.42	33.3%
	Mean	3.69	41.3%
	SD	1.45	12.4%
	% SD	39.5%	29.9%
Control urine N° 2	08.05.2007	3.84	60.0%
	30.05.2007	2.78	53.8%
	01.06.2007	3.62	58.0%
	19.06.2007	4.23	47.0%
	21.06.2007	4.25	72.5%
	11.07.2007	4.01	100.8%
	12.07.2007	3.63	64.9%
	13.07.2007	3.70	71.2%
	14.07.2007	4.52	68.2%
	17.07.2007	3.05	50.2%
	Mean	3.76	64.7%
	SD	0.54	15.4%
	% SD	14.3%	23.8%

SD: standard deviation

In order to take into account the inter-day variability, we decided to correct urinary concentrations of 8OHdG for workers with results obtained each day for control urines. For that purpose, we calculated the mean concentration of 8OHdG in control urines (Table 5.9), and we corrected urinary concentrations for workers using Equation 5.2:

$$[8OHdG]_{corrected} = [8OHdG]_{measured} \cdot \frac{[8OHdG]_{mean\ control}}{[8OHdG]_{measured\ control}} \quad \text{Equation 5.2}$$

where $[8OHdG]_{corrected}$ is the corrected concentration of 8OHdG in worker's urine;
 $[8OHdG]_{measured}$ is the concentration of 8OHdG in worker's urine measured by LC-MS/MS and quantified with a calibration curve;
 $[8OHdG]_{mean\ control}$ is the mean concentration of 8OHdG in control urine (Table 5.9);
 $[8OHdG]_{measured\ control}$ is the concentration of 8OHdG in control urine measured the same day as the worker's urine.

Among all the volunteers, we decided to separate results obtained for workers in the metro construction site from those obtained for workers in the bus depots. This choice was motivated by the differences in the activities of the workers and the production of particle

types in these workplaces. We also decided to regroup non-smokers and former smokers, who stopped to smoke for at least one year, in order to increase the population of non-smokers and to improve the robustness of statistical analyses. This choice was also motivated by a previous study on effects of smoking cessation on oxidative DNA modification, which showed that urinary levels of 8OHdG decreased significantly already four weeks after cessation, and that this decrease continued during the 26 following weeks (Priemé *et al*, 1998).

In order to ascertain that urinary levels of 8OHdG can be normalized to creatinine, we tested the correlation between 8OHdG (raw data, without creatinine adjustment) and creatinine with the Spearman's rank correlation coefficient. The Spearman's coefficient was 0.364 ($n=91$), and indicated that 8OHdG and creatinine were very well correlated ($p<0.001$), as shown in Figure 5.14. This result suggests that 8OHdG and creatinine are excreted by the same mechanisms in the kidney, and that urinary levels of 8OHdG can be normalized to creatinine.

Figure 5.14: Correlation between urinary levels of 8OHdG (raw data, without creatinine adjustment) and those of creatinine. Population: non-smokers and former smokers, without workers of the metro construction site ($n=91$). $p<0.001$ with the Spearman's rank correlation coefficient.

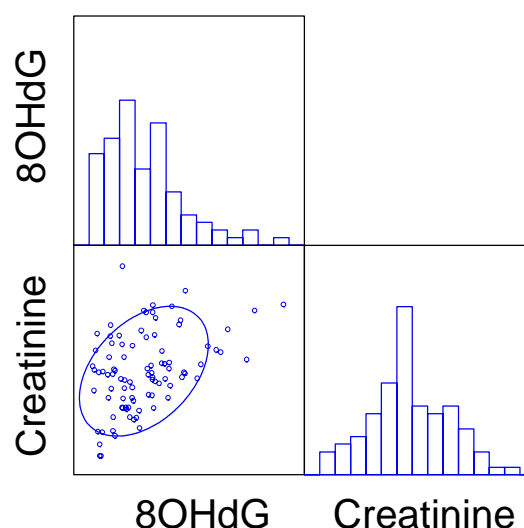


Figure 5.15 shows box plots of urinary concentrations of 8OHdG (normalized to creatinine), while numerical values are reported in Annex. Table 5.10 shows the matrix of pairwise comparison probabilities for non-smokers and former smokers in bus depots, and Table 5.11 for smokers in bus depots. We notice that urinary levels of 8OHdG increased for non-smokers between day 1 before the shift and day 2 after the shift ($p<0.05$, see Table 5.10), while those of smokers did not change much during the same period. These results may be due to the fact that non-smokers began day 1 before the shift with low levels of 8OHdG, and two days of exposure at the workplace were sufficient to induce oxidative stress. On the contrary, smokers had already high levels of 8OHdG on day 1 before the shift, and two consecutive days of

exposure were not sufficient to induce significant changes in oxidative stress status. It should be stressed that on Monday morning before the shift, even if urinary levels of 8OHdG were higher for smokers than for non-smokers/former smokers, the difference between both groups was not significant ($p > 0.05$ with Mann-Whitney U-test). Nevertheless, we already mentioned above that many studies pointed out significant differences between smokers and non-smokers. Our result may be due to the low number of participants. Levels of 8OHdG increased regularly for non-smokers during both days, but for smokers, we notice a decrease between day 1 after the shift and day 2 before the shift. A possible explanation of this trend may be that the defense mechanism of smokers is always activated due to the constant exposure to oxidants contained in cigarette smoke, and that this defense mechanism allowed to decrease quickly the oxidative stress during sleep between the two days of work. One of the scientists involved in the present research project was included as volunteer at each sampling site, and was surveyed five times. Results obtained on Monday morning before the shift for this volunteer allowed us to assess roughly the intra-individual variability of urinary levels of 8OHdG. We found out that mean urinary level of 8OHdG was $2.44 (\pm 0.54) \mu\text{g/g}$ creatinine ($n=5$), which corresponds to a variability of 22.0%. This result indicates that the control values of 8OHdG did not vary much for this person.

Figure 5.15: Box plots of urinary concentrations of 8OHdG for workers in bus depots (without metro construction site). The central horizontal line marks the median. Boxes show the range within which the central 50% of the values fall, while whiskers contain top and bottom 25% of the values. Asterisks mark outside values ($1.5 \cdot$ previous value).

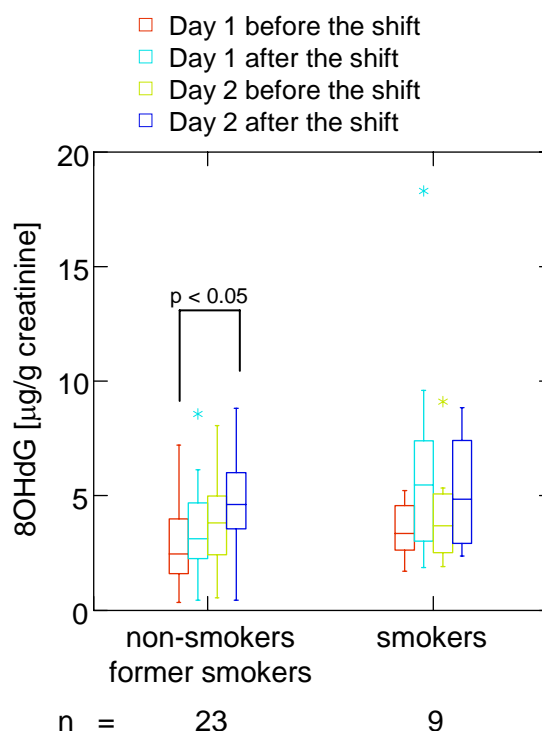


Table 5.10: Matrix of pairwise comparison probabilities obtained by analysis of variance (Bonferroni adjustment) for urinary levels of 8OHdG. Population: non-smokers and former smokers, without workers of the metro construction site. n=23.

	Day 1 before shift	Day 1 after shift	Day 2 before shift	Day 2 after shift
Day 1 before shift	1.000			
Day 1 after shift	1.000	1.000		
Day 2 before shift	0.646	1.000	1.000	
Day 2 after shift	0.034 *	0.380	1.000	1.000

*: difference statistically significant ($p < 0.05$).

Table 5.11: Matrix of pairwise comparison probabilities obtained by analysis of variance (Bonferroni adjustment) for urinary levels of 8OHdG. Population: smokers, without workers of the metro construction site. n=9.

	Day 1 before shift	Day 1 after shift	Day 2 before shift	Day 2 after shift
Day 1 before shift	1.000			
Day 1 after shift	0.387	1.000		
Day 2 before shift	1.000	0.981	1.000	
Day 2 after shift	1.000	1.000	1.000	1.000

Since urinary concentrations of 8OHdG were normalized to creatinine, we must ensure that the increase of 8OHdG during both days of work for non-smokers was not due to a decrease of creatinine during the same period. As shown with the box plots of Figure 5.16 (numerical values in Annex) and the matrix of pairwise comparison probabilities of Tables 5.12 and 5.13, urinary creatinine decreased for non-smokers, but this decrease was not statistically significant ($p > 0.05$). The difference was significant only between samples of Monday evening and Tuesday evening. Therefore, the increase of 8OHdG for non-smokers during both days is not explained exclusively by the decrease of creatinine during the same period.

Figure 5.16: Box plots of urinary concentrations of creatinine for workers in bus depots (without metro construction site). The central horizontal line marks the median. Boxes show the range within which the central 50% of the values fall, while whiskers contain top and bottom 25% of the values. Asterisks mark outside values ($1.5 \cdot$ previous value).

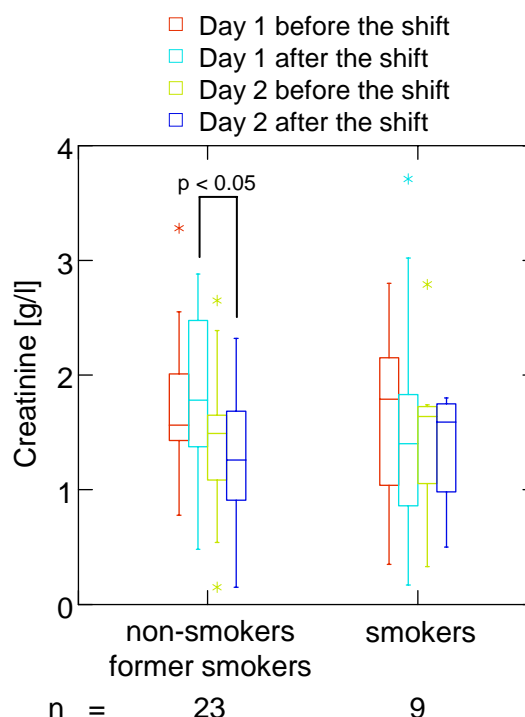


Table 5.12: Matrix of pairwise comparison probabilities obtained by analysis of variance (Bonferroni adjustment) for urinary levels of creatinine. Population: non-smokers and former smokers, without workers of the metro construction site. $n=23$.

	Day 1 before shift	Day 1 after shift	Day 2 before shift	Day 2 after shift
Day 1 before shift	1.000			
Day 1 after shift	1.000	1.000		
Day 2 before shift	0.990	0.410	1.000	
Day 2 after shift	0.092	0.026 *	1.000	1.000

*: difference statistically significant ($p < 0.05$).

Table 5.13: Matrix of pairwise comparison probabilities obtained by analysis of variance (Bonferroni adjustment) for urinary levels of creatinine. Population: smokers, without workers of the metro construction site. $n=9$.

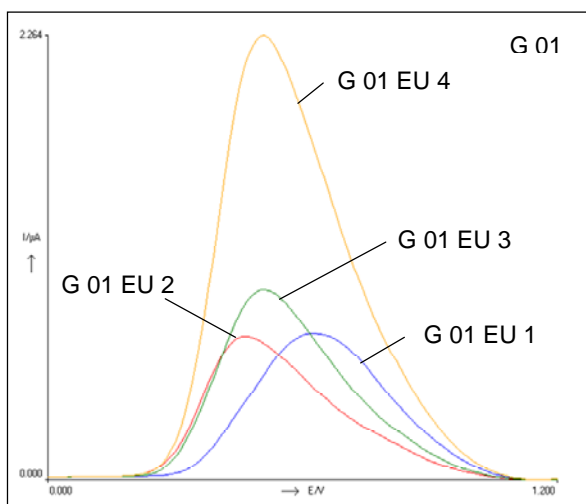
	Day 1 before shift	Day 1 after shift	Day 2 before shift	Day 2 after shift
Day 1 before shift	1.000			
Day 1 after shift	1.000	1.000		
Day 2 before shift	1.000	1.000	1.000	
Day 2 after shift	1.000	1.000	1.000	1.000

5.3.5 Levels of urinary antioxidants for workers in bus depots

In order to check whether the oxidative stress status for workers in the bus depots was followed by a response of the defense mechanisms through an increase of antioxidants, we measured urinary levels of antioxidants using the sensor manufactured by EDEL Therapeutics S.A. Figure 5.17 shows typical voltammetric measurements of urine samples obtained with the sensor. The integrated surface area of each curve is proportional to the number of antioxidants able to undergo redox reaction in the potential range of 0 to +1.2 V. Another

important parameter of these voltammetric measurements is the potential for which the redox reaction takes place, since this potential is a characteristic of the antioxidant. However, this parameter has not been considered within the framework of the present study, because we did not have enough time to analyze antioxidants commonly found in the organism (ascorbic acid, glutathione...) and to compare the signals with those obtained with urine samples.

Figure 5.17: Example of voltammetric measurements of urine samples using the antioxidant redox sensor manufactured by EDEL Therapeutics S.A. Urine samples of worker “G 01 EU” of Monday morning (1), Monday evening (2), Tuesday morning (3) and Tuesday evening (4).



As for 8OHdG, we tested the correlation between antioxidants and creatinine with the Spearman's rank correlation coefficient, in order to ascertain that urinary levels of antioxidants could be normalized to creatinine. The Spearman's rank correlation coefficient was 0.169 (n=91), while the critical value for $p=0.05$ was 0.173. This result indicates that antioxidants and creatinine were not significantly correlated, as shown in Figure 5.18, and may be due to the fact that the sensor detected many compounds, some of which being excreted in urine by the same mechanism as creatinine and the others by a passive excretion. Nevertheless, the Spearman's coefficient was very near the critical value, and therefore we decided to adjust to creatinine.

Figure 5.18: Correlation between urinary levels of antioxidants (raw data, without creatinine adjustment) and those of creatinine. Population: non-smokers and former smokers, without workers of the metro construction site (n=91). $p>0.05$ with the Spearman's rank correlation coefficient.

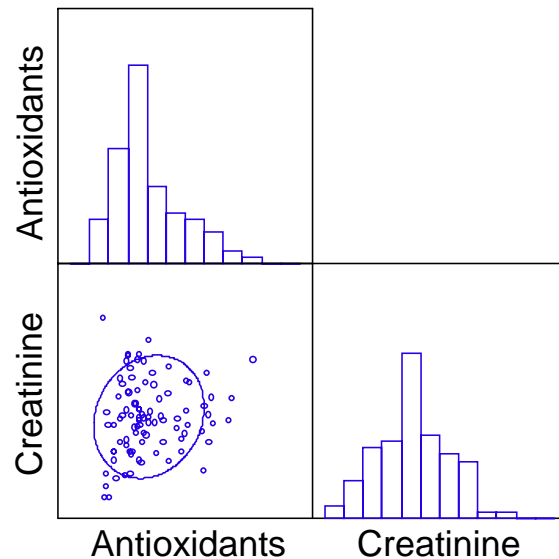


Figure 5.19 shows box plots of urinary levels of antioxidants (normalized to creatinine), while numerical values are reported in Annex. As for 8OHdG and creatinine, an analysis of variance was performed in order to test whether the evolution of urinary levels of antioxidants was statistically significant. Matrix of pairwise comparison probabilities are reported in Table 5.14 for non-smokers, and in Table 5.15 for smokers. We notice that urinary levels of antioxidants increased for non-smokers between day 1 before the shift and day 2 after the shift, but this increase was not significant ($p>0.05$). Moreover, we notice that levels of antioxidants were very stable between day 1 before the shift and day 2 before the shift, and began to increase only during day 2, while levels of 8OHdG began to increase already during day 1 (see Figure 5.15). Obviously, this trend suggests that the antioxidant response began approximately one day after the oxidative stress, and would confirm the hierarchical oxidative stress model (Tier 1) discussed in Chapter 1 (see Figure 1.2). On the other hand, levels of antioxidants were not statistically different for smokers between both days, but a daily increase followed by a decrease during night was observed. As for 8OHdG, we assessed roughly the intra-individual variability of urinary levels of antioxidants. For that purpose, we used the results obtained with the volunteer who was surveyed five times. We found out that urinary level of antioxidants was $792.3 (\pm 233.2)$ /g creatinine (n=5), which corresponds to a variability of 29.4%. This result indicates that the control values of antioxidants did not vary much for this person.

Figure 5.19: Box plots of urinary concentrations of antioxidants in their reduced state for workers in bus depots (without metro construction site). The central horizontal lines mark the median. Boxes show the range within which the central 50% of the values fall, while whiskers contain top and bottom 25% of the values. Asterisks mark outside values ($1.5 \cdot$ previous value), and empty circles mark far outside values ($3 \cdot$ previous value).

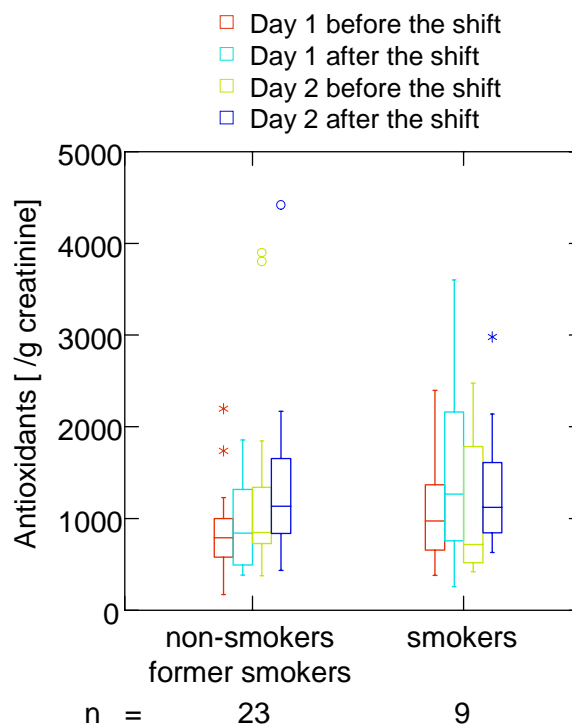


Table 5.14: Matrix of pairwise comparison probabilities obtained by analysis of variance (Bonferroni adjustment) for urinary levels of antioxidants. Population: non-smokers and former smokers, without workers of the metro construction site. n=23.

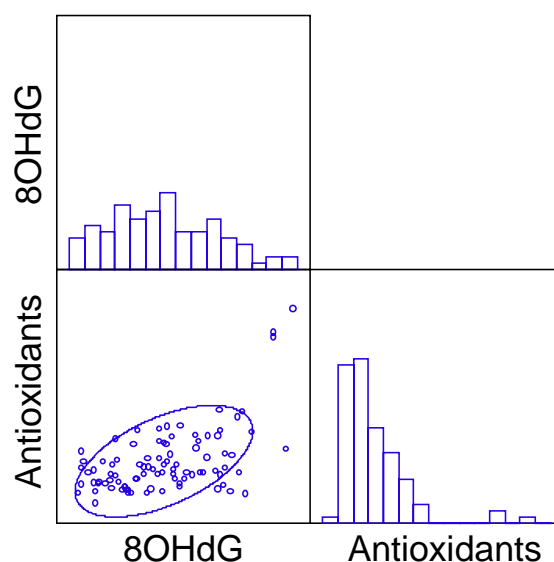
	Day 1 before shift	Day 1 after shift	Day 2 before shift	Day 2 after shift
Day 1 before shift	1.000			
Day 1 after shift	1.000	1.000		
Day 2 before shift	0.499	1.000	1.000	
Day 2 after shift	0.095	0.269	1.000	1.000

Table 5.15: Matrix of pairwise comparison probabilities obtained by analysis of variance (Bonferroni adjustment) for urinary levels of antioxidants. Population: smokers, without workers of the metro construction site. n=9.

	Day 1 before shift	Day 1 after shift	Day 2 before shift	Day 2 after shift
Day 1 before shift	1.000			
Day 1 after shift	1.000	1.000		
Day 2 before shift	1.000	1.000	1.000	
Day 2 after shift	1.000	1.000	1.000	1.000

A non-parametric method was used to check the correlation between urinary levels of 8OHdG and those of antioxidants. The Spearman's rank correlation coefficient was 0.422 (n=91) between urinary levels of 8OHdG and those of antioxidants, indicating an excellent correlation between both parameters ($p < 0.001$), as shown in Figure 5.20. This result indicates that oxidative damages on DNA were accompanied by a response of defense mechanisms through an increase of antioxidants in a reduced state.

Figure 5.20: Correlation between urinary levels of 8OHdG and those of antioxidants (both adjusted to creatinine). Population: non-smokers and former smokers, without workers of the metro construction site (n=91). $p < 0.001$ with the Spearman's rank correlation coefficient.



5.4 Conclusion

A new analytical method for urinary concentrations of 8OHdG was successfully developed and used for the quantification of 8OHdG of workers in bus depots. The following points summarize main results obtained during the field campaign:

- Urinary concentrations of 8OHdG increased significantly ($p < 0.05$) for non-smoking workers during two consecutive days of exposure in bus depots. Therefore, working in bus depots during this period induced oxidative damages to DNA.
- On the first day before the shift, urinary concentrations of 8OHdG were higher for smokers than for non-smokers, but the difference was not statistically significant ($p > 0.05$).
- Urinary concentrations of antioxidants increased for non-smoking workers during two consecutive days of exposure in bus depots, but the difference was not statistically significant ($p > 0.05$).
- Urinary concentrations of 8OHdG and those of antioxidants were very well correlated ($p < 0.001$), indicating that an increase of oxidative damages on DNA was accompanied by a response of defense mechanisms through a production of antioxidants. Moreover, the increase of antioxidants began approximately one day after that of 8OHdG, giving some weight to the theory of the hierarchical oxidative stress model proposed by Nel *et al* (2006).

5.5 References

- Adachi S., Zeisig M., Möller L., 1995. Improvements in the analytical method for 8-hydroxydeoxyguanosine in nuclear DNA. *Carcinogenesis*, 16 (2), 253-258.
- Akagi S., Nagake Y., Kasahara J., Sarai A., Kihara T., Morimoto H., Yano A., Nakao K., Nanba K., Ichikawa H., Makino H., 2003. Significance of 8-hydroxy-2'-deoxyguanosine levels in patients with chronic renal failure. *Nephrology*, 8 (4), 192-195.
- Barr D.B., Wilder L.C., Caudill S.P., Gonzalez A.J., Needham L.L., Pirkle J.L., 2005. Urinary creatinine concentrations in the U.S. population: implications for urinary biologic monitoring measurements. *Environmental Health Perspectives*, 113 (2), 192-200.
- Behndig A.F., Mudway I.S., Brown J.L., Stenfors N., Helleday R., Duggan S.T., Wilson S.J., Boman C., Cassee F.R., Frew A.J., Kelly F.J., Sandström T., Blomberg A., 2006. Airway antioxidant and inflammatory responses to diesel exhaust exposure in healthy humans. *European Respiratory Journal*, 27 (2), 359-365.
- Bogdanov M.B., Beal M.F., McCabe D.R., Griffin R.M., Matson W.R., 1999. A carbon column-based liquid chromatography electrochemical approach to routine 8-hydroxy-2'-deoxyguanosine measurements in urine and other biologic matrices: a one-year evaluation of methods. *Free Radical Biology & Medicine*, 27 (5/6), 647-666.
- Breton J., Sichel F., Bianchini F., Prevost V., 2003. Measurement of 8-hydroxy-2'-deoxyguanosine by a commercially available ELISA test: comparison with HPLC/electrochemical detection in calf thymus DNA and determination in human serum. *Analytical Letters*, 36 (1), 123-134.
- Cadet J., Douki T., Ravanat J.-L., 1997. Artifacts associated with the measurement of oxidized DNA bases. *Environmental Health Perspectives*, 105 (10), 1034-1039.
- Carrieri M., Trevisan A., Bartolucci G.B., 2001. Adjustment to concentration-dilution of spot urine samples: correlation between specific gravity and creatinine. *International Archives of Occupational and Environmental Health*, 74 (1), 63-67.
- Chiou C.-C., Chang P.-Y., Chan E.-C., Wu T.-L., Tsao K.-C., Wu J.T., 2003. Urinary 8-hydroxydeoxyguanosine and its analogs as DNA marker of oxidative stress: development of an ELISA and measurement in both bladder and prostate cancers. *Clinica Chimica Acta*, 334 (1/2), 87-94.
- Cho S.-H., Jung B.H., Lee S.H., Lee W.-Y., Kong G., Chung B.C., 2006. Direct determination of nucleosides in the urine of patients with breast cancer using column-

-
- switching liquid chromatography–tandem mass spectrometry. *Biomedical Chromatography*, 20 (11), 1229-1236.
- Cooke M.S., Singh R., Hall G.K., Mistry V., Duarte T.L., Farmer P.B., Evans M.D., 2006. Evaluation of enzyme-linked immunosorbent assay and liquid chromatography–tandem mass spectrometry methodology for the analysis of 8-oxo-7,8-dihydro-2'-deoxyguanosine in saliva and urine. *Free Radical Biology & Medicine*, 41 (12), 1829-1836.
 - Crow B., Bishop M., Kovalcik K., Norton D., George J., Bralley J.A., 2008. A simple and cost effective method for the quantification of 8-hydroxy-2'-deoxyguanosine from urine using liquid chromatography tandem mass spectrometry. *Biomedical Chromatography*, 22 (4), 394-401.
 - Culp S.J., Cho B.P., Kadlubar F.F., Evans F.E., 1989. Structural and conformational analyses of 8-hydroxy-2'-deoxyguanosine. *Chemical Research in Toxicology*, 2 (6), 416-422.
 - Delfino R.J., Staimer N., Tjoa T., Polidori A., Arhami M., Gillen D.L., Kleinman M.T., Vaziri N.D., Longhurst J., Zaldivar F., Sioutas C., 2008. Circulating biomarkers of inflammation, antioxidant activity, and platelet activation are associated with primary combustion aerosols in subjects with coronary artery disease. *Environmental Health Perspectives*, 116 (7), 898-906.
 - de Martinis B.S., Bianchi M.D.L.P., 2002. Methodology for urinary 8-hydroxy-2'-deoxyguanosine analysis by HPLC with electrochemical detection. *Pharmacological Research*, 46 (2), 129-131.
 - de Zwart L.L., Meerman J.H.N., Commandeur J.N.M., Vermeulen N.P.E., 1999. Biomarkers of free radical damage applications in experimental animals and in humans. *Free Radical Biology & Medicine*, 26 (1/2), 202-226.
 - Fanou L.A., Mobio T.A., Creppy E.E., Fayomi B., Fustoni S., Møller P., Kyrtopoulos S., Georgiades P., Loft S., Sanni A., Skov H., Øvrebø S., Autrup H., 2006. Survey of air pollution in Cotonou, Benin - air monitoring and biomarkers. *Science of the Total Environment*, 358 (1/3), 85-96.
 - Germadnik D., Pilger A., Rüdiger H.W., 1997. Assay for the determination of urinary 8-hydroxy-2'-deoxyguanosine by high-performance liquid chromatography with electrochemical detection. *Journal of Chromatography B*, 689 (2), 399-403.

-
- Gupta R.C., Arif J.M., 2001. An improved ^{32}P -postlabeling assay for the sensitive detection of 8-oxodeoxyguanosine in tissue DNA. *Chemical Research in Toxicology*, 14 (8), 951-957.
 - Helbock H.J., Beckman K.B., Shigenaga M.K., Walter P.B., Woodall A.A., Yeo H.C., Ames B.N., 1998. DNA oxidation matters: the HPLC-electrochemical detection assay of 8-oxo-deoxyguanosine and 8-oxo-guanine. *Proceedings of the National Academy of Sciences of the United States of America*, 95 (1), 288-293.
 - Hofer T., Möller L., 2002. Optimization of the workup procedure for the analysis of 8-oxo-7,8-dihydro-2'-deoxyguanosine with electrochemical detection. *Chemical Research in Toxicology*, 15 (3), 426-432.
 - Hu C.-W., Wang C.-J., Chang L.W., Chao M.-R., 2006 (a). Clinical-scale high-throughput analysis of urinary 8-oxo-7,8-dihydro-2'-deoxyguanosine by isotope-dilution liquid chromatography-tandem mass spectrometry with on-line solid-phase extraction. *Clinical Chemistry*, 52 (7), 1381-1388.
 - Hu C.-W., Pan C.-H., Huang Y.-L., Wu M.-T., Chang L.W., Wang C.-J., Chao M.-R., 2006 (b). Effects of arsenic exposure among semiconductor workers: a cautionary note on urinary 8-oxo-7,8-dihydro-2'-deoxyguanosine. *Free Radical Biology & Medicine*, 40 (7), 1273-1278.
 - Hua Y., Wainhaus S.B., Yang Y., Shen L., Xiong Y., Xu X., Zhang F., Bolton J.L., van Breemen R.B., 2001. Comparison of negative and positive ion electrospray tandem mass spectrometry for the liquid chromatography tandem mass spectrometry analysis of oxidized deoxynucleosides. *Journal of the American Society for Mass Spectrometry*, 12 (1), 80-87.
 - Irie M., Asami S., Nagata S., Miyata M., Kasai H., 2001. Relationships between perceived workload, stress and oxidative DNA damage. *International Archives of Occupational and Environmental Health*, 74 (2), 153-157.
 - Irie M., Tamae K., Iwamoto-Tanaka N., Kasai H., 2005. Occupational and lifestyle factors and urinary 8-hydroxydeoxyguanosine. *Cancer Science*, 96 (9), 600-606.
 - Jaffe M., 1886. Measurement of creatinine using picric acid. *Zeitschrift für Physiologische Chemie*, 10, 391-400.
 - Kasai H., Iwamoto-Tanaka N., Miyamoto T., Kawanami K., Kawanami S., Kido R., Ikeda M., 2001. Life style and urinary 8-hydroxydeoxyguanosine, a marker of oxidative DNA

damage: effects of exercise, working conditions, meat intake, body mass index, and smoking. *Japanese Journal of Cancer Research*, 92 (1), 9-15.

- Kasai H., 2003. A new automated method to analyze urinary 8-hydroxydeoxyguanosine by a high-performance liquid chromatography-electrochemical detector system. *Journal of Radiation Research*, 44 (2), 185-189.
- Kim J.Y., Mukherjee S., Ngo L., Christiani D.C., 2004. Urinary 8-hydroxy-2'-deoxyguanosine as a biomarker of oxidative DNA damage in workers exposed to fine particulates. *Environmental Health Perspectives*, 112 (6), 666-671.
- Kono Y., Nakamura K., Kimura H., Nishii N., Watanabe A., Banba K., Miura A., Nagase S., Sakuragi S., Kusano K.F., Matsubara H., Ohe T., 2006. Elevated levels of oxidative DNA damage in serum and myocardium of patients with heart failure. *Circulation Journal*, 70 (8), 1001-1005.
- Konopka T., Król K., Kopeć W., Gerber H., 2007. Total antioxidant status and 8-hydroxy-2'-deoxyguanosine levels in gingival and peripheral blood of periodontitis patients. *Archivum Immunologiae et Therapiae Experimentalis*, 55 (6), 417-425.
- Kvasníková V., Samcová E., Jursová A., Jelínek I., 2003. Determination of 8-hydroxy-2'-deoxyguanosine in untreated urine by capillary electrophoresis with UV detection. *Journal of Chromatography A*, 985 (1/2), 513-517.
- Lai C.-H., Liou S.-H., Lin H.-C., Shih T.-S., Tsai P.-J., Chen J.-S., Yang T., Jaakkola J.J.K., Strickland P.T., 2005. Exposure to traffic exhausts and oxidative DNA damage. *Occupational and Environmental Medicine*, 62 (4), 216-222.
- Li N., Kim S., Wang M., Froines J., Sioutas C., Nel A., 2002. Use of a stratified oxidative stress model to study the biological effects of ambient concentrated and Diesel exhaust particulate matter. *Inhalation Toxicology*, 14 (5), 459-486.
- Lin H.-S., Jenner A.M., Ong C.N., Huang S.H., Whiteman M., Halliwell B., 2004. A high-throughput and sensitive methodology for the quantification of urinary 8-hydroxy-2'-deoxyguanosine: measurement with gas chromatography-mass spectrometry after single solid-phase extraction. *Biochemical Journal*, 380 (2), 541-548.
- Liu A.-L., Lu W.-Q., Wang Z.-Z., Chen W.-H., Lu W.-H., Yuan J., Nan P.-H., Sun J.-Y., Zou Y.-L., Zhou L.-H., Zhang C., Wu T.-C., 2006. Elevated levels of urinary 8-hydroxy-2'-deoxyguanosine, lymphocytic micronuclei, and serum glutathione S-transferase in workers exposed to coke oven emissions. *Environmental Health Perspectives*, 114 (5), 673-677.

-
- Liu X., Meng Z., 2005. Effects of airborne fine particulate matter on antioxidant capacity and lipid peroxidation in multiple organs of rats. *Inhalation Toxicology*, 17 (9), 467-473.
 - Lodovici M., Caldini S., Luceri C., Bambi F., Boddi V., Dolaro P., 2005. Active and passive smoking and lifestyle determinants of 8-oxo-7,8-dihydro-2'-deoxyguanosine levels in human leukocyte DNA. *Cancer Epidemiology, Biomarkers & Prevention*, 14 (12), 2975-2977.
 - Malayappan B., Garrett T.J., Segal M., Leeuwenburgh C., 2007. Urinary analysis of 8-oxoguanine, 8-oxoguanosine, fapy-guanine and 8-oxo-2'-deoxyguanosine by high-performance liquid chromatography-electrospray tandem mass spectrometry as a measure of oxidative stress. *Journal of Chromatography A*, 1167 (1), 54-62.
 - Marczynski B., Rozynek P., Hellichhausen H.-J., Korn M., Baur X., 1997. Detection of 8-hydroxydeoxyguanosine, a marker of oxidative DNA damage, in white blood cells of workers occupationally exposed to styrene. *Archives of Toxicology*, 71 (8), 496-500.
 - Matayatsuk C., Wilairat P., 2008. Quantitative determination of 8-hydroxy-2'-deoxyguanosine as a biomarker of oxidative stress in thalassemic patients using HPLC with an electrochemical detector. *Journal of Analytical Chemistry*, 63 (1), 52-56.
 - Mei S.-R., Yao Q.-H., Cai L.-S., Xing J., Xu G.-W., Wu C.-Y., 2003. Capillary electrophoresis with end-column amperometric detection of urinary 8-hydroxy-2'-deoxyguanosine. *Electrophoresis*, 24 (9), 1411-1415.
 - Mei S., Yao Q., Wu C., Xu G., 2005. Determination of urinary 8-hydroxy-2'-deoxyguanosine by two approaches - capillary electrophoresis and GC/MS: an assay for in vivo oxidative DNA damage in cancer patients. *Journal of Chromatography B*, 827 (1), 83-87.
 - Mizoue T., Kasai H., Kubo T., Tokunaga S., 2006. Leanness, smoking, and enhanced oxidative DNA damage. *Cancer Epidemiology, Biomarkers & Prevention*, 15 (3), 582-585.
 - Nel A., Xia T., Mädler L., Li N., 2006. Toxic potential of materials at the nanolevel. *Science*, 311 (5761), 622-627.
 - Nilsson R., Nordlinder R., Moen B.E., Øvrebø S., Bleie K., Skorve A.H., Hollund B.E., Tagesson C., 2004. Increased urinary excretion of 8-hydroxydeoxyguanosine in engine room personnel exposed to polycyclic aromatic hydrocarbons. *Occupational and Environmental Medicine*, 61 (8), 692-696.

-
- Park E.-M., Shigenaga M.K., Degan P., Korn T.S., Kitzler J.W., Wehr C.M., Kolachana P., Ames B.N., 1992. Assay of excised oxidative DNA lesions: isolation of 8-oxoguanine and its nucleoside derivatives from biological fluids with a monoclonal antibody column. *Proceedings of the National Academy of Sciences of the United States of America*, 89 (8), 3375-3379.
 - Priemé H., Loft S., Klarlund M., Grønbæk K., Tønnesen P., Poulsen H.E., 1998. Effect of smoking cessation on oxidative DNA modification estimated by 8-oxo-7,8-dihydro-2'-deoxyguanosine excretion. *Carcinogenesis*, 19 (2), 347-351.
 - Prieto-Simón B., Cortina M., Campàs M., Calas-Blanchard C., 2008. Electrochemical biosensors as a tool for antioxidant capacity assessment. *Sensors and Actuators B: Chemical*, 129 (1), 459-466.
 - Randerath K., Reddy M.V., Gupta R.C., 1981. ³²P-labeling test for DNA damage. *Proceedings of the National Academy of Sciences of the United States of America*, 78 (10), 6126-6129.
 - Rebelo I.A., Piedade J.A.P., Oliveira-Brett A.M., 2004. Development of an HPLC method with electrochemical detection of femtomoles of 8-oxo-7,8-dihydroguanine and 8-oxo-7,8-dihydro-2'-deoxyguanosine in the presence of uric acid. *Talanta*, 63 (2), 323-331.
 - Sabatini L., Barbieri A., Tosi M., Roda A., Violante F.S., 2005. A method for routine quantitation of urinary 8-hydroxy-2'-deoxyguanosine based on solid-phase extraction and micro-high-performance liquid chromatography/electrospray ionization tandem mass spectrometry. *Rapid Communications in Mass Spectrometry*, 19 (2), 147-152.
 - Samcová E., Marhol P., Opekar F., Langmaier J., 2004. Determination of urinary 8-hydroxy-2'-deoxyguanosine in obese patients by HPLC with electrochemical detector. *Analytica Chimica Acta*, 516 (1/2), 107-110.
 - Singh R, McEwan M., Lamb J.H., Santella R.M., Farmer P.B., 2003. An improved liquid chromatography/tandem mass spectrometry method for the determination of 8-oxo-7,8-dihydro-2'-deoxyguanosine in DNA samples using immunoaffinity column purification. *Rapid Communications in Mass Spectrometry*, 17 (2), 126-134.
 - Tagesson C., Källberg M., Klintenberg C., Starkhammar H., 1995. Determination of urinary 8-hydroxydeoxyguanosine by automated coupled-column high performance liquid chromatography: a powerful technique for assaying *in vivo* oxidative DNA damage in cancer patients. *European Journal of Cancer*, 31A (6), 934-940.

-
- Weiss D.J., Lunte C.E., 2000. Detection of a urinary biomarker for oxidative DNA damage 8-hydroxydeoxyguanosine by capillary electrophoresis with electrochemical detector. *Electrophoresis*, 21 (10), 2080-2085.
 - Xiao G.G., Wang M., Li N., Loo J.A., Nel A.E., 2003. Use of proteomics to demonstrate a hierarchical oxidative stress response to Diesel exhaust particle chemicals in a macrophage cell line. *Journal of Biological Chemistry*, 278 (50), 50781-50790.
 - Yao Q.-H., Mei S.-R., Weng Q.-F., Zhang P.-D., Yang Q., Wu C.-Y., Xu G.-W., 2004. Determination of urinary oxidative DNA damage marker 8-hydroxy-2'-deoxyguanosine and the association with cigarette smoking. *Talanta*, 63 (3), 617-623.
 - Yin B., Whyatt R.M., Perera F.P., Randall M.C., Cooper T.B., Santella R.M., 1995. Determination of 8-hydroxydeoxyguanosine by an immunoaffinity chromatography-monoclonal antibody-based ELISA. *Free Radical Biology & Medicine*, 18 (6), 1023-1032.
 - Zeisig M., Hofer T., Cadet J., Moller L., 1999. ³²P-postlabeling high-performance liquid chromatography (³²P-HPLC) adapted for analysis of 8-hydroxy-2'-deoxyguanosine. *Carcinogenesis*, 20 (7), 1241-1245.

Chapter 6 – Correlations between oxidative stress and exposure parameters

6.1 Introduction

8-hydroxy-2'-deoxyguanosine (8OHdG) has been widely used as a biomarker of oxidative DNA damage in many studies. As we mentioned in the previous Chapter, the aim of these studies was usually to compare urinary levels of 8OHdG for people exposed to pollutants with those obtained for a non-exposed control population. However, several studies tried to link oxidative stress with occupational or lifestyle factors. Table 6.1 shows selected publications where 8OHdG was found to be associated with exposure parameters or dietary factors. We notice that particulate matter (PM_{2.5} or PM₁₀) and many metals were already associated with increased urinary levels of 8OHdG in previous studies. Moreover, several personal data, such as age, body mass index (BMI) or food intake may also play a role in the oxidative stress process. Nevertheless, it must be stressed that several other studies did not end up with the same conclusions. For instance, Yoshida *et al* (2006) did not find any correlation between 8OHdG and age, or BMI. These differences may be due to variations in sample size, sample composition, methods for the determination of 8OHdG and exposure parameters, and statistical treatments.

Table 6.1: List of selected studies where urinary levels of 8OHdG were correlated with occupational or lifestyle factors.

Parameter	Association with 8OHdG	n	p-value	References
Smoking status	Positive	170	$p < 0.001$	Chuang <i>et al</i> , 2003
PM _{2.5}	Positive	300	$p < 0.001$	Rossner <i>et al</i> , 2008
PM ₁₀	Positive	300	$p < 0.001$	
Vanadium in PM _{2.5}	Positive	51	$p < 0.01$	Sørensen <i>et al</i> , 2005
Chromium in PM _{2.5}	Positive	51	$p < 0.01$	
PM _{2.5}	Positive	N/A	$p < 0.05$	Kim <i>et al</i> , 2004
Vanadium in PM _{2.5}	Positive	N/A	$p < 0.05$	
Manganese in PM _{2.5}	Positive	N/A	$p < 0.05$	
Nickel in PM _{2.5}	Positive	N/A	$p < 0.05$	
Lead in PM _{2.5}	Positive	N/A	$p < 0.05$	
Mercury	Positive	48	$p < 0.01$	Chen <i>et al</i> , 2005
CO ₂	Positive	344	$p < 0.01$	Lu <i>et al</i> , 2007
Total volatile organic compounds	Positive	344	$p = 0.05$	
Age	Negative	100	$p < 0.001$	Tamura <i>et al</i> , 2006
BMI	Negative	372	$p < 0.01$	Irie <i>et al</i> , 2005
Average number of working hours per day	Positive	372	$p < 0.01$	
Involvement in work	Positive	372	$p < 0.01$	
Average number of cigarettes smoked per day	Positive	372	$p < 0.01$	
Soybean products consumption	Negative	372	$p < 0.01$	
Light-colored vegetables consumption	Negative	372	$p < 0.05$	
Rice consumption	Negative	372	$p < 0.05$	
Intake of vitamin	Negative	217	$p = 0.02$	Wu <i>et al</i> , 2003

N/A: not available.

Within the framework of the present research project, we tested the correlation between 8OHdG and exposure parameters described in Chapters 3 and 4, in order to identify parameters which would be responsible for the increase of urinary levels of 8OHdG during work. The main problem of this part of the project was that we had the participation of only 40 volunteers to test 34 exposure parameters. Therefore, the robustness of the statistical analysis was seriously reduced, and we have to be careful with the interpretation of the results. In the present Chapter, we will discuss correlations between 8OHdG and exposure parameters, and we will present different statistical models describing urinary levels of 8OHdG as a function of several exposure parameters.

6.2 Material and methods

Statistical analyses were performed using SYSTAT for Windows, version 10.2.

For statistical treatments, we took into account non-smokers and former smokers, without workers of the metro construction site. Indeed, we have shown in Chapter 5 that the increase of 8OHdG over a two-day period of shift was statistically significant only for this population.

Among the 34 exposure parameters described in Chapter 3 and 4, we decided not to take into account ozone, since ozone levels in the workplaces were negligible. Parameters were all used as continuous variables. In the case of results below the limit of detection, we considered the half value of the limit of detection.

Correlations between all the exposure parameters presented in Chapters 3 and 4 were tested with the Spearman's rank correlation coefficient, and were considered significant when $p < 0.05$. For all the exposure parameters, we considered mean values over an 8-hour period of shift measured with stationary samplings.

Correlations between 8OHdG and personal data, lifestyle factors and exposure parameters were also tested with the Spearman's rank correlation coefficient, and were considered significant when $p < 0.05$. For correlations with personal data and lifestyle factors, we considered values of 8OHdG obtained in urine samples collected on Monday morning before the shift (control). For correlations with exposure parameters, we considered the difference between urinary levels of 8OHdG after the shift and those before the shift. Since the field campaign was conducted over a two-day period, we had two values per worker, one for each sampling day. This choice allowed us to have a higher number of values to test the different correlations between 8OHdG and exposure parameters. For PM₄, OC, EC and OC/EC, we considered results obtained with personal samplings, since these values are more representative of the real exposure of each worker.

The normal distribution of all the parameters was tested using skewness and kurtosis values, which measure the symmetry of a distribution about its mean. The distribution was not considered normal when the absolute value of the skewness/standard error (SE) of skewness ratio and that of the kurtosis/SE of kurtosis ratio were both higher than 2. In this case, the logarithm of the parameter was calculated, and the distribution was tested again. For each parameter, we considered the method which presented the best symmetry, using either the log-transformed values or the non-transformed ones. Indeed, since the presence of a few outliers may have great incidence on statistical treatments (especially for the multiple regression analysis), it was important to consider normally distributed parameters.

We performed a multiple regression analysis using a stepwise method (backward) in order to describe the evolution of urinary levels of 8OHdG (dependant variable) as a function of

several exposure parameters (independent variables). For that purpose, we tested many combinations of five or six parameters (including personal data) which were not correlated together, and we used for each parameter either non-transformed or log-transformed values. Indeed, statistical models need to use parameters with normal distributions, since the presence of outliers may have important influences on the model.

6.3 Results and discussion

6.3.1 *Correlations between exposure parameters*

Table 6.2 shows Spearman's rank correlation coefficients between exposure parameters. We found 81 significant correlations (either positive or negative) out of 528, which represent 15.3% of all the tested correlations. We notice that several parameters which have been measured using the same instrument were strongly correlated, such as particle number, surface area and mass concentrations measured using the scanning mobility particle sizer (SMPS); or NO, NO₂ and NO_x measured using the NO_x analyzer. For the three parameters related to the SMPS, the correlation is not a surprise, since the instrument measures the particle size distribution, and this data is then used to calculate the three parameters. For NO and NO₂, the strong correlation indicates that both gases are emitted by the same sources (motor vehicles). We also notice the same kind of correlation between iron (Fe), copper (Cu) and manganese (Mn), suggesting that these transition metals are emitted by the same sources, such as brakes (Gasser and Perrenoud, 2007). An interesting finding is the correlation between OC and NO/NO₂/NO_x. We remind that OC may be emitted either directly by incomplete combustion of carbonaceous fuels or by gas-to-particle conversion of volatile organic compounds (VOCs), while NO_x are exclusively emitted by motor vehicles. Thus, the correlation between OC and NO_x suggests that both compounds are emitted by the same sources, and that the presence of OC in the bus depots is mainly due to the exhaust gas of buses, and not to the activities of workers.

Several parameters related to the particle surface reactivity (Knudsen flow reactor) are also correlated. For instance, for the five probe gases used with the Knudsen flow reactor (N(CH₃)₃, NH₂OH, CF₃COOH, HCl and O₃), results given in molecule/mg are always correlated with those given in molecule/cm². Moreover, results obtained with several probe gases are correlated, the most important correlation being between CF₃COOH and HCl. This is due to the fact that both probe gases react with the same functional groups (basic sites of different strength) on the particle surface.

Table 6.2: Spearman's rank correlation coefficients between exposure parameters. For all the exposure parameters, mean concentration over an 8-hour period of shift was considered. n=14, except for some cases due to missing values. Cases highlighted in green: p<0.05.

Relative humidity																																																																																																																																																																																																																																																																																																																																																																																																																																																																																																																																																																																																																																																																																																																																																																																																																																																																										
Temperature																																																																																																																																																																																																																																																																																																																																																																																																																																																																																																																																																																																																																																																																																																																																																																																																																																																																										
Mn																																																																																																																																																																																																																																																																																																																																																																																																																																																																																																																																																																																																																																																																																																																																																																																																																																																																										
Cu																																																																																																																																																																																																																																																																																																																																																																																																																																																																																																																																																																																																																																																																																																																																																																																																																																																																										
Fe																																																																																																																																																																																																																																																																																																																																																																																																																																																																																																																																																																																																																																																																																																																																																																																																																																																																										
O ₃ γ ₀																																																																																																																																																																																																																																																																																																																																																																																																																																																																																																																																																																																																																																																																																																																																																																																																																																																																										
O ₃ [molecule/cm ²]																																																																																																																																																																																																																																																																																																																																																																																																																																																																																																																																																																																																																																																																																																																																																																																																																																																																										
O ₃ [molecule/mg]																																																																																																																																																																																																																																																																																																																																																																																																																																																																																																																																																																																																																																																																																																																																																																																																																																																																										
HCl γ ₀																																																																																																																																																																																																																																																																																																																																																																																																																																																																																																																																																																																																																																																																																																																																																																																																																																																																										
HCl [molecule/cm ²]																																																																																																																																																																																																																																																																																																																																																																																																																																																																																																																																																																																																																																																																																																																																																																																																																																																																										
HCl [molecule/mg]																																																																																																																																																																																																																																																																																																																																																																																																																																																																																																																																																																																																																																																																																																																																																																																																																																																																										
CF ₃ COOH γ ₀																																																																																																																																																																																																																																																																																																																																																																																																																																																																																																																																																																																																																																																																																																																																																																																																																																																																										
CF ₃ COOH [molecule/cm ²]																																																																																																																																																																																																																																																																																																																																																																																																																																																																																																																																																																																																																																																																																																																																																																																																																																																																										
CF ₃ COOH [molecule/mg]																																																																																																																																																																																																																																																																																																																																																																																																																																																																																																																																																																																																																																																																																																																																																																																																																																																																										
NH ₂ OH γ ₀																																																																																																																																																																																																																																																																																																																																																																																																																																																																																																																																																																																																																																																																																																																																																																																																																																																																										
NH ₂ OH [molecule/cm ²]																																																																																																																																																																																																																																																																																																																																																																																																																																																																																																																																																																																																																																																																																																																																																																																																																																																																										
NH ₂ OH [molecule/mg]																																																																																																																																																																																																																																																																																																																																																																																																																																																																																																																																																																																																																																																																																																																																																																																																																																																																										
N(CH ₃) ₃ γ ₀																																																																																																																																																																																																																																																																																																																																																																																																																																																																																																																																																																																																																																																																																																																																																																																																																																																																										
N(CH ₃) ₃ [molecule/cm ²]																																																																																																																																																																																																																																																																																																																																																																																																																																																																																																																																																																																																																																																																																																																																																																																																																																																																										
N(CH ₃) ₃ [molecule/mg]																																																																																																																																																																																																																																																																																																																																																																																																																																																																																																																																																																																																																																																																																																																																																																																																																																																																										
NO ₂ /NO _x																																																																																																																																																																																																																																																																																																																																																																																																																																																																																																																																																																																																																																																																																																																																																																																																																																																																										
NO _x																																																																																																																																																																																																																																																																																																																																																																																																																																																																																																																																																																																																																																																																																																																																																																																																																																																																										
NO ₂																																																																																																																																																																																																																																																																																																																																																																																																																																																																																																																																																																																																																																																																																																																																																																																																																																																																										
NO																																																																																																																																																																																																																																																																																																																																																																																																																																																																																																																																																																																																																																																																																																																																																																																																																																																																										
Mean aerodynamic diameter																																																																																																																																																																																																																																																																																																																																																																																																																																																																																																																																																																																																																																																																																																																																																																																																																																																																										
LQ1-DC surface area																																																																																																																																																																																																																																																																																																																																																																																																																																																																																																																																																																																																																																																																																																																																																																																																																																																																										
PM _{0.7} [μg/m ³]																																																																																																																																																																																																																																																																																																																																																																																																																																																																																																																																																																																																																																																																																																																																																																																																																																																																										
PM _{0.7} [μm ² /cm ³]																																																																																																																																																																																																																																																																																																																																																																																																																																																																																																																																																																																																																																																																																																																																																																																																																																																																										
PM _{0.7} [particle/cm ³]																																																																																																																																																																																																																																																																																																																																																																																																																																																																																																																																																																																																																																																																																																																																																																																																																																																																										
PM ₄																																																																																																																																																																																																																																																																																																																																																																																																																																																																																																																																																																																																																																																																																																																																																																																																																																																																										
OC/EC																																																																																																																																																																																																																																																																																																																																																																																																																																																																																																																																																																																																																																																																																																																																																																																																																																																																										
EC																																																																																																																																																																																																																																																																																																																																																																																																																																																																																																																																																																																																																																																																																																																																																																																																																																																																										
OC																																																																																																																																																																																																																																																																																																																																																																																																																																																																																																																																																																																																																																																																																																																																																																																																																																																																										
OC	OC	0.386	0.053	0.179	-0.084	0.102	0.063	0.084	0.190	-0.242	0.182	0.825	0.811	0.993	0.650	0.650	0.650	0.650	0.650	0.650	0.650	0.650	0.650	0.650	0.650	0.650	0.650	0.650	0.650	0.650	0.650	0.650	0.650	0.650	0.650	0.650	0.650	0.650	0.650	0.650	0.650	0.650	0.650	0.650	0.650	0.650	0.650	0.650	0.650	0.650	0.650	0.650	0.650	0.650	0.650	0.650	0.650	0.650	0.650	0.650	0.650	0.650	0.650	0.650	0.650	0.650	0.650	0.650	0.650	0.650	0.650	0.650	0.650	0.650	0.650	0.650	0.650	0.650	0.650	0.650	0.650	0.650	0.650	0.650	0.650	0.650	0.650	0.650	0.650	0.650	0.650	0.650	0.650	0.650	0.650	0.650	0.650	0.650	0.650	0.650	0.650	0.650	0.650	0.650	0.650	0.650	0.650	0.650	0.650	0.650	0.650	0.650	0.650	0.650	0.650	0.650	0.650	0.650	0.650	0.650	0.650	0.650	0.650	0.650	0.650	0.650	0.650	0.650	0.650	0.650	0.650	0.650	0.650	0.650	0.650	0.650	0.650	0.650	0.650	0.650	0.650	0.650	0.650	0.650	0.650	0.650	0.650	0.650	0.650	0.650	0.650	0.650	0.650	0.650	0.650	0.650	0.650	0.650	0.650	0.650	0.650	0.650	0.650	0.650	0.650	0.650	0.650	0.650	0.650	0.650	0.650	0.650	0.650	0.650	0.650	0.650	0.650	0.650	0.650	0.650	0.650	0.650	0.650	0.650	0.650	0.650	0.650	0.650	0.650	0.650	0.650	0.650	0.650	0.650	0.650	0.650	0.650	0.650	0.650	0.650	0.650	0.650	0.650	0.650	0.650	0.650	0.650	0.650	0.650	0.650	0.650	0.650	0.650	0.650	0.650	0.650	0.650	0.650	0.650	0.650	0.650	0.650	0.650	0.650	0.650	0.650	0.650	0.650	0.650	0.650	0.650	0.650	0.650	0.650	0.650	0.650	0.650	0.650	0.650	0.650	0.650	0.650	0.650	0.650	0.650	0.650	0.650	0.650	0.650	0.650	0.650	0.650	0.650	0.650	0.650	0.650	0.650	0.650	0.650	0.650	0.650	0.650	0.650	0.650	0.650	0.650	0.650	0.650	0.650	0.650	0.650	0.650	0.650	0.650	0.650	0.650	0.650	0.650	0.650	0.650	0.650	0.650	0.650	0.650	0.650	0.650	0.650	0.650	0.650	0.650	0.650	0.650	0.650	0.650	0.650	0.650	0.650	0.650	0.650	0.650	0.650	0.650	0.650	0.650	0.650	0.650	0.650	0.650	0.650	0.650	0.650	0.650	0.650	0.650	0.650	0.650	0.650	0.650	0.650	0.650	0.650	0.650	0.650	0.650	0.650	0.650	0.650	0.650	0.650	0.650	0.650	0.650	0.650	0.650	0.650	0.650	0.650	0.650	0.650	0.650	0.650	0.650	0.650	0.650	0.650	0.650	0.650	0.650	0.650	0.650	0.650	0.650	0.650	0.650	0.650	0.650	0.650	0.650	0.650	0.650	0.650	0.650	0.650	0.650	0.650	0.650	0.650	0.650	0.650	0.650	0.650	0.650	0.650	0.650	0.650	0.650	0.650	0.650	0.650	0.650	0.650	0.650	0.650	0.650	0.650	0.650	0.650	0.650	0.650	0.650	0.650	0.650	0.650	0.650	0.650	0.650	0.650	0.650	0.650	0.650	0.650	0.650	0.650	0.650	0.650	0.650	0.650	0.650	0.650	0.650	0.650	0.650	0.650	0.650	0.650	0.650	0.650	0.650	0.650	0.650	0.650	0.650	0.650	0.650	0.650	0.650	0.650	0.650	0.650	0.650	0.650	0.650	0.650	0.650	0.650	0.650	0.650	0.650	0.650	0.650	0.650	0.650	0.650	0.650	0.650	0.650	0.650	0.650	0.650	0.650	0.650	0.650	0.650	0.650	0.650	0.650	0.650	0.650	0.650	0.650	0.650	0.650	0.650	0.650	0.650	0.650	0.650	0.650	0.650	0.650	0.650	0.650	0.650	0.650	0.650	0.650	0.650	0.650	0.650	0.650	0.650	0.650	0.650	0.650	0.650	0.650	0.650	0.650	0.650	0.650	0.650	0.650	0.650	0.650	0.650	0.650	0.650	0.650	0.650	0.650	0.650	0.650	0.650	0.650	0.650	0.650	0.650	0.650	0.650	0.650	0.650	0.650	0.650	0.650	0.650	0.650	0.650	0.650	0.650	0.650	0.650	0.650	0.650	0.650	0.650	0.650	0.650	0.650	0.650	0.650	0.650	0.650	0.650	0.650	0.650	0.650	0.650	0.650	0.650	0.650	0.650	0.650	0.650	0.650	0.650	0.650	0.650	0.650	0.650	0.650	0.650	0.650	0.650	0.650	0.650	0.650	0.650	0.650	0.650	0.650	0.650	0.650	0.650	0.650	0.650	0.650	0.650	0.650	0.650	0.650	0.650	0.650	0.650	0.650	0.650	0.650	0.650	0.650	0.650	0.650	0.650	0.650	0.650	0.650	0.650	0.650	0.650	0.650	0.650	0.650	0.650	0.650	0.650	0.650	0.650	0.650	0.650	0.650	0.650	0.650	0.650	0.650	0.650	0.650	0.650	0.650	0.650	0.650	0.650	0.650	0.650	0.650	0.650	0.650	0.650	0.650	0.650	0.650	0.650	0.650	0.650	0.650	0.650	0.650	0.650	0.650	0.650	0.650	0.650	0.650	0.650	0.650	0.650	0.650	0.650	0.650	0.650	0.650	0.650	0.650	0.650	0.650	0.650	0.650	0.650	0.650	0.650	0.650	0.650	0.650	0.650	0.650	0.650	0.650	0.650	0.650	0.650	0.650	0.650	0.650	0.650	0.650	0.650	0.650	0.650	0.650	0.650	0.650	0.650	0.650	0.650	0.650	0.650	0.650	0.650	0.650	0.650	0.650	0.650	0.650	0.650	0.650	0.650	0.650	0.650	0.650	0.650	0.650	0.650	0.650	0.650	0.650	0.650	0.650	0.650	0.650	0.650	0.650	0.650	0.650	0.650	0.650	0.650	0.650	0.650	0.650	0.650	0.650	0.650	0.650	0.650	0.650	0.650	0.650	0.650	0.650	0.650	0.650	0.650	0.650	0.650	0.650	0.650	0.650	0.650	0.650	0.650	0.650	0.650	0.650	0.650	0.650	0.650	0.650	0.650	0.650	0.650	0.650	0.650	0.650	0.650	0.650	0.650	0.650	0.650	0.650	0.650	0.650	0.650	0.650	0.650	0.650	0.650	0.650	0.650	0.650	0.650	0.650	0.650	0.650	0.650	0.650	0.650	0.650	0.650	0.650	0.650	0.650	0.650	0.650	0.650	0.650	0.650	0.650	0.650	0.650	0.650	0.650	0.650	0.650	0.650	0.650	0.650	0.650	0.650	0.650	0.650	0.650	0.650	0.650	0.650	0.650	0.650	0.650	0.650	0.650	0.650	0.650	0.650	0.650	0.650	0.650	0.650	0.650	0.650	0.650	0.650	0.650	0.650	0.650	0.650	0.650	0.650	0.650	0.650	0.650	0.650	0.650	0.650	0.650	0.650	0.650	0.650	0.650	0.650	0.650	0.650	0.650	0.650	0.650	0.650	0.650	0.650	0.650	0.650	0.650	0.650	0.650	0.650	0.650	0.650	0.650

Table 6.2 also shows many additional correlations, but some of them may be due to coincidence, the data collected during the field campaign being very limited (n=14).

6.3.2 Correlations between 8OHdG and personal data, lifestyle factors and exposure parameters

Table 6.3 shows Spearman's rank correlation coefficients between 8OHdG and personal data. No significant correlation was found. Nevertheless, previous studies did not end up with the same conclusions concerning correlations with personal data and dietary factors. For instance, several publications reported correlations between urinary levels of 8OHdG and age (Tamura *et al*, 2006), BMI, perceived workload, alcohol consumption and food intake (Irie *et al*, 2005), and arthritis (Rall *et al*, 2000). Within the framework of the present research project, the absence of correlation indicates that these parameters are not confounding factors explaining the increase of urinary levels of 8OHdG.

Table 6.3: Spearman's rank correlation coefficients between 8OHdG and personal data. For 8OHdG, urinary levels of Monday morning before the shift (control) were considered. Population: non-smokers and former smokers, without workers of the metro construction site.

Personal data	n	Spearman's ρ
Age	22	-0.410
Height	22	0.039
Weight	22	0.337
BMI	22	0.352
Alcohol consumption	22	-0.346
Meat intake	22	0.124
Fruit intake	22	-0.131
Drug intake	22	-0.115
Vitamin intake	22	0.399
Heart diseases	22	0.374
Pulmonary diseases	22	-0.204
Articulation problems	22	-0.177
Sport practice	21	0.123
Years of employment	22	-0.206

Table 6.4 shows Spearman's rank correlation coefficients between 8OHdG and exposure parameters. We found correlations between 8OHdG and several particle surface characteristics, such as the reactivity of PM₄ toward O₃ (positive correlations) and N(CH₃)₃ (negative correlations). We found the strongest correlations between 8OHdG and the reactivity of PM₄ toward O₃ (p<0.01). As mentioned in Chapter 4, O₃ probe is supposed to react in the Knudsen flow reactor with carbon-carbon double bonds on the particle surface (Reaction 4.9 in Table 4.2). Thus, this result suggests that the presence of unsaturated aliphatic groups induces oxidative DNA damage, and may be explained by the fact that

carbon-carbon double bonds can react with radicals, such as certain reactive oxygen species (ROS), and participate to the propagation of radical chain reactions (Matyjaszewski and Davis, 2002). Moreover, it has been reported that alkenes enhance DNA damages (Zuniga *et al.*, 2006).

Table 6.4: Spearman's rank correlation coefficients between 8OHdG and exposure parameters. For 8OHdG, the difference between urinary levels after the shift and those before the shift was considered (two values per worker, one for each sampling day). For exposure parameters, mean values over an 8-hour period of shift were considered. Population: non-smokers and former smokers, without workers of the metro construction site.

Measurement method	Exposure parameter	n	Spearman's ρ
Personal sampling	OC	45	0.226
	EC	45	0.074
	OC/EC	45	0.026
	PM ₄	45	0.023
Scanning mobility particle sizer (SMPS)	PM _{0.7} number [particle/cm ³]	33	0.015
	PM _{0.7} surface area [$\mu\text{m}^2/\text{cm}^3$]	33	0.043
	PM _{0.7} mass [$\mu\text{g}/\text{m}^3$]	33	0.043
LQ1-DC	Particle surface area	45	0.153
Cascade impactor	Mean aerodynamic diameter	45	-0.229
NO _x analyzer	NO	32	0.422 *
	NO ₂	32	0.440 *
	NO _x	32	0.422 *
	NO ₂ /NO _x	32	-0.051
Knudsen flow reactor	N(CH ₃) ₃ [molecule/mg]	45	-0.320 *
	N(CH ₃) ₃ [molecule/cm ²]	33	-0.437 *
	N(CH ₃) ₃ γ_0	45	-0.361 *
	NH ₂ OH [molecules/mg]	41	-0.354 *
	NH ₂ OH [molecules/cm ²]	29	-0.306
	NH ₂ OH γ_0	41	0.363 *
	CF ₃ COOH [molecule/mg]	45	0.153
	CF ₃ COOH [molecule/cm ²]	33	-0.026
	CF ₃ COOH γ_0	45	0.358 *
	HCl [molecule/mg]	45	0.029
	HCl [molecule/cm ²]	33	0.000
	HCl γ_0	45	0.373 *
	O ₃ [molecule/mg]	45	0.422 **
	O ₃ [molecule/cm ²]	33	0.557 **
	O ₃ γ_0	45	0.448 **
Atomic absorption spectrometer	Fe	45	0.305 *
	Cu	45	0.353 *
	Mn	45	0.227
Direct reading instrument	Temperature	45	-0.084
	Relative humidity	45	-0.026

* : $p < 0.05$

** : $p < 0.01$

We also found negative correlation between 8OHdG and the reactivity of PM₄ toward N(CH₃)₃ ($p < 0.05$). This probe gas is supposed to react in the Knudsen flow reactor with acids on the particle surface (Reaction 4.1 of Table 4.2), and is a good indicator of the oxidation

state of the particle surface. We noticed in Chapter 4 that O_3 and $N(CH_3)_3$ probes had opposite reactivity towards particulate matter collected in the bus depots, and therefore, it is not a surprise to find out also opposite correlations toward 8OHdG.

We also found positive correlations with the uptake coefficient γ_0 of the five probe gases of the Knudsen flow reactor, except for that of $N(CH_3)_3$ which has a negative correlation. These results indicate that the faster particles react with probe gas, the more 8OHdG is produced. This phenomenon suggests that the quantification of functional groups on the particle surface is perhaps not sufficient to explain the particle reactivity, and that the reaction kinetics is also an important parameter to consider. Indeed, even if these functional groups are present in large amounts on the particle surface, their reaction kinetics should be high enough to induce important oxidative damages in the body. Nevertheless, we are aware that the uptake coefficients were measured in the gas phase, while particles are in solution after entering the body. Therefore, we are not sure that the γ_0 values represent the real kinetics in the body. This question should be investigated further through measurements of particle reactivity in solution. To our knowledge, it is the first time that the correlation between 8OHdG and particle surface characteristics is investigated.

In addition to the surface functional groups, we also found positive correlations between 8OHdG and NO_x concentrations in the bus depots. This result is not a surprise, since NO and NO_2 are known as oxidizing compounds. Even if NO is not strong enough to attack directly the DNA strand, NO metabolism produces reactive compounds, known as “reactive nitrogen oxide species” (RNOS), which initiate oxidative stress through formation of peroxynitrite ($ONOO^-$) and nitroxyl (NO^-) ions (Burney *et al*, 1999; Miranda *et al*, 2000; Pacher *et al*, 2007). Moreover, it has been clearly reported that oxidative DNA damages induced by peroxynitrite predominantly occur on guanine, through an oxidation on C_8 of the compound (Niles *et al*, 2006).

We also found significant correlations with particulate iron and copper concentrations. This result was also expected, since many studies have demonstrated the implication of these metals in oxidative stress (Nakano *et al*, 2003; Park *et al*, 2006). Indeed, iron and copper are both involved in the Fenton reaction, in which superoxide anion and hydroxyl radical are produced (Stohs and Bagchi, 1995; Meneghini, 1997; Turi *et al*, 2004). Moreover, iron (II)

and copper (II) have also the ability to interact directly with DNA in-between the bases, and therefore to produce ROS near the DNA strand.

Finally, we did not find any correlation with other exposure parameters, even with the particle concentrations, or with OC and EC. However, previous studies found out positive correlations with $PM_{2.5}$ and PM_{10} (see Table 6.1).

6.3.3 Normality test

Table 6.5 shows results obtained for the normality test. According to these results, the following parameters were not normally distributed: OC, OC/EC, PM_4 , $PM_{0.7}$ [particle/cm³], CF_3COOH [molecule/mg], CF_3COOH γ_0 , HCl [molecule/mg], HCl [molecule/cm²], HCl γ_0 . We calculated the logarithm of these parameters, and we tested the normal distribution again (Table 6.6). Values obtained for the log-transformed parameters fitted better, and therefore we decided to consider these values for the forthcoming statistical treatments (multiple regression analysis).

Table 6.5: Normality test using skewness and kurtosis values. Population: non-smokers and former smokers, without workers of the metro construction site.

	Skewness	SE of Skewness	Skewness/SE	Kurtosis	SE of Kurtosis	Kurtosis/SE
δ 8OHdG	0.419	0.354	1.184	2.428	0.695	3.494 *
OC	1.130	0.35	3.229 *	3.799	0.688	5.522 *
EC	0.328	0.35	0.937	0.077	0.688	0.112
OC/EC	2.253	0.35	6.437 *	4.696	0.688	6.826 *
PM ₄	4.162	0.35	11.891 *	22.399	0.688	32.557 *
PM _{0.7} [particle/cm ³]	2.527	0.403	6.270 *	6.013	0.788	7.631 *
PM _{0.7} [µm ² /cm ³]	0.822	0.403	2.040 *	1.180	0.788	1.497
PM _{0.7} [µg/m ³]	0.003	0.403	0.007	-0.456	0.788	0.579
LQ1-DC surface area	-0.337	0.35	0.963	-0.959	0.688	1.394
Mean aerodynamic diameter	0.730	0.35	2.086 *	0.425	0.688	0.618
NO	-0.015	0.414	0.036	-1.016	0.809	1.256
NO ₂	-1.053	0.414	2.543 *	-0.485	0.809	0.600
NO _x	-0.146	0.414	0.353	-0.736	0.809	0.910
NO ₂ /NO _x	-0.382	0.414	0.923	-1.134	0.809	1.402
N(CH ₃) ₃ [molecule/mg]	1.128	0.35	3.223 *	-0.167	0.688	0.243
N(CH ₃) ₃ [molecule/cm ²]	1.019	0.403	2.529 *	-0.604	0.788	0.766
N(CH ₃) ₃ γ ₀	-0.664	0.35	1.897	-1.018	0.688	1.480
NH ₂ OH [molecule/mg]	0.648	0.365	1.775	-1.172	0.717	1.635
NH ₂ OH [molecule/cm ²]	1.582	0.427	3.705 *	1.215	0.833	1.459
NH ₂ OH γ ₀	1.451	0.365	3.975 *	0.762	0.717	1.063
CF ₃ COOH [molecule/mg]	1.565	0.35	4.471 *	1.579	0.688	2.295 *
CF ₃ COOH [molecule/cm ²]	1.293	0.403	3.208 *	0.955	0.788	1.212
CF ₃ COOH γ ₀	1.938	0.35	5.537 *	2.257	0.688	3.281 *
HCl [molecule/mg]	2.387	0.35	6.820 *	5.014	0.688	7.288 *
HCl [molecule/cm ²]	1.714	0.403	4.253 *	1.943	0.788	2.466 *
HCl γ ₀	2.024	0.35	5.783 *	2.558	0.688	3.718 *
O ₃ [molecule/mg]	1.103	0.35	3.151 *	-0.647	0.688	0.940
O ₃ [molecule/cm ²]	0.819	0.403	2.032 *	-1.158	0.788	1.470
O ₃ γ ₀	0.206	0.35	0.589	-1.233	0.688	1.792
Fe	0.650	0.35	1.857	-0.263	0.688	0.382
Cu	0.539	0.35	1.540	-1.026	0.688	1.491
Mn	0.500	0.35	1.429	-0.316	0.688	0.459
Temperature	0.578	0.35	1.651	-0.643	0.688	0.935
Relative humidity	0.590	0.35	1.686	-0.132	0.688	0.192

SE: standard error.

*: absolute value of the skewness/SE of skewness, or that of the kurtosis/SE of kurtosis, > 2.

Table 6.6: Normality test for log-transformed parameters using skewness and kurtosis values. Population: non-smokers and former smokers, without workers of the metro construction site.

	Skewness	SE of Skewness	Skewness/SE	Kurtosis	SE of Kurtosis	Kurtosis/SE
log OC	-0.522	0.35	1.491	1.644	0.688	2.390 *
log OC/EC	0.720	0.35	2.057 *	1.011	0.688	1.469
log PM ₄	-0.308	0.35	0.880	0.533	0.688	0.775
log PM _{0.7} [particle/cm ³]	-0.079	0.403	0.196	1.878	0.788	2.383 *
log CF ₃ COOH γ_0	1.014	0.35	2.897 *	-0.626	0.688	0.910
log HCl [molecule/mg]	0.970	0.35	2.771 *	0.176	0.688	0.256
log HCl [molecule/cm ²]	0.465	0.403	1.154	-1.11	0.788	1.409
log HCl γ_0	0.775	0.35	2.214 *	-0.883	0.688	1.283

SE: standard error.

*: absolute value of the skewness/SE of skewness, or that of the kurtosis/SE of kurtosis, > 2.

6.3.4 Statistical models

In addition to the univariate analysis to test the correlation between 8OHdG and each exposure parameter separately, we tried to find statistical models allowing to describe at best the evolution of urinary levels of 8OHdG as a function of several exposure parameters. We tested a total of 19 combinations with parameters which were not correlated together, and the best models that we obtained, based on the adjusted R^2 -value, are reported in Table 6.7. 13 models for which R^2 adjusted < 0.200 are not shown in this table, since they explain less than 20% of the increase of 8OHdG.

One outlier from bus depot 3 (G 15 EU) was removed for several models proposed in Table 6.7. The outlier was one of the researchers involved in the present project, who spent almost 48 hours in a row in the bus depot. Therefore, it is possible that, in addition to the exposure to particulate matter and pollutants in the bus depot, the tiredness and the stress due to the field campaign played a role in biological effects.

Table 6.7: List of different statistical models describing the evolution of urinary levels of 8OHdG as a function of exposure parameters, obtained by multiple regression analysis. Population: non-smokers and former smokers, without workers of the metro construction site. Among the 19 tested models, only those for which R^2 adjusted > 0.200 are shown in this table. Models are sorted by R^2 adjusted.

Model	Result
Model 6.1	$8\text{OHdG } [\mu\text{g/g creatinine}] = 4.202(\pm 2.081) \cdot \log \text{OC } [\mu\text{g/m}^3]$ $p=0.062$ $+ 270545(\pm 172292) \cdot \text{PM}_{0.7} \text{ surface area } [\mu\text{m}^2/\text{cm}^3]$ $p=0.137$ $+ 24.593(\pm 7.985) \cdot \text{NO}_2/\text{NO}_x$ $p=0.008$ $- 9.977(\pm 3.526)$ $p=0.013$ $n = 19^a$ $p = 0.007$ $R^2 = 0.546$ $R^2 \text{ adjusted} = 0.455$
Model 6.2	$8\text{OHdG } [\mu\text{g/g creatinine}] = 1.113(\pm 0.568) \cdot \log \text{PM}_4 [\mu\text{g/m}^3]$ $p=0.060$ $+ 0.004(\pm 0.001) \cdot \text{NO}_x$ $p=0.000$ $- 4.018(\pm 1.293)$ $p=0.004$ $n = 31^a$ $p = 0.000$ $R^2 = 0.476$ $R^2 \text{ adjusted} = 0.438$
Model 6.3	$8\text{OHdG } [\mu\text{g/g creatinine}] = 0.004(\pm 0.002) \cdot \text{LQ1-DC surface area } [\mu\text{m}^2/\text{cm}^3]$ $p=0.148$ $+ 0.920(\pm 0.205) \cdot \log \text{CF}_3\text{COOH } \gamma_0$ $p=0.000$ $- 0.158(\pm 0.054) \cdot \text{BMI } [\text{kg/m}^2]$ $p=0.005$ $+ 6.958(\pm 1.868)$ $p=0.001$ $n = 44^a$ $p = 0.000$ $R^2 = 0.447$ $R^2 \text{ adjusted} = 0.405$
Model 6.4	$8\text{OHdG } [\mu\text{g/g creatinine}] = 1.021(\pm 0.213) \cdot \log \text{CF}_3\text{COOH } \gamma_0$ $p=0.000$ $- 2.002(\pm 0.715) \cdot \log \text{OC/EC}$ $p=0.008$ $+ 0.941(\pm 0.508) \cdot \log \text{PM}_4 [\mu\text{g/m}^3]$ $p=0.071$ $+ 3.907(\pm 1.143)$ $p=0.001$ $n = 44^a$ $p = 0.000$ $R^2 = 0.403$ $R^2 \text{ adjusted} = 0.358$
Model 6.5	$8\text{OHdG } [\mu\text{g/g creatinine}] = 0.799(\pm 0.247) \cdot \log \text{CF}_3\text{COOH } \gamma_0$ $p=0.002$ $- 0.298(\pm 0.157) \cdot \text{mean aerodynamic diameter } [\mu\text{m}]$ $p=0.065$ $- 0.205(\pm 0.064) \cdot \text{BMI } [\text{kg/m}^2]$ $p=0.002$ $+ 9.767(\pm 1.978)$ $p=0.000$ $n = 45$ $p = 0.000$ $R^2 = 0.375$ $R^2 \text{ adjusted} = 0.329$
Model 6.6	$8\text{OHdG } [\mu\text{g/g creatinine}] = 2.956(\pm 1.475) \cdot \log \text{OC } [\mu\text{g/m}^3]$ $p=0.052$ $+ 0.007(\pm 0.002) \cdot \text{Cu } [\mu\text{g/m}^3]$ $p=0.007$ $- 0.224(\pm 0.140) \cdot \text{mean aerodynamic diameter } [\mu\text{m}]$ $p=0.119$ $- 0.172(\pm 0.058) \cdot \text{BMI } [\text{kg/m}^2]$ $p=0.005$ $+ 0.388(\pm 2.546)$ $p=0.880$ $n = 44^a$ $p = 0.001$ $R^2 = 0.388$ $R^2 \text{ adjusted} = 0.325$

^a One outlier from bus depot 3 (G 15 EU) removed.

According to the first model proposed in Table 6.7, $\log \text{OC}$, surface area of $\text{PM}_{0.7}$ and NO_2/NO_x ratio explain 45% of the increase of urinary levels of 8OHdG. The implication of OC in this model can be explained by the fact that the organic fraction of particulate matter gathers hundreds of compounds, including alkanes, alkenes, aromatics, polycyclic aromatic hydrocarbons (PAHs), oxygenated compounds (including aldehydes, ketones and carboxylic acids), amino compounds, and nitrates (Schlesinger *et al*, 2006). Among these compounds, PAHs are of prime interest, because they can be converted to quinones, which are involved in redox reactions and produce ROS (Penning *et al*, 1999). Therefore, the implication of OC in

the statistical model is not a surprise. The implication of the surface area of $PM_{0.7}$ was also expected, since previous studies stressed the importance of the particle surface area in the ability to induce oxidative stress (Stone *et al*, 1998; Donaldson *et al*, 2000; Dick *et al*, 2003). Thus, this model may give some weight to the importance of the “surface area” metrics in the measurement of particle concentration. As for NO_2/NO_x ratio, the role of nitric oxides in oxidative stress has already been discussed above. The presence of the NO_2/NO_x ratio in this model may be due to the fact that NO_2 is a stronger oxidizing agent than NO .

The second model proposed in Table 6.7 involves PM_4 and NO_x , and explains more than 40% of the increase of urinary levels of 8OHdG. The simultaneous presence of these two compounds in the model suggests that the main problem of occupational exposure of workers is not due to their activities in the mechanical yard, but rather to the passage of motor vehicles and buses near their workplace.

The third model proposed in Table 6.7 involves particle surface area measured using the LQ1-DC, reaction kinetics between particles and CF_3COOH in the Knudsen flow reactor ($CF_3COOH \gamma_0$) and BMI, and explains 40% of the increase of urinary levels of 8OHdG. As already mentioned above, the implication of the reaction kinetics between particles and one of the probe gases suggests that the quantification of functional groups on the particle surface is perhaps not sufficient to explain the particle reactivity. In this third model, as well as in Models 6.5 and 6.6, BMI has a negative incidence on urinary levels of 8OHdG. This result is consistent with previous studies (Loft *et al*, 1992; Irie *et al*, 2005).

We remind that these statistical models proposed in Table 6.7 have been obtained with limited data, and therefore we have to be careful with the interpretations discussed above. Rather, these statistical models provide information on possible parameters involved in the increase of urinary levels of 8OHdG.

6.4 Conclusion

The robustness of the statistical analysis was seriously reduced due to the low number of volunteers and the high number of exposure parameters that we wanted to test.

However, several correlations between urinary levels of 8OHdG and exposure parameters were found. Results confirmed the importance of particle surface characteristics in the

oxidative stress process, since the reactivity of PM₄ toward O₃ and N(CH₃)₃ were found to strongly influence 8OHdG. Moreover, the uptake coefficient γ_0 of all the probe gases used in the Knudsen flow reactor was also significantly correlated to 8OHdG, and suggested that the quantification of the number of surface functional groups is perhaps not sufficient by itself to explain the particle reactivity. We also found out that NO_x concentrations in the bus depots, as well as iron and copper levels, had a significant influence on urinary levels of 8OHdG.

Finally, we proposed several statistical models obtained by multiple regression analysis and describing urinary levels of 8OHdG as a function of exposure parameters. These models gave some weight to the influence of particle surface area and NO_x, despite the limited data used for statistical treatments.

6.5 References

- Burney S., Caulfield J.L., Niles J.C., Wishnok J.S., Tannenbaum S.R., 1999. The chemistry of DNA damage from nitric oxide and peroxynitrite. *Mutation Research/Fundamental and Molecular Mechanisms of Mutagenesis*, 424 (1/2), 37-49.
- Chen C., Qu L., Li B., Xing L., Jia G., Wang T., Gao Y., Zhang P., Li M., Chen W., Chai Z., 2005. Increased oxidative DNA damage, as assessed by urinary 8-hydroxy-2'-deoxyguanosine concentrations, and serum redox status in persons exposed to mercury. *Clinical Chemistry*, 51 (4), 759-767.
- Chuang C.-Y., Lee C.-C., Chang Y.-K., Sung F.-C., 2003. Oxidative DNA damage estimated by urinary 8-hydroxydeoxyguanosine: influence of taxi driving, smoking and areca chewing. *Chemosphere*, 52 (7), 1163-1171.
- Dick C.A.J., Brown D.M., Donaldson K., Stone V., 2003. The role of free radicals in the toxic and inflammatory effects of four different ultrafine particle types. *Inhalation Toxicology*, 15 (1), 39-52.
- Donaldson K., Stone V., Gilmour P.S., Brown D.M., MacNee W., 2000. Ultrafine particles: mechanisms of lung injury. *Philosophical Transactions of the Royal Society A: Mathematical, Physical & Engineering Sciences*, 358 (1775), 2741-2749.
- Gasser M., Perrenoud A., 2007. Eigenschaften und Toxizität von Bremsstaubpartikeln. Master thesis; Swiss Federal Institute of Technology (Zürich, Switzerland), University of Bern (Switzerland) and Institute for Work and Health (Lausanne, Switzerland).

-
- Irie M., Tamae K., Iwamoto-Tanaka N., Kasai H., 2005. Occupational and lifestyle factors and urinary 8-hydroxydeoxyguanosine. *Cancer Science*, 96 (9), 600-606.
 - Kim J.Y., Mukherjee S., Ngo L., Christiani D.C., 2004. Urinary 8-hydroxy-2'-deoxyguanosine as a biomarker of oxidative DNA damage in workers exposed to fine particulates. *Environmental Health Perspectives*, 112 (6), 666-671.
 - Loft S., Vistisen K., Ewertz M., Tjønneland A., Overvad K., Poulsen H.E., 1992. Oxidative DNA damage estimated by 8-hydroxydeoxyguanosine excretion in humans: influence of smoking, gender and body mass index. *Carcinogenesis*, 13 (12), 2241-2247.
 - Lu, C.-Y., Ma, Y.-C., Lin, J.-M., Chuang, C.-Y., Sung, F.-C., 2007. Oxidative DNA damage estimated by urinary 8-hydroxydeoxyguanosine and indoor air pollution among non-smoking office employees. *Environmental Research*, 103, 331-337.
 - Matyjaszewski K., Davis T.P., 2002. Handbook of Radical Polymerization. John Wiley & Sons, Inc.
 - Meneghini R., 1997. Iron homeostasis, oxidative stress, and DNA damage. *Free Radical Biology & Medicine*, 23 (5), 783-792.
 - Miranda K.M., Espey M.G., Wink D.A., 2000. A discussion of the chemistry of oxidative and nitrosative stress in cytotoxicity. *Journal of Inorganic Biochemistry*, 79 (1/4), 237-240.
 - Nakano M., Kawanishi Y., Kamohara S., Uchida Y., Shiota M., Inatomi Y., Komori T., Miyazawa K., Gondo K., Yamasawa I., 2003. Oxidative DNA damage (8-hydroxydeoxyguanosine) and body iron status: a study on 2507 healthy people. *Free Radical Biology & Medicine*, 35 (7), 826-832.
 - Niles J.C., Wishnok J.S., Tannenbaum S.R., 2006. Peroxynitrite-induced oxidation and nitration products of guanine and 8-oxoguanine: structures and mechanisms of product formation. *Nitric Oxide: Biology and Chemistry*, 14 (2), 109-121.
 - Pacher P., Beckman J.S., Liaudet L., 2007. Nitric oxide and peroxynitrite in health and disease. *Physiological Reviews*, 87 (1), 315-424.
 - Park S., Nam H., Chung N., Park J.-D., Lim Y., 2006. The role of iron in reactive oxygen species generation from diesel exhaust particles. *Toxicology in Vitro*, 20 (6), 851-857.
 - Penning T.M., Burczynski M.E., Hung C.-F., McCoull K.D., Palackal N.T., Tsuruda L.S., 1999. Dihydrodiol dehydrogenases and polycyclic aromatic hydrocarbon activation: generation of reactive and redox active o-quinones. *Chemical Research in Toxicology*, 12 (1), 1-18.

-
- Rall L.C., Roubenoff R., Meydani S.N., Han S.N., Meydani M., 2000. Urinary 8-hydroxy-2'-deoxyguanosine (8-OHdG) as a marker of oxidative stress in rheumatoid arthritis and aging: effect of progressive resistance training. *Journal of Nutritional Biochemistry*, 11 (11/12), 581-584.
 - Rossner P. Jr, Svecova V., Milcova A., Lnenickova Z., Solansky I., Sram R.J., 2008. Seasonal variability of oxidative stress markers in city bus drivers - Part I. Oxidative damage to DNA. *Mutation Research/Fundamental and Molecular Mechanisms of Mutagenesis*, 642 (1/2), 14-20.
 - Schlesinger R.B., Kunzli N., Hidy G.M., Gotschi T., Jerrett M., 2006. The health relevance of ambient particulate matter characteristics: coherence of toxicological and epidemiological inferences. *Inhalation Toxicology*, 18 (2), 95-125.
 - Sørensen M., Schins R.P.F., Hertel O., Loft S., 2005. Transition metals in personal samples of PM_{2.5} and oxidative stress in human volunteers. *Cancer Epidemiology, Biomarkers & Prevention*, 14 (5), 1340-1343.
 - Stohs S.J., Bagchi D., 1995. Oxidative mechanisms in the toxicity of metal ions. *Free Radical Biology & Medicine*, 18 (2), 321-336.
 - Stone V., Shaw J., Brown D.M., MacNee W., Faux S.P., Donaldson K., 1998. The role of oxidative stress in the prolonged inhibitory effect of ultrafine carbon black on epithelial cell function. *Toxicology in Vitro*, 12 (6), 649-659.
 - Tamura S., Tsukahara H., Ueno M., Maeda M., Kawakami H., Sekine K., Mayumi M., 2006. Evaluation of a urinary multi-parameter biomarker set for oxidative stress in children, adolescents and young adults. *Free Radical Research*, 40 (11), 1198-1205.
 - Turi J.L., Yang F., Garrick M.D., Piantadosi C.A., Ghio A.J., 2004. The iron cycle and oxidative stress in the lung. *Free Radical Biology & Medicine*, 36 (7), 850-857.
 - Wu M.-T., Pan C.-H., Huang Y.-L., Tsai P.-J., Chen C.-J., Wu T.-N., 2003. Urinary excretion of 8-hydroxy-2-deoxyguanosine and 1-hydroxypyrene in coke-oven workers. *Environmental and Molecular Mutagenesis*, 42 (2), 98-105.
 - Yoshida J., Kumagai S., Tabuchi T., Kosaka H., Akasaka S., Kasai H., Oda H., 2006. Negative association between serum dioxin level and oxidative DNA damage markers in municipal waste incinerator workers. *International Archives of Occupational and Environmental Health*, 79 (2), 115-122.

-
- Zuniga M.A., Dai J., Wehunt M.P., Zhou Q., 2006. DNA oxidative damage by terpene catechols as analogues of natural terpene quinone methide precursors in the presence of Cu(II) and/or NADH. *Chemical Research in Toxicology*, 19 (6), 828-836.

Chapter 7 - Conclusion and perspectives

We know for a long time that exposure to particulate matter is associated with a range of adverse health effects, including cancer, pulmonary and cardiovascular diseases. However, mechanisms by which particles influence health are complex, and many points remain unclear. Over the past 10 years, publications strongly suspected particles to cause these adverse effects through the production of reactive oxygen species (ROS), and thereby to cause oxidative stress in biological systems. Moreover, particle surface characteristics seem to play a central role in the ability of particles to generate ROS.

The present research project was undertaken in order to better understand the mechanisms by which exposure to particulate matter induces adverse health effects. The first point of the project was to check whether exposure to particulate matter was linked to oxidative stress. Secondly, we wanted to identify which particle surface characteristics are involved in the production of ROS.

In order to answer these questions, we decided to undertake a study in workplaces where high levels of particulate matter were expected. Indeed, since activities of workers in many occupational situations are responsible for the release of important amounts of particles, workers are often in first line to suffer acute exposure to particles.

The study undertaken in bus depots allowed us firstly to measure significant increases of 8-hydroxy-2'-deoxyguanosine (8OHdG), the selected oxidative stress biomarker, in non-smoking workers exposed over a two-day period. Results obtained confirmed that 8OHdG is an interesting biomarker of oxidative DNA damages. Therefore this compound should be retained for forthcoming projects involving the assessment of oxidative stress. The analytical method developed using LC-MS/MS was suitable within the framework of the present project. Nevertheless, in the case of epidemiological studies involving hundreds or thousands of volunteers, this analytical method would cause some problems due to the time-consuming nature of the analysis. Within the framework of a forthcoming research project, the Particles and Health Group (Institute for Work and Health) has planned to develop a new analytical

method using enzyme-linked immuno-sorbent assay (ELISA), which is known to be much faster than LC-MS/MS.

According to results obtained for 8OHdG and antioxidants, we found out that the hierarchical oxidative stress model was applicable to explain the physiological response of workers. An interesting point is that biological response to oxidative stress took place at very low levels of PM₄.

For the second point of the present research project, the work undertaken in the laboratory of Dr Michel J. Rossi confirmed the importance of particle surface characteristics in the oxidative stress process. In addition to the quantification of several functional groups located on the surface of particles, we also decided to study the reaction kinetics. Correlations between reaction kinetics and oxidative stress were unexpected, and this point needs to be investigated further. Nevertheless, these measurements were undertaken in the gas-phase, while reactions involving particles in humans take place in solution. Therefore, we are not sure that the reaction kinetics measured using the Knudsen flow reactor reflect real kinetics in the body. This question should be investigated further, through measurements of the particle reactivity in solution. Such a project is ongoing at the Institute for Work and Health.

Even if this research project pointed out associations between several exposure parameters and oxidative stress, some questions remain open, such as the influence of psycho-social factors on oxidative stress. This point was not studied within the framework of the present work, but will be the subject of a future research project, which is in preparation at the Institute for Work and Health.

Chapter 8 - Annexes

8.1 Questionnaire

L'ensemble des données recueillies par ce questionnaire sera traité de manière à garantir la confidentialité. Votre employeur ne recevra aucune information vous concernant personnellement.

Si vous souhaitez participer à cette étude, nous vous remercions de répondre aussi complètement que possible à toutes les questions.

Nom : _____

Prénom : _____

Année de naissance : _____

Taille : _____

Poids : _____

Nom de l'entreprise dans laquelle vous travaillez actuellement :

Depuis combien d'années travaillez-vous dans cette entreprise ? _____ an(s)

Quel est votre poste de travail ? _____

Durant les deux jours qui ont précédé cette étude, avez-vous été exposé aux polluants (barbecue, parking, ...) ? ☐ oui ☐ non

Si oui, précisez : _____

Etes-vous fumeur ou ancien fumeur ?

☐ Non, je n'ai jamais fumé.

☐ Oui, je suis ancien fumeur : j'ai fumé environ _____ cigarettes par jour pendant _____ an(s), et j'ai arrêté il y a _____ an(s).

☐ Oui, je suis fumeur actif : je fume environ _____ cigarettes par jour.

Consommez-vous de l'alcool ?

- ☐ Non, je ne bois jamais d'alcool.
- ☐ Oui, je bois moins d'1 verre d'alcool par jour.
- ☐ Oui, je bois entre 1 et 3 verre(s) d'alcool par jour.
- ☐ Oui, je bois plus de 3 verres d'alcool par jour.

Combien d'heures par semaine faites-vous du sport ? _____**Souffrez-vous d'une insuffisance rénale ? ☐ oui ☐ non****Avez-vous des problèmes d'articulations (arthrose, rhumatisme) ? ☐ oui ☐ non****Avez-vous déjà eu des problèmes cardiaques ? ☐ oui ☐ non****Souffrez-vous de maladies allergiques ou respiratoires (rhume des foins, asthme, bronchite, allergies, ...) ? ☐ oui ☐ non****Si oui, le(s)quel(s) ? _____****Prenez-vous régulièrement des médicaments ? ☐ oui ☐ non****Si oui, le(s)quel(s) ? _____****Combien en prenez-vous ? _____****Prenez-vous régulièrement des vitamines ? ☐ oui ☐ non****Si oui, la(les)quelle(s) ? _____****Combien en prenez-vous ? _____****Mangez-vous de la viande ?**

- ☐ Non, je ne mange jamais de viande.
- ☐ Oui, je mange de la viande 1-3 fois par semaine.
- ☐ Oui, je mange de la viande lors d'un repas sur deux.
- ☐ Oui, je mange de la viande à chaque repas (midi/soir).

Mangez-vous des fruits ?

- ☐ Non, je ne mange jamais de fruit.
- ☐ Oui, je mange moins de 1 fruit par jour.
- ☐ Oui, je mange 1-2 fruits par jour.
- ☐ Oui, je mange plus de 2 fruits par jour.

8.2 Stationary sampling

	Temperature [°C]	Relative humidity [%]	PM ₄ [µg/m ³]	Organic Carbon [µg/m ³]	Elemental Carbon [µg/m ³]
Limit of detection	min: -35°C ^a max: 55°C ^a	min: 0% ^a max: 100% ^a	22.1 ^b	13.9 ^b	3.2 ^b
Bus depot 1 27.03.2006 day	22.3	33.2	78.3 (±4.6)	27.5 (±6.1)	17.0 (±2.4)
Bus depot 1 28.03.2006 day	20.6	44.6	63.2 (±3.6)	29.8 (±5.3)	15.2 (±1.9)
Bus depot 2 22.05.2006 day	23.2	42.9	50.9 (±10.1)	25.0 (±10.0)	7.1 (±3.7)
Bus depot 2 22.05.2006 night	23.2	53.3	21.4 (±9.1)	27.2 (±10.8)	6.9 (±3.9)
Bus depot 2 23.05.2006 day	22.6	36.4	53.3 (±8.4)	22.6 (±8.0)	6.2 (±2.8)
Bus depot 2 23.05.2006 night	21.4	30.7	42.0 (±8.8)	32.8 (±11.5)	7.0 (±3.6)
Bus depot 3 06.06.2006 day	24.9	29.9	45.7 (±12.0)	25.7 (±9.4)	8.1 (±3.6)
Bus depot 3 06.06.2006 night	21.3	43.7	18.8 (±13.5)	19.8 (±8.6)	6.2 (±3.7)
Bus depot 3 07.06.2006 day	24.1	26.4	41.2 (±11.9)	26.0 (±9.6)	6.2 (±3.2)
Bus depot 3 07.06.2006 night	19.5	33.8	31.0 (±14.2)	11.5 (±5.9)	N/D
Metro construction site 11.12.2006 day	7.8	53.6	48.4 (±6.5)	31.6 (±8.3)	5.8 (±2.5)
Metro construction site 12.12.2006 day	9.3	49.6	87.4 (±5.4)	17.8 (±4.3)	2.3 (±1.1)
Bus depot 2 12.02.2007 day	20.9	39.5	50.2 (±7.0)	32.0 (±8.1)	8.7 (±2.6)
Bus depot 2 13.02.2007 day	20.7	35.7	67.0 (±7.7)	37.7 (±8.8)	6.1 (±2.2)

	Fe [ng/m ³]	Cu [ng/m ³]	Mn [ng/m ³]	PM _{0.7} number [particle/cm ³]	PM _{0.7} mass [µg/m ³]	PM _{0.7} surface area [µm ² /cm ³]	LQ1-DC surface area [µm ² /cm ³]
Limit of detection	7.0 ^b	3.5 ^b	2.1 ^b	min: 2 ^a max: 10 ^{8a}			min: 1 ^a max: 2000 ^a
Bus depot 1 27.03.2006 day	1402.5 (±140.3)	140.5 (±14.1)	10.8 (±1.1)	N/A	N/A	N/A	318
Bus depot 1 28.03.2006 day	1157.6 (±115.8)	68.6 (±6.9)	6.8 (±0.7)	N/A	N/A	N/A	289
Bus depot 2 22.05.2006 day	2138.9 (±213.9)	31.3 (±3.1)	26.4 (±2.6)	10624	26.5	400	153
Bus depot 2 22.05.2006 night	572.4 (±57.2)	13.1 (±1.3)	7.4 (±0.7)	12129	36.9	526	170
Bus depot 2 23.05.2006 day	2552.5 (±255.3)	64.1 (±6.4)	26.8 (±2.7)	7194	14.8	228	168
Bus depot 2 23.05.2006 night	1532.7 (±153.3)	20.5 (±2.1)	18.4 (±1.8)	2770	4.6	76	95
Bus depot 3 06.06.2006 day	393.7 (±39.4)	10.2 (±1.0)	48.2 (±4.8)	42498	39.0	799	230
Bus depot 3 06.06.2006 night	2487.3 (±248.7)	135.8 (±13.6)	22.9 (±2.3)	9614	18.0	303	119
Bus depot 3 07.06.2006 day	252.8 (±25.3)	13.6 (±1.4)	2.0 (±0.2)	11242	16.5	281	191
Bus depot 3 07.06.2006 night	430.9 (±43.1)	13.9 (±1.4)	3.7 (±0.4)	10999	10.8	206	106
Metro construction site 11.12.2006 day	2461.7 (±246.2)	13.4 (±1.3)	52.4 (±5.2)	30090	32.8	674	418
Metro construction site 12.12.2006 day	6024.6 (±602.5)	69.7 (±7.0)	467.1 (±46.7)	27208	26.7	494	292
Bus depot 2 12.02.2007 day	2049.6 (±205.0)	223.4 (±22.3)	29.7 (±3.0)	11729	23.1	360	252
Bus depot 2 13.02.2007 day	3765.1 (±376.5)	148.4 (±14.8)	28.1 (±2.8)	10850	22.9	357	250

	Mean aerodynamic diameter [μm]	NO [ppb]	NO ₂ [ppb]	NO _x [ppb]	O ₃ [ppb]
Limit of detection		0.5 ^a	0.5 ^a	0.5 ^a	0.5 ^a
Bus depot 1 27.03.2006 day	3.9 (± 4.8)	479	124	603	1.5
Bus depot 1 28.03.2006 day	3.4 (± 4.4)	382	109	491	1.3
Bus depot 2 22.05.2006 day	3.2 (± 2.9)	N/A	N/A	N/A	2.3
Bus depot 2 22.05.2006 night	2.8 (± 3.6)	N/A	N/A	N/A	3.7
Bus depot 2 23.05.2006 day	5.5 (± 2.1)	N/A	N/A	N/A	2.3
Bus depot 2 23.05.2006 night	6.5 (± 1.8)	N/A	N/A	N/A	4.8
Bus depot 3 06.06.2006 day	1.5 (± 4.7)	599	42	641	1.0
Bus depot 3 06.06.2006 night	5.0 (± 3.2)	245	23	268	16.3
Bus depot 3 07.06.2006 day	1.8 (± 4.0)	291	19	310	7.7
Bus depot 3 07.06.2006 night	5.0 (± 5.3)	106	10	116	9.4
Metro construction site 11.12.2006 day	6.6 (± 3.4)	282	54	334	1.4
Metro construction site 12.12.2006 day	5.8 (± 3.0)	265	44	308	2.4
Bus depot 2 12.02.2007 day	3.4 (± 3.6)	851	145	996	2.4
Bus depot 2 13.02.2007 day	3.3 (± 3.7)	711	126	837	1.1

Results: mean values over an 8-hour period of shift.

Values between brackets: uncertainty due to the analytical method, except for the mean aerodynamic diameter (standard deviation).

^a data provided by the manufacturer

^b determined by the mean of the blank measures plus three times the standard deviation of the blank measures

N/A: not available

N/D: not detected (below the limit of detection)

8.3 Personal sampling

Personal information				PM ₄ [µg/m ³]		Organic Carbon [µg/m ³]		Elemental Carbon [µg/m ³]	
Worker	Workplace	Date	Status	day 1	day 2	day 1	day 2	day 1	day 2
L 01	Bus depot 1	27/28.03.2006 day	smoker	413 (±28)	137 (±15)	107 (±29)	63 (±20)	17 (±6)	11 (±5)
L 02	Bus depot 1	27/28.03.2006 day	non-smoker	120 (±15)	99 (±12)	51 (±18)	34 (±13)	10 (±5)	10 (±5)
L 03	Bus depot 1	27/28.03.2006 day	former smoker	89 (±11)	60 (±8)	57 (±18)	40 (±14)	10 (±5)	12 (±5)
L 04	Bus depot 1	27/28.03.2006 day	former smoker	96 (±12)	44 (±5)	48 (±17)	34 (±12)	14 (±6)	9 (±4)
L 05	Bus depot 1	27/28.03.2006 day	non-smoker	228 (±18)	59 (±8)	67 (±20)	32 (±12)	8 (±4)	7 (±4)
L 06	Bus depot 1	27/28.03.2006 day	former smoker	122 (±7)	122 (±7)	49 (±10)	46 (±9)	12 (±2)	9 (±2)
L 07	Bus depot 1	27/28.03.2006 day	non-smoker	84 (±5)	60 (±3)	27 (±6)	28 (±5)	16 (±2)	15 (±2)
G 01 EU	Bus depot 2	22/23.05.2006 day	non-smoker	103 (±14)	155 (±17)	33 (±12)	45 (±15)	10 (±4)	7 (±4)
G 02 EU	Bus depot 2	22/23.05.2006 day	smoker	125 (±16)	82 (±11)	63 (±19)	49 (±14)	8 (±4)	4 (±2)
G 03 EU	Bus depot 2	22/23.05.2006 day	smoker	299 (±24)	222 (±20)	206 (±43)	110 (±27)	32 (±8)	9 (±4)
G 04 EU	Bus depot 2	22/23.05.2006 day	non-smoker	56 (±12)	48 (±12)	36 (±13)	32 (±12)	6 (±4)	4 (±3)
G 05 EU	Bus depot 2	22/23.05.2006 day	non-smoker	66 (±11)	N/D	33 (±11)	25 (±9)	7 (±3)	7 (±3)
G 06 EU	Bus depot 2	22/23.05.2006 night	non-smoker	570 (±40)	83 (±14)	66 (±22)	45 (±16)	3 (±3)	6 (±4)
G 07 EU	Bus depot 2	22/23.05.2006 night	smoker	176 (±21)	67 (±12)	135 (±34)	79 (±23)	15 (±6)	10 (±5)
G 08 EU	Bus depot 2	22/23.05.2006 night	former smoker	32 (±10)	80 (±14)	45 (±15)	38 (±14)	8 (±4)	3 (±3)
G 09 EU	Bus depot 2	22/23.05.2006 night	former smoker	77 (±15)	67 (±13)	44 (±16)	24 (±10)	9 (±5)	N/D
G 10 EU	Bus depot 2	22/23.05.2006 night	former smoker	66 (±14)	23 (±8)	43 (±15)	36 (±13)	9 (±5)	N/D
G 11 EU	Bus depot 2	22/23.05.2006 night	smoker	120 (±25)	272 (±25)	110 (±35)	224 (±48)	16 (±9)	5 (±3)
G 12 EU	Bus depot 3	06/07.06.2006 day	non-smoker	17 (±12)	112 (±17)	44 (±14)	40 (±13)	12 (±5)	6 (±3)
G 13 EU	Bus depot 3	06/07.06.2006 day	former smoker	66 (±15)	116 (±18)	47 (±15)	44 (±6)	9 (±4)	7 (±2)
G 14 EU	Bus depot 3	06/07.06.2006 day	smoker	97 (±17)	108 (±16)	73 (±20)	62 (±14)	9 (±4)	8 (±4)
G 15 EU	Bus depot 3	06/07.06.2006 day	non-smoker	17 (±7)	24 (±9)	18 (±7)	15 (±18)	5 (±2)	4 (±4)
G 16 EU	Bus depot 3	06/07.06.2006 night	former smoker	27 (±15)	85 (±19)	36 (±13)	38 (±14)	3 (±3)	N/D
G 17 EU	Bus depot 3	06/07.06.2006 night	smoker	207 (±25)	92 (±20)	134 (±33)	56 (±18)	12 (±5)	3 (±3)
M1	Metro construction site	11/12.12.2006 day	non-smoker	N/A	N/A	N/A	N/A	N/A	N/A
M2	Metro construction site	11/12.12.2006 day	smoker	95 (±19)	N/A	66 (±21)	N/A	7 (±4)	N/A
M3	Metro construction site	11/12.12.2006 day	smoker	N/A	N/A	N/A	N/A	N/A	N/A
M4	Metro construction site	11/12.12.2006 day	non-smoker	185 (±32)	N/A	66 (±25)	N/A	N/D	N/A
M5	Metro construction site	11/12.12.2006 day	smoker	219 (±35)	211 (±18)	88 (±30)	60 (±17)	12 (±8)	4 (±2)
M6	Metro construction site	11/12.12.2006 day	smoker	466 (±40)	356 (±24)	147 (±39)	144 (±31)	13 (±7)	4 (±3)
M7	Metro construction site	11/12.12.2006 day	non-smoker	107 (±21)	33 (±10)	90 (±27)	N/D	8 (±5)	N/D
M8	Metro construction site	11/12.12.2006 day	N/A	179 (±22)	N/A	70 (±22)	N/A	9 (±5)	N/A
G 02 HU	Bus depot 2	12/13.02.2007 day	smoker	200 (±21)	209 (±20)	119 (±29)	135 (±31)	9 (±4)	6 (±3)
G 03 HU	Bus depot 2	12/13.02.2007 day	smoker	91 (±20)	155 (±20)	69 (±23)	67 (±20)	13 (±6)	11 (±5)
G 04 HU	Bus depot 2	12/13.02.2007 day	non-smoker	85 (±14)	197 (±23)	52 (±16)	92 (±25)	7 (±4)	5 (±3)
G 05 HU	Bus depot 2	12/13.02.2007 day	non-smoker	64 (±4)	67 (±5)	40 (±6)	45 (±7)	5 (±1)	5 (±1)
G 06 HU	Bus depot 2	12/13.02.2007 day	non-smoker	46 (±13)	85 (±16)	37 (±13)	47 (±16)	10 (±4)	6 (±4)
G 08 HU	Bus depot 2	12/13.02.2007 day	former smoker	N/D	83 (±16)	47 (±16)	46 (±16)	10 (±5)	10 (±5)
G 10 HU	Bus depot 2	12/13.02.2007 day	former smoker	19 (±13)	10 (±12)	41 (±15)	58 (±19)	9 (±5)	9 (±5)
G 18 HU	Bus depot 2	12/13.02.2007 day	non-smoker	24 (±9)	86 (±14)	24 (±9)	41 (±13)	5 (±3)	5 (±3)

Results: mean concentrations over an 8-hour period of shift.

Values between brackets: uncertainty due to the analytical method.

N/A: not available.

N/D: not detected (below the limit of detection).

8.4 Uptake measurements on aerosols collected in the workplaces using the Knudsen flow reactor

	$\text{N}(\text{CH}_3)_3$	NH_2OH	CF_3COOH	HCl	O_3
Bus depot 1 27.03.2006 day	(a) $6.6 (\pm 2.1) \cdot 10^{14}$ (b) not available	(a) $1.3 (\pm 0.1) \cdot 10^{17}$ (b) not available	(a) $1.9 (\pm 1.1) \cdot 10^{15}$ (b) not available	(a) $7.4 (\pm 0.8) \cdot 10^{15}$ (b) not available	(a) $4.7 (\pm 0.8) \cdot 10^{16}$ (b) not available
Bus depot 1 28.03.2006 day	(a) not detected (b) not available	(a) $6.2 (\pm 0.7) \cdot 10^{16}$ (b) not available	(a) $1.9 (\pm 0.6) \cdot 10^{15}$ (b) not available	(a) $7.1 (\pm 0.7) \cdot 10^{15}$ (b) not available	(a) $3.3 (\pm 0.7) \cdot 10^{16}$ (b) not available
Bus depot 2 22.05.2006 day	(a) $3.6 (\pm 3.7) \cdot 10^{14}$ (b) $7.0 (\pm 7.3) \cdot 10^{12}$	(a) $6.0 (\pm 1.0) \cdot 10^{16}$ (b) $1.2 (\pm 0.2) \cdot 10^{15}$	(a) $1.0 (\pm 0.1) \cdot 10^{16}$ (b) $2.0 (\pm 0.2) \cdot 10^{14}$	(a) $2.4 (\pm 0.1) \cdot 10^{16}$ (b) $4.8 (\pm 0.3) \cdot 10^{14}$	(a) $6.4 (\pm 11.1) \cdot 10^{15}$ (b) $1.2 (\pm 2.2) \cdot 10^{14}$
Bus depot 2 23.05.2006 night	(a) $3.4 (\pm 0.5) \cdot 10^{15}$ (b) $7.2 (\pm 1.2) \cdot 10^{13}$	(a) $1.5 (\pm 0.1) \cdot 10^{17}$ (b) $3.0 (\pm 0.3) \cdot 10^{15}$	(a) $2.5 (\pm 0.2) \cdot 10^{16}$ (b) $5.2 (\pm 0.5) \cdot 10^{14}$	(a) $7.7 (\pm 0.2) \cdot 10^{16}$ (b) $1.6 (\pm 0.1) \cdot 10^{15}$	(a) $1.2 (\pm 1.7) \cdot 10^{16}$ (b) $2.5 (\pm 3.5) \cdot 10^{14}$
Bus depot 2 23.05.2006 day	(a) $1.3 (\pm 0.3) \cdot 10^{15}$ (b) $6.7 (\pm 1.4) \cdot 10^{13}$	(a) $1.0 (\pm 0.1) \cdot 10^{17}$ (b) $5.1 (\pm 0.4) \cdot 10^{15}$	(a) $4.7 (\pm 0.5) \cdot 10^{15}$ (b) $2.4 (\pm 0.2) \cdot 10^{14}$	(a) $1.5 (\pm 0.1) \cdot 10^{16}$ (b) $7.5 (\pm 0.5) \cdot 10^{14}$	(a) $5.8 (\pm 6.0) \cdot 10^{15}$ (b) $2.9 (\pm 3.0) \cdot 10^{14}$
Bus depot 2 23.05.2006 night	not detected	not available	(a) $3.8 (\pm 0.7) \cdot 10^{15}$ (b) $5.4 (\pm 1.1) \cdot 10^{13}$	(a) $5.7 (\pm 0.9) \cdot 10^{15}$ (b) $8.0 (\pm 1.3) \cdot 10^{13}$	not detected
Bus depot 3 06.06.2006 day	(a) $2.0 (\pm 0.5) \cdot 10^{15}$ (b) $1.5 (\pm 0.3) \cdot 10^{13}$	(a) $3.1 (\pm 1.2) \cdot 10^{16}$ (b) $2.4 (\pm 0.9) \cdot 10^{14}$	(a) $5.6 (\pm 1.1) \cdot 10^{15}$ (b) $4.3 (\pm 0.8) \cdot 10^{13}$	(a) $1.8 (\pm 0.1) \cdot 10^{16}$ (b) $1.4 (\pm 0.1) \cdot 10^{14}$	not detected
Bus depot 3 06.06.2006 night	(a) $1.9 (\pm 0.7) \cdot 10^{15}$ (b) $4.5 (\pm 1.5) \cdot 10^{13}$	(a) $3.0 (\pm 1.4) \cdot 10^{16}$ (b) $6.9 (\pm 3.3) \cdot 10^{14}$	(a) $1.1 (\pm 0.1) \cdot 10^{16}$ (b) $2.5 (\pm 0.3) \cdot 10^{14}$	(a) $2.5 (\pm 0.1) \cdot 10^{16}$ (b) $5.8 (\pm 0.4) \cdot 10^{14}$	not detected
Bus depot 3 07.06.2006 day	(a) $2.8 (\pm 0.4) \cdot 10^{15}$ (b) $2.8 (\pm 0.4) \cdot 10^{13}$	(a) $2.1 (\pm 1.3) \cdot 10^{16}$ (b) $2.0 (\pm 1.3) \cdot 10^{14}$	(a) $2.7 (\pm 0.8) \cdot 10^{15}$ (b) $2.7 (\pm 0.8) \cdot 10^{13}$	(a) $1.2 (\pm 0.1) \cdot 10^{16}$ (b) $1.2 (\pm 0.1) \cdot 10^{14}$	not detected
Bus depot 3 07.06.2006 night	(a) $3.8 (\pm 0.5) \cdot 10^{15}$ (b) $3.6 (\pm 0.5) \cdot 10^{13}$	(a) $2.5 (\pm 2.2) \cdot 10^{16}$ (b) $2.4 (\pm 2.1) \cdot 10^{14}$	(a) $1.3 (\pm 1.2) \cdot 10^{15}$ (b) $1.2 (\pm 1.1) \cdot 10^{13}$	(a) $8.6 (\pm 2.1) \cdot 10^{15}$ (b) $8.1 (\pm 2.0) \cdot 10^{13}$	not detected
Metro construction site 11.12.2006 day	(a) $7.4 (\pm 5.9) \cdot 10^{14}$ (b) $4.5 (\pm 3.6) \cdot 10^{12}$	not detected	(a) $1.5 (\pm 1.3) \cdot 10^{15}$ (b) $9.1 (\pm 7.8) \cdot 10^{12}$	(a) $2.4 (\pm 0.1) \cdot 10^{16}$ (b) $1.5 (\pm 0.1) \cdot 10^{14}$	not detected
Metro construction site 12.12.2006 day	not detected	not detected	(a) $3.2 (\pm 1.1) \cdot 10^{15}$ (b) $5.4 (\pm 1.8) \cdot 10^{13}$	(a) $3.0 (\pm 0.1) \cdot 10^{16}$ (b) $5.0 (\pm 0.3) \cdot 10^{14}$	not detected
Bus depot 2 12.02.2007 day	not detected	(a) $2.8 (\pm 1.4) \cdot 10^{16}$ (b) $3.3 (\pm 1.7) \cdot 10^{14}$	(a) $3.7 (\pm 1.1) \cdot 10^{15}$ (b) $4.4 (\pm 1.3) \cdot 10^{13}$	(a) $7.0 (\pm 0.9) \cdot 10^{15}$ (b) $8.3 (\pm 1.2) \cdot 10^{13}$	(a) $2.3 (\pm 0.1) \cdot 10^{17}$ (b) $2.7 (\pm 0.2) \cdot 10^{15}$
Bus depot 2 13.02.2007 day	not detected	(a) $1.6 (\pm 1.2) \cdot 10^{16}$ (b) $2.3 (\pm 1.8) \cdot 10^{14}$	(a) $1.4 (\pm 0.1) \cdot 10^{16}$ (b) $2.0 (\pm 0.2) \cdot 10^{14}$	(a) $2.4 (\pm 0.1) \cdot 10^{16}$ (b) $3.5 (\pm 0.2) \cdot 10^{14}$	(a) $2.7 (\pm 0.1) \cdot 10^{17}$ (b) $4.0 (\pm 0.3) \cdot 10^{15}$

(a) molecule/mg

(b) molecule/cm²

Results: mean values of duplicates.

Values between brackets: combined uncertainty due to the measurement of the mass, surface area and uptake.

8.5 Urinary concentrations of 8-hydroxy-2'-deoxyguanosine

Personal information				8-hydroxy-2'-deoxyguanosine [µg/g creatinine]			
Worker	Workplace	Date	Status	day 1 before shift	day 1 after shift	day 2 before shift	day 2 after shift
L 01	Bus depot 1	27/28.03.2006 day	smoker	4.57	5.47	4.11	7.41
L 02	Bus depot 1	27/28.03.2006 day	non-smoker	1.16	1.17	0.96	1.66
L 03	Bus depot 1	27/28.03.2006 day	former smoker	2.94	5.29	6.12	5.42
L 04	Bus depot 1	27/28.03.2006 day	former smoker	5.93	5.00	5.15	6.83
L 05	Bus depot 1	27/28.03.2006 day	non-smoker	4.35	5.87	6.42	6.36
L 06	Bus depot 1	27/28.03.2006 day	former smoker	5.76	6.14	6.92	6.71
L 07	Bus depot 1	27/28.03.2006 day	non-smoker	1.70	1.03	1.41	1.86
G 01 EU	Bus depot 2	22/23.05.2006 day	non-smoker	2.29	5.47	3.84	3.72
G 02 EU	Bus depot 2	22/23.05.2006 day	smoker	3.60	9.60	4.81	4.85
G 03 EU	Bus depot 2	22/23.05.2006 day	smoker	2.52	1.87	1.91	2.92
G 04 EU	Bus depot 2	22/23.05.2006 day	non-smoker	N/A	2.64	3.66	4.03
G 05 EU	Bus depot 2	22/23.05.2006 day	non-smoker	2.77	2.19	2.17	3.57
G 06 EU	Bus depot 2	22/23.05.2006 night	non-smoker	3.08	2.44	3.56	3.56
G 07 EU	Bus depot 2	22/23.05.2006 night	smoker	3.26	3.24	3.27	3.57
G 08 EU	Bus depot 2	22/23.05.2006 night	former smoker	1.61	2.53	3.82	4.62
G 09 EU	Bus depot 2	22/23.05.2006 night	former smoker	1.95	3.20	3.66	4.16
G 10 EU	Bus depot 2	22/23.05.2006 night	former smoker	3.48	3.04	8.06	4.55
G 11 EU	Bus depot 2	22/23.05.2006 night	smoker	2.64	3.02	2.40	2.62
G 12 EU	Bus depot 3	06/07.06.2006 day	non-smoker	0.34	0.44	0.55	0.45
G 13 EU	Bus depot 3	06/07.06.2006 day	former smoker	0.97	1.32	0.74	1.81
G 14 EU	Bus depot 3	06/07.06.2006 day	smoker	3.36	7.40	5.34	7.83
G 15 EU	Bus depot 3	06/07.06.2006 day	non-smoker	2.63	2.33	2.70	8.82
G 16 EU	Bus depot 3	06/07.06.2006 night	former smoker	5.92	4.34	8.05	5.08
G 17 EU	Bus depot 3	06/07.06.2006 night	smoker	5.23	6.68	9.11	4.95
M1	Metro yard	11/12.12.2006 day	non-smoker	6.62	8.03	N/A	N/A
M2	Metro construction site	11/12.12.2006 day	smoker	2.04	3.86	N/A	N/A
M3	Metro construction site	11/12.12.2006 day	smoker	3.10	3.03	N/A	1.87
M4	Metro construction site	11/12.12.2006 day	non-smoker	3.93	2.77	5.56	4.49
M5	Metro construction site	11/12.12.2006 day	smoker	14.67	10.40	7.97	9.29
M6	Metro construction site	11/12.12.2006 day	smoker	3.50	4.47	2.66	2.32
M7	Metro construction site	11/12.12.2006 day	non-smoker	3.02	2.47	2.49	3.53
M8	Metro construction site	11/12.12.2006 day	N/A	1.85	1.34	N/A	N/A
G 02 HU	Bus depot 2	12/13.02.2007 day	smoker	4.89	18.31	N/A	8.84
G 03 HU	Bus depot 2	12/13.02.2007 day	smoker	1.71	1.98	2.63	2.37
G 04 HU	Bus depot 2	12/13.02.2007 day	non-smoker	1.01	4.38	3.85	5.94
G 05 HU	Bus depot 2	12/13.02.2007 day	non-smoker	2.09	4.23	4.12	6.63
G 06 HU	Bus depot 2	12/13.02.2007 day	non-smoker	2.25	3.12	2.95	5.87
G 08 HU	Bus depot 2	12/13.02.2007 day	former smoker	0.45	1.82	1.60	3.32
G 10 HU	Bus depot 2	12/13.02.2007 day	former smoker	7.21	8.57	4.11	6.07
G 18 HU	Bus depot 2	12/13.02.2007 day	non-smoker	3.99	3.73	4.83	4.96

N/A: not available

8.6 Urinary concentrations of creatinine

Personal information				Creatinine [g/l]			
Worker	Workplace	Date	Status	day 1 before shift	day 1 after shift	day 2 before shift	day 2 after shift
L 01	Bus depot 1	27/28.03.2006 day	smoker	0.35	0.17	0.33	0.50
L 02	Bus depot 1	27/28.03.2006 day	non-smoker	2.01	1.78	2.31	1.99
L 03	Bus depot 1	27/28.03.2006 day	former smoker	2.15	1.15	1.45	0.90
L 04	Bus depot 1	27/28.03.2006 day	former smoker	1.53	1.35	1.42	1.11
L 05	Bus depot 1	27/28.03.2006 day	non-smoker	1.67	2.24	1.66	1.90
L 06	Bus depot 1	27/28.03.2006 day	former smoker	1.96	2.55	2.65	1.86
L 07	Bus depot 1	27/28.03.2006 day	non-smoker	1.56	2.13	2.14	0.55
G 01 EU	Bus depot 2	22/23.05.2006 day	non-smoker	2.22	0.48	0.95	2.32
G 02 EU	Bus depot 2	22/23.05.2006 day	smoker	2.80	1.08	2.79	1.00
G 03 EU	Bus depot 2	22/23.05.2006 day	smoker	2.15	3.71	1.61	1.80
G 04 EU	Bus depot 2	22/23.05.2006 day	non-smoker	N/A	2.43	2.39	0.92
G 05 EU	Bus depot 2	22/23.05.2006 day	non-smoker	1.27	2.52	1.97	0.94
G 06 EU	Bus depot 2	22/23.05.2006 night	non-smoker	1.10	2.52	1.59	0.34
G 07 EU	Bus depot 2	22/23.05.2006 night	smoker	1.85	1.83	1.74	1.64
G 08 EU	Bus depot 2	22/23.05.2006 night	former smoker	1.50	1.40	1.11	1.38
G 09 EU	Bus depot 2	22/23.05.2006 night	former smoker	1.78	2.88	1.64	1.68
G 10 EU	Bus depot 2	22/23.05.2006 night	former smoker	0.95	2.62	0.61	1.69
G 11 EU	Bus depot 2	22/23.05.2006 night	smoker	1.04	1.72	1.71	1.80
G 12 EU	Bus depot 3	06/07.06.2006 day	non-smoker	1.63	1.89	1.23	2.17
G 13 EU	Bus depot 3	06/07.06.2006 day	former smoker	1.54	1.49	1.53	1.26
G 14 EU	Bus depot 3	06/07.06.2006 day	smoker	1.07	1.40	1.67	0.97
G 15 EU	Bus depot 3	06/07.06.2006 day	non-smoker	2.11	2.64	0.54	0.15
G 16 EU	Bus depot 3	06/07.06.2006 night	former smoker	0.78	1.41	0.15	0.79
G 17 EU	Bus depot 3	06/07.06.2006 night	smoker	1.04	0.86	0.61	0.98
M1	Metro construction site	11/12.12.2006 day	non-smoker	1.42	1.24	N/A	N/A
M2	Metro construction site	11/12.12.2006 day	smoker	2.96	1.77	N/A	N/A
M3	Metro construction site	11/12.12.2006 day	smoker	5.98	3.05	N/A	4.38
M4	Metro construction site	11/12.12.2006 day	non-smoker	1.87	1.28	2.21	1.91
M5	Metro construction site	11/12.12.2006 day	smoker	1.05	1.73	2.74	1.89
M6	Metro construction site	11/12.12.2006 day	smoker	2.09	1.96	1.46	1.26
M7	Metro construction site	11/12.12.2006 day	non-smoker	1.04	1.48	1.63	1.16
M8	Metro construction site	11/12.12.2006 day	N/A	2.45	1.97	N/A	N/A
G 02 HU	Bus depot 2	12/13.02.2007 day	smoker	2.28	0.80	N/A	1.59
G 03 HU	Bus depot 2	12/13.02.2007 day	smoker	1.79	3.02	1.50	1.75
G 04 HU	Bus depot 2	12/13.02.2007 day	non-smoker	3.28	0.56	1.49	1.31
G 05 HU	Bus depot 2	12/13.02.2007 day	non-smoker	2.55	1.45	1.06	0.94
G 06 HU	Bus depot 2	12/13.02.2007 day	non-smoker	1.42	0.79	1.37	0.75
G 08 HU	Bus depot 2	12/13.02.2007 day	former smoker	1.57	1.11	1.58	1.28
G 10 HU	Bus depot 2	12/13.02.2007 day	former smoker	1.43	1.74	0.95	1.51
G 18 HU	Bus depot 2	12/13.02.2007 day	non-smoker	1.52	1.88	1.59	1.16

N/A: not available

8.7 Urinary concentrations of antioxidants

Personal information				Antioxidants [/g creatinine]			
Worker	Workplace	Date	Status	day 1 before shift	day 1 after shift	day 2 before shift	day 2 after shift
L 01	Bus depot 1	27/28.03.2006 day	smoker	2394.29	3600.00	2354.60	2978.00
L 02	Bus depot 1	27/28.03.2006 day	non-smoker	582.40	628.65	617.75	498.99
L 03	Bus depot 1	27/28.03.2006 day	former smoker	958.60	837.39	934.48	1163.33
L 04	Bus depot 1	27/28.03.2006 day	former smoker	782.35	1372.59	847.89	2169.37
L 05	Bus depot 1	27/28.03.2006 day	non-smoker	588.62	477.68	1218.07	434.21
L 06	Bus depot 1	27/28.03.2006 day	former smoker	867.86	1247.06	374.34	829.03
L 07	Bus depot 1	27/28.03.2006 day	non-smoker	1013.46	424.88	606.07	1112.73
G 01 EU	Bus depot 2	22/23.05.2006 day	non-smoker	389.64	1643.75	1077.89	1020.26
G 02 EU	Bus depot 2	22/23.05.2006 day	smoker	671.43	2161.11	656.63	2140.00
G 03 EU	Bus depot 2	22/23.05.2006 day	smoker	380.93	337.47	418.01	627.78
G 04 EU	Bus depot 2	22/23.05.2006 day	non-smoker	N/A	702.88	435.15	1626.09
G 05 EU	Bus depot 2	22/23.05.2006 day	non-smoker	1000.00	508.73	513.71	1134.04
G 06 EU	Bus depot 2	22/23.05.2006 night	non-smoker	1130.91	384.52	1510.69	1797.06
G 07 EU	Bus depot 2	22/23.05.2006 night	smoker	654.59	803.28	776.44	840.85
G 08 EU	Bus depot 2	22/23.05.2006 night	former smoker	799.33	1452.14	1458.56	839.13
G 09 EU	Bus depot 2	22/23.05.2006 night	former smoker	634.27	473.96	838.41	711.90
G 10 EU	Bus depot 2	22/23.05.2006 night	former smoker	797.89	384.35	3804.28	701.18
G 11 EU	Bus depot 2	22/23.05.2006 night	smoker	1718.27	756.40	1212.28	949.44
G 12 EU	Bus depot 3	06/07.06.2006 day	non-smoker	385.28	1295.77	1069.11	930.41
G 13 EU	Bus depot 3	06/07.06.2006 day	former smoker	885.06	1082.55	835.29	1572.22
G 14 EU	Bus depot 3	06/07.06.2006 day	smoker	974.77	1267.14	469.46	1171.13
G 15 EU	Bus depot 3	06/07.06.2006 day	non-smoker	688.63	451.14	1764.81	4420.00
G 16 EU	Bus depot 3	06/07.06.2006 night	former smoker	2197.44	535.46	3900.00	1510.13
G 17 EU	Bus depot 3	06/07.06.2006 night	smoker	1367.31	1645.35	2473.77	1123.47
M1	Metro construction site	11/12.12.2006 day	non-smoker	N/A	N/A	N/A	N/A
M2	Metro construction site	11/12.12.2006 day	smoker	422.64	635.59	N/A	N/A
M3	Metro construction site	11/12.12.2006 day	smoker	357.02	604.26	N/A	N/A
M4	Metro construction site	11/12.12.2006 day	non-smoker	413.90	552.34	408.14	642.41
M5	Metro construction site	11/12.12.2006 day	smoker	2031.43	946.82	647.45	952.91
M6	Metro construction site	11/12.12.2006 day	smoker	779.90	690.82	790.41	2103.17
M7	Metro construction site	11/12.12.2006 day	non-smoker	805.77	638.51	911.66	1140.52
M8	Metro construction site	11/12.12.2006 day	N/A	N/A	N/A	N/A	N/A
G 02 HU	Bus depot 2	12/13.02.2007 day	smoker	998.25	2871.25	N/A	1611.95
G 03 HU	Bus depot 2	12/13.02.2007 day	smoker	402.23	257.28	563.33	678.29
G 04 HU	Bus depot 2	12/13.02.2007 day	non-smoker	170.43	1857.14	1844.30	1754.20
G 05 HU	Bus depot 2	12/13.02.2007 day	non-smoker	453.73	1004.83	911.32	2048.94
G 06 HU	Bus depot 2	12/13.02.2007 day	non-smoker	462.68	953.16	809.49	1641.33
G 08 HU	Bus depot 2	12/13.02.2007 day	former smoker	577.71	772.97	667.72	895.31
G 10 HU	Bus depot 2	12/13.02.2007 day	former smoker	1737.06	1339.66	802.11	568.87
G 18 HU	Bus depot 2	12/13.02.2007 day	non-smoker	1226.32	1492.55	786.79	1668.10

N/A: not available

Remerciements

Ce projet de thèse a nécessité un travail de plus de 4 ans, et n'aurait pas pu aller jusqu'à son terme sans le soutien et la participation de plusieurs personnes, que je tiens à remercier.

A l'IST :

- *Prof. Michel Guillemin*, pour son accueil chaleureux à l'IST, et pour avoir accepté d'être le Directeur de thèse.
- *Dr Jean-Jacques Sauvain*, pour avoir supervisé la partie du travail effectuée à l'IST, et pour l'équipe de choc que nous avons formée lors de la campagne d'échantillonnage sur le terrain.
- *Dr Michael Riediker*, pour les nombreuses discussions que nous avons eues sur le projet, et les précieux conseils qu'il m'a donnés.
- *Ferdinando Storti*, le plus « arménien » des Arménois !
- *Dr Michèle Berode* et son équipe, pour les analyses de métaux, de créatinine et les tests de comètes (*Christine Arnoux, Christine Kohler, Patricia Stephan, Monique Strebel, Coralie Roncadin* et *Mikaël Versel*).
- *Prof. Marcel-André Boillat* et l'équipe de médecins, pour les prises de sang effectuées sur le terrain (*Dr Sophie-Maria Praz-Christinaz, Dr David Kursner* et *Dr Frédéric Regamey*).
- *Dr Cong Khanh Huynh* et son équipe, pour les analyses des aldéhydes (*Philippe Boiteux*).
- *Dr Jérôme Lavoué*, pour son aide lors du traitement statistique.
- La Direction et les secrétaires, sans qui je n'aurais pas eu mes sous à la fin de chaque mois !
- Tous les collègues de l'IST, qui sont trop nombreux pour être cités !

A l'EPFL :

- *Dr Michel J. Rossi*, pour avoir supervisé la partie du travail effectuée à l'EPFL, et pour tout l'enseignement dont il m'a fait part durant ces quatre années.
- *Flavio Comino*, « il maestro » du tournevis et de la clé imbus, pour nous avoir notamment fabriqué deux racks qui nous ont bien servis lors du transport des appareils de mesure sur le terrain.

-
- *Prof. Hubert van den Bergh*, qui m'a permis d'effectuer une grosse partie du projet au sein de son Laboratoire de Pollution Atmosphérique et Sol.
 - Tous les collègues du Groupe Chimie Hétérogène : *Dr Pascal Pratte*, *Dr Federico Karagulian*, *Dr Christophe Delval*, le futur *Dr Simone Chiesa*, *Blanca Alonso Alvarez*, *Dr Mireille Crittin* et *Gaëlle Théodoloz*.

Collaborations externes :

- *Prof. Francelyne Marano*, de l'Université Paris VII, pour nous avoir donné l'opportunité de participer au projet NANOTOX.
- *Dr Jorge Boczkowski*, *Dr Sophie Lanone* et *Lyes Tabet*, de l'Institut National de la Santé Et de la Recherche Médicale (INSERM), pour la collaboration sur le projet concernant les nanotubes de carbone.
- *Dr Philippe Tacchini*, de l'entreprise EDEL Therapeutics S.A., pour les mesures d'antioxydants.

Jury de thèse :

- *Prof. Valentin Rousson*, pour avoir accepté d'être le Président du Jury.
- *Dr Thomas Kuhlbusch*, qui s'est beaucoup investi en tant qu'Expert externe et qui m'a donné de précieux conseils sur le projet et sur le mémoire de thèse.

Je tiens également à remercier tous les employés qui se sont portés volontaires pour participer à cette étude, ainsi que les principaux responsables des dépôts de bus pour nous avoir permis d'effectuer les mesures sur place.

Finalement, je voudrais remercier mes parents et ma sœur pour leur soutien et leur patience tout au long de ces quatre années.

Curriculum Vitae

Ari SETYAN



Date of birth: June 21st, 1974
Place of birth: Sion (Switzerland)
Citizenship: Switzerland
Marital status: single
Address: Avenue de Budé, 14
1202 Genève
Switzerland
E-mail: ari.setyan@gmail.com

Education

- 2004-2009 Institut universitaire romand de Santé au Travail (IST; Lausanne, Switzerland) and Ecole Polytechnique Fédérale de Lausanne (EPFL; Lausanne, Switzerland);
PhD Thesis in Life Sciences, under the supervision of Prof. Michel Guillemin and Dr Michel J. Rossi;
- Assessment of occupational exposure to Diesel exhaust particles;
- Development and validation of an analytical method of 8-hydroxy-2'-deoxyguanosine by LC-MS/MS;
- Characterization of surface functional groups present on particles.
- 1997-2002 University of Geneva (Switzerland);
Chemistry Diploma. Diploma Work under the supervision of Dr Patrick Edder and Dr Didier Ortellì (Food Control Authority of Geneva);
- Development and validation of an analytical method of 5 avermectines by HPLC (fluorescence detector).
- 1993-1997 University of Geneva (Switzerland);
Undergraduate studies of Medicine.
- 1989-1993 Collège Sismondi (Geneva, Switzerland);
Federal Maturity, type B (Latin).

Professional experiences

- Oct-Dec 2003 Ecole Polytechnique Fédérale de Lausanne (EPFL; Lausanne, Switzerland);
Trainee in electrochemical engineering, under the supervision of Prof. Christos Comninellis (Group of Electrochemical Engineering);
- Electrochemical deposition of gold nanoparticles on gold electrodes;
 - Study of electrochemical properties of boron-doped diamond electrodes.
- Feb-Jul 2003 Firmenich S.A. (Geneva, Switzerland);
Trainee in analytical chemistry, under the supervision of Dr Thierry Stora (Division Recherche Analyse et Perception);
- Study of physicochemical properties of raw materials used in fragrances.
- Aug 1994 Hôpital Cantonal Universitaire de Genève (Geneva, Switzerland);
Trainee in medicine, under the supervision of Martine Micallef (bloc opératoire de la Clinique de Pédiatrie);
- Medical assistance.

Languages

French: mother tongue

English: fluent

German: good knowledge

Armenian: fluent

Professional skills

Analytical chemistry: LC-MS/MS, HPLC, GC-MS.

Heterogeneous chemistry: Knudsen flow reactor.

Microsoft Office: Word, Excel, PowerPoint.

Statistics: Systat.

Acquisition and analysis of scientific data: LabView, Igor Pro.

List of publications

Peer-review

- **Setyan A.**, Sauvain J.-J., Riediker M., Guillemin M., Rossi M.J., 2009. Characterization of surface functional groups present on laboratory-generated and ambient aerosol particles by means of heterogeneous titration reactions. *Journal of Aerosol Science*, 40 (6), 534-548.
- **Setyan A.**, Sauvain J.-J., Rossi M.J., 2009. The use of heterogeneous chemistry for the characterization of functional groups at the gas/particle interface of soot and TiO₂ nanoparticles. *Physical Chemistry Chemical Physics*, 11 (29), 6205-6217.
- Tabet L., Bussy C., Amara N., **Setyan A.**, Grodet A., Rossi M.J., Pairon J.-C., Boczkowski J., Lanone S., 2009. Adverse effects of industrial multi-walled carbon nanotubes on human pulmonary cells. *Journal of Toxicology and Environmental Health, Part A: Current Issues*, 72 (2), 60-73.
- **Setyan A.**, Sauvain J.-J., Storti F., Deslarzes S., Tacchini P., Wild P., Guillemin M., Rossi M.J., Riediker M., 2009. Oxidative DNA damage and antioxidant response in workers exposed to fine particles in bus depots. In preparation.

Conference proceedings, abstracts

- **Setyan A.**, Sauvain J.-J., Rossi M.J., 2005. Characterization of surface functional groups present on soot and on laboratory-generated secondary aerosols. *Chimia*, 59 (9), p. 665.
- **Setyan A.**, Sauvain J.-J., Riediker M., Guillemin M., Rossi M.J., 2006. Characterization of surface functional groups present on aerosols. Proceedings of the International Conference on the COST Action 633 (Particulate Matter: Properties Related to Health Effects); Vienna, April 3rd-5th, 2006; p. 98.
- **Setyan A.**, 2006. Assessment of particulate exposure and surface characteristics in association with levels of biomarkers of oxidative stress. Proceedings of the 10th-ETH Conference on Combustion Generated Particles (Book of Abstracts: Posters); Zürich, August 21st-23rd, 2006; p. 55.
- **Setyan A.**, Sauvain J.-J., Riediker M., Rossi M.J., Guillemin M., 2006. Assessment of particulate exposure and surface characteristics in association with levels of biomarkers of oxidative stress. *Chimia*, 60 (7/8), p. 475.

-
- **Setyan A.**, Sauvain J.-J., Riediker M., Rossi M.J., Guillemin M., 2007. Assessment of Diesel exhaust particulate exposure and surface characteristics in association with levels of oxidative stress biomarkers. Proceedings of the CHUV Research Day (Biomedical Imaging); Lausanne, February 1st, 2007; N° EHU-20, p. 34.
 - **Setyan A.**, Sauvain J.-J., Riediker M., Guillemin M., Rossi M.J., 2007. Characterization of surface functional groups present on field-sampled aerosols. Proceedings of the General Assembly of the European Geosciences Union; Vienna, April 15th-20th, 2007; N° 02590.
 - Sauvain J.-J., **Setyan A.**, Riediker M., Rossi M.J., Guillemin M., 2007. Assessment of Diesel exhaust particulate exposure and surface characteristics in association with levels of oxidative stress biomarkers. Proceedings of the Public Conference on Particles and Health - State of the Research and Policy Implications; Lausanne, May 16th, 2007; p. 13.
 - **Setyan A.**, 2007. Assessment of particulate exposure and surface characteristics in association with urinary levels of oxidative stress biomarkers. Proceedings of the 11th-ETH Conference on Combustion Generated Particles (Book of Abstract: Papers); Zürich, August 13th-15th, 2007; p. 47.
 - **Setyan A.**, Sauvain J.-J., Riediker M., Rossi M.J., Guillemin M., 2007. Assessment of diesel exhaust particulate exposure and surface characteristics in association with levels of oxidative stress biomarkers. Proceedings of the European Aerosol Conference; Salzburg, September 9th-14th, 2007; N° T01A055.
 - **Setyan A.**, Sauvain J.-J., Riediker M., Rossi M.J., Guillemin M., 2007. Levels of oxidative stress biomarkers in workers exposed to diesel exhaust particulate. *Chimia*, 61 (7/8), p. 426.
 - Riediker M., **Setyan A.**, 2007. Particules à l'intérieur des bâtiments et des véhicules. *Bulletin de l'Association Romande pour la Protection des Eaux et de l'Air (ARPEA)*, 43 (234), p. 29-33.
 - **Setyan A.**, Sauvain J.-J., Riediker M., Rossi M.J., Guillemin M., 2008. Assessment of Diesel exhaust particulate exposure and surface characteristics in association with levels of oxidative stress biomarkers. Proceedings of the CHUV Research Day (Regenerative Medicine); Lausanne, January 17th, 2008; N° EHU-10, p. 14.
 - **Setyan A.**, Sauvain J.-J., Guillemin M., Rossi M.J., Riediker M., 2008. Assessment of diesel exhaust particulate exposure and surface characteristics in association with levels of oxidative stress biomarkers. *American Journal of Respiratory and Critical Care Medicine*, 177 (Abstracts Issue), p. A428.

-
- **Setyan A.**, 2008. Assessment of Diesel exhaust particulate exposure and surface characteristics in association with levels of oxidative stress biomarkers. Proceedings of the 12th-ETH Conference on Combustion Generated Particles (Book of Abstract: Posters); Zürich, June 23rd-25th, 2008; p. 32.
 - **Setyan A.**, Sauvain J.-J., Riediker M., Rossi M.J., Guillemin M., 2008. Assessment of Diesel exhaust particulate exposure and surface characteristics in association with levels of oxidative stress biomarkers. Proceedings of the European Aerosol Conference; Thessaloniki, August 24th-29th, 2008; N° T09A024P.
 - **Setyan A.**, Sauvain J.-J., Riediker M., Rossi M.J., Guillemin M., 2008. Assessment of Diesel exhaust particulate exposure and surface characteristics in association with levels of oxidative stress biomarker. *Chimia*, 62 (7/8), p. 572.
 - Tabet L., Bussy C., Amara N., **Setyan A.**, Grodet A., Rossi M.J., Pairon J.-C., Boczkowski J., Lanone S., 2008. Adverse effects of industrial multi-walled carbon nanotubes on human pulmonary cells. Proceedings of the Nanosafe, International Conference on Safe Production and Use of Nanomaterials; Grenoble, November 3rd-7th, 2008; N° P4-12.
 - **Setyan A.**, Sauvain J.-J., Rossi M.J., Guillemin M., Riediker M., 2009. Assessment of occupational exposure to Diesel exhaust particles in association with levels of oxidative stress biomarkers. Proceedings of the 1st NanoImpactNet Conference; Lausanne, March 23rd-27th, 2009; p. 57.

Impressum

Centre d'Impression et de Reprographie (CIR)
Centre Hospitalier Universitaire Vaudois (CHUV)
Rue du Bugnon 46 - BH10
CH - 1011 Lausanne

cir@chuv.ch

Imprimé en juillet 2009